RADC-TR-76-101, Volume V (of seven)
Final Technical Report
February 1978

APPLICATIONS OF MULTICONDUCTOR TRANSMISSION LINE THEORY TO THE PREDICTION OF CABLE COUPLING, Prediction of Crosstalk Involving Twisted Wire Pairs

Jack W. McKnight
Clayton R. Paul

University of Kentucky

Approved for public release; distribution unlimited.

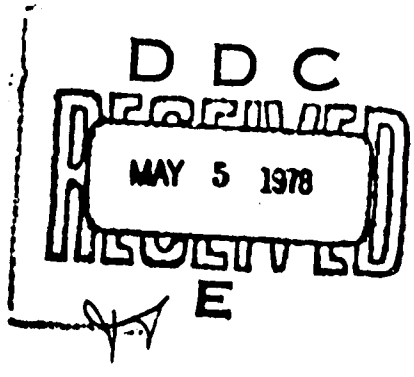

ROME AIR DEVELOPMENT CENTER
Air Force Systems Command
Griffiss Air Force Base, New York 13441

This report has been reviewed by the RADC Information Office (OI) and is releasable to the National Technical Information Service (NTIS). At NTIS it will be releasable to the general public, including foreign nations.

RADC-TR-76-101, Vol V (of seven) has been reviewed and is approved for publication.

APPROVED: James C. Brodock

JAMES C. BRODOCK
Project Engineer

APPROVED: Lester E. Treankler

LESTER E. TREANKLER, Lt Col, USAF
Assistant Chief
Reliability & Compatibility Division

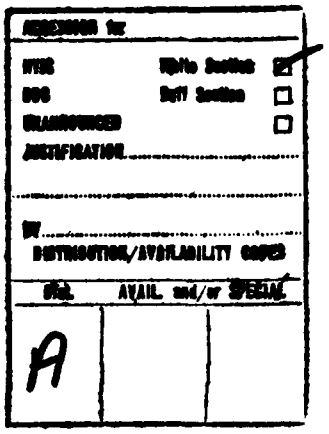

FOR THE COMMANDER: John P. Huss

JOHN P. HUSS
Acting Chief, Plans Office

If your address has changed or if you wish to be removed from the RADC mailing list, or if the addressee is no longer employed by your organization, please notify RADC (RBCT) Griffiss AFB NY 13441. This will assist us in maintaining a current mailing list.

Do not return this copy. Retain or destroy.

(18) FAD (19) TR 76 101 VOL 5

UNCLASSIFIED

SECURITY CLASSIFICATION OF THIS PAGE *(When Data Entered)*

REPORT DOCUMENTATION PAGE	READ INSTRUCTIONS BEFORE COMPLETING FORM
1. REPORT NUMBER RADC-TR-76-101, Vol V (of seven)	2. GOVT ACCESSION NO.
	3. RECIPIENT'S CATALOG NUMBER (9)
(6) 4. TITLE (and Subtitle) APPLICATIONS OF MULTICONDUCTOR TRANSMISSION LINE THEORY TO THE PREDICTION OF CABLE COUPLING. Prediction of Crosstalk Involving Twisted Wire Pairs.	5. TYPE OF REPORT & PERIOD COVERED Final Technical Report.
	6. PERFORMING ORG. REPORT NUMBER N/A
(10) 7. AUTHOR(s) Jack W. McKnight Clayton R. Paul (Volume 5.)	(15) 8. CONTRACT OR GRANT NUMBER(s) F30602-75-C-0118
9. PERFORMING ORGANIZATION NAME AND ADDRESS University of Kentucky Department of Electrical Engineering Lexington, KY 40506	10. PROGRAM ELEMENT, PROJECT, TASK AREA & WORK UNIT NUMBERS 62702F (16) 23380305 (17) 11
11. CONTROLLING OFFICE NAME AND ADDRESS Rome Air Development Center (RBCT) Griffiss AFB NY 13441	(11) 12. REPORT DATE Feb 78
	13. NUMBER OF PAGES 234
14. MONITORING AGENCY NAME & ADDRESS *(if different from Controlling Office)* Same	15. SECURITY CLASS. *(of this report)* UNCLASSIFIED (12) 247 p.
	15a. DECLASSIFICATION/DOWNGRADING SCHEDULE N/A

16. DISTRIBUTION STATEMENT *(of this Report)*

Approved for public release; distribution unlimited.

17. DISTRIBUTION STATEMENT *(of the abstract entered in Block 20, if different from Report)*

Same

18. SUPPLEMENTARY NOTES

RADC Project Engineer: James Brodock (RBCT)

19. KEY WORDS *(Continue on reverse side if necessary and identify by block number)*

Electromagnetic Compatibility	Wire-to-Wire Coupling
Cable Coupling	Crosstalk
Transmission Lines	Twisted Pairs
Multiconductor Transmission Lines	Twisted Wires

20. ABSTRACT *(Continue on reverse side if necessary and identify by block number)*

A transmission line model of the twisted wire pair is presented which may be used to compute electromagnetic coupling between the twisted wire pair and other circuits. The model is derived by representing the transmission line for the twisted wire pair as a cascade of uniform loops and "abruptly" nonuniform twists. The overall transmission line matrix is found by cascading the chain parameter matrices, which represent the loops, with the permutation matrices, that represent the twists. Comparisons are presented between the twisted wire pair, the straight wire pair, and the single wire circuit configurations to de-

DD FORM 1 JAN 73 1473 EDITION OF 1 NOV 65 IS OBSOLETE

UNCLASSIFIED

SECURITY CLASSIFICATION OF THIS PAGE *(When Data Entered)*

404 922

termine the relative effectiveness in the reduction of electromagnetic coupling. Experimental results are compared to the model predictions which verify that the chain parameter model is accurate to within ± 3 dB for frequencies such that the line is electrically short (i.e. $1/10(\lambda)$). Finally a second model, the low frequency model, is presented and is shown to be as accurate as the chain parameter model in the prediction of coupling at low frequencies. This low frequency model is very appealing in that it is conceptually much easier to model and also less time consuming, computationally.

PREFACE

This effort was conducted by The University of Kentucky under the sponsorship of the Rome Air Development Center Post-Doctoral Program for RADC's Compatibility Branch. Mr. Jim Brodock of RADC was the task project engineer and provided overall technical direction and guidance.

The RADC Post-Doctoral Program is a cooperative venture between RADC and some sixty-five universities eligible to participate in the program. Syracuse University (Department of Electrical Engineering), Purdue University (School of Electrical Engineering), Georgia Institute of Technology (School of Electrical Engineering), and State University of New York at Buffalo (Department of Electrical Engineering) act as prime contractor schools with other schools participating via sub-contracts with the prime schools. The U.S. Air Force Academy (Department of Electrical Engineering), Air Force Institute of Technology (Department of Electrical Engineering), and the Naval Post Graduate School (Department of Electrical Engineering) also participate in the program.

The Post-Doctoral Program provides an opportunity for faculty at participating universities to spend up to one year full time on exploratory development and problem-solving efforts with the post-doctorals splitting their time between the customer location and their educational institutions. The program is totally customer-funded with current projects

being undertaken for Rome Air Development Center (RADC), Space and Missile Systems Organization (SAMSO), Aeronautical Systems Division (ASD), Electronics Systems Division (ESD), Air Force Avionics Laboratory (AFAL), Foreign Technology Division (FTD), Air Force Weapons Laboratory (AFWL), Armament Development and Test Center (ADTC), Air Force Communications Service (AFCS), Aerospace Defense Command (ADC), Hq USAF, Defense Communications Agency (DCA), Navy, Army, Aerospace Medical Division (AMD), and Federal Aviation Administration (FAA).

Further information about the RADC Post-Doctoral Program can be obtained from Mr. Jacob Scherer, RADC/RBC, Griffiss AFB, NY, 13441, telephone Autovon 587-2543, commercial (315) 330-2543.

The authors of this report are Jack W. McKnight and Clayton R. Paul. Jack W. McKnight received the BSEE and MSEE degrees from the University of Kentucky, Lexington, Kentucky 40506 in December 1973 and December 1977, respectively. He is currently a research assistant with the Department of Electrical Engineering, University of Kentucky. Clayton R. Paul received the BSEE degree from The Citadel (1963), the MSEE degree from Georgia Institute of Technology (1964), and the Ph.D. degree from Purdue University (1970). He is currently an Associate Professor with the Department of Electrical Engineering, University of Kentucky, Lexington, Kentucky 40506.

The authors wish to acknowledge the capable efforts of Mrs. Maude Terhune in typing this manuscript.

TABLE OF CONTENTS

Chapter		Page
I	INTRODUCTION	1
	1.1 Rationale for Using Twisted Pairs	2
	1.2 Discussion of the Modeling Technique	15
II	DERIVATION OF THE PREDICTION MODELS	23
	2.1 General Discussion	23
	2.2 Single Wire Receptor Model	25
	2.3 The Straight Wire Pair Receptor Model	35
	2.4 The Twisted Wire Pair Receptor Model	43
	2.5 Special Considerations	55
	2.6 Other Excitation Configurations	64
III	EXPERIMENTAL RESULTS	67
	3.1 General Discussion	67
	3.2 Experimental Procedure	67
	3.3 Discussion of Graph Formats	73
	3.4 Single Wire Results	80
	3.5 Straight Wire Pair Results	81
	3.6 Twisted Wire Pair Results	82
	3.7 Low Impedance Loads	83
	3.8 Summary	89
IV	THE LOW FREQUENCY MODEL	92
	4.1 Introduction	92
	4.2 Inductive Coupling	93
	4.2.1 The Twisted Wire Pair	93
	4.2.2 The Straight Wire Pair	100
	4.2.3 Comparison of the Inductive Coupling Models	103
	4.3 Capacitive Coupling	104
	4.3.1 The Twisted Wire Pair	104
	4.3.2 The Straight Wire Pair	109
	4.3.3 Comparison of the Capacitive Coupling Models	109

Chapter Page

4.4 Generator Circuit Currents and Voltages 112
4.5 The Mutual Inductances and Capacitances of The Segments 113
4.6 The Total Coupling Equation 115
4.7 The Coupling Model For Other Excitation Configurations 116
4.7.1 Inductive Coupling 117
4.7.2 Capacitive Coupling 120
4.7.3 The Total Coupling Model 123
4.8 Prediction Accuracies of the Low Frequency Model 125
4.9 Further Observations Based on the Low Frequency Model 129
4.10 Balanced Load Configurations 138

V SUMMARY 154

APPENDIX A 158

APPENDIX B 191

APPENDIX C 208

BIBLIOGRAPHY 233

LIST OF TABLES

Table		Page
I	Cross reference for loadings and circuit separations in Appendix A	78
II	Cross reference for loadings and circuit separations in Appendix B	84
III	Cross reference for loadings and circuit separations in Appendix C	127
IV	Computed comparison of low frequency model and chain parameter model for unbalanced load configuration and 1 ohm loads	132
V	Computed comparison of low frequency model and chain parameter model for unbalanced load configuration and 50 ohm loads	134
VI	Computed comparison of low frequency model and chain parameter model for unbalanced load configuration and 1000 ohm loads	136
VII	Computed comparison of low frequency model and chain parameter model for balanced load configuration and 1 ohm loads	147
VIII	Computed comparison of low frequency model and chain parameter model for balanced load configuration and 50 ohm loads	149
IX	Computed comparison of low frequency model and chain parameter model for balanced load configuration and 1000 ohm loads	151

LIST OF FIGURES

Figure		Page
1-1	The twisted wire pair	3
1-2	Two-wire system	4
1-3	Relation of area in receptor circuit to inductive coupling	6
1-4	Superposition of representative sources for induction and capacitive coupling components	8
1-5	(a) Inductive component of coupling representation	10
	(b) Capacitive component of coupling representation	10
1-6	(a) The straight wire pair receptor configuration	12
	(b) Circuit cross section	12
1-7	(a) The twisted wire pair receptor configuration	14
	(b) Circuit cross section	14
1-8	The currents induced in adjacent loops	16
1-9	The abruptly non-uniform representation of the twisted wire pair	19
1-10	The cascade of chain parameter matrices for each loop to obtain the overall transmission line chain parameter matrix	21
2-1	(a) Cross section of two-wire circuit configuration showing assumption of no dielectric insulation	24
	(b) Cross section of straight wire pair and twisted wire pair circuit configurations showing assumption of no dielectric insulation	24
2-2	(a) Single wire receptor configuration	26
	(b) Straight wire pair receptor configuration	26
	(c) Twisted wire pair receptor configuration	26

Figure		Page
2-3	The per-unit-length parameters for the single wire receptor configuration	27
2-4	Imaging technique	31
2-5	Terminal system for single wire receptor configuration	33
2-6	The per-unit-length parameters for the straight wire pair receptor configuration	36
2-7	Terminal system for straight wire pair receptor configuration	41
2-8	The "abruptly" nonumiform TL model of the twisted wire pair receptor configuration	45
2-9	The "abruptly" nonuniform portion or twist	46
2-10	The additional twist for an even number of loops	50
2-11	The cascade of matrices $\underset{\sim}{\Phi}$ and $\underset{\sim}{P}$ to determine the overall TL matrix for the twisted wire pair	52
2-12	(a) The TL representation for an odd number of loops	53
	(b) The TL representation for an even number of loops	53
2-13	(a) Special configuration for the twisted wire pair	58
	(b) Special configuration for the twisted wire pair	58
2-14	The experimental configuration	63
2-15	(a) Single wire configuration with voltage source in each circuit	65
	(b) Straight wire pair configuration with voltage source in each circuit	65
	(c) Twisted wire pair configuration with voltage source in each circuit	65
3-1	(a) Photograph of the experimental setup	69
	(b) Photograph of the experimental setup	69
3-2	The experimental setup	70

Figure

3-3 Cross section showing the [illegible] mental setup . . . . .

3-4 (a) Single wire configurat[illegible] that is used in plotting [illegible] model results . . . .

(b) Straight wire pair [illegible] labeling that is used [illegible] and model results . .

(c) Twisted wire pair [illegible] labeling that is used [illegible] and model results . .

3-5 Typical graph of transfer rat[illegible] 1000 ohm loads . . . . . .

3-6 Typical graph of transfer rat[illegible] 50 ohm loads . . . . . .

3-7 Low impedance load pl[illegible] . . .

3-8 Low impedance load plot [illegible] . .

3-9 Low impedance load plot [illegible] . .

3-10 Low impedance load plot [illegible] . .

4-1 The low frequency [illegible] the twisted wire pair . .

4-2 Net flux representati[illegible] .

4-3 The inductive [illegible] for one loop of the twisted w[illegible] .

4-4 The overall inductive [illegible] sentation for the twisted w[illegible] .

4-5 The resulting representati[illegible] the TWP when the [illegible] superimposed . . . . .

4-6 The inductive components [illegible] wire pair (SWP) . . . . .

Figure		Page
4-7	The resulting representation of inductive coupling for the SWP when the components of inductive coupling are superimposed	102
4-8	The capacitive component of coupling for a single loop of the TWP	105
4-9	The overall capacitive components of coupling for the TWP	107
4-10	The reduced representation of capacitive coupling for the TWP	108
4-11	The overall capacitive components of coupling for the SWP	110
4-12	The reduced representation of capacitive coupling for the SWP	111
4-13	The TWP as the generator circuit	118
4-14	The net flux induced in the single wire due to the currents in each of the above two wires	119
4-15	(a) The inductive coupling components in the single wire induced by the TWP generator circuit . . .	121
	(b) The inductive coupling components in the single wire induced by the SWP generator circuit . . .	121
4-16	The capacitive coupling model for the twisted wire pair generator circuit configuration.	122
4-17	The balanced load configuration for the TWP	139
4-18	The representation of the balanced load configuration for the TWP	141
4-19	(a) The inductive components of coupling in the TWP balanced load configuration	143
	(b) The capacitive components of coupling in the TWP balanced load configuration	143
4-20	(a) The reduced inductive component of coupling representation for the TWP balanced load configuration	144
	(b) The reduced capacitive component of coupling representation for the TWP balanced load configuration	144

I. INTRODUCTION

High performance military as well as commercial aircraft contain numerous sophisticated electronic subsystems. The various electronic subsystems are interconnected by wires (cylindrical conductors with cylindrical dielectric insulation) which are grouped into tightly packed bundles. The close proximity of the wires in these cable bundles enhances the electromagnetic interaction (crosstalk) between the electronic subsystems which the wires interconnect. Generally this unintended coupling of electromagnetic energy is detrimental to the system performance. Shielding individual wires and use of twisted pairs are examples of techniques which have been used to reduce this interference.

In the initial design of an electronic system as well as retrofit of present systems, there is a need to model the electromagnetic coupling in cable bundles so that the required interference suppression measures can be determined. The main objective of this work is the development of a model which will predict crosstalk in which twisted pairs are involved.

1.1 Rationale for Using Twisted Pairs

Twisted wire pairs are two identical wires that typically have touching insulations (See Fig. 1-1(a)). The twisting effect stems from progressively rotating the cross-sectional axis of these two wires as the distance along the line increases (See Fig. 1-1(b)).

In addition to physically holding the wires together, the twisting of wire pairs tends to eliminate inductive coupling (inductive cross-talk). As a preliminary to understanding the mechanism of inductive coupling, consider the simple two-wire line shown in Fig. 1-2. The line axis is denoted by x and the line is of total length ℓ. This simple two-wire line consists of a generator circuit and a receptor circuit. The generator circuit consists of a wire, the "generator wire", and a reference plane for the line voltages. The receptor circuit consists of another wire, the "receptor wire", and the reference plane. Typically one end of the generator circuit is excited and the voltages V_{0R} and $V_{\ell R}$ at each end of the receptor circuit are measured to determine the induced signals. Portions of these induced signals are directly related to the area of the loop formed by the receptor circuit and the reference plane as illustrated by the shaded area of Fig. 1-2(a)[1]. To prove this, one can show that the per-unit-length mutual inductance between the generator and receptor circuits and thus the inductive

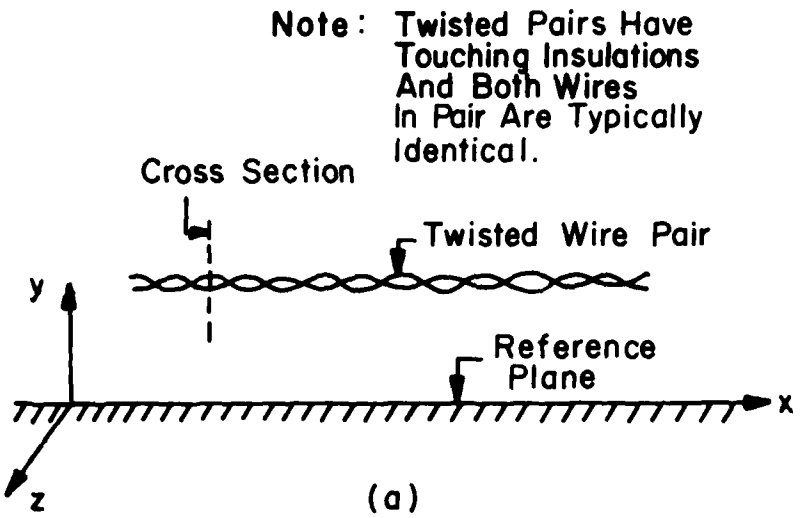

(a)

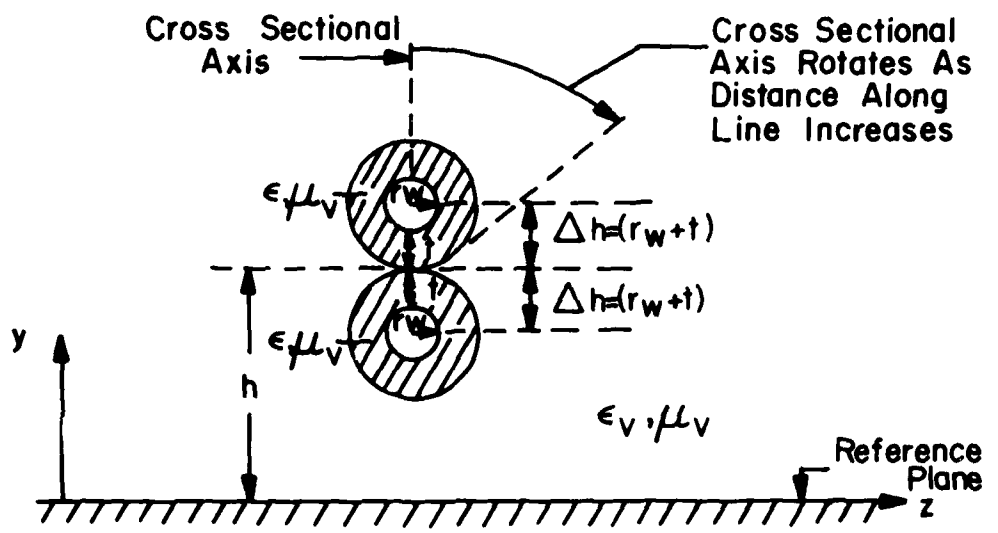

ϵ_v = Permittivity Of Free Space
μ_v = Permeability Of Free Space
ϵ = Permittivity Of Wire Insulation

(b)

Fig. 1-1.

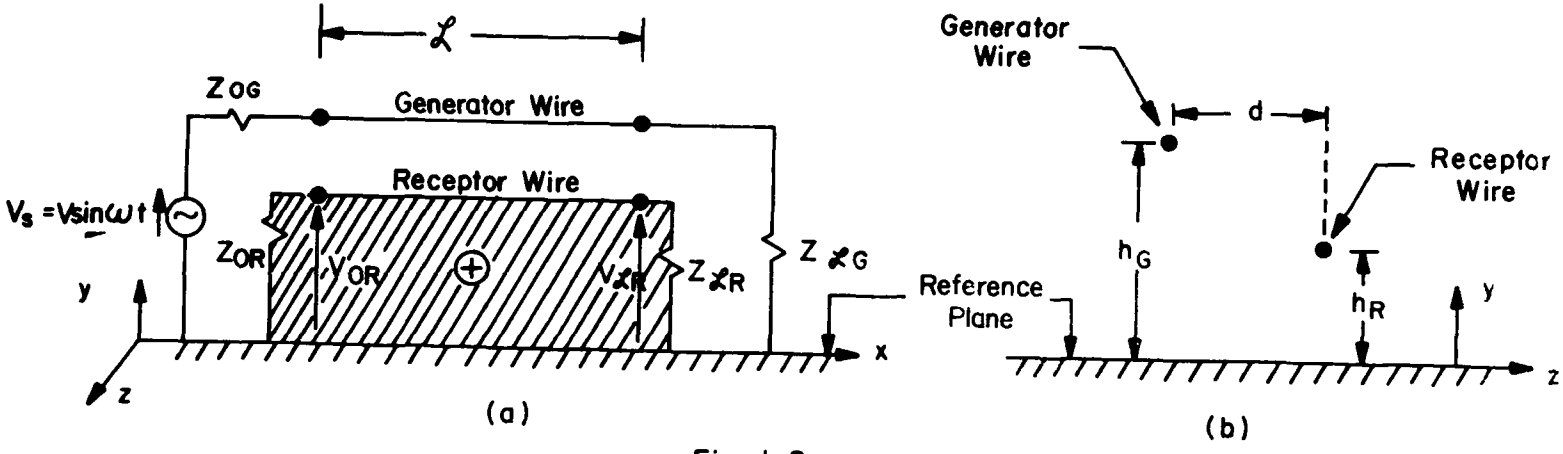
ℓ
Z OG
Generator Wire
Receptor Wire
V_S = V sin ω t
Z OR
V OR
V ℓR
Z ℓR
Z ℓG
y
x
z
(a)
Generator Wire
d
Receptor Wire
h_G
h_R
Reference Plane
y
z
(b)

Fig. 1-2.

coupling is related to the loop area (See Fig. 1-3). The generator wire current, I_G, in a small Δx section of the generator wire will produce a magnetic flux density, B_r, at a distance r from the generator wire of $B_r = \frac{\mu_v I_G}{2\pi r}$ [1]. By integrating the component of this field, B_n, which is normal to the vertical plane formed by the receptor circuit directly beneath the receptor wire, one can obtain the total flux ϕ_T which links a Δx portion of the receptor circuit as

$$\phi_T = \int B_n \, da \tag{1-1}$$

where $da = h_R \Delta x$. This flux will induce a voltage in the receptor circuit and cause an incremental current to flow in the receptor wire. The per-unit-length mutual inductance between the generator and receptor circuit, ℓ_m, is related to the flux and current by the equation

$$\ell_m = \frac{\phi_T}{I_G \Delta x} \tag{1-2}$$

Thus the per-unit-length mutual inductance is dependent upon the loop area of the receptor circuit.

Similarly, the voltage of the generator circuit produces an electric field intensity between the generator wire and the receptor wire. This electric field intensity causes a displacement current

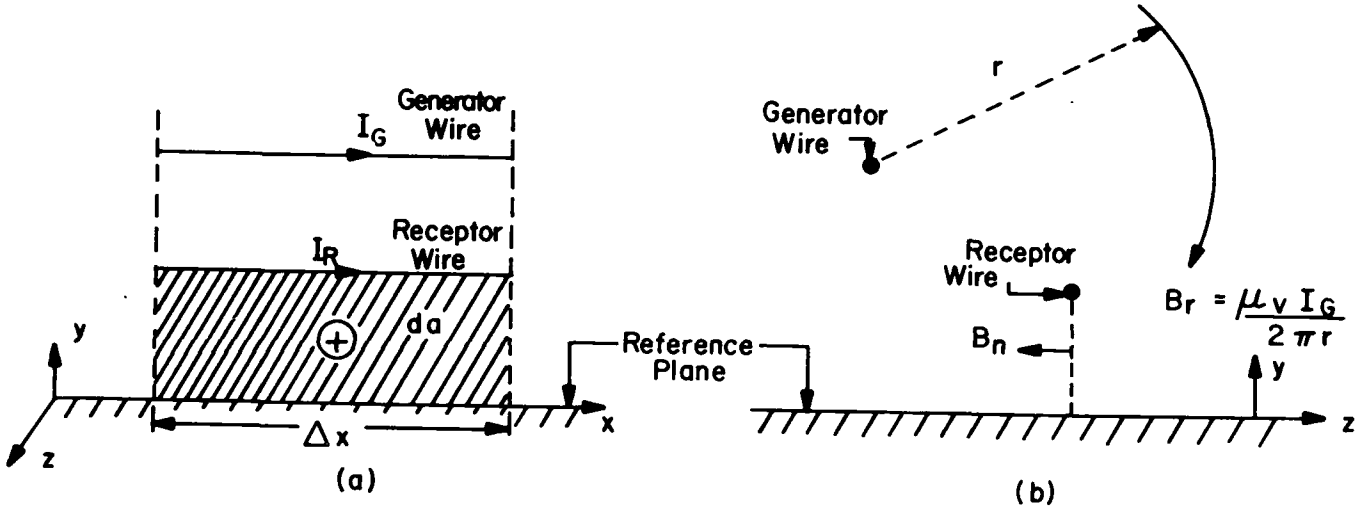
Generator Wire
I_G
Receptor Wire
I_R
da
y
z
x
Δx
(a)
Reference Plane
r
Generator Wire
Receptor Wire
B_n
$B_r = \frac{\mu_v I_G}{2\pi r}$
y
z
(b)

Fig. 1 - 3.

to flow between the generator and receptor wires which may be represented as a per-unit-length mutual capacitance, c_m.

Intuitively, the induced coupling or crosstalk can be considered, for a sufficiently small frequency, to be a superposition of the portions of the coupling due to the mutual inductance ("inductive coupling") and the mutual capacitance ("capacitive coupling") between the generator and receptor circuits. This has been proven in [2] by obtaining an exact solution for the coupled transmission line equations which represent the circuit interactions for the TEM mode of propagation. From these equations it was shown in [2] that as the frequency of excitation of the generator circuit becomes sufficiently small, one obtains the equivalent circuit shown in Fig. 1-4 where $I_{G_{DC}}$ and $V_{G_{DC}}$ are the D.C. (zero frequency) values of current and voltage of the generator wire, respectively, and are given by

$$I_{G_{DC}} = \frac{V_s}{Z_{0G} + Z_{\ell G}} \tag{1-3}$$

$$V_{G_{DC}} = \frac{Z_{\ell G}}{Z_{0G} + Z_{\ell G}} \; V_s \tag{1-4}$$

For the circuit in Fig. 1-4, clearly the net induced terminal voltages in the receptor circuit, V_{0R} and $V_{\ell R}$, may be considered to be the super-

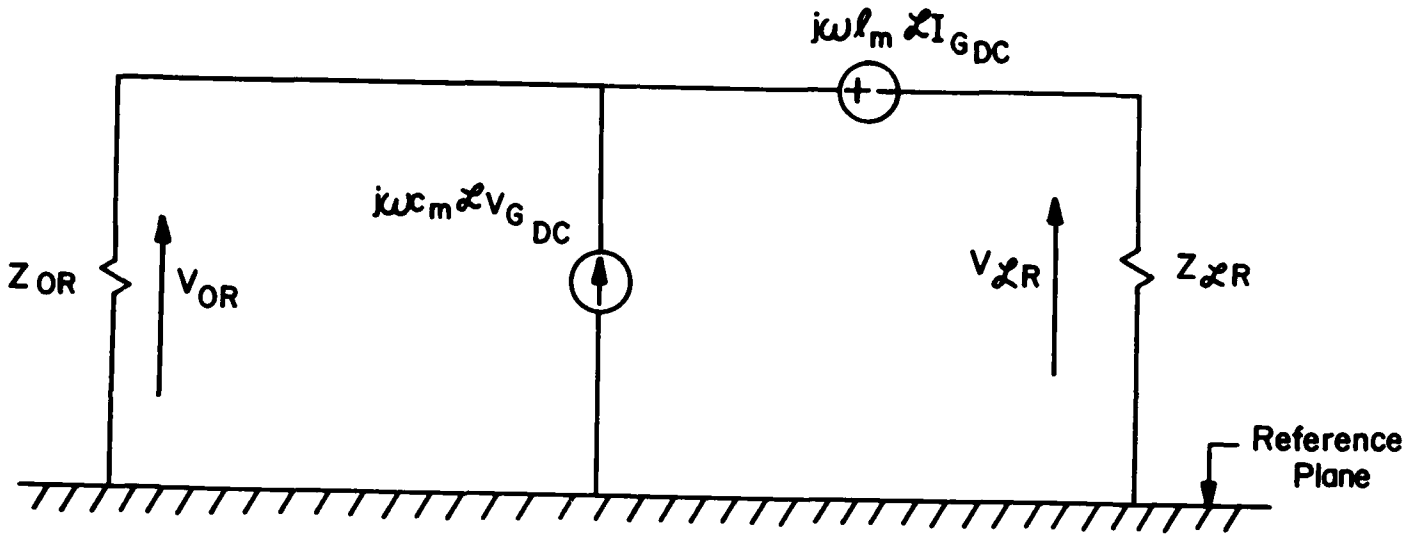
$j\omega l_m \mathcal{L} I_{G_{DC}}$
$j\omega c_m \mathcal{L} V_{G_{DC}}$
Z_{OR}
V_{OR}
$V_{\mathcal{L}R}$
$Z_{\mathcal{L}R}$
Reference Plane

Fig. 1-4.

position of the capacitive (V_{0R}^{CAP} and $V_{\ell R}^{CAP}$) and inductive (V_{0R}^{IND} and $V_{\ell R}^{IND}$) portions of the couplings as shown in Fig. 1-5 where $V_{0R} = V_{0R}^{IND} + V_{0R}^{CAP}$ and $V_{\ell R} = V_{\ell R}^{IND} + V_{\ell R}^{CAP}$. These individual components are easily calculated from Fig. 1-5 as

$$V_{0R}^{IND} = j\omega \ell_m \ell I_{G_{DC}} \left(\frac{Z_{0R}}{Z_{0R} + Z_{\ell R}}\right) \tag{1-5a}$$

$$V_{\ell R}^{IND} = -j\omega \ell_m \ell I_{G_{DC}} \left(\frac{Z_{\ell R}}{Z_{0R} + Z_{\ell R}}\right) \tag{1-5b}$$

and

$$V_{0R}^{CAP} = j\omega c_m \ell V_{G_{DC}} \left(\frac{Z_{0R} Z_{\ell R}}{Z_{0R} + Z_{\ell R}}\right) \tag{1-6a}$$

$$V_{\ell R}^{CAP} = j\omega c_m \ell V_{G_{DC}} \left(\frac{Z_{0R} Z_{\ell R}}{Z_{0R} + Z_{\ell R}}\right) \tag{1-6b}$$

Also in [2] it was shown that the inductive coupling dominates the capacitive coupling in V_{0R} if

$$Z_{\ell G} Z_{\ell R} << Z_{CG} Z_{CR} \tag{1-7}$$

where $Z_{CG}(Z_{CR})$ is the characteristic impedance of the generator (receptor) circuit in the presence of the receptor (generator) circuit. Similarly the inductive coupling dominates the capacitive coupling in $V_{\ell R}$ if

$$Z_{\ell G} Z_{0R} << Z_{CG} Z_{CR} \tag{1-8}$$

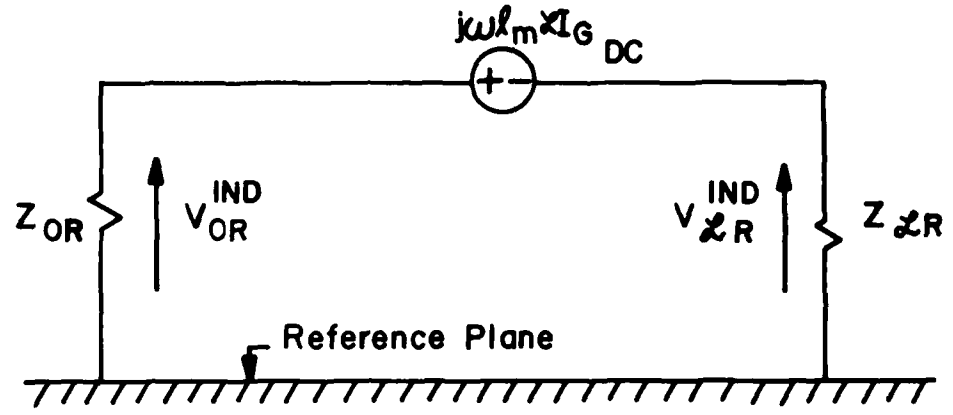
$j\omega l_m \ell I_{G_{DC}}$
Z_{OR}
V_{OR}^{IND}
$V_{\ell R}^{IND}$
$Z_{\ell R}$
Reference Plane

(a)

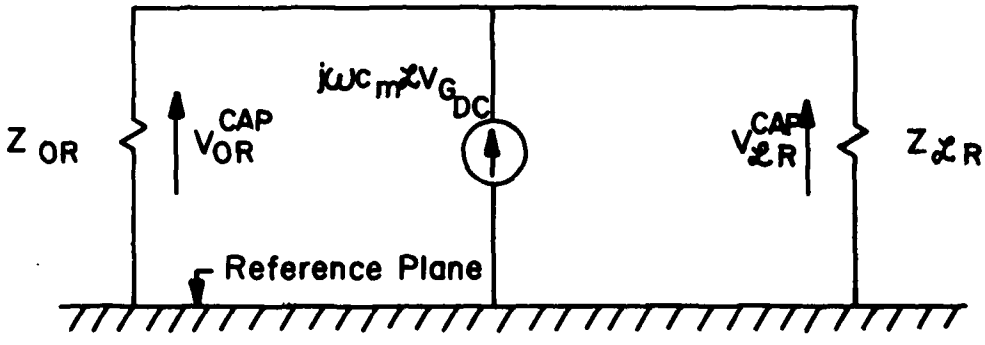
$j\omega c_m \ell V_{G_{DC}}$
Z_{OR}
V_{OR}^{CAP}
$V_{\ell R}^{CAP}$
$Z_{\ell R}$
Reference Plane

(b)

Fig. 1-5.

Capacitive coupling dominates inductive coupling when the above inequalities are reversed. From this we see that inductive coupling predominates for "low" impedances and conversely for "high" impedances.

Generally, twisted pairs are used to connect power distribution circuits which typically have very low terminal impedances. They are used in these situations with the intent of reducing the inductive coupling to or from these types of circuits and the rationale is generally based on the above reasoning for the simple two-wire circuit. However, twisted pairs have been used to connect high impedance devices and it will be shown that the twisted pairs have virtually no effect on reducing the crosstalk to or from these types of high impedance circuits.

From the above discussion, it seems that in order to reduce the inductive coupling one must reduce the loop area of the receptor circuit. This can be done in several ways. One is to reduce the height of the receptor wire above the reference plane. A second method is to shorten the length of the line and a third method is to add a second wire to the receptor circuit that is tied to the reference plane at one end (See Fig. 1-6). The length and height of wires above the reference plane are generally minimized in the installation

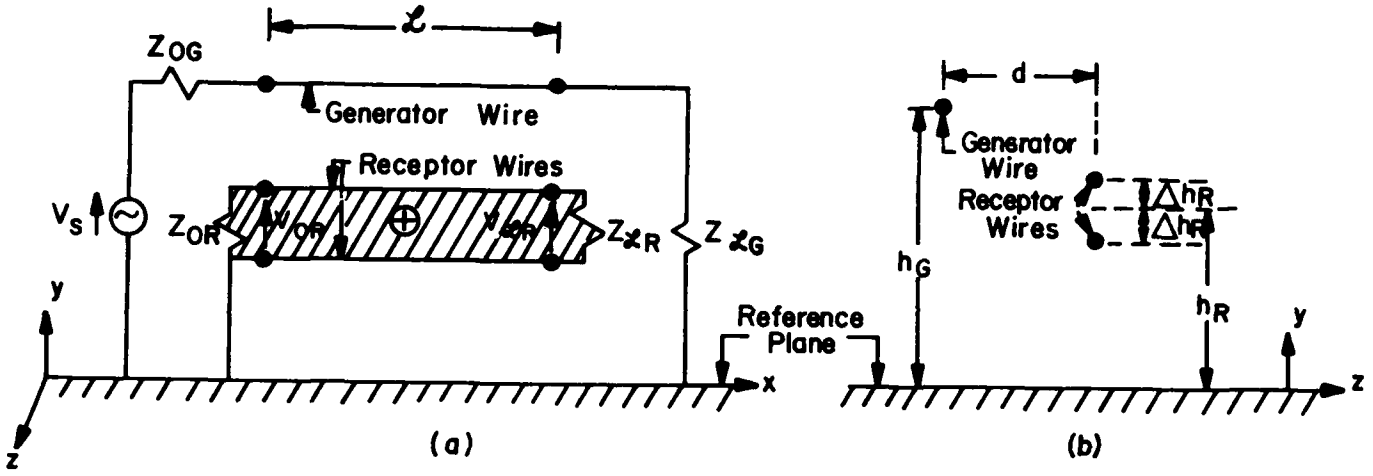
ℓ
Z_OG
Generator Wire
Receptor Wires
V_S
Z_OR
V_oh
V_oh
Z_ℓR
Z_ℓG
y
x
z
Reference Plane
(a)
d
Generator Wire
Receptor Wires
Δh_R
Δh_R
h_G
h_R
y
z
(b)

Fig. 1-6.

of the wire bundles. [illegible]
ribs, hydraulic lines, etc., pla
above the aircraft struct[illegible]
is often used to further re[illegible]
that by using this third method [illegible]
tively reduced by moving the w[illegible]
each other, i.e. reducing [illegible]
nection of the receptor circuit t[illegible]
is only made at one end. This pra[illegible]
to eliminate an additional loop betwe[illegible]
plane.

A further reduction of [illegible]
twisting the two wires of th[illegible]
Fig. 1-7(a). The total flux [illegible]
will depend upon the correspond[illegible]
of the generator wire, I_{G_1}, as [illegible]
rents induced in these loops w[illegible]
in Fig. 1-7(a). In this ideal [illegible]
same wire in adjacent loops appe[illegible]
inductive coupling contributi[illegible]
of the receptor circuit when th[illegible]

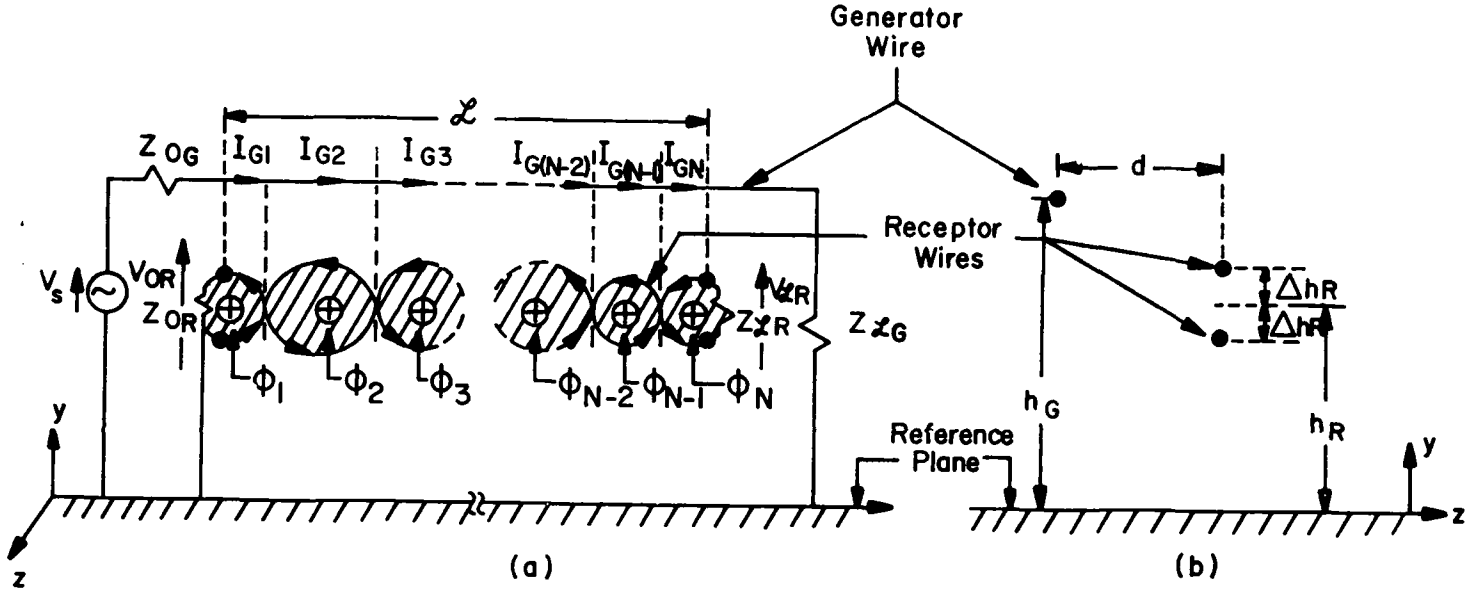
Generator
Wire
$\mathcal{L}$
Z_{OG}
I_{G1} I_{G2} I_{G3} $I_{G(N-2)}$ $I_{G(N-1)}$ I_{GN}
d
Receptor
Wires
V_S
V_{OR}
Z_{OR}
Φ_1 Φ_2 Φ_3 Φ_{N-2} Φ_{N-1} Φ_N
$V_{\mathcal{L}R}$
$Z_{\mathcal{L}R}$
$Z_{\mathcal{L}G}$
Δh_R
Δh_R
h_G
h_R
Reference
Plane
y
z
(a)
(b)

Fig. 1-7.

odd number of loops the overall coupling appears to be effectively that of one loop. This has long been the accepted convention in the reasoning for using twisted wire pairs [3, 8].

However, consider the following fallacy in this reasoning. The generator circuit currents, I_{G_i}, of Fig. 1-7(a) are not actually in phase. As the frequency of excitation is lowered, however, they become more closely in phase. Thus, the fluxes induced in the individual loops, ϕ_i, are not in phase and the corresponding currents of wire in adjacent loops induced by ϕ_i and ϕ_{i+1} do not cancel exactly as previously assumed. The currents induced in adjacent loops such as I_a and I_b in Fig. 1-8 will be complex numbers. Even though they have approximately the same magnitudes, the phases are different and they cannot cancel exactly. Clearly this will only occur for some "high frequency" such that the length of a loop is not electrically short.

1.2 Discussion of the Modeling Technique

Previous work on twisted and straight wire pairs have typically described the fields resulting from twisted and straight wire pairs when excited with voltage sources in free space without reference conductors or planes [3, 4, 5]. These works do not attempt to

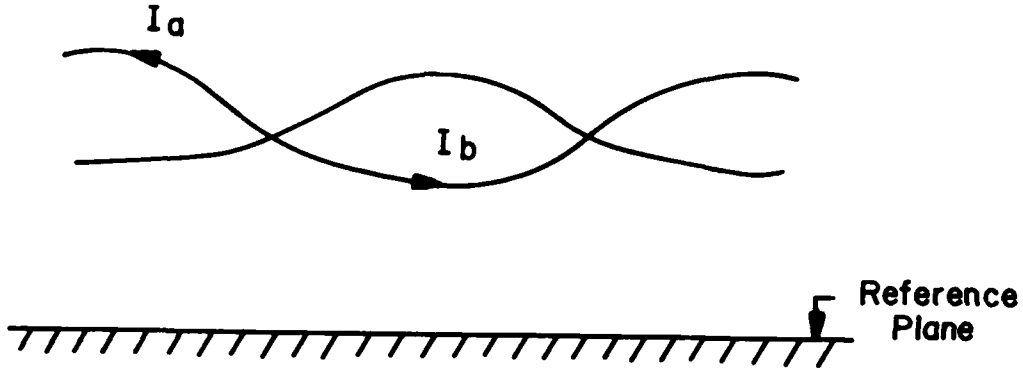

Fig. 1-8.

describe the effect of mutual coupling of the pairs with other circuits.

The objective of this work will be to examine the prediction of crosstalk either to or from twisted pairs. This will be done by (a) determining a transmission line (TL) model for predicting the coupling to twisted wire pairs, (b) experimentally correlating the predictions, and (c) simplifying the model where possible.

One of the difficulties in obtaining a TL model for twisted pair circuits is that conventional TL models generally assume uniform lines. Lines are said to be uniform if cross-sectional views of the line at every point along the line are identical, i.e., the wires do not exhibit any cross-sectional variation along the line and are parallel to each other and the reference plane [1]. The reasons for assuming uniform lines are mainly due to the ease of calculating the per-unit-length parameters of the model and the ease of solution of the resulting differential equations [1]. In calculating the per-unit-length capacitance and inductance parameters (self terms as well as mutual terms), one may select any section of a uniform line since all other sections are identical. For nonuniform lines, this is no longer true and the calculation of the per-unit-length parameters becomes more difficult. In addition, if the line is nonuniform the per-unit length

quantities will be functions of the axis variable, x. Consequently, the TL equations will be nonconstant coefficient differential equations which are much more difficult to solve than constant coefficient ones, e.g., Bessel's equation [1].

One straightforward technique for obtaining approximate solutions of nonuniform lines is to model the line as a cascade of uniform lines. This technique has been successfully applied to several types of nonuniform lines [6, 7] and can be classified as modeling a "smoothly" nonuniform line as an "abruptly" nonuniform one.

The technique used in this work will involve a similar method for modeling twisted wire pairs. In this model each loop is considered as a separate transmission line pair excited by a corresponding adjacent section of generator line. Each loop, although "smoothly" nonuniform, will be modeled as a pair of parallel wires as shown in Fig. 1-9. The per-unit-length chain parameter matrix of each single uniform loop and corresponding adjacent section of the generator wire is easily determined [1]. Assuming that the junction between adjacent loops is "abruptly" nonuniform (i.e. the twist takes place over a zero interval of distance) the chain parameter matrices may be cascaded (with appropriate interchange of voltage and current variables at the junctions) to obtain the overall transmission line chain parameter

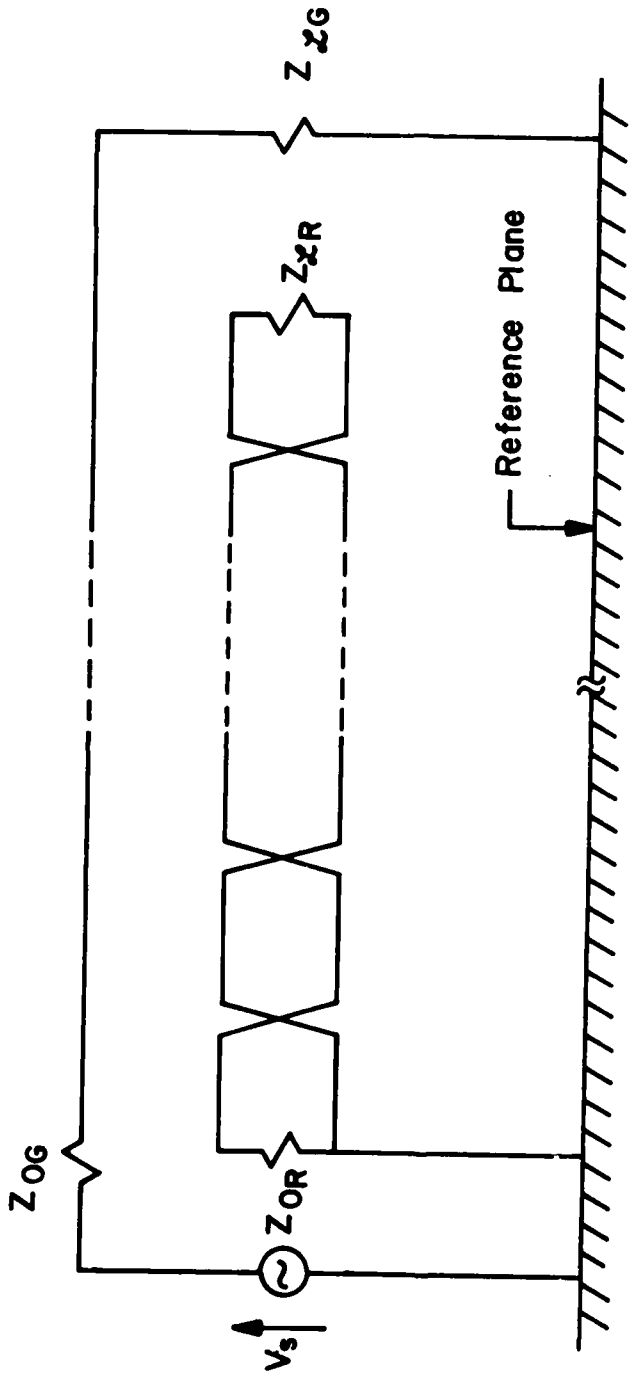

Fig. 1-9.

matrix (See Figs. 1-9 and 1-10). Once the overall TL has been modeled as this cascade, the terminal conditions are used with the resulting overall chain parameter matrix to solve for the induced receptor circuit voltages. This model will be discussed in Chapter II.

Although this model (referred to as the chain parameter model) will be shown to provide very accurate predictions of the coupling to or from twisted pair circuits, the computation time is somewhat excessive. In order to simplify the computation, a model valid for "low" frequencies was developed. This model is an approximation to the chain parameter model and will be discussed in Chapter IV. Although it seems to be virtually impossible to determine the highest frequency for which this model is valid, it appears, from the extensive experimental and computed results, to be valid for frequencies such that the line is electrically short, e.g., $\ell < 1/20\ \lambda$ where λ is a wavelength. For this range of frequencies, the low frequency model yields predictions that are virtually identical to those of the more complex chain parameter model and both model predictions are within a few percent of the experimental results. One outstanding advantage of this model is that the per-frequency computation time is virtually trivial and considerably less than the chain parameter model. An additional advantage is that, in the low frequency model, the signals

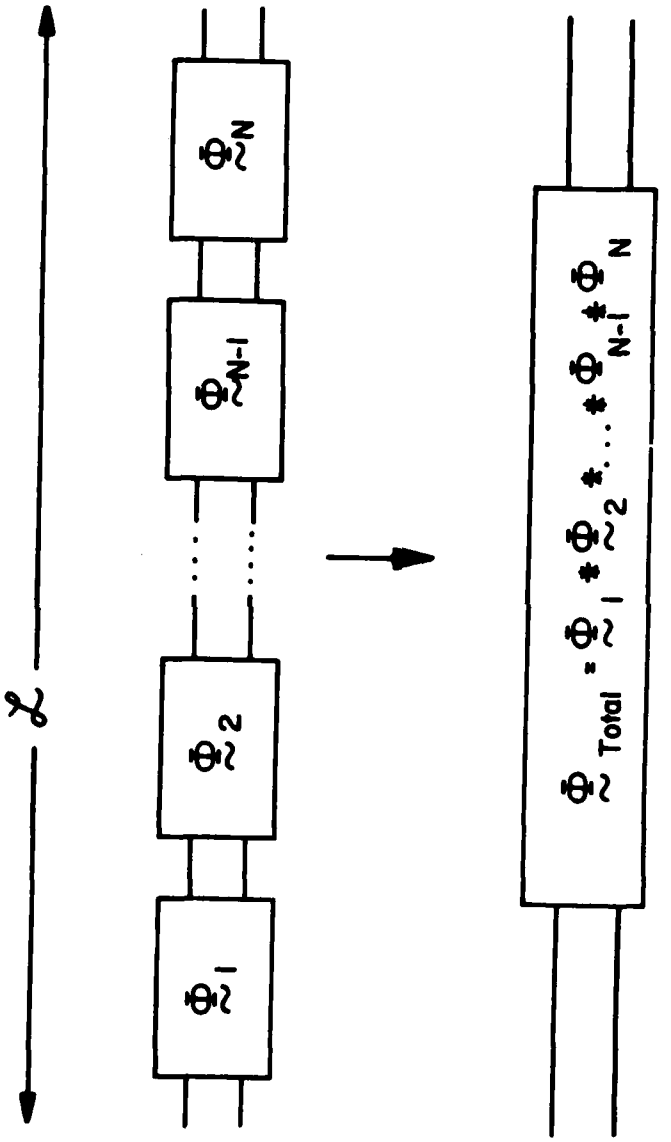
ℓ
$\Theta_{\tilde{i}}^{N}$
$\Theta_{\tilde{i}}^{N-1}$
$\Theta_{\tilde{i}}^{2}$
$\Theta_{\tilde{i}}^{1}$
$\Theta_{\tilde{i}\,\text{Total}} = \Theta_{\tilde{i}}^{1} * \Theta_{\tilde{i}}^{2} * \ldots * \Theta_{\tilde{i}}^{N-1} * \Theta_{\tilde{i}}^{N}$

Fig. I-10.

induced at each end of the receptor circuit, V_{0R} and $V_{\ell R}$, are separated into inductive and capacitive components. One can then easily determine the relative magnitudes of the components. In fact, it is shown that twisting the pair of wires reduces the total coupling more for low impedance loads than for high impedance loads (as has long been intuitively assumed). It is also shown that the total coupling is predominately capacitive for high impedance loads and usually inductive for lower impedance loads. However, exceptions to this statement will be shown and, in fact we will find in some instances that although one can effectively eliminate inductive coupling by using twisted wire pairs, there exists a limit on the reduction in total coupling due to the capacitive coupling component. This very interesting fact has apparently not been noted before.

II. DERIVATION OF THE PREDICTION MODELS

2.1 General Discussion

In order to evaluate the effectiveness of using twisted pairs to reduce crosstalk over the use of other wire configurations, one must decide which other wire configurations will be used for comparison. The natural choice would be to compare the crosstalk resulting from the single wire receptor circuit shown in Fig. 1-2 and the straight wire pair receptor circuit shown in Fig. 1-6 to the twisted pair receptor circuit shown in Fig. 1-7. As discussed in Chapter I, the twisted wire pair receptor circuit should be the most effective in reducing interference followed by the straight wire pair receptor circuit and then the single wire receptor circuit.

In modeling all three of these configurations there are certain assumptions that will be used which simplify the mathematics. First, the wires are assumed to have no insulating dielectric (See Fig. 2-1). Thus the permittivities and permeabilities of the insulations are considered to be that of free space, ϵ_v and μ_v, respectively and are therefore considered lossless. Secondly, the conductors are considered to be perfect conductors.

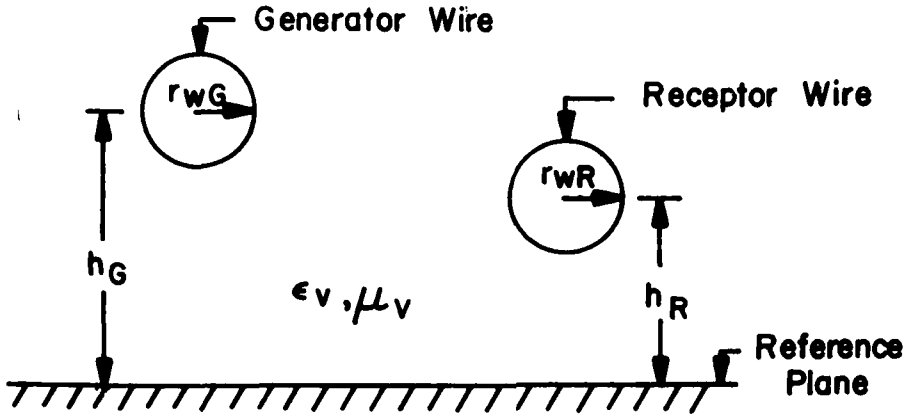
Generator Wire
r_{wG}
Receptor Wire
r_{wR}
h_G
ϵ_v, μ_v
h_R
Reference Plane

(a)

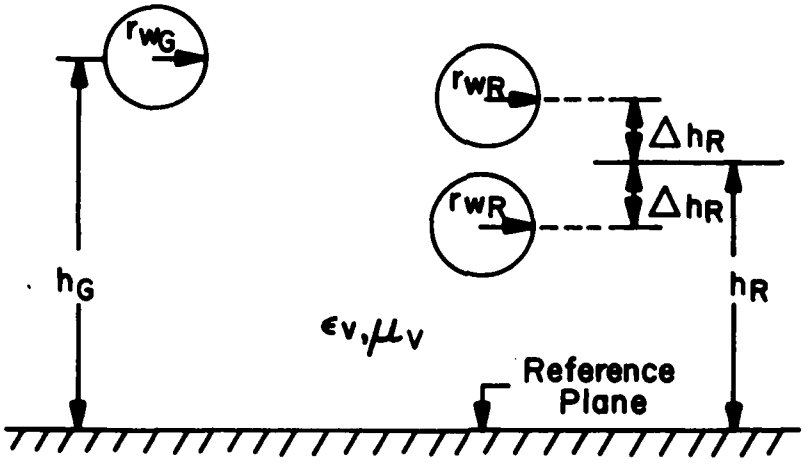
r_{wG}
r_{wR}
Δh_R
r_{wR}
Δh_R
h_G
h_R
ϵ_v, μ_v
Reference Plane

(b)

Fig. 2-1.

These three configurations will be modeled by first determining the chain parameter matrix of the overall transmission line (TL) and then incorporating the end conditions (i.e., loading and voltage excitation sources) to complete the model (See Fig. 2-2(a), (b), (c)).

2.2 Single Wire Receptor Model

In developing the TL equations and resulting chain parameter matrix for the single wire receptor model, one can characterize an electrically short Δx section of the line with lumped, per-unit-length parameters of self inductance, ℓ_G and ℓ_R, mutual inductance ℓ_m, self capacitance, c_G and c_R, and mutual capacitance, c_m as shown in Fig. 2-3[2]. The TL equations were derived from the circuit of Fig. 2-3 in [2] and in the limit as $\Delta x \to 0$ they were found to be,

$$\frac{dV_G(x)}{dx} = -j\omega \ell_G I_G(x) - j\omega \ell_m I_R(x) \tag{2-1a}$$

$$\frac{dV_R(x)}{dx} = -j\omega \ell_m I_G(x) - j\omega \ell_R I_R(x) \tag{2-1b}$$

$$\frac{dI_G(x)}{dx} = -j\omega (c_G + c_m) V_G(x) + j\omega c_m V_R(x) \tag{2-1c}$$

$$\frac{dI_R(x)}{dx} = j\omega c_m V_G(x) - j\omega (c_R + c_m) V_R(x) \tag{2-1d}$$

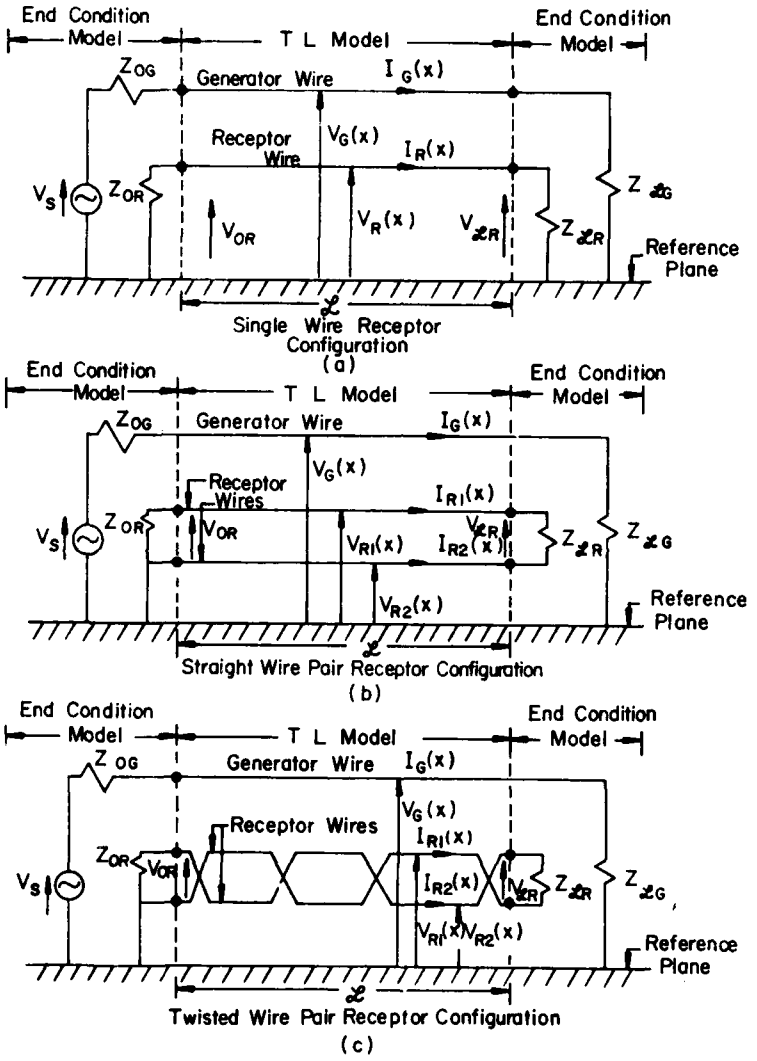
End Condition Model
T L Model
End Condition Model
Z_{OG}
Generator Wire
$I_G(x)$
Receptor Wire
$V_G(x)$
$I_R(x)$
V_S
Z_{OR}
V_{OR}
$V_R(x)$
$V_{\ell R}$
$Z_{\ell R}$
$Z_{\ell G}$
Reference Plane
ℓ
Single Wire Receptor Configuration
(a)
End Condition Model
T L Model
End Condition Model
Z_{OG}
Generator Wire
$I_G(x)$
$V_G(x)$
Receptor Wires
$I_{R1}(x)$
V_S
Z_{OR}
V_{OR}
$V_{R1}(x)$
$I_{R2}(x)$
$V_{\ell R}$
$Z_{\ell R}$
$Z_{\ell G}$
$V_{R2}(x)$
Reference Plane
ℓ
Straight Wire Pair Receptor Configuration
(b)
End Condition Model
T L Model
End Condition Model
Z_{OG}
Generator Wire
$I_G(x)$
$V_G(x)$
Receptor Wires
$I_{R1}(x)$
Z_{OR}
V_S
V_{OR}
$I_{R2}(x)$
$V_{\ell R}$
$Z_{\ell R}$
$Z_{\ell G}$
$V_{R1}(x)$
$V_{R2}(x)$
Reference Plane
ℓ
Twisted Wire Pair Receptor Configuration
(c)

Fig. 2-2

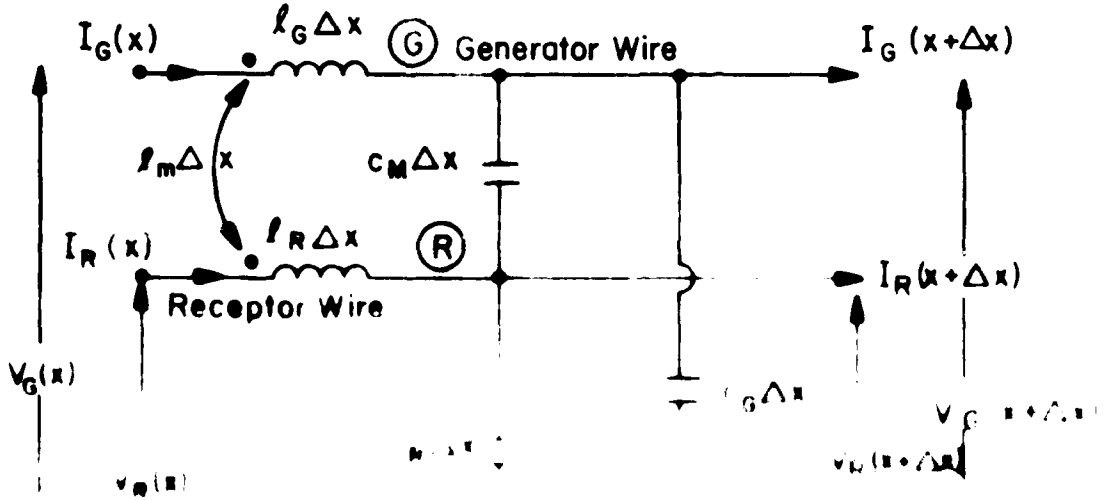
$I_G(x)$
$\ell_G \Delta x$
G
Generator Wire
$I_G(x+\Delta x)$
$\ell_m \Delta x$
$c_M \Delta x$
$I_R(x)$
$\ell_R \Delta x$
R
$I_R(x+\Delta x)$
Receptor Wire
$V_G(x)$

By relating the voltages and currents at one end of the line, $V_G(\ell)$, $V_R(\ell)$, $I_G(\ell)$ and $I_R(\ell)$, to the voltage and currents at the other end of the line, $V_G(0)$, $V_R(0)$, $I_G(0)$ and $I_R(0)$, a solution to these TL equations is provided by the matrix chain parameters [1,2];

$$\begin{bmatrix} \underline{V}(\ell) \\ \underline{I}(\ell) \end{bmatrix} = \begin{bmatrix} \underset{\sim}{\Phi}_{11}(\ell) & \underset{\sim}{\Phi}_{12}(\ell) \\ \underset{\sim}{\Phi}_{21}(\ell) & \underset{\sim}{\Phi}_{22}(\ell) \end{bmatrix} \begin{bmatrix} \underline{V}(0) \\ \underline{I}(0) \end{bmatrix} \tag{2-2}$$

where

$$\underline{V}(\ell) = \begin{bmatrix} V_G(\ell) \\ V_R(\ell) \end{bmatrix} \qquad \underline{V}(0) = \begin{bmatrix} V_G(0) \\ V_R(0) \end{bmatrix}$$

$$\underline{I}(\ell) = \begin{bmatrix} I_G(\ell) \\ I_R(\ell) \end{bmatrix} \qquad \underline{I}(0) = \begin{bmatrix} I_G(0) \\ I_R(0) \end{bmatrix} \tag{2-3}$$

and an nxm matrix with n rows and m columns is denoted by $\underset{\sim}{M}$ and an nx1 vector is denoted by $\underline{V}$. The entry in the i-th row and j-th column of a matrix $\underset{\sim}{M}$ is denoted by $[\underset{\sim}{M}]_{ij}$.

For the assumptions in Section 2-1, the matrix chain parameters in (2-2) become [2]

$$\underset{\sim}{\Phi}_{11}(\ell) = \cos(\beta\ell)\,\underset{\sim}{1}_2 \tag{2-4a}$$

$$\underset{\sim}{\Phi}_{12}(\ell) = -j\,v\sin(\beta\ell)\,\underset{\sim}{L} = -j\omega\ell\left\{\frac{\sin(\beta\ell)}{\beta\ell}\right\}\,\underset{\sim}{L} \tag{2-4b}$$

$$\underset{\sim}{\Phi}_{21}(\mathcal{L}) = -j\, v \sin(\beta \mathcal{L})\, \underset{\sim}{C} = -j\omega \mathcal{L} \left\{\frac{\sin(\beta \mathcal{L})}{\beta \mathcal{L}}\right\} \underset{\sim}{C} \tag{2-4c}$$

$$\underset{\sim}{\Phi}_{22}(\mathcal{L}) = \cos(\beta \mathcal{L})\, \underset{\sim}{1}_2 \tag{2-4d}$$

where β is the phase constant given by

$$\beta = \frac{\omega}{v} = \frac{2\pi}{\lambda} \tag{2-5}$$

ω is the radian frequency of excitation, λ is a wavelength at this frequency,

$$\lambda = v/f \tag{2-6}$$

and v is the velocity of propagation in the surrounding medium,

$$v = \frac{1}{\sqrt{\mu_v \epsilon_v}} \tag{2-7}$$

The per-unit-length inductance and capacitance matrices $\underset{\sim}{L}$ and $\underset{\sim}{C}$, respectively, are given by [2]

$$\underset{\sim}{L} = \begin{bmatrix} \ell_G & \ell_m \\ \ell_m & \ell_R \end{bmatrix} \tag{2-8a}$$

$$\underset{\sim}{C} = \begin{bmatrix} (c_G + c_m) & -c_m \\ -c_m & (c_R + c_m) \end{bmatrix} \tag{2-9}$$

and

$$\underset{\sim}{1}_2 = \begin{bmatrix} 1 & 0 \\ 0 & 1 \end{bmatrix} \tag{2-9}$$

where the n x n identity matrix, denoted by $\underset{\sim}{1}_n$, has ones on the main diagonal and zeros elsewhere, i.e., $[\underset{\sim}{1}_n]_{ii} = 1$ and $[\underset{\sim}{1}_n]_{ij} = 0$ $i, j = 1, \ldots, n$ and $i \neq j$. The matrices $\underset{\sim}{L}$ and $\underset{\sim}{C}$ satisfy, for a homogeneous medium [2],

$$\underset{\sim}{L}\ \underset{\sim}{C} = \mu_v \epsilon_v \underset{\sim}{1}_2 = \frac{1}{v^2}\underset{\sim}{1}_2 \tag{2-10}$$

The entries in $\underset{\sim}{L}$ may be determined from the following general result for multiconductor transmission lines [1, 9]. Consider a pair of wires above a reference or ground plane shown in Fig. 2-4. From [1, 9], the entries in $\underset{\sim}{L}$ are given by

$$[\underset{\sim}{L}]_{ii} = \frac{\mu_v}{2\pi} \ell n \left(\frac{2h_i}{r_{wi}}\right)$$

$$[\underset{\sim}{L}]_{\substack{ij \\ i \neq j}} = \frac{\mu_v}{2\pi} \ell n \left(\frac{d_{ij}^*}{d_{ij}}\right) \tag{2-11b}$$

$$d_{ij}^* = \sqrt{(h_i + h_j)^2 + d_{ij}^2 - (h_i - h_j)^2} \tag{2-11c}$$

$$= \sqrt{d_{ij}^2 + 4h_i h_j}$$

For the single wire receptor configuration shown in Fig. 2-1(a), we obtain

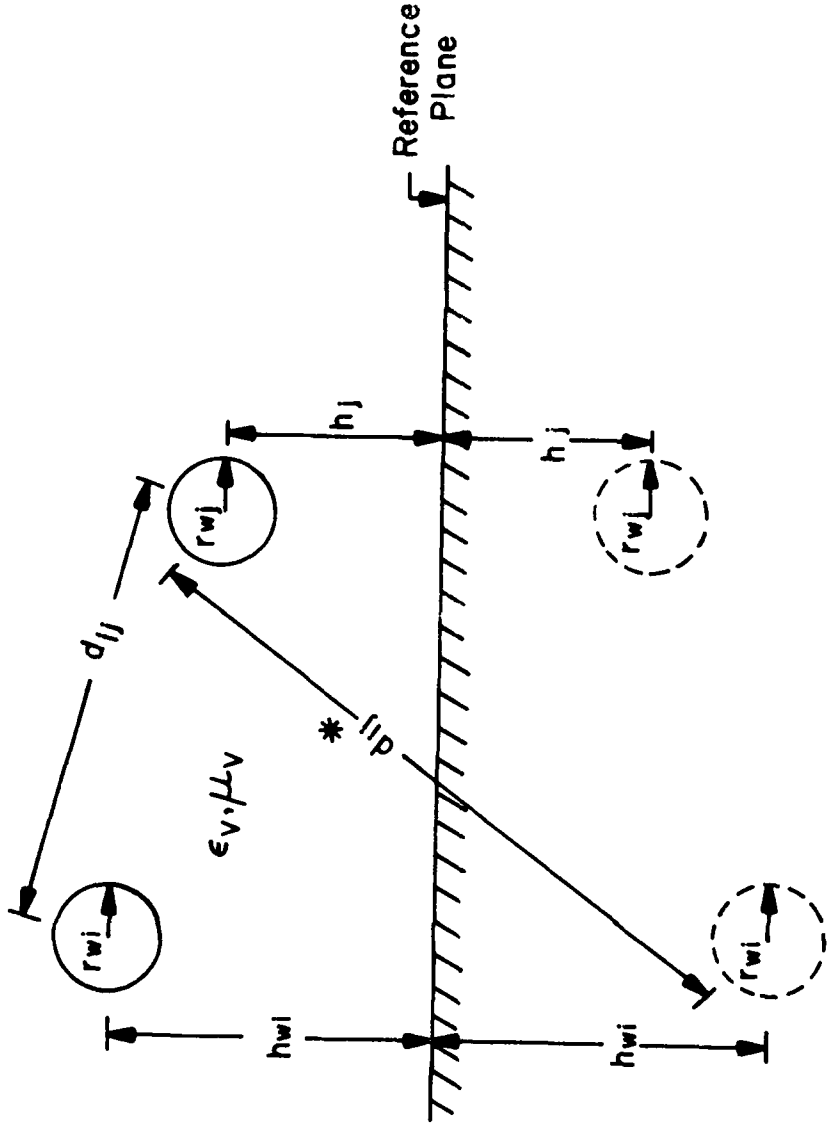
Reference Plane
h_j
h_j
r_{wj}
r_{wj}
d_{ij}
ϵ_v, μ_v
l_{ip}
r_{wi}
r_{wi}
h_{wi}
h_{wi}

Fig. 2-4

$$\ell_G = \frac{\mu_v}{2\pi} \ell n \left(\frac{2h_G}{r_{\omega G}}\right) \tag{2-12a}$$

$$\ell_R = \frac{\mu_v}{2\pi} \ell n \left(\frac{2h_R}{r_{\omega G}}\right) \tag{2-12b}$$

$$\ell_m = \frac{\mu_v}{2\pi} \ell n \left(\frac{\sqrt{d^2 + 4h_G h_R}}{d}\right) \tag{2-12c}$$

$$= \frac{\mu_v}{4\pi} \ell n \left(1 + \frac{4h_G h_R}{d^2}\right)$$

The capacitance matrix $\underset{\sim}{C}$ is determined from (2-10) where

$$\underset{\sim}{C} = \mu_v \epsilon_v \underset{\sim}{L}^{-1} \tag{2-13}$$

Once the overall transmission line matrix has been determined, the terminal conditions will be modeled and added. The terminating loads, voltages and currents are as shown in Fig. 2-5. From this diagram, the termination equations are found to be

$$V_G(0) = V_s - I_G(0) Z_{0G} \tag{2-14a}$$

$$V_R(0) = - I_R(0) Z_{0R} \tag{2-14b}$$

and

$$V_G(\mathcal{L}) = Z_{\mathcal{L}G} I_G(\mathcal{L}) \tag{2-15a}$$

$$V_R(\mathcal{L}) = Z_{\mathcal{L}R} I_R(\mathcal{L}) \tag{2-15b}$$

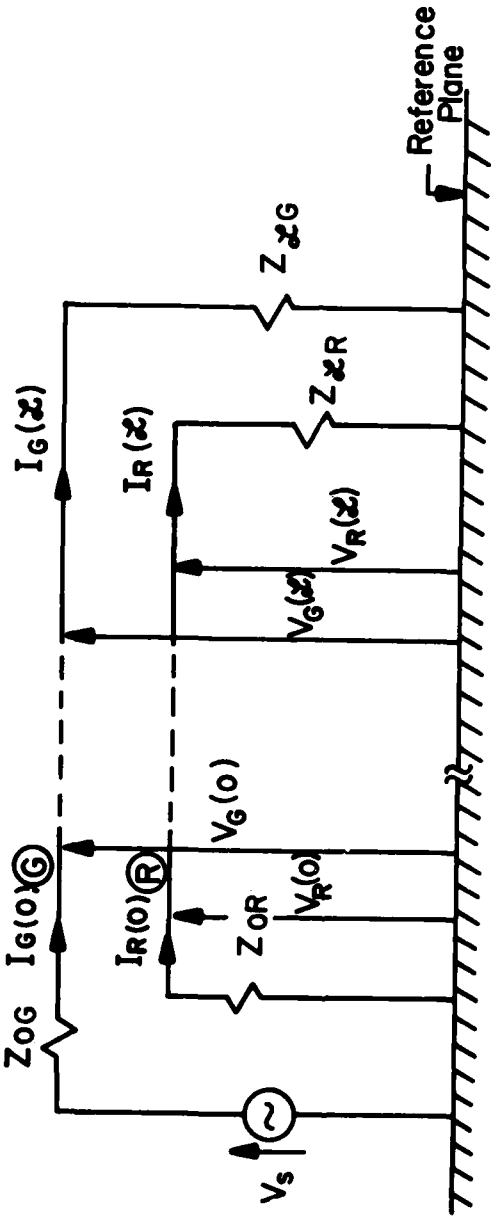
Reference Plane
$Z_{\ell G}$
$Z_{\ell R}$
$I_G(\ell)$
$I_R(\ell)$
$V_R(\ell)$
$V_G(\ell)$
$V_G(0)$
$V_R(0)$
Z_{OR}
$I_{R(0)}$
$I_{G(0)}$
Z_{OG}
V_S
G
R
0
ℓ

Fig. 2-5.

In matrix form, these becomme

$$\underline{V}(0) = \underline{V} - \underset{\sim}{Z}_0 \, \underline{I}(0) \tag{2-16}$$

and

$$\underline{V}(\mathcal{L}) = \underset{\sim}{Z}_{\mathcal{L}} \, \underline{I}(\mathcal{L}) \tag{2-17}$$

where

$$\underline{V}(0) = \begin{bmatrix} V_G(0) \\ V_R(0) \end{bmatrix} \qquad \underline{V}(\mathcal{L}) = \begin{bmatrix} V_G(\mathcal{L}) \\ V_R(\mathcal{L}) \end{bmatrix} \qquad \underline{V} = \begin{bmatrix} V_s \\ 0 \end{bmatrix}$$

$$\underline{I}(0) = \begin{bmatrix} I_G(0) \\ I_R(0) \end{bmatrix} \qquad \underline{I}(\mathcal{L}) = \begin{bmatrix} I_G(\mathcal{L}) \\ I_R(\mathcal{L}) \end{bmatrix} \tag{2-18}$$

$$\underset{\sim}{Z}_0 = \begin{bmatrix} Z_{0G} & 0 \\ 0 & Z_{0R} \end{bmatrix} \qquad \underset{\sim}{Z}_{\mathcal{L}} = \begin{bmatrix} Z_{\mathcal{L}G} & 0 \\ 0 & Z_{\mathcal{L}R} \end{bmatrix}$$

If the matrix equation (2-2) is expanded, one obtains the following,

$$\underline{V}(\mathcal{L}) = \underset{\sim}{\Phi}_{11}(\mathcal{L}) \, \underline{V}(0) + \underset{\sim}{\Phi}_{12}(\mathcal{L}) \underline{I}(0) \tag{2-19}$$

$$\underline{I}(\mathcal{L}) = \underset{\sim}{\Phi}_{21}(\mathcal{L}) \, \underline{V}(0) + \underset{\sim}{\Phi}_{22}(\mathcal{L}) \, \underline{I}(0) \tag{2-20}$$

By substituting (2-16) and (2-17) into (2-19) and (2-20), equations for the terminal currents of the line, $V_G(0)$, $V_G(\mathcal{L})$ and $V_R(0) \triangleq V_{0R}$, $V_R(\mathcal{L}) \triangleq V_{\mathcal{L}R}$, are obtained in terms of the input voltage V_s as

$$[\underset{\sim}{\Phi}_{11}(\mathcal{L})\underset{\sim}{Z}_0 - \underset{\sim}{\Phi}_{12}(\mathcal{L}) - \underset{\sim}{Z}_{\mathcal{L}}\underset{\sim}{\Phi}_{21}(\mathcal{L})\underset{\sim}{Z}_0 + \underset{\sim}{Z}_{\mathcal{L}}\underset{\sim}{\Phi}_{22}(\mathcal{L})]\underline{I}(0) = [\underset{\sim}{\Phi}_{11}(\mathcal{L}) - \underset{\sim}{Z}_{\mathcal{L}}\underset{\sim}{\Phi}_{21}(\mathcal{L})]\underline{V} \tag{2-21a}$$

$$\underline{I}(\mathcal{L}) = \underset{\sim}{\Phi}_{21}(\mathcal{L})\underline{V} + [\underset{\sim}{\Phi}_{22}(\mathcal{L}) - \underset{\sim}{\Phi}_{21}(\mathcal{L})\underset{\sim}{Z}_0]\underline{I}(0) \tag{2-21b}$$

The (two) simultaneous equations in (2-21a) are solved for the terminal currents at x = 0. The terminal currents at x = $\mathcal{L}$ are then found directly from (2-21b). The terminal voltages are then found from (2-16) and (2-17).

2.3 The Straight Wire Pair Receptor Model

The straight wire pair receptor model is derived in much the same way as the single wire receptor model. Referring to Fig. 2-1(b) and the assumptions made in Section 2-1, one can characterize an electrically short Δx section of the line with lumped, per-unit-length parameters of self inductance (ℓ_{GG}, ℓ_{11} and ℓ_{22}), mutual inductance (ℓ_{G1}, ℓ_{G2}, and ℓ_{12}), self capacitance (c_{GG}, c_{11} and c_{22}), and mutual capacitance (c_{G1}, c_{G2}, and c_{12}) as shown in Fig. 2-6.

In Fig. 2-1(b), one of the wires in the receptor circuit is designated as wire # 1 and the other is designated as wire # 2. This numbering is somewhat irrelevant since both receptor wires will be assumed to be identical. However, the numbering will become import-

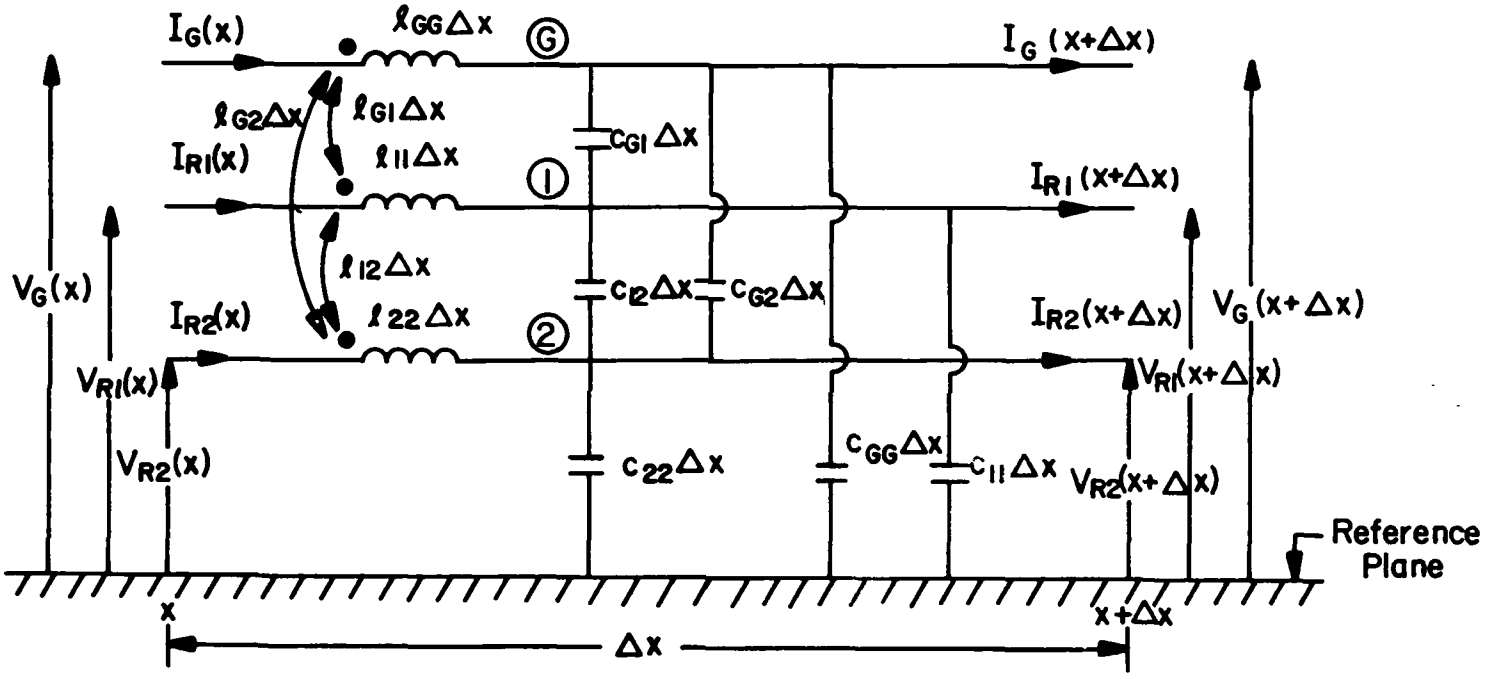
$I_G(x)$
$\ell_{GG}\Delta x$
G
$I_G(x+\Delta x)$
$\ell_{G2}\Delta x$
$\ell_{G1}\Delta x$
$C_{G1}\Delta x$
$I_{R1}(x)$
$\ell_{11}\Delta x$
1
$I_{R1}(x+\Delta x)$
$\ell_{12}\Delta x$
$C_{12}\Delta x$
$C_{G2}\Delta x$
$V_G(x)$
$I_{R2}(x)$
$\ell_{22}\Delta x$
2
$I_{R2}(x+\Delta x)$
$V_G(x+\Delta x)$
$V_{R1}(x)$
$V_{R1}(x+\Delta x)$
$V_{R2}(x)$
$C_{22}\Delta x$
$C_{GG}\Delta x$
$C_{11}\Delta x$
$V_{R2}(x+\Delta x)$
Reference Plane
x
$x+\Delta x$
Δx

Fig. 2-6.

ant in deriving the twisted pair model in Section 2-3 when the number of loops in a twisted pair is odd. The transmission line equations become, in the limit as $\Delta x \to 0$,

$$\frac{dV_G(x)}{dx} = -j\omega \ell_{GG} I_G(x) - j\omega \ell_{G1} I_{R1}(x) - j\omega \ell_{G2} I_{R2}(x) \qquad (2\text{-}22a)$$

$$\frac{dV_{R1}(x)}{dx} = -j\omega \ell_{G1} I_G(x) - j\omega \ell_{11} I_{R1}(x) - j\omega \ell_{12} I_{R2}(x) \qquad (2\text{-}22b)$$

$$\frac{dV_{R2}(x)}{dx} = -j\omega \ell_{G2} I_G(x) - j\omega \ell_{12} I_{R1}(x) - j\omega \ell_{22} I_{R2}(x) \qquad (2\text{-}22c)$$

$$\frac{dI_G(x)}{dx} = -j\omega (c_{GG} + c_{G1} + c_{G2}) V_G(x) + j\omega c_{G1} V_{R1}(x) + j\omega c_{G2} V_{R2}(x) \qquad (2\text{-}22d)$$

$$\frac{dI_{R1}(x)}{dx} = j\omega c_{G1} V_G(x) - j\omega (c_{11} + c_{G1} + c_{12}) V_{R1}(x) + j\omega c_{12} V_{R2}(x) \qquad (2\text{-}22e)$$

$$\frac{dI_{R2}(x)}{dx} = j\omega c_{G2} V_G(x) + j\omega c_{12} V_{R1}(x) - j\omega (c_{22} + c_{G2} + c_{12}) V_{R2}(x) \qquad (2\text{-}22f)$$

By relating the voltages and currents at one end of the line ($x = \ell$), $V_G(\ell)$, $V_{R1}(\ell)$, $V_{R2}(\ell)$, $I_G(\ell)$, $I_{R1}(\ell)$, and $I_{R2}(\ell)$, to the voltages and currents at the other end of the line ($x = 0$), $V_G(0)$, $V_{R1}(0)$, $V_{R2}(0)$, $I_G(0)$, $I_{R1}(0)$, and $I_{R2}(0)$, a solution to these transmission line equations is again provided by the matrix chain parameters shown in (2-2) where,

$$\underline{V}(\ell) = \begin{bmatrix} V_G(\ell) \\ V_{R1}(\ell) \\ V_{R2}(\ell) \end{bmatrix} \qquad \underline{V}(0) = \begin{bmatrix} V_G(0) \\ V_{R1}(0) \\ V_{R2}(0) \end{bmatrix}$$

$$\underline{I}(\ell) = \begin{bmatrix} I_G(\ell) \\ I_{R1}(\ell) \\ I_{R2}(\ell) \end{bmatrix} \qquad \underline{I}(0) = \begin{bmatrix} I_G(0) \\ I_{R1}(0) \\ I_{R2}(0) \end{bmatrix} \tag{2-23}$$

This overall chain parameter matrix, $\underset{\sim}{\Phi}(\ell)$, of the line relates these terminal voltages and currents as

$$\begin{bmatrix} \underline{V}(\ell) \\ \underline{I}(\ell) \end{bmatrix} = \begin{bmatrix} \underset{\sim}{\Phi}_{11}(\ell) & \underset{\sim}{\Phi}_{12}(\ell) \\ \underset{\sim}{\Phi}_{21}(\ell) & \underset{\sim}{\Phi}_{22}(\ell) \end{bmatrix} \begin{bmatrix} \underline{V}(0) \\ \underline{I}(0) \end{bmatrix} \tag{2-24}$$

where $\underset{\sim}{\Phi}_{ij}$ are now 3×3 matrices given by [1]

$$\underset{\sim}{\Phi}_{11}(\mathcal{L}) = \cos(\beta\mathcal{L})\,\underset{\sim}{1}_3 \tag{2-25a}$$

$$\underset{\sim}{\Phi}_{12}(\mathcal{L}) = -j\,v\sin(\beta\mathcal{L})\,\underset{\sim}{L} \tag{2-25b}$$

$$\underset{\sim}{\Phi}_{21}(\mathcal{L}) = -j\,v\sin(\beta\mathcal{L})\,\underset{\sim}{C} \tag{2-25c}$$

$$\underset{\sim}{\Phi}_{22}(\mathcal{L}) = \cos(\beta\mathcal{L})\,\underset{\sim}{1}_3 \tag{2-25d}$$

The 3 x 3 per-unit-length inductance and capacitance matrices, $\underset{\sim}{L}$ and $\underset{\sim}{C}$, respectively, are given by

$$\underset{\sim}{L} = \begin{bmatrix} \ell_{GG} & \ell_{G1} & \ell_{G2} \\ \ell_{G1} & \ell_{11} & \ell_{12} \\ \ell_{G2} & \ell_{12} & \ell_{22} \end{bmatrix} \tag{2-26a}$$

$$\underset{\sim}{C} = \begin{bmatrix} (c_{GG} + c_{G1} + c_{G2}) & -c_{G1} & -c_{G2} \\ -c_{G1} & (c_{11} + c_{G1} + c_{12}) & -c_{12} \\ -c_{G2} & -c_{12} & (c_{22} + c_{G2} + c_{12}) \end{bmatrix} \tag{2-26b}$$

Again, because of the assumption of a homogeneous surrounding medium (free space), $\underset{\sim}{C}$ is found from $\underset{\sim}{L}$ via (2-13). The entries in $\underset{\sim}{L}$ are found from the general result in (2-11) and Fig. 2-1(b) as

$$\ell_{GG} = \frac{\mu_v}{2\pi} \ell n \left(\frac{2h_G}{r_{wG}}\right) \qquad (2\text{-}27a)$$

$$\ell_{11} = \frac{\mu_v}{2\pi} \ell n \left(\frac{2(h_R + \Delta h)}{r_{wR}}\right) \qquad (2\text{-}27b)$$

$$\ell_{22} = \frac{\mu_v}{2\pi} \ell n \left(\frac{2(h_R - \Delta h)}{r_{wR}}\right) \qquad (2\text{-}27c)$$

$$\ell_{G1} = \frac{\mu_v}{4\pi} \ell n \left(1 + \frac{4h_G(h_R + \Delta h)}{(d^2 + (h_R + \Delta h_R - h_G)^2)}\right) \qquad (2\text{-}27d)$$

$$\ell_{G2} = \frac{\mu_v}{4\pi} \ell n \left(1 + \frac{4h_G(h_R - \Delta h)}{(d^2 + (h_R - \Delta h_R - h_G)^2)}\right) \qquad (2\text{-}27e)$$

$$\ell_{12} = \frac{\mu_v}{4\pi} \ell n \left(1 + \frac{4(h_R + \Delta h)(h_R - \Delta h)}{4(\Delta h)^2}\right) \qquad (2\text{-}27f)$$

$$= \frac{\mu_v}{4\pi} \ell n \left(\frac{h_R}{\Delta h}\right)$$

In deriving (2-27), we have assumed that receptor wire # 1 lies directly above receptor wire # 2. It is, of course, possible to derive the equations for the case in which the two wires lie side by side. In an actual cable bundle, either of these situations is a possibility so we have arbitrarily presumed the first case.

The equations for the termination networks are obtained from Fig. 2-7 as

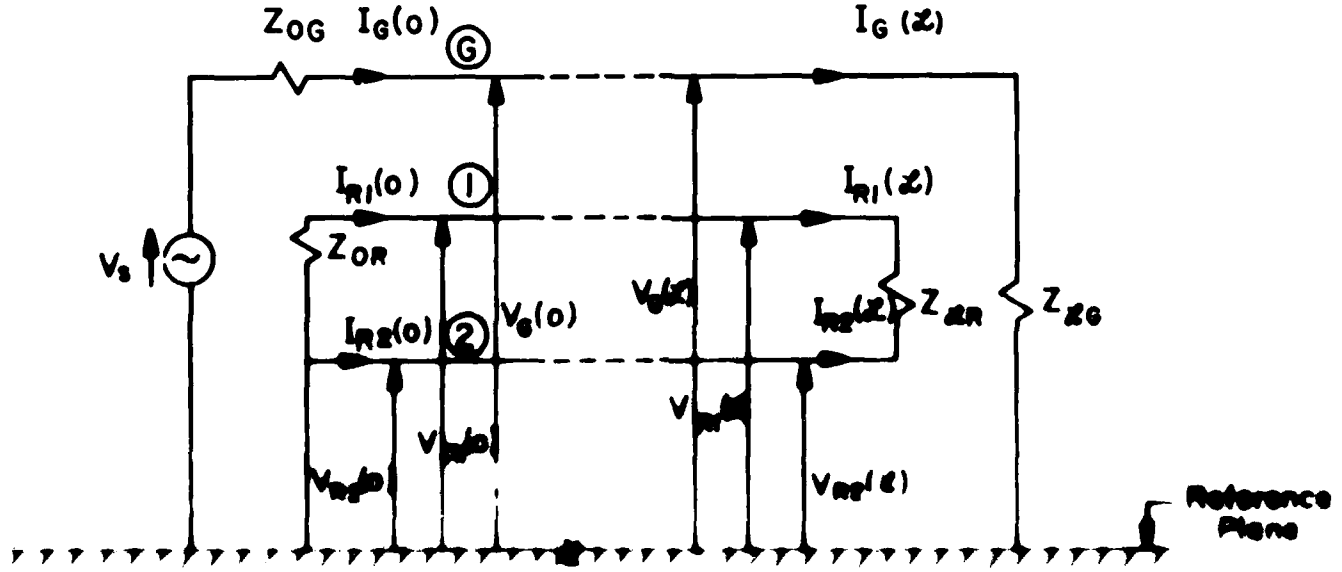
Z_{OG} $I_G(0)$
G
$I_G(\ell)$
$I_{R1}(0)$
1
$I_{R1}(\ell)$
V_s
Z_{OR}
$I_{R2}(0)$
2
$V_0(0)$
$V_0(\ell)$
$I_{R2}(\ell)$
Z_{2R}
Z_{2G}
$V_{R2}(0)$
$V_{R2}(\ell)$
Reference Plane

$$V_G(0) = V_s - Z_{0G}\, I_G(0) \tag{2-28a}$$

$$V_{R1}(0) = - Z_{0R}\, I_{R1}(0) \tag{2-28b}$$

$$V_{R2}(0) = 0 \tag{2-28c}$$

$$I_G(\mathcal{L}) = \left(\frac{1}{Z_{\mathcal{L}G}}\right) V_G(\mathcal{L}) \tag{2-28d}$$

$$I_{R1}(\mathcal{L}) = \left(\frac{1}{Z_{\mathcal{L}R}}\right) (V_{R1}(\mathcal{L}) - V_{R2}(\mathcal{L})) \tag{2-28e}$$

$$I_{R2}(\mathcal{L}) = \left(\frac{1}{Z_{\mathcal{L}R}}\right) (V_{R2}(\mathcal{L}) - V_{R1}(\mathcal{L})) \tag{2-28f}$$

Writing equations (2-28) in matrix form gives

$$\underline{V}(0) = \underline{V} - \underset{\sim}{Z}_0\, \underline{I}(0) \tag{2-29a}$$

$$\underline{I}(\mathcal{L}) = \underset{\sim}{Y}_{\mathcal{L}}\, \underline{V}(\mathcal{L}) \tag{2-29b}$$

where

$$\underline{V}(0) = \begin{bmatrix} V_G(0) \\ V_{R1}(0) \\ V_{R2}(0) \end{bmatrix} \qquad \underline{V}(\mathcal{L}) = \begin{bmatrix} V_G(\mathcal{L}) \\ V_{R1}(\mathcal{L}) \\ V_{R2}(\mathcal{L}) \end{bmatrix} \qquad \underline{V} = \begin{bmatrix} V_s \\ 0 \\ 0 \end{bmatrix}$$

$$\underline{I}(0) = \begin{bmatrix} I_G(0) \\ I_{R1}(0) \\ I_{R2}(0) \end{bmatrix} \qquad \underline{I}(\ell) = \begin{bmatrix} I_G(\ell) \\ I_{R1}(\ell) \\ I_{R2}(\ell) \end{bmatrix} \tag{2-30}$$

$$\underset{\sim}{Z}_0 = \begin{bmatrix} Z_{0G} & 0 & 0 \\ 0 & Z_{0R} & 0 \\ 0 & 0 & 0 \end{bmatrix} \qquad \underset{\sim}{Y}_\ell = \begin{bmatrix} \left(\frac{1}{Z_{\ell G}}\right) & 0 & 0 \\ 0 & \left(\frac{1}{Z_{\ell R}}\right) & -\left(\frac{1}{Z_{\ell R}}\right) \\ 0 & -\left(\frac{1}{Z_{\ell R}}\right) & \left(\frac{1}{Z_{\ell R}}\right) \end{bmatrix}$$

Substituting (2-29) into (2-24) yields equations similar to (2-21);

$$[\underset{\sim}{Y}_\ell \underset{\sim}{\Phi}_{11}(\ell) \underset{\sim}{Z}_0 - \underset{\sim}{Y}_\ell \underset{\sim}{\Phi}_{12}(\ell) - \underset{\sim}{\Phi}_{21}(\ell) \underset{\sim}{Z}_0 + \underset{\sim}{\Phi}_{22}(\ell)]\, \underline{I}(0) =$$

$$[\underset{\sim}{Y}_\ell \underset{\sim}{\Phi}_{11}(\ell) - \underset{\sim}{\Phi}_{21}(\ell)]\, \underline{V} \tag{2-31a}$$

$$\underline{I}(\ell) = \underset{\sim}{\Phi}_{21}(\ell)\, \underline{V} + [\underset{\sim}{\Phi}_{22}(\ell) - \underset{\sim}{\Phi}_{21}(\ell) \underset{\sim}{Z}_0]\, \underline{I}(0) \tag{2-31b}$$

The (three) simultaneous equations in (2-31a) are then solved for the terminal currents at $x = 0$. The terminal currents at $x = \ell$ are then found directly from (2-31b).

2.4 The Twisted Wire Pair Receptor Model

The model of the twisted wire pair receptor is somewhat similar to that of the straight wire pair receptor. The line is modeled as a

cascade of loops. Each loop consists of a uniform section of parallel wires of length ℓ_s and nonuniform wire interchange sections or twists at each end of the uniform sections as shown in Fig. 2-8. The chain parameter matrix for the uniform sections of each of these loops $\underset{\sim}{\Phi}_s(\ell_s)$, can be easily found and is of the same form as the chain parameter matrix for the straight wire pair in (2-24) and (2-25) with ℓ in (2-25) replaced by ℓ_s.

We have assumed that both wires in the twisted receptor pair are identical. This is a reasonable assumption and is the usual practice since in a twisted pair, both of the wires are presumed to carry the same current. Clearly the dependence of each section's chain parameter matrix on the cross-sectional dimensions of the line resides solely in the per-unit-length inductance matrix whose entries are given in (2-11). Therefore, with the important assumption that the wires in the twisted pair are identical, the per-unit-length inductance and capacitance matrices for each uniform section of length ℓ_s will be identical even though wires # 1 and # 2 alternate cross sectional line positions.

The problems of modeling the "abruptly" nonuniform portion or twist still remains. This can, however, be represented quite simply if the twist is considered to take place over a zero interval of distance. Referring to Fig. 2-9 it can be seen that the physical significance of

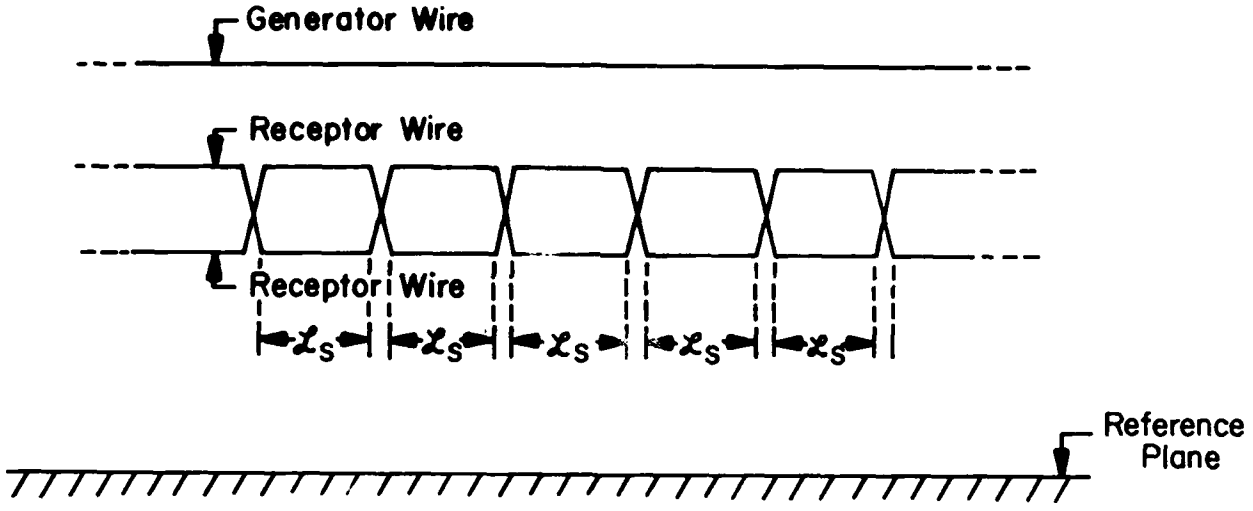
Generator Wire
Receptor Wire
Receptor Wire
$\mathcal{L}_s$
$\mathcal{L}_s$
$\mathcal{L}_s$
$\mathcal{L}_s$
$\mathcal{L}_s$
Reference Plane

Fig. 2-8.

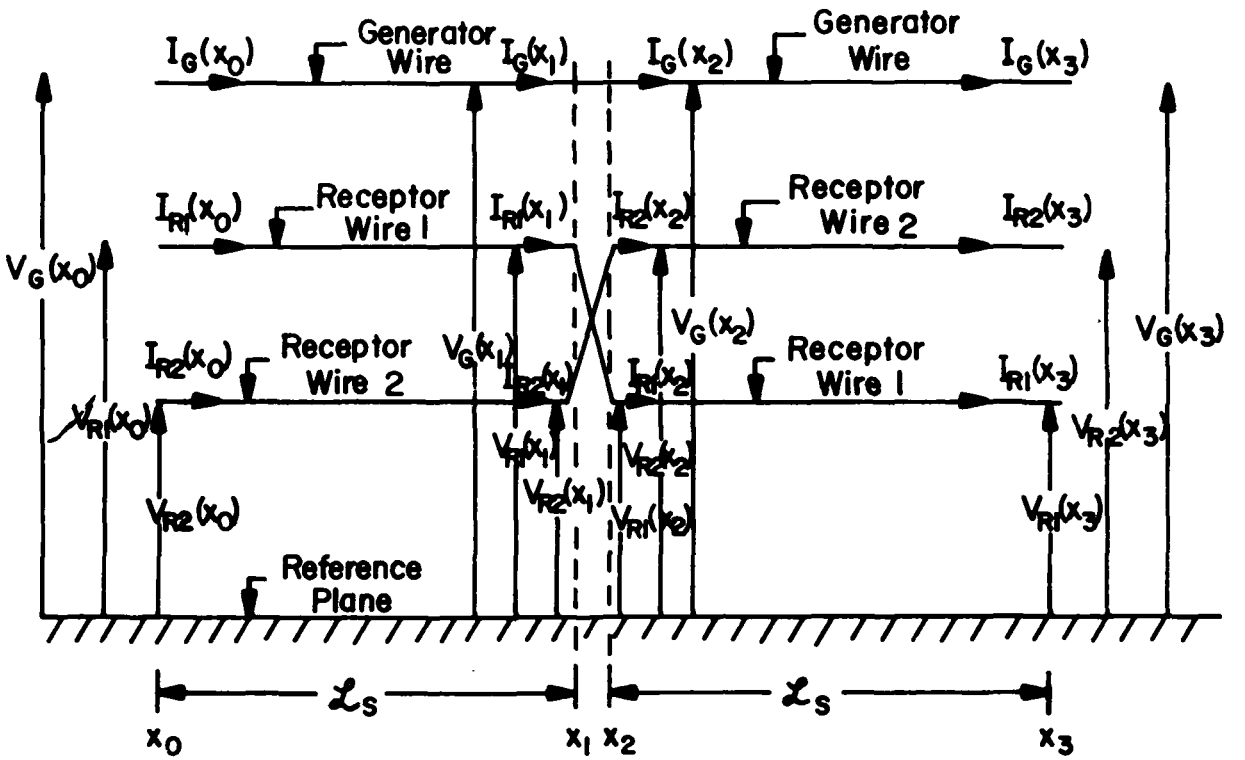
$I_G(x_0)$
Generator Wire
$I_G(x_1)$
$I_G(x_2)$
Generator Wire
$I_G(x_3)$
$I_{R1}(x_0)$
Receptor Wire 1
$I_{R1}(x_1)$
$I_{R2}(x_2)$
Receptor Wire 2
$I_{R2}(x_3)$
$V_G(x_0)$
$V_G(x_1)$
$V_G(x_2)$
$V_G(x_3)$
$I_{R2}(x_0)$
Receptor Wire 2
$I_{R2}(x_1)$
$I_{R1}(x_2)$
Receptor Wire 1
$I_{R1}(x_3)$
$V_{R1}(x_0)$
$V_{R1}(x_1)$
$V_{R2}(x_2)$
$V_{R2}(x_3)$
$V_{R2}(x_0)$
$V_{R2}(x_1)$
$V_{R1}(x_2)$
$V_{R1}(x_3)$
Reference Plane
$\mathcal{L}_s$
$\mathcal{L}_s$
x_0
x_1 x_2
x_3

Fig. 2-9.

the twist is to reverse the position of the receptor wires # 1 and # 2. From Fig. 2-9 the following two equations can be written,

$$\begin{bmatrix} V_G(x_1) \\ V_{R1}(x_1) \\ V_{R2}(x_1) \\ I_G(x_1) \\ I_{R1}(x_1) \\ I_{R2}(x_1) \end{bmatrix} = \underset{\sim}{\Phi}_s(\ell_s) \begin{bmatrix} V_G(x_0) \\ V_{R1}(x_0) \\ V_{R2}(x_0) \\ I_G(x_0) \\ I_{R1}(x_0) \\ I_{R2}(x_0) \end{bmatrix} \tag{2-32}$$

and

$$\begin{bmatrix} V_G(x_3) \\ V_{R2}(x_3) \\ V_{R1}(x_3) \\ I_G(x_3) \\ I_{R2}(x_3) \\ I_{R1}(x_3) \end{bmatrix} = \underset{\sim}{\Phi}_s(\ell_s) \begin{bmatrix} V_G(x_2) \\ V_{R2}(x_2) \\ V_{R1}(x_2) \\ I_G(x_2) \\ I_{R2}(x_2) \\ I_{R1}(x_2) \end{bmatrix} \tag{2-33}$$

where $\underset{\sim}{\Phi}_s(\ell_s)$ is the chain parameter matrix formed over the uniform section of the loop of length ℓ_s. The chain parameter matrices in (2-32) and (2-33) are identical since we assume that the wires in the twisted pair are identical.

Note in Fig. 2-9 that if, as assumed, the twist takes place over a zero distance, then,

$$
\begin{aligned}
x_1 &= x_2 \\
I_G(x_2) &= I_G(x_1) \\
I_{R1}(x_2) &= I_{R1}(x_1) \\
I_{R2}(x_2) &= I_{R2}(x_1) \\
V_G(x_2) &= V_G(x_1) \\
V_{R1}(x_2) &= V_{R1}(x_1) \\
V_{R2}(x_2) &= V_{R2}(x_1)
\end{aligned}
\tag{2-34}
$$

Equation (2-34) can be written in matrix form as

$$
\begin{bmatrix} V_G(x_2) \\ V_{R2}(x_2) \\ V_{R1}(x_2) \\ I_G(x_2) \\ I_{R2}(x_2) \\ I_{R1}(x_2) \end{bmatrix} = \underset{\sim}{P} \begin{bmatrix} V_G(x_1) \\ V_{R1}(x_1) \\ V_{R2}(x_1) \\ I_G(x_1) \\ I_{R1}(x_1) \\ I_{R2}(x_1) \end{bmatrix} \tag{2-35}
$$

Note the ordering of the voltage and current variables in the two vectors in (2-35). $\underset{\sim}{P}$ is a 6x6 permutation matrix given by

$$
\underset{\sim}{P} = \begin{bmatrix} \hat{\underset{\sim}{P}} & {}_3\underset{\sim}{0}_3 \\ {}_3\underset{\sim}{0}_3 & \hat{\underset{\sim}{P}} \end{bmatrix} \tag{2-36}
$$

where $\hat{\underset{\sim}{P}}$ is given by

$$
\hat{\underset{\sim}{P}} = \begin{bmatrix} 1 & 0 & 0 \\ 0 & 0 & 1 \\ 0 & 1 & 0 \end{bmatrix} \tag{2-37}
$$

and $\underset{n}{0}\underset{\sim}{}\underset{m}{}$ is an nxm zero matrix with $[\underset{n}{0}\underset{\sim}{}\underset{m}{}]_{ij} = 0$ for i = 1, ... n, and j = 1, ..., m. Combining (2-32), (2-33) and (2-35), the matrix product $\underset{\sim}{\Phi}_s \underset{\sim}{P} \underset{\sim}{\Phi}_s$ relates the voltages and currents at x_3 to those at x_0 as

$$\begin{bmatrix} V_G(x_3) \\ V_{R2}(x_3) \\ V_{R1}(x_3) \\ I_G(x_3) \\ I_{R2}(x_3) \\ I_{R1}(x_3) \end{bmatrix} = \underset{\sim}{\Phi}_s \underset{\sim}{P} \underset{\sim}{\Phi}_s \begin{bmatrix} V_G(x_0) \\ V_{R1}(x_0) \\ V_{R2}(x_0) \\ I_G(x_0) \\ I_{R1}(x_0) \\ I_{R2}(x_0) \end{bmatrix} \tag{2-38}$$

Note that the voltage and current variables in the two vectors in (2-38) are not in the same order. This is because the number of sections modeled in Fig. 2-9 is even. To arrange the voltage and current variables in both vectors in the natural order as in (2-23) we introduce an additional interchange section or twist at $x = x_3$ as shown in Fig. 2-10. The twist length $x_4 - x_3$ is again zero. This results in

$$\begin{bmatrix} V_G(x_4) \\ V_{R1}(x_4) \\ V_{R2}(x_4) \\ I_G(x_4) \\ I_{R1}(x_4) \\ I_{R2}(x_4) \end{bmatrix} = \underset{\sim}{P} \underset{\sim}{\Phi}_s \underset{\sim}{P} \underset{\sim}{\Phi}_s \begin{bmatrix} V_G(x_0) \\ V_{R1}(x_0) \\ V_{R2}(x_0) \\ I_G(x_0) \\ I_{R1}(x_0) \\ I_{R2}(x_0) \end{bmatrix} \tag{2-39}$$

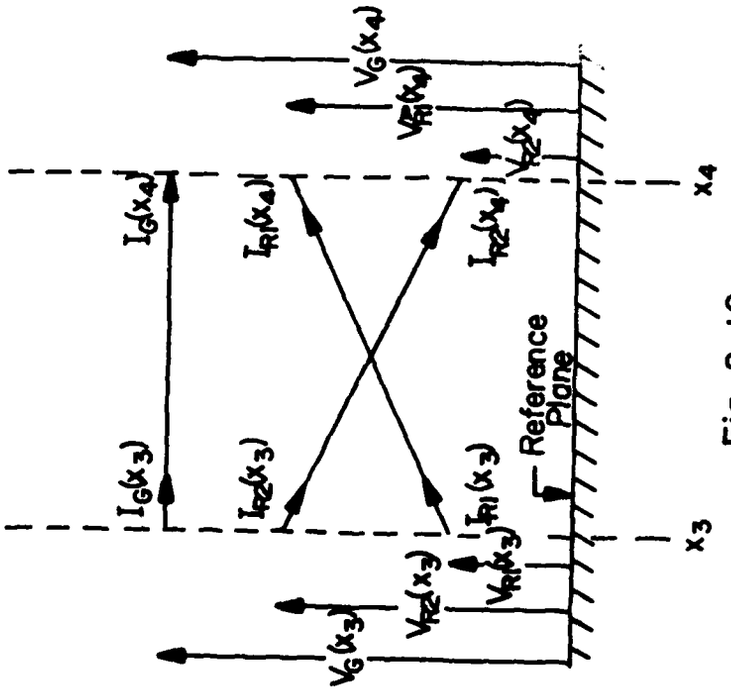
$V_G(x_4)$
$V_{R1}(x_4)$
$V_{R2}(x_4)$
$I_G(x_4)$
$I_{R1}(x_4)$
$I_{R2}(x_4)$
x_4
Reference Plane
$I_G(x_3)$
$I_{R2}(x_3)$
$I_{R1}(x_3)$
$V_{R2}(x_3)$
$V_{R1}(x_3)$
$V_G(x_3)$
x_3

Fig. 2-10.

and the voltage and current variables in both vectors are in the same order.

The additional twist added from x_3 to x_4 clearly does not affect the line behavior and is only used to properly sequence the voltage and current variables in the chain parameter matrix relation for a pair of adjacent sections. Therefore, the overall TL matrix for the line consisting of N loops can be modeled as a cascade of matrices $\underset{\sim}{\Phi}_s$ and $\underset{\sim}{P}$ as shown in Fig. 2-11.

It is interesting to note at this point that the overall transmission line chain parameter matrix, $\underset{\sim}{\Phi}_T$, for the entire length of the line can be written in a compact form in terms of $\underset{\sim}{\Phi}_s$ and $\underset{\sim}{P}$. The equations will depend on whether there is an even or odd number of loops. For an odd number of loops (See Fig. 2-12a) the overall chain parameter matrix is given by

$$\begin{bmatrix} V_G(\ell) \\ V_{R1}(\ell) \\ V_{R2}(\ell) \\ I_G(\ell) \\ I_{R1}(\ell) \\ I_{R2}(\ell) \end{bmatrix} = \underbrace{[\underset{\sim}{\Phi}_s \underset{\sim}{P}\, \underset{\sim}{\Phi}_s \underset{\sim}{P} \cdots \underset{\sim}{\Phi}_s \underset{\sim}{P}\, \underset{\sim}{\Phi}_s]}_{\underset{\sim}{\Phi}_T} \begin{bmatrix} V_G(0) \\ V_{R1}(0) \\ V_{R2}(0) \\ I_G(0) \\ I_{R1}(0) \\ I_{R2}(0) \end{bmatrix} \quad (2\text{-}40)$$

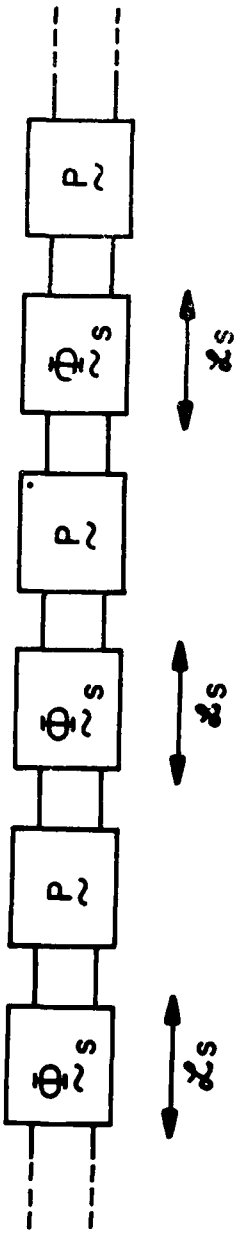

Fig. 2-11.

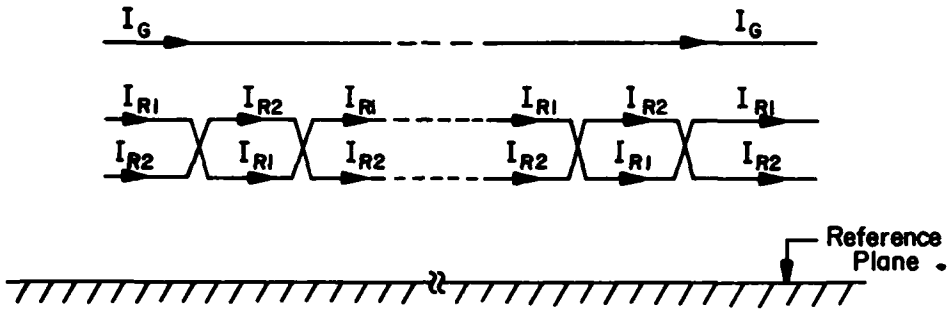
I_G
I_G
I_{R1} I_{R2} I_{R1} I_{R1} I_{R2} I_{R1}
I_{R2} I_{R1} I_{R2} I_{R2} I_{R1} I_{R2}
Reference Plane

(a)

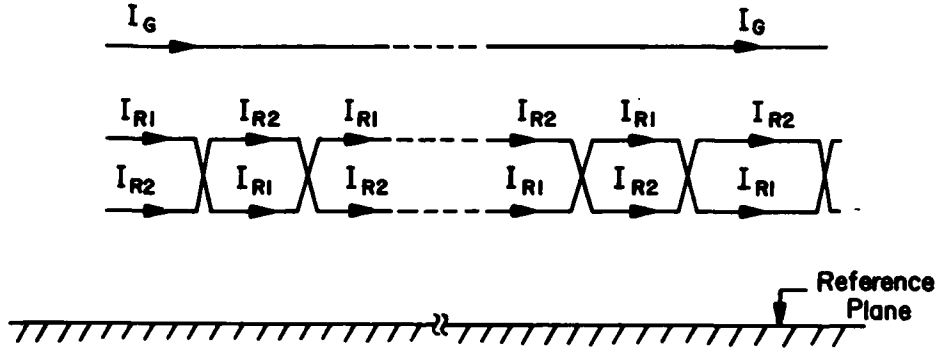
I_G
I_G
I_{R1} I_{R2} I_{R1} I_{R2} I_{R1} I_{R2}
I_{R2} I_{R1} I_{R2} I_{R1} I_{R2} I_{R1}
Reference Plane

(b)

Fig. 2-12.

Note that in (2-40) the $\underset{\sim}{\Phi}_T$ matrix product begins and ends with $\underset{\sim}{\Phi}_s$ and the voltages and currents in the left-hand side vector of the equation are in the same sequence as in the right-hand side vector. Thus no additional interchange matrix is required. However, for an even number of sections (See Fig. 2-12b), we have

$$\begin{bmatrix} V_G(\ell) \\ V_{R1}(\ell) \\ V_{R2}(\ell) \\ I_G(\ell) \\ V_{R1}(\ell) \\ V_{R2}(\ell) \end{bmatrix} = \underbrace{[\underset{\sim}{P}\,\underset{\sim}{\Phi}_s\,\underset{\sim}{P}\,\underset{\sim}{\Phi}_s \cdots \underset{\sim}{P}\,\underset{\sim}{\Phi}_s]}_{\underset{\sim}{\Phi}_T} \begin{bmatrix} V_G(0) \\ V_{R1}(0) \\ V_{R2}(0) \\ I_G(0) \\ I_{R1}(0) \\ I_{R2}(0) \end{bmatrix} \qquad (2\text{-}41)$$

Note that the proper sequence of entries in the vectors on the left and right sides of (2-41) are obtained by adding a $\underset{\sim}{P}$ matrix at the end of the TL cascade of chain parameter matrices. This does not change the values of voltages or currents in the equations since it ideally takes place over a zero interval of distance and only serves to properly sequence the voltages and currents on both sides of (2-41). It is now apparent from (2-40) and (2-41) that the overall chain parameter matrix of the entire line, $\underset{\sim}{\Phi}_T$, can be written as

$$\underset{\sim}{\Phi}_T = \underset{\sim}{\Phi}_s \left(\underset{\sim}{P}\,\underset{\sim}{\Phi}_s\right)^{N-1} \qquad \begin{matrix} \text{for odd \# of loops} \\ (N \text{ odd}) \end{matrix} \qquad (2\text{-}42a)$$

and

$$\underset{\sim}{\Phi}_T = (\underset{\sim}{P}\,\underset{\sim}{\Phi}_s)^N \qquad \text{for even } N$$
$$(N \text{ odd})$$

where N is the number of loops.

The terminal network equations for the twisted ... the same as those for the straight wire pair case wh ... (2-29) and (2-30) and illustrated in Fig. 2-7. Sinc ... careful to sequence the voltages and current varia ... sponding voltage vectors, $\underline{V}(\ell)$ and $\underline{V}(0)$, and corres... vectors, $\underline{I}(\ell)$ and $\underline{I}(0)$, the overall matrix chain para... for the line given by

$$\begin{bmatrix} \underline{V}(\ell) \\ \underline{I}(\ell) \end{bmatrix} = \underset{\sim}{\Phi}_T \begin{bmatrix} \underline{V}(0) \\ \underline{I}(0) \end{bmatrix}$$

may be used directly with these terminal equations ... equations for the terminal currents given in (2-...

2.5 Special Considerations

Note that for the abruptly nonuniform mode ... two-... pair, one is required to find the overall chain parameter ... $\underset{\sim}{\Phi}_T$, of the entire line which is given as a product of the ...

$\underset{\sim}{P}$ and $\underset{\sim}{\Phi}_s$ in (2-42). Computationally, (2-42) requires that we find N products of 6x6 matrices. Computing $\underset{\sim}{P}\ \underset{\sim}{\Phi}_s$ is trivial since this requires only an interchange of certain rows of $\underset{\sim}{\Phi}_s$ (See (2-36) and (2-37). However, we must still compute N products of 6x6 matrices at each frequency. This can obviously be a time consuming operation, especially when the response of the line is desired at a large number of frequencies. One would prefer to obtain this product in some compact form without resorting to direct matrix multiplications. To determine whether this is possible, we examine the form of this matrix product. The equations for the overall chain parameter matrix in (2-42) become

$$\underset{\sim}{\Phi}_T = \underset{\sim}{\Phi}_s (\underset{\sim}{P}\ \underset{\sim}{\Phi}_s)^{N-1} \qquad \text{(N odd)} \qquad \text{(2-44a)}$$

$$= \underset{\sim}{\Phi}_s (\underbrace{\underset{\sim}{P}\ \underset{\sim}{\Phi}_s \underset{\sim}{P}\ \underset{\sim}{\Phi}_s \cdots \underset{\sim}{P}\ \underset{\sim}{\Phi}_s}_{N-1})$$

$$\underset{\sim}{\Phi}_T = (\underset{\sim}{P}\ \underset{\sim}{\Phi}_s)^{N} \qquad \text{(N even)}$$

$$= (\underbrace{\underset{\sim}{P}\ \underset{\sim}{\Phi}_s \underset{\sim}{P}\ \underset{\sim}{\Phi}_s \cdots \underset{\sim}{P}\ \underset{\sim}{\Phi}_s}_{N}) \qquad \text{(2-44b)}$$

Extensive examination of these products revealed no simplification. Therefore, the matrix products are obtained by direct computation in the computed results to be presented.

However, for certain wire configurations, the result is simplified considerably and no matrix products as in (2-44) need be obtained. Consider the special configurations shown in Fig. 2-13. In these two configurations, the receptor wires lie either above or below the generator wire and are symmetric with respect to a vertical line through the generator wire. For these two physical configurations, we observe that due to symmetry

$$\ell_{G1} = \ell_{G2} \tag{2-45a}$$

$$\ell_{11} = \ell_{22} \tag{2-45b}$$

Thus $\underset{\sim}{L}$ becomes

$$\underset{\sim}{L} = \begin{bmatrix} \ell_{GG} & \ell_{G1} & \ell_{G1} \\ \ell_{G1} & \ell_{11} & \ell_{12} \\ \ell_{G1} & \ell_{12} & \ell_{11} \end{bmatrix} \tag{2-46}$$

Clearly, because of symmetry, we also obtain

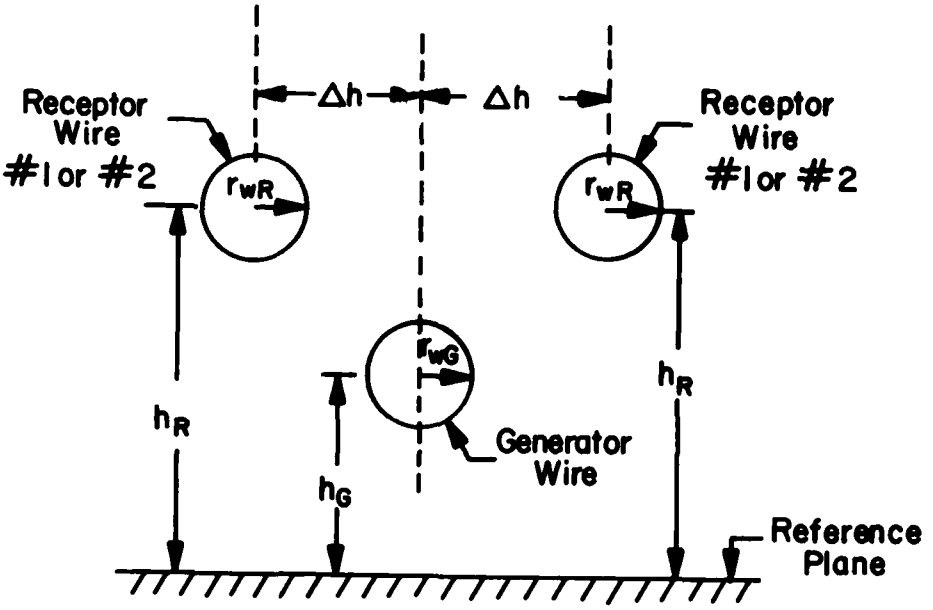
Receptor
Wire
#1 or #2
Δh
Δh
Receptor
Wire
#1 or #2
r_{wR}
r_{wR}
r_{wG}
h_R
h_G
h_R
Generator
Wire
Reference
Plane

(a)

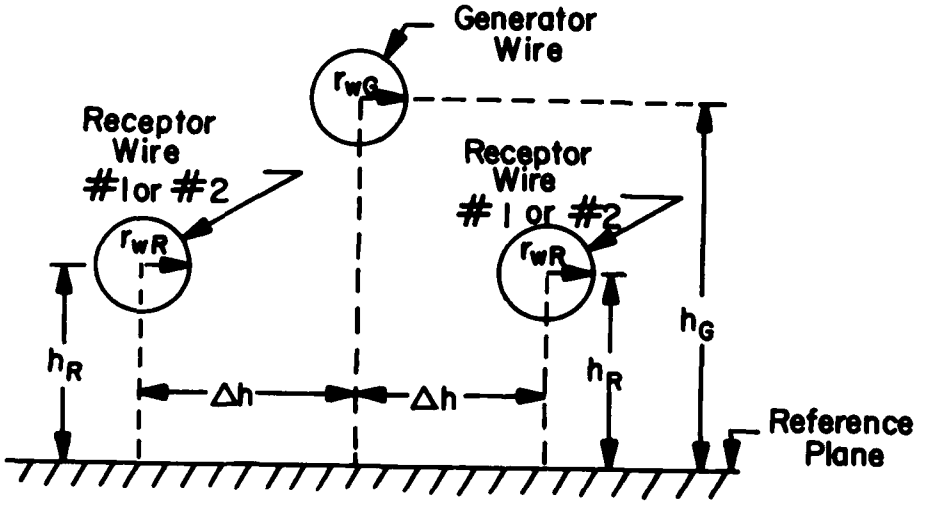
Generator
Wire
r_{wG}
Receptor
Wire
#1 or #2
Receptor
Wire
#1 or #2
r_{wR}
r_{wR}
h_R
h_R
h_G
Δh
Δh
Reference
Plane

(b)

Fig. 2-13.

$$c_{G1} = c_{G2} \tag{2-47a}$$

$$c_{11} = c_{22} \tag{2-47b}$$

and $\underset{\sim}{C}$ becomes

$$\underset{\sim}{C} = \begin{bmatrix} (c_{GG} + 2c_{G1}) & -c_{G1} & -c_{G1} \\ -c_{G1} & (c_{11} + c_{12} + c_{G1}) & -c_{12} \\ -c_{G1} & -c_{12} & (c_{11} + c_{12} + c_{G1}) \end{bmatrix} \tag{2-48}$$

$\underset{\sim}{C}$ has the same structure as $\underset{\sim}{L}$. Note that these relations, because of the assumed symmetry, hold even if the wires have dielectric insulations (the dielectric insulations of the receptor wires are logically assumed to be identical in type and thickness)! For this configuration, we can write the matrix product $\underset{\sim}{P}\,\underset{\sim}{\Phi}\,\underset{\sim}{P}$ as

$$\underset{\sim}{P}\underset{\sim}{\Phi}_s\underset{\sim}{P} = \begin{bmatrix} \hat{\underset{\sim}{P}} & \underset{3\sim 3}{0} \\ \underset{3\sim 3}{0} & \hat{\underset{\sim}{P}} \end{bmatrix} \begin{bmatrix} \cos(\beta \ell)\,\underset{\sim}{1}_3 & -jv\sin(\beta\ell)\,\underset{\sim}{L} \\ -jv\sin(\beta\ell_s)\,\underset{\sim}{C} & \cos(\beta\ell_s)\,\underset{\sim}{1}_3 \end{bmatrix} \begin{bmatrix} \hat{\underset{\sim}{P}} & \underset{3\sim 3}{0} \\ \underset{3\sim 3}{0} & \hat{\underset{\sim}{P}} \end{bmatrix} \tag{2-49}$$

$$= \begin{bmatrix} \hat{\underset{\sim}{P}} & \underset{3\sim 3}{0} \\ \underset{3\sim 3}{0} & \hat{\underset{\sim}{P}} \end{bmatrix} \begin{bmatrix} \cos(\beta\ell_s)\,\hat{\underset{\sim}{P}} & -jv\sin(\beta\ell_s)\,\underset{\sim}{L}\,\hat{\underset{\sim}{P}} \\ -jv\sin(\beta\ell_s)\,\underset{\sim}{C}\,\hat{\underset{\sim}{P}} & \cos(\beta\ell_s)\,\hat{\underset{\sim}{P}} \end{bmatrix}$$

$$= \begin{bmatrix} \cos(\beta \ell_s)\, \hat{\underset{\sim}{P}}\, \hat{\underset{\sim}{P}} & -jv\sin(\beta \ell_s)\, \hat{\underset{\sim}{P}}\, \underset{\sim}{L}\, \hat{\underset{\sim}{P}} \\ -jv\sin(\beta \ell_s)\, \hat{\underset{\sim}{P}}\, \underset{\sim}{C}\, \hat{\underset{\sim}{P}} & \cos(\beta \ell_s)\, \hat{\underset{\sim}{P}}\, \hat{\underset{\sim}{P}} \end{bmatrix}$$

But, note that

$$\hat{\underset{\sim}{P}}\, \hat{\underset{\sim}{P}} = \begin{bmatrix} 1 & 0 & 0 \\ 0 & 0 & 1 \\ 0 & 1 & 0 \end{bmatrix} \begin{bmatrix} 1 & 0 & 0 \\ 0 & 0 & 1 \\ 0 & 1 & 0 \end{bmatrix} = \begin{bmatrix} 1 & 0 & 0 \\ 0 & 1 & 0 \\ 0 & 0 & 1 \end{bmatrix} = \underset{\sim}{1}_3 \qquad (2\text{-}50)$$

Also by using the forms of $\underset{\sim}{L}$ and $\underset{\sim}{C}$ in (2-46) and (2-48) for this configuration, one will obtain the important result

$$\hat{\underset{\sim}{P}}\, \underset{\sim}{L}\, \hat{\underset{\sim}{P}} = \underset{\sim}{L} \qquad (2\text{-}51a)$$

$$\hat{\underset{\sim}{P}}\, \underset{\sim}{C}\, \hat{\underset{\sim}{P}} = \underset{\sim}{C} \qquad (2\text{-}51b)$$

Applying the results of (2-50) and (2-51) to (2-49) we obtain

$$\hat{\underset{\sim}{P}}\, \underset{\sim}{\Phi}_s\, \hat{\underset{\sim}{P}} = \begin{bmatrix} \cos(\beta \ell_s)\, \underset{\sim}{1}_3 & -jv\sin(\beta \ell_s)\, \underset{\sim}{L} \\ -jv\sin(\beta \ell_s)\, \underset{\sim}{C} & \cos(\beta \ell_s)\, \underset{\sim}{1}_3 \end{bmatrix} \qquad (2\text{-}52)$$

$$= \underset{\sim}{\Phi}_s$$

The matrix products in (2-44) for several values of N are

$$\underset{\sim}{\Phi}_T = \Phi_s \qquad N = 1$$

$$\underset{\sim}{\Phi}_T = \underset{\sim}{P}\,\underset{\sim}{\Phi}_s\,\underset{\sim}{P}\,\underset{\sim}{\Phi}_s \qquad N = 2$$

$$= (\underset{\sim}{P}\,\underset{\sim}{\Phi}_s\,\underset{\sim}{P})\,\underset{\sim}{\Phi}_s \tag{2-53}$$

$$\underset{\sim}{\Phi}_T = \underset{\sim}{\Phi}_s\underset{\sim}{P}\,\underset{\sim}{\Phi}_s\,\underset{\sim}{P}\,\underset{\sim}{\Phi}_s \qquad N = 3$$

$$= \underset{\sim}{\Phi}_s(\underset{\sim}{P}\,\underset{\sim}{\Phi}_s\,\underset{\sim}{P})\;\underset{\sim}{\Phi}_s$$

$$\underset{\sim}{\Phi}_T = \underset{\sim}{P}\,\underset{\sim}{\Phi}_s\underset{\sim}{P}\,\underset{\sim}{\Phi}_s\underset{\sim}{P}\,\underset{\sim}{\Phi}_s\underset{\sim}{P}\,\underset{\sim}{\Phi}_s \qquad N = 4$$

$$= (\underset{\sim}{P}\,\underset{\sim}{\Phi}_s\,\underset{\sim}{P})\,\underset{\sim}{\Phi}_s\,(\underset{\sim}{P}\,\underset{\sim}{\Phi}_s\underset{\sim}{P})\,\underset{\sim}{\Phi}_s$$

From this grouping, one immediately observes with the result in (2-52) that

$$\underset{\sim}{\Phi}_T = (\underset{\sim}{\Phi}_s)^N \tag{2-54}$$

Note, however, that this is simply the chain parameter matrix of the straight wire pair, i.e.,

$$\underset{\sim}{\Phi}_T = \underset{\sim}{\Phi}_s{}^N\,(\mathcal{L}_s) = \underset{\sim}{\Phi}(\mathcal{L}) \tag{2-55}$$

This astonishing result shows that for the special configurations in Fig. 2-13, the twisting of the receptor pair has absolutely no effect! Note that this result holds regardless of whether the receptor wires have insulation and is based solely on the symmetry of the physical configuration and the assumption that the two receptor wires are

identical.

In a practical situation in which the generator and receptor wires are immersed in a large, random cable bundle, one could argue that the physical configuration of the receptor wires in Fig. 2-13 probably does not occur. Therefore, it is important to examine other cases. Note that if one accepts the assumption that there is some other configuration in which the twisting of the receptor wires has some effect, namely reducing the coupling over that from the untwisted case (the straight wire receptor pair), then the configuration in Fig. 2-13 would represent an upper bound on the coupling for other configurations.

The physical configuration which was investigated experimentally is shown in Fig. 2-14. For this configuration, the center of the receptor pair is located at the same height above the reference plane as the generator wire. Observe that in a practical situation, the two receptor wires will have touching insulations (the receptor pair is simply twisted together). Thus Δh will be the sum of each wire radius and associated insulation thickness (See Fig. 1-1b). From a practical standpoint, Δh will be quite small. Thus one might make the following approximations:

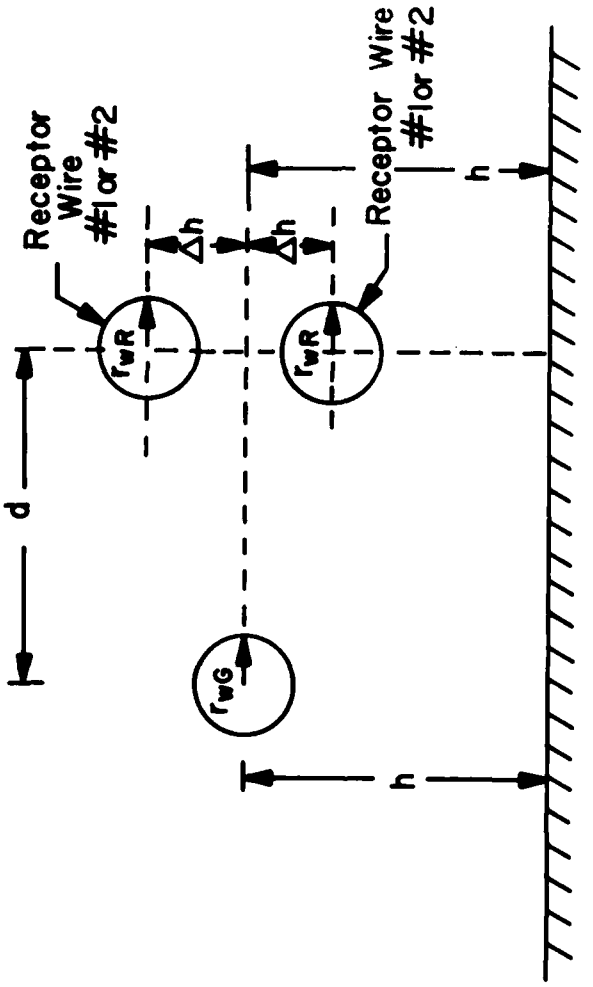

Fig. 2-14.

$$
\begin{aligned}
\ell_{G1} &\cong \ell_{G2} \\
\ell_{11} &\cong \ell_{22} \\
c_{G1} &\cong c_{G2} \\
c_{11} &\cong c_{22}
\end{aligned}
\qquad (2\text{-}56)
$$

Note that when these approximations are valid we obtain the same result as for the special symmetric configurations in Fig. 2-13; the twist has no effect! Clearly, the twist will have some effect over the straight wire pair since (2-56) are approximations. For (2-56) to be exact, we would need to require that the two receptor wire positions be identical; a physically impossible situation. We will find in Chapter III that for relatively "high" impedance loads that the twist has virtually no effect for the "side-by-side" configuration in Fig. 2-14. However, we will find that for very "low" impedance loads, the twist has a dramatic effect.

2.6 Other Excitation Configurations

We will also be interested in investigating the configurations in Fig. 2-15 in which the voltage excitation source, V_s, is located in the twisted pair circuit, for Fig. 2-15(c) and correspondingly located for Fig. 2-15(a) and (b). In these cases, the induced voltages, V_{0R} and

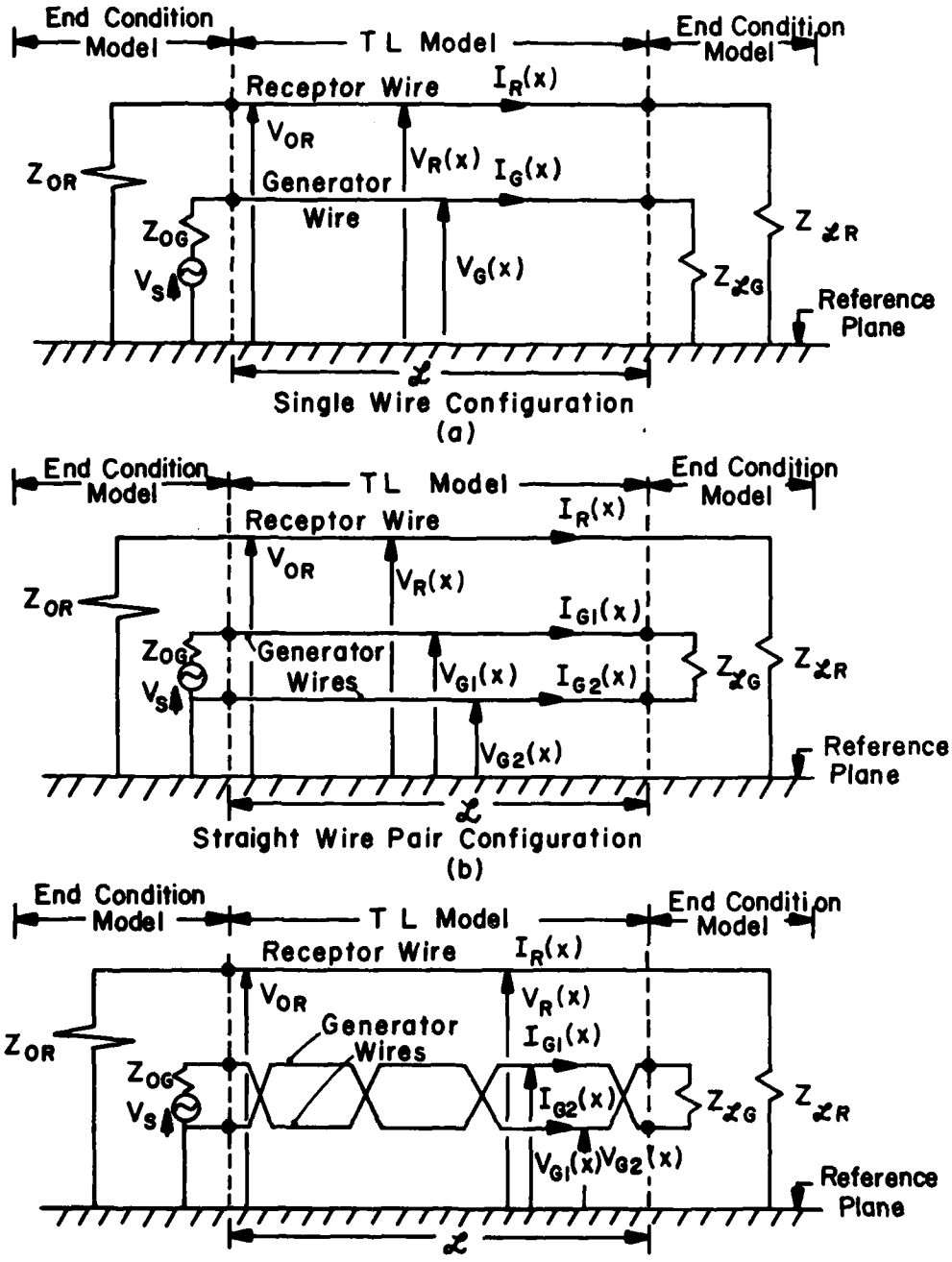
End Condition Model
T L Model
End Condition Model
Receptor Wire
$I_R(x)$
V_{OR}
$V_R(x)$
$I_G(x)$
Z_{OR}
Generator Wire
Z_{OG}
V_S
$V_G(x)$
$Z_{\ell R}$
$Z_{\ell G}$
Reference Plane
ℓ
Single Wire Configuration
(a)
End Condition Model
T L Model
End Condition Model
Receptor Wire
$I_R(x)$
V_{OR}
$V_R(x)$
$I_{G1}(x)$
Z_{OR}
Z_{OG}
Generator Wires
V_S
$V_{G1}(x)$
$I_{G2}(x)$
$Z_{\ell G}$
$Z_{\ell R}$
$V_{G2}(x)$
Reference Plane
ℓ
Straight Wire Pair Configuration
(b)
End Condition Model
T L Model
End Condition Model
Receptor Wire
$I_R(x)$
V_{OR}
$V_R(x)$
$I_{G1}(x)$
Z_{OR}
Generator Wires
Z_{OG}
V_S
$I_{G2}(x)$
$Z_{\ell G}$
$Z_{\ell R}$
$V_{G1}(x)V_{G2}(x)$
Reference Plane
ℓ
(c)
Twisted Wire Pair Configuration

Fig. 2-15

$V_{\ell R}$, are at the ends of the single wire which was the generator circuit in all previous cases.

The chain parameter models previously derived can be similarly obtained for these cases. Clearly the overall chain parameter matrix of the line for all these cases will be of the same form as for the circuits in Fig. 2-2. Note for Fig. 2-15, the wires (and consequently the line voltages and currents) have been relabeled. For example, the generator wire in Fig. 2-2(a) becomes the receptor wire in Fig. 2-15(a). Obviously one can write the chain parameter matrix entries and the equations for the terminal conditions for Fig. 2-15 in the same fashion as was done for the configurations in Fig. 2-2.

Computed and experimental results for the circuit configurations in Fig. 2-2 and Fig. 2-15 will be obtained in the following chapters.

III. EXPERIMENTAL RESULTS

3.1 General Discussion

This chapter deals with experimental verification of the models derived in Chapter II. Although the object of this work is to predict the coupling involving twisted wire pairs, a comparison of the effectiveness in reducing coupling between the twisted wire pair configuration, the single wire configuration, and the straight wire pair configuration will be made. In order to determine the accuracy of the straight wire pair and twisted wire pair models, the circuit configurations of Fig. 2-2(b) and Fig. 2-15(b) (the straight wire pair configuration) and Fig. 2-2(c) and Fig. 2-15(c) (the twisted wire pair configuration) will be examined experimentally. Experimental measurements for the single wire configuration of Fig. 2-2(a) and Fig. 2-15(a) will not be made since this particular model has previously been verified experimentally and was found to be sufficiently accurate [10, 11].

3.2 Experimental Procedure

The circuits in Fig. 2-2 and Fig. 2-15 were constructed of # 20 gauge solid copper wires with radii of 16 mils and having polyvinyl

chloride insulation 17 mils in thickness. The circuit lengths were 15' - 5$\frac{1}{4}$" (ℓ = 15' - 5$\frac{1}{4}$" in Fig. 2-2) and the circuits were mounted on a 2' by 15' - 11" aluminum ground plane 1/8" in thickness as shown in Fig. 3-1 and Fig. 3-2. The resistors which terminate the ends of the circuits were constructed by inserting small resistors into BNC connectors to facilitate their removal and replacement.

Two basic circuit separation configurations will be investigated for the twisted and straight wire pair configurations. Referring to Fig. 3-3, the circuit separation, d, will be 2 cm or .1451805 cm, the latter of which will be obtained when the insulations of the wires in both circuits are touching. These two circuit separations will be referred to as the 2 cm and Touching cases. The height, h, in Fig. 3-3 will be 2 cm in all experiments. This height was obtained by supporting the wires above the ground plane by small styrofoam blocks that had an average height of 2 cm. The 2 cm and Touching circuit separations were obtained by taping the wires to the styrofoam blocks. The separations Δh in Fig. 3-3 will be equivalent to the sum of the wire radius and insulation thickness, i.e., Δh = 33 mils.

The experimental data were taken from 20 Hz to 100 MHz for the Touching cases and 1 KHz to 100 MHz for the 2 cm cases. The reason for the difference in frequency ranges, is due to the fact that the

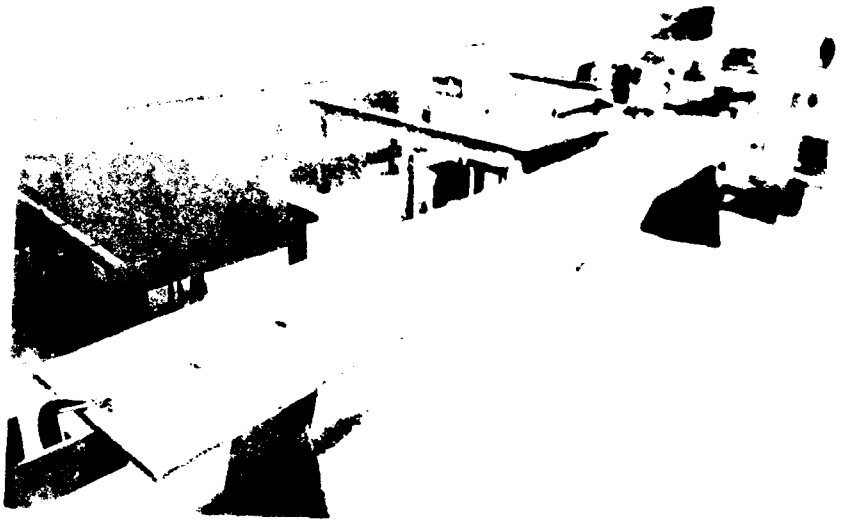

(b)

Fig. 3-1

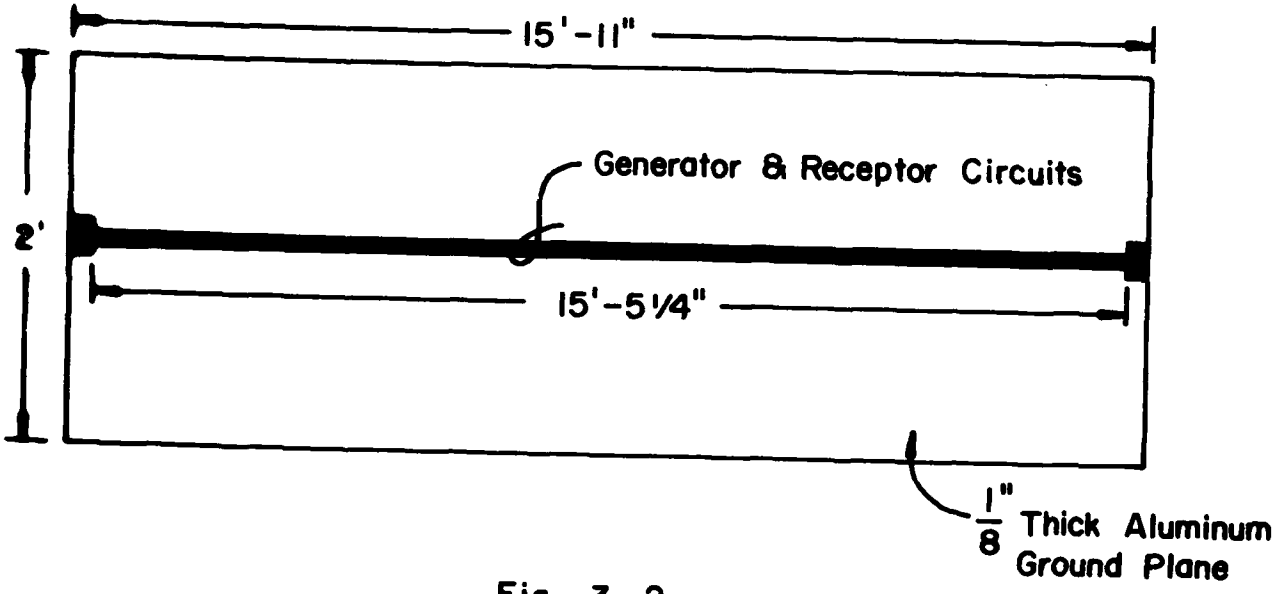
15'-11"
2'
Generator & Receptor Circuits
15'-5 1/4"
1/8" Thick Aluminum
Ground Plane

Fig. 3-2

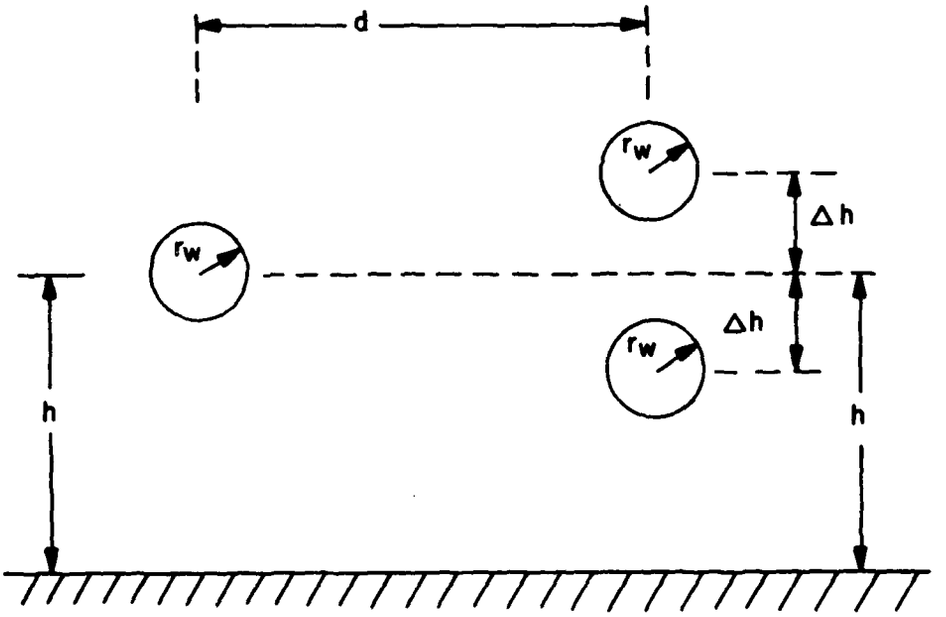

h = 2 cm
r_w = 16 mils
Δh = 33 mils

Fig. 3-3.

measurement equipment used in the experiment does not have the needed sensitivity at the lower frequencies when the circuits were separated by 2 cm. The circuit lengths, ℓ, are one wavelength long at approximately 64 MHz (computed assuming free space propagation). Therefore, this frequency range (20 Hz to 100 Mz) will permit investigation of circuit responses for electrically short to electrically long cable lengths ($\ell = 3.14 \times 10^{-7}\lambda$ to $\ell = 1.56845\lambda$). Measurements were taken at discrete frequencies; 20 Hz, 25 Hz, 30 Hz, 40 Hz, ---, 90 Hz, 100 Hz, 150 Hz, 200 Hz, 250 Hz, 300 Hz, ---, 900 Hz, 1KHz, 1.5 KHz, 2.0 KHz, 2.5 KHz, 3.0 KHz, 4.0 KHz, ---, 9.0 KHz, 10 KHz, 15 KHz, 20 KHz, 25KHz, 30 KHz, 40 KHz, ---, 90 KHz, 100 KHz, 150 KHz, 200 KHz, 250 KHz, 300 KHz, 400 KHz, ---, 900 KHz, 1 MHz, 1.5 MHz, 2.0 MHz, 2.5 MHz, 3.0 MHz, 4.0 MHz, ---, 9 MHz, 10 MHz, 15 MHz, 20 MHz, 25 MHz, 30 MHz, 40 MHz, ---, 90 MHz, 100 MHz. The data points are connected by straight lines on the graph to facilitate the interpretation of the results. The apparatus used for measurement and excitation of the line are:

	Frequency Range
(1) HP 8405A Vector Voltmeter	1 MHz → 100 MHz
(2) HP 3400A RMS Voltmeter	20 Hz → 1 MHz

		Frequency Range
(3) HP 205AG	Audio Signal Generator	20 Hz → 15 KHz
(4) HP 8601A	Generator/Sweeper	1 MHz → 100 MHz
(5) Wavetek 134	Sweep Generator	15 KHz → 1 MHz
(6) Tektronix DC502	Counter	20 Hz → 100 MHz

The input voltage source V_s in Fig. 2-2 and Fig. 2-15 was a one-volt sinusoidal source. This was obtained, experimentally, by monitoring the oscillator output and adjusting it to provide one volt. The ratio of the received voltage to V_s = 1 volt is plotted versus frequency in all graphs. Although the received voltages are phasors with a magnitude and phase, only the magnitudes are plotted versus frequency.

3.3 Discussion of Graph Formats

The experimental results for the received voltages of the straight and twisted wire pair configurations, discussed in Section 3-2, have been plotted versus frequency in Appendix A and B. The computed results using the models of the three circuit configurations discussed in Chapter II, for the circuits in Fig. 2-2 and Fig. 2-15 are also plotted on these graphs. The model predictions and experimental results for the three circuit configurations in Fig. 2-2 or Fig. 2-15 are placed on the same graph in order to determine the model accur-

acies and also to compare the effectiveness of each configuration in reducing crosstalk.

To facilitate labeling of the graphs, we will refer to Fig. 3-4. In all cases either V_1 or V_2 will be zero. If $V_1 = 1$ and $V_2 = 0$, this corresponds to the configurations of Fig. 2-2. If $V_1 = 0$ and $V_2 = 1$, this corresponds to the configurations of Fig. 2-15. Note also that the termination impedances are labeled as R_{01}, $R_{\ell 1}$, R_{02}, $R_{\ell 2}$ which implies that they are purely resistive as is the case in our computed results (and approximately so in the experimental situation). For $V_1 = 1$ and $V_2 = 0$, the received (plotted) voltage is V_{02}. For $V_1 = 0$ and $V_2 = 1$, the received (plotted) voltage is V_{01}. Typical graphs are shown in Fig. 3-5 for 1000 ohm loads and Fig. 3-6 for 50 ohm loads. Note, in these graphs, that besides showing the values of the resistive loads, the circuit separation and the value of V_1 and V_2 are also given. The circuit separation will always be labeled as either "2 cm" or "Touching" as discussed in Section 3.2.

The graphs of "assorted" loadings, which consist of all permutations of 50 ohm and 1000 ohm resistors, are given in Appendix A. Appendix A consists of 50 ohm and 1000 ohm assorted loadings along with varying the circuit separation, V_1, and V_2. Table I shows a cross reference for the particular loading, voltage, and circuit sepa-

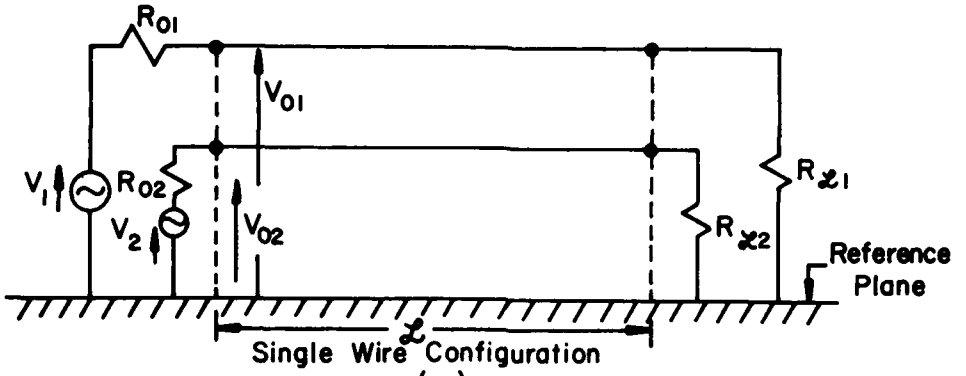

Single Wire Configuration
(a)

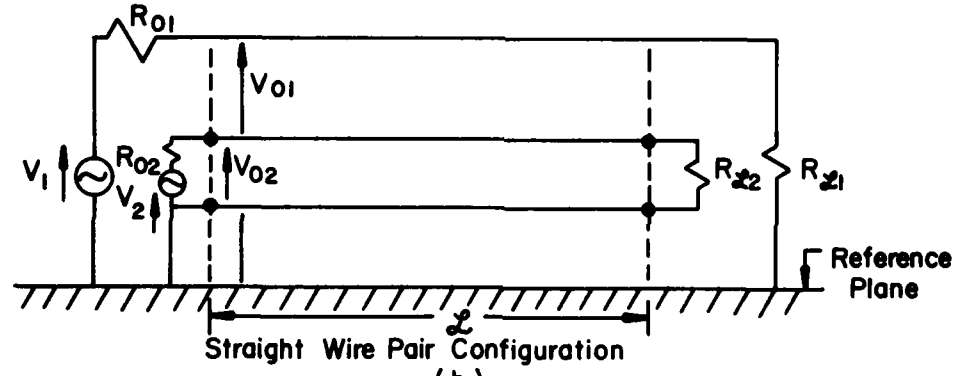

Straight Wire Pair Configuration
(b)

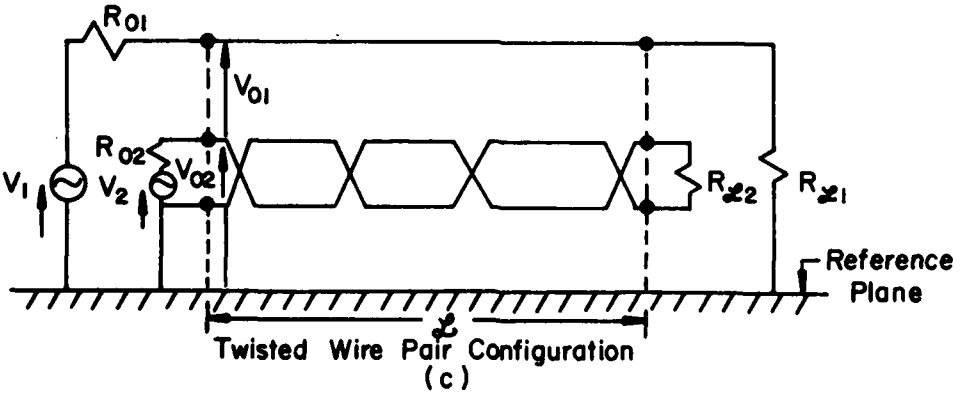

Twisted Wire Pair Configuration
(c)

Fig. 3-4

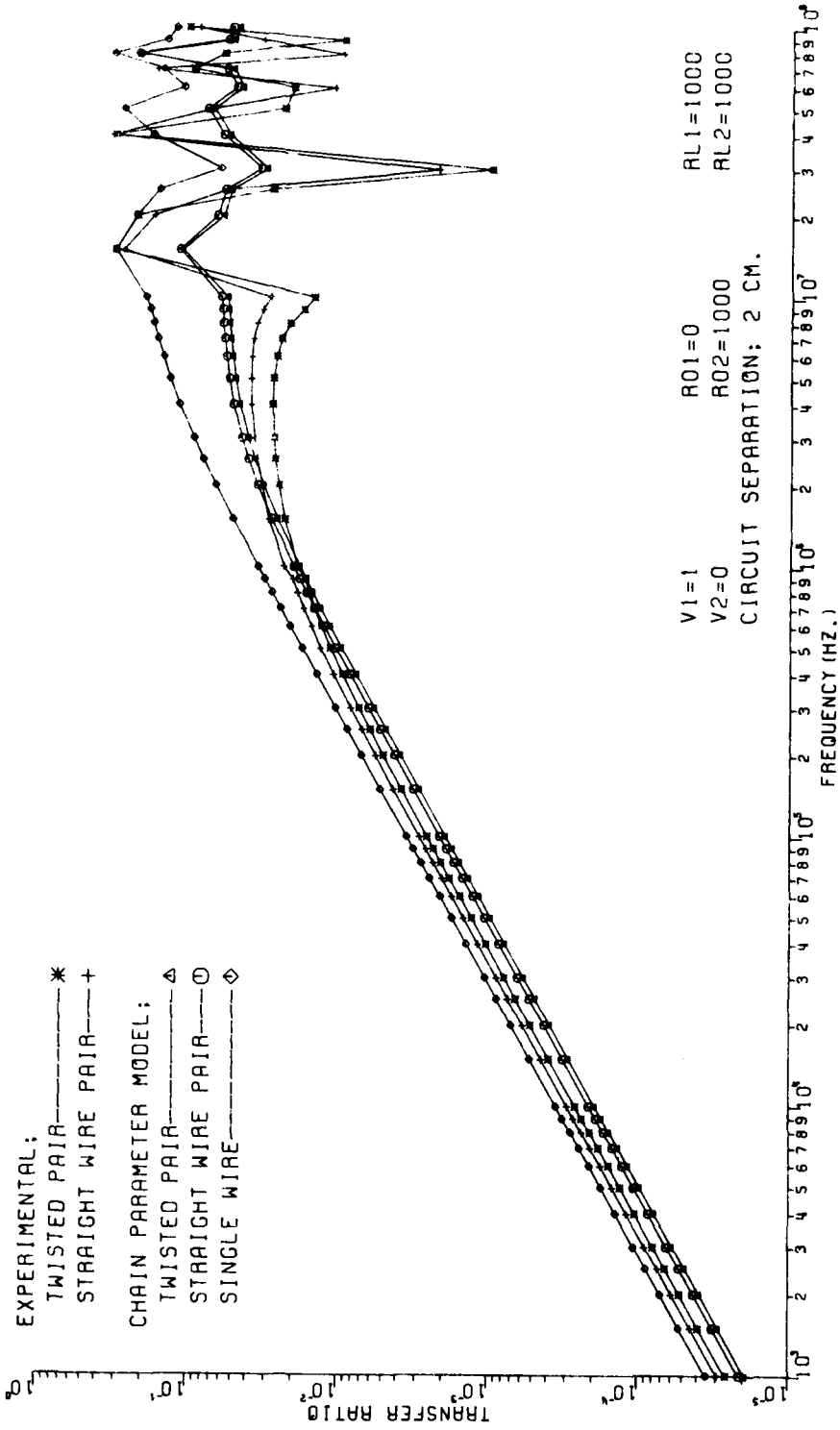
EXPERIMENTAL:
TWISTED PAIR
STRAIGHT WIRE PAIR
CHAIN PARAMETER MODEL:
TWISTED PAIR
STRAIGHT WIRE PAIR
SINGLE WIRE
TRANSFER RATIO
FREQUENCY (HZ.)
V1=1
V2=0
RO1=0
RO2=1000
RL1=1000
RL2=1000
CIRCUIT SEPARATION: 2 CM.

Fig. 3-5

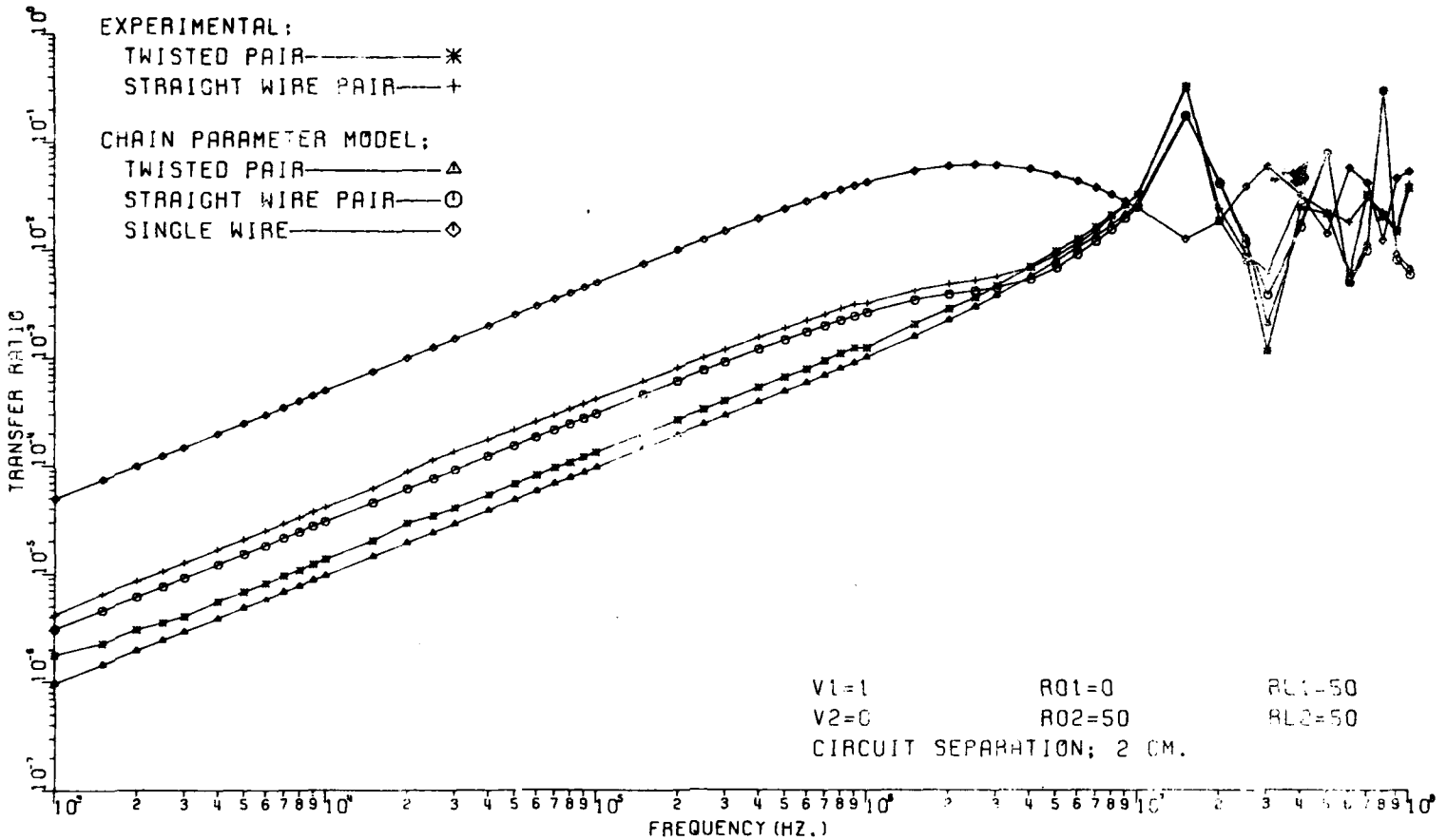
EXPERIMENTAL:
TWISTED PAIR
STRAIGHT WIRE PAIR
CHAIN PARAMETER MODEL:
TWISTED PAIR
STRAIGHT WIRE PAIR
SINGLE WIRE
TRANSFER RATIO
FREQUENCY (HZ.)
V1=1
R01=0
RL1=50
V2=0
R02=50
RL2=50
CIRCUIT SEPARATION; 2 CM.

Fig. 3-6

TABLE I

Circuit Separation	V_1(volts)	V_2(volts)	R01(Ω)	R02(Ω)	RL1(Ω)	RL2(Ω)	Fig.
Touching	1	0	0	50	50	50	A-1
Touching	1	0	0	50	50	1000	A-2
Touching	1	0	0	50	1000	50	A-3
Touching	1	0	0	50	1000	1000	A-4
Touching	1	0	0	1000	50	50	A-5
Touching	1	0	0	1000	50	1000	A-6
Touching	1	0	0	1000	1000	50	A-7
Touching	1	0	0	1000	1000	1000	A-8
Touching	0	1	50	0	50	50	A-9
Touching	0	1	50	0	50	1000	A-10
Touching	0	1	50	0	1000	50	A-11
Touching	0	1	50	0	1000	1000	A-12
Touching	0	1	1000	0	50	50	A-13
Touching	0	1	1000	0	50	1000	A-14
Touching	0	1	1000	0	1000	50	A-15
Touching	0	1	1000	0	1000	1000	A-16

TABLE I (continued)

Circuit Separation	V_1(volts)	V_2(volts)	R01(Ω)	R02(Ω)	RL1(Ω)	RL2(Ω)	Fig.
2 cm	1	0	0	50	50	50	A-17
2 cm	1	0	0	50	50	1000	A-18
2 cm	1	0	0	50	1000	50	A-19
2 cm	1	0	0	50	1000	1000	A-20
2 cm	1	0	0	1000	50	50	A-21
2 cm	1	0	0	1000	50	1000	A-22
2 cm	1	0	0	1000	1000	50	A-23
2 cm	1	0	0	1000	1000	1000	A-24
2 cm	0	1	50	0	50	50	A-25
2 cm	0	1	50	0	50	1000	A-26
2 cm	0	1	50	0	1000	50	A-27
2 cm	0	1	50	0	1000	1000	A-28
2 cm	0	1	1000	0	50	50	A-29
2 cm	0	1	1000	0	50	1000	A-30
2 cm	0	1	1000	0	1000	50	A-31
2 cm	0	1	1000	0	1000	1000	A-32

ration for the graphs in Appendix A. Appendix A represents an even number of loops (226) in the twisted wire pair model and experimental data.

3.4 Single Wire Results

As previously mentioned, there were no experimental measurements taken for the single wire configuration of Fig. 3-4(a) since this work has previously been done [10, 11]. As was shown in Chapter II, the single wire configuration is much simpler, computationally, than the other two configurations. One might therefore be interested in determining whether this simpler model will provide a reasonable prediction of the twisted wire pair case. Although one might suspect that this model would not be able to predict the twisted wire pair case, examples will be shown for which it does provide accurate predictions. This suggests that for these loadings, the twisting of the wire pair has no effect on reducing the coupling; a rather remarkable observation.

Referring to Appendix A, note that for "high" impedance loads, i.e., 1000 ohms, the model for the single wire configuration predicts the coupling for the twisted wire pair configuration very well. The error for this "high" impedance loading being between 1.75 db and 5.5 db for the Touching cases and 3 db and 6 db for the 2 cm separa-

tion cases. However, for "low" impedance loads, i.e., 50 ohms, the model of the single wire configuration does not predict twisted wire pair coupling very well. The error for this "low" impedance loading being between 6 db and 25 db for the Touching cases and between 10 db and 32 db for the 2 cm separation cases. From the results shown in Appendix A, it appears that the error in using the single wire model to predict twisted wire pair coupling increases as the load impedances decrease and circuit separation increases.

3.5 Straight Wire Pair Results

In looking at the experimental results and the model predictions for the straight wire pair configuration in Appendix A, one can see that the model is very accurate in predicting the coupling for this configuration. The error for this model as compared to the experimental results (50 ohm and 1000 ohm loadings) is between 6 db and 8.25 db for the Touching cases and between 3.5 db and 4.25 db for the 2 cm separation cases.

As was the case for the single wire model, the straight wire pair model also does very well in predicting coupling for the twisted wire pair configuration for "high" impedance loads, i.e., 1000 ohms, and not so well for "low" impedance loads, i.e., 50 ohms.

Referring again to Appendix A, the error incurred in using the straight wire pair model to predict coupling in the twisted wire pair case is between 0 db and 3.2 db for the Touching cases and between 2 db and 7 db for the 2 cm separation cases. Even though the straight wire pair model provides much better predictions of the twisted wire pair coupling for "low" impedance loads than that of the single wire model, the predictions are still not very accurate. The error in predicting twisted wire pair coupling using the straight wire pair model again increases with a decrease in load impedance and increased circuit separation.

3.6 Twisted Wire Pair Results

The model for the twisted wire pair case compares very well with the twisted wire pair experimental results, as shown in Appendix A. The error in predicting twisted wire pair coupling (50 ohm and 1000 ohm loads) is between 2.95 db and 3.35 db for the Touching cases and between 3.2 db and 3.5 db for the 2 cm separation cases.

From Appendix A one can see that the straight wire pair model is almost as accurate as the twisted wire pair model in predicting twisted pair coupling for "high" impedance loads, i.e., 1000 ohms. However, for "low" impedance loads, i.e., 50 ohms, or where the

straight wire pair model does not accurately predict twisted wire pair coupling, the twisted wire pair model is very accurate. This "low" impedance load coupling is clearly shown in Fig. 3-4 where the coupling to twisted wire pairs is 10.25 db lower than the coupling to straight wire pairs. It would appear from this that the twist does, in fact, matter for "low" impedance loads and has no effect for high impedance loads.

3.7 Low Impedance Loads

As discussed in sections 3.4, 3.5, and 3.6, it appears that the prediction of twisted wire pair coupling cannot be accurately achieved using the single wire and straight wire pair models for low impedance loads. In order to further investigate the effects of low impedance loads on coupling for the circuits of Fig. 3-4, measurements were taken for the particular loadings listed in Table II. Table II refers to the figures of Appendix B which are plots of the results for 25 ohm, 10 ohm, 5 ohm, and 1 ohm loads on both circuits. Typical plots of the "low" impedance loads are shown in Fig. 3-7 through Fig. 3-10 where the circuit separation is 2 cm. The twisted wire pair results again represent an even number of loops (226) for these figures and those in Appendix B.

TABLE II

Circuit Separation	V_1 (volts)	V_2 (volts)	R01(Ω)	R02(Ω)	RL1(Ω)	RL2(Ω)	Fig.
Touching	1	0	0	25	25	25	B-1
Touching	1	0	0	10	10	10	B-2
Touching	1	0	0	5	5	5	B-3
Touching	1	0	0	1	1	1	B-4
Touching	0	1	25	0	25	25	B-5
Touching	0	1	10	0	10	10	B-6
Touching	0	1	5	0	5	5	B-7
Touching	0	1	1	0	1	1	B-8
2 cm	1	0	0	25	25	25	B-9
2 cm	1	0	0	10	10	10	B-10
2 cm	1	0	0	5	5	5	B-11
2 cm	1	0	0	1	1	1	B-12
2 cm	0	1	25	0	25	25	B-13
2 cm	0	1	10	0	10	10	B-14
2 cm	0	1	5	0	5	5	B-15
2 cm	0	1	1	0	1	1	B-16

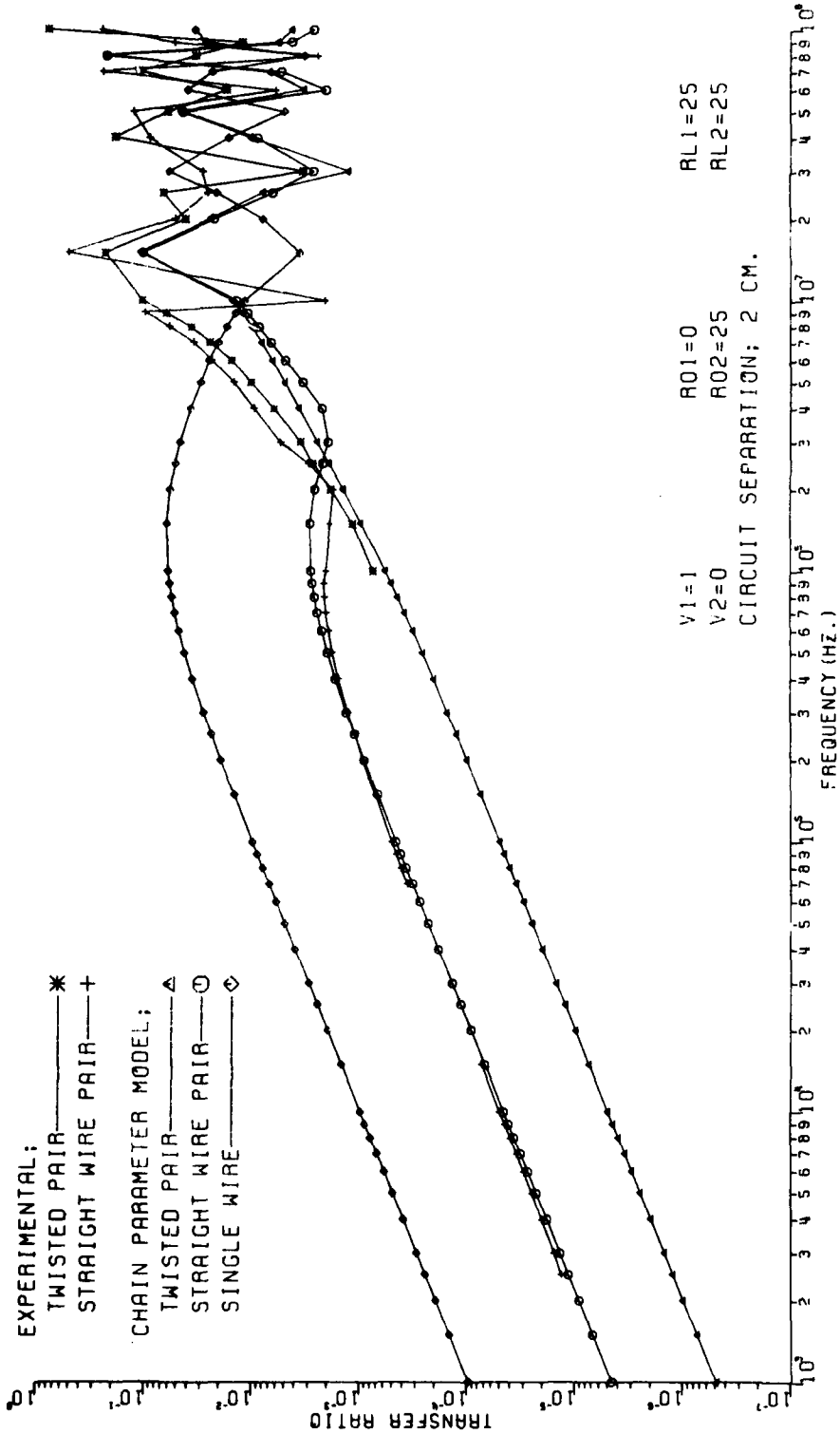
EXPERIMENTAL:
TWISTED PAIR
STRAIGHT WIRE PAIR
CHAIN PARAMETER MODEL:
TWISTED PAIR
STRAIGHT WIRE PAIR
SINGLE WIRE
TRANSFER RATIO
FREQUENCY (HZ.)
V1=1
V2=0
RO1=0
RO2=25
RL1=25
RL2=25
CIRCUIT SEPARATION; 2 CM.

Fig. 3-7

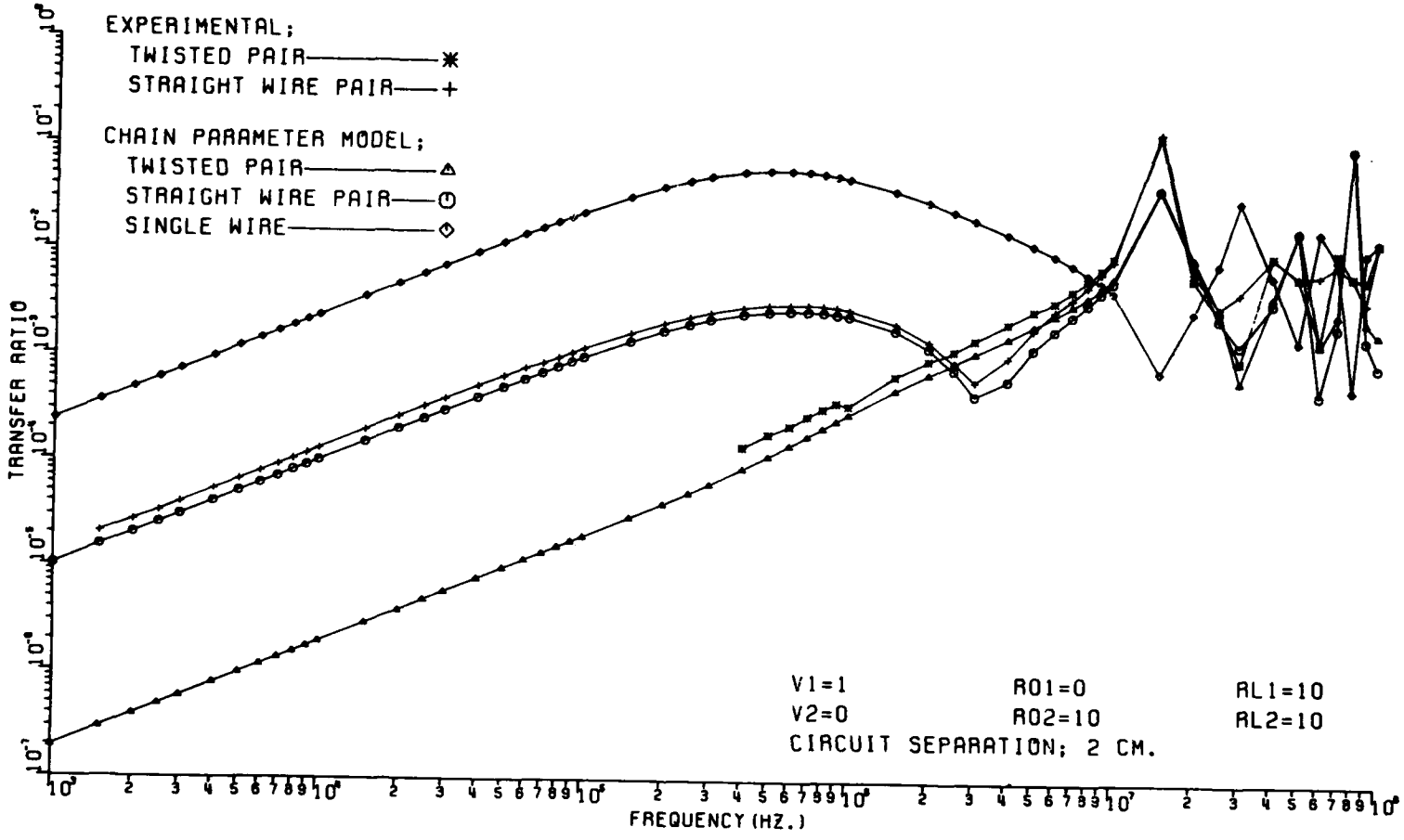
EXPERIMENTAL;
TWISTED PAIR
STRAIGHT WIRE PAIR
CHAIN PARAMETER MODEL;
TWISTED PAIR
STRAIGHT WIRE PAIR
SINGLE WIRE
TRANSFER RATIO
FREQUENCY (HZ.)
V1=1
V2=0
R01=0
R02=10
RL1=10
RL2=10
CIRCUIT SEPARATION; 2 CM.

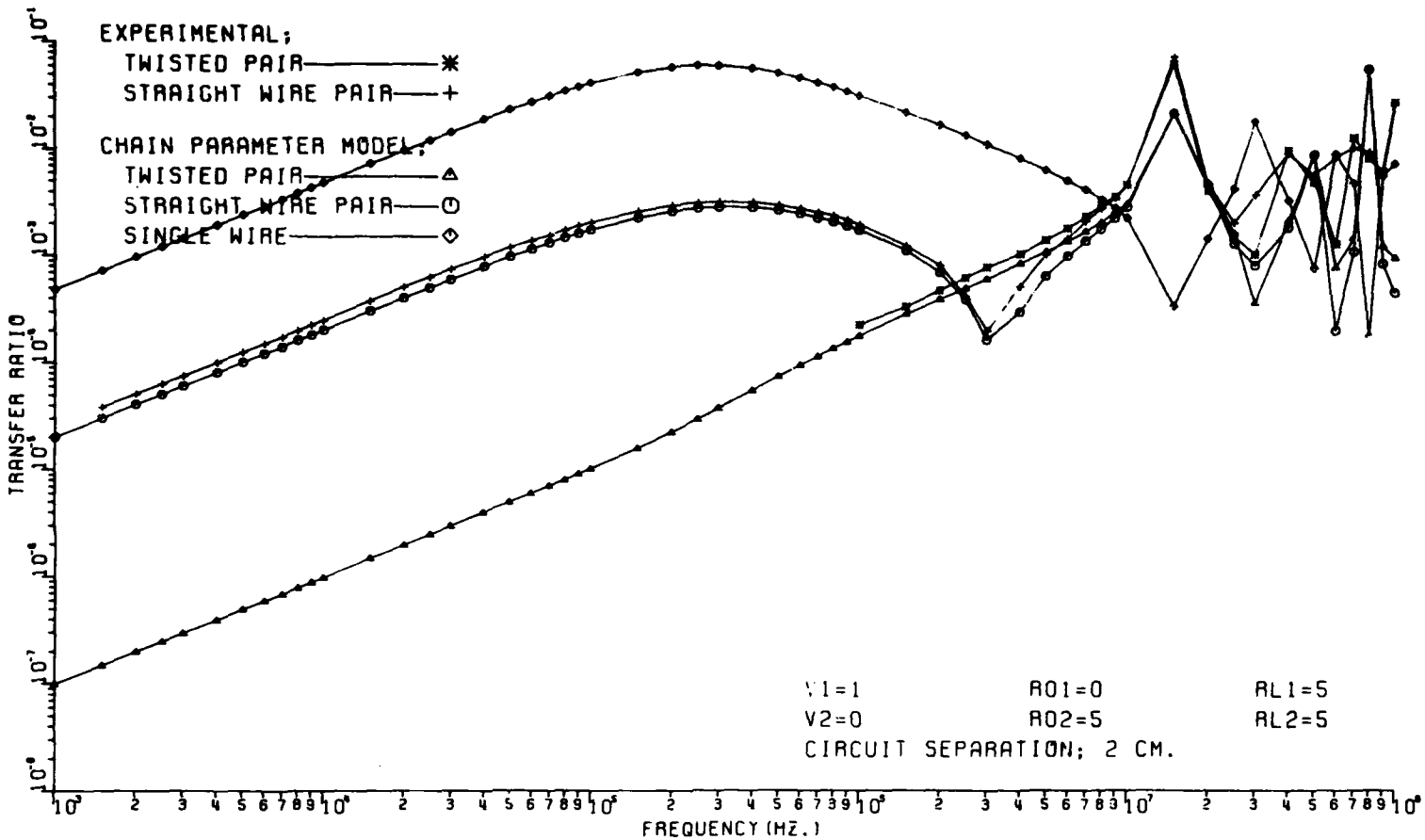
EXPERIMENTAL;
TWISTED PAIR
STRAIGHT WIRE PAIR
CHAIN PARAMETER MODEL;
TWISTED PAIR
STRAIGHT WIRE PAIR
SINGLE WIRE
TRANSFER RATIO
FREQUENCY (HZ.)
V1=1
V2=0
R01=0
R02=5
RL1=5
RL2=5
CIRCUIT SEPARATION; 2 CM.

Fig. 3-9

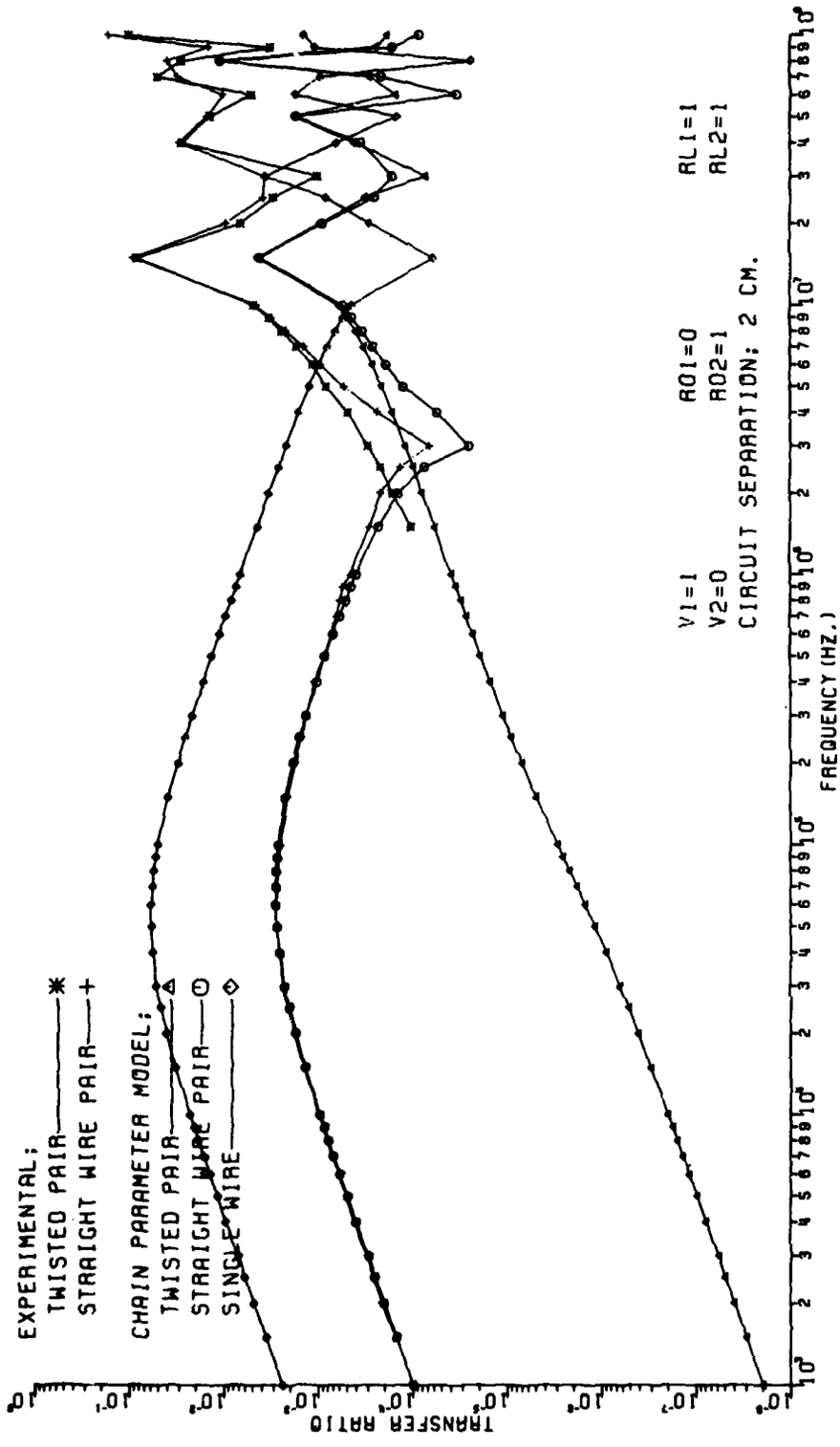
EXPERIMENTAL;
TWISTED PAIR
STRAIGHT WIRE PAIR
CHAIN PARAMETER MODEL;
TWISTED PAIR
STRAIGHT WIRE PAIR
SINGLE WIRE
TRANSFER RATIO
FREQUENCY (HZ.)
V1=1
V2=0
RO1=0
RO2=1
RL1=1
RL2=1
CIRCUIT SEPARATION: 2 CM.

Fig. 3-10

In comparing the single wire model predictions with the twisted wire pair experimental results shown in Appendix B, one observes that these plots further verify the previous observation that the error in predicting twisted wire pair coupling by using the single wire model increases with lower impedance loads and larger circuit separation. Although the error is not as large, the same is true for the straight wire pair model. The major point here, is that the twisting of wire pairs dramatically reduces the coupling as compared to single wire and straight wire pair configurations for "low" impedance loads. This is apparent in Fig. 3-7 through Fig. 3-10, where the consistent reduction of values of the load impedances shows a proportional decrease in coupling for the twisted wire pair over the single wire and straight wire pair results.

3.8 Summary

The models of the straight wire pair and twisted wire pair configurations proved to be very accurate in predicting the corresponding experimental results. The results, of course, are not as dependable in the standing wave region (the region in which the line length is greater than $1/10\,\lambda$) which is apparent from the plots in Appendix A and Appendix B above approximately 10^7 Hertz.

It appears that for "high" impedance loads, twisting the wire pair has virtually no effect in reducing coupling as compared to the straight wire pair. Therefore, for these load impedance levels, the simpler straight wire pair model (or even the single wire model) will suffice for predicting the twisted pair coupling. However, for "low" impedance loads the effect of twisting the wire pair has a dramatic effect and neither the straight wire pair nor the single wire models provide any adequate predictions of the twisted pair results.

It is difficult to precisely define the range of loads which are considered to be either "high" or "low" impedance since it does not appear to be feasible to solve the transmission line equations in literal form for either the straight wire pair or twisted wire pair configurations. However, the single wire configuration has been solved in literal form in [2] and from an examination of the resulting equations, one can define the terms "high" impedance and "low" impedance to be those impedances greater than or less than, respectively, the characteristic impedance of the single wire above ground (approximately 275 ohms).

It would be advantageous, computationally, to find a simpler approximate model of the twisted wire pair that would not only provide a reasonable prediction of the coupling for the twisted pair case but

would also separate the total coupling into capacitive and inductive components. This separation was illustrated for the single wirecase in Chapter II. A simpler model is justified by the fact that twisted pairs are usually randomly oriented in cable bundles. Therefore even an "exact" model would not accurately predict the coupling for this realistic situation. Also, the previously derived chain parameter model of the twisted wire pair is very time consuming, computationally, since one must multiply, at each frequency, the chain parameter matrices for the uniform sections of the line (each loop). For the problem investigated here, this requires 226 multiplications of 6×6 matrices at each frequency.

A simpler, approximate model for predicting twisted pair coupling will be derived in the following chapter. This model not only provides accurate (within 3 db) predictions of the twisted pair coupling for frequencies such that the line is electrically short and is virtually trivial, computationally, but also provides considerable insight into the twisted pair coupling phenomenon.

IV. THE LOW FREQUENCY MODEL

4.1 Introduction

In determining simpler coupling models for the twisted wire pair and straight wire pair configurations, the lines will be assumed to be electrically short (i.e. $\ell \leq 1/20\,\lambda$). This assumption will allow considerable simplifications in the resulting model which are justifiable, at least, intuitively. The basic technique used in deriving these models will be the superposition of the coupling due to the mutual inductance ("inductive coupling") and the mutual capacitance ("capacitive coupling") which was discussed for the single wire configuration in Chapter I and can be shown to be correct for this case for electrically short lines [2]. The inductive and capacitive coupling contributions will be determined separately and their magnitude will be added together to determine the magnitude of total coupling for each model.

The following derivations are not rigorous nor are they intended to be. In order to obtain rigorous justification for these models, one must solve the terminal current equations of Chapter II in literal

form (as opposed to a numerical solution) as was done for the single wire configuration in [2] and observe the resulting simplification of these equations as the frequency is decreased. For the straight wire pair and twisted wire pair configurations, this would involve great difficulty as should be evident from Chapter II. Therefore it does not appear feasible to approach the solution in this manner. Instead, we will rely on extending the result for the single wire configuration in a logically consistent manner to the straight wire pair and twisted wire pair configurations.

4.2 Inductive Coupling

4.2.1 The Twisted Wire Pair

In order to determine the inductive coupling for the twisted wire pair receptor configuration shown in Fig. 2-2(c), the total inductive coupling will be taken to be the sum of the inductive coupling contributions for each loop. The "abruptly" nonuniform model for this situation is shown in Fig. 4-1. For each section or loop in Fig. 4-1, the net flux, ϕ_i, penetrating a loop is the difference in the fluxes penetrating the area between one of the wires in the twisted pair at height h_1 and the reference plane, and the area between the other wire at height h_2 and the reference plane (See Fig. 4-2).

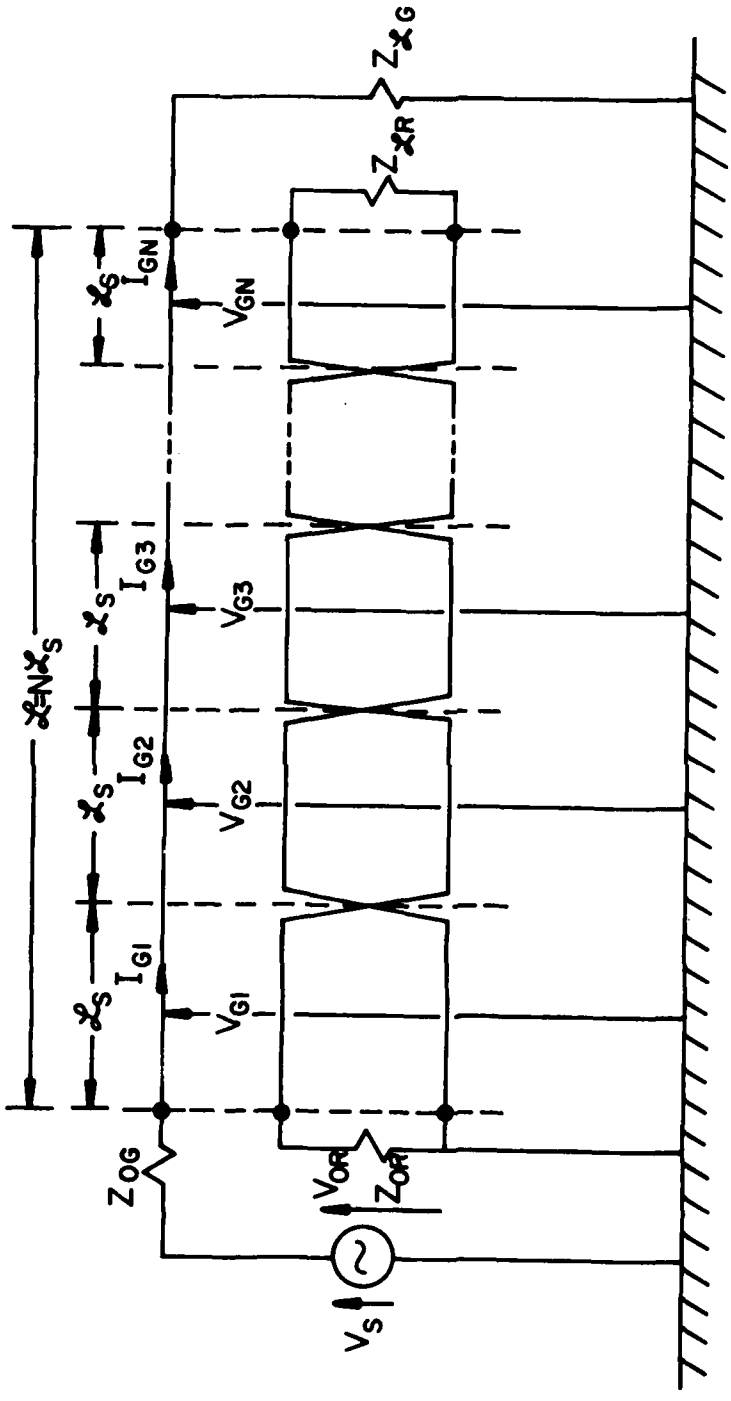
$Z_{\lambda G}$
$Z_{\lambda R}$
λ_G
I_{GN}
V_{GN}
I_{G3}
V_{G3}
I_{G2}
V_{G2}
I_{G1}
V_{G1}
$\lambda_N\lambda_S$
λ_S
Z_{OG}
V_{OR}
Z_{OR}
V_S

Fig. 4-1

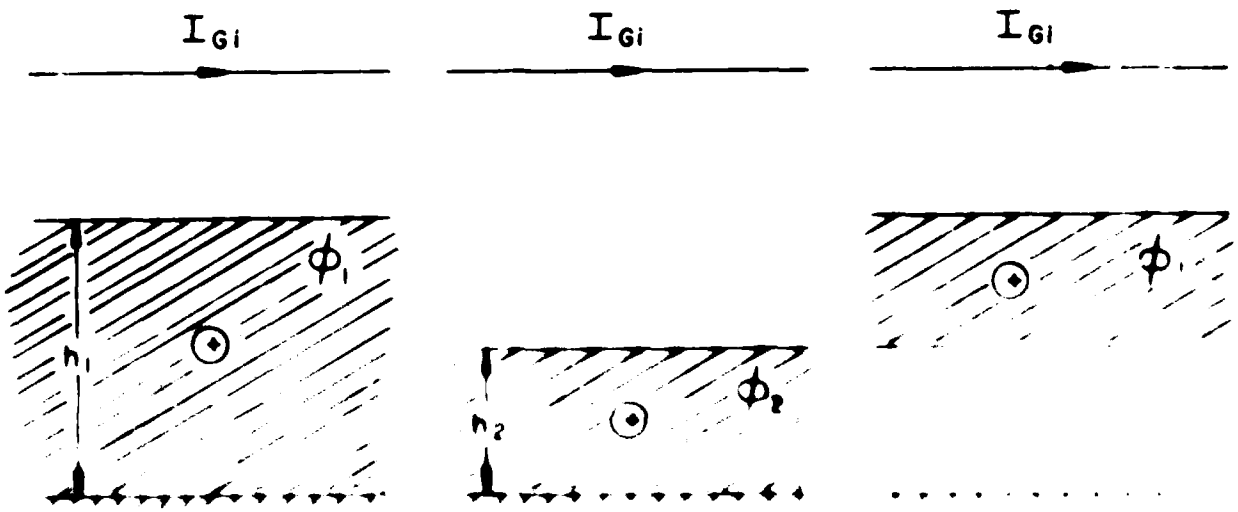
I_{Gi}
I_{Gi}
I_{Gi}
Φ_1
h_1
Φ_2
h_2
Φ_1

Since the line (and consequently each loop) is electrically short, we may assume that the current in each generator section, I_{G_i}, is independent of position along that section and we may represent the effect of this net flux, ϕ_i, as equivalent induced voltage sources as shown in Fig. 4-3. The mutual inductances, ℓ_{G1} and ℓ_{G2}, are between the single generator wire and each of the wires in the twisted pair [2] (See Section 2-3 and Section 4-5). If the components of inductive coupling are represented for every loop of Fig. 4-1, the result would be as shown in Fig. 4-4. Since the twist between each loop is assumed to take place over a zero interval of distance, we can "untwist" the receptor circuit of Fig. 4-1 and superimpose the inductive components of coupling into one representative voltage source, V_{TWP}^{IND}, as shown in Fig. 4-5 where

$$V_{TWP}^{IND} = j\omega \mathcal{L}_s(\ell_{G1} I_{G1} + \ell_{G2} I_{G2} + \cdots - \ell_{G1} I_{G2} - \ell_{G2} I_{G1}) \qquad (4\text{-}1)$$

$$= j\omega \mathcal{L}_s (\ell_{G1} - \ell_{G2}) \{I_{G1} - I_{G2} + I_{G3} - \cdots\}$$

$$= j\omega \mathcal{L}_s \ell_m (XI_{TWP})$$

and

$$\ell_m = \ell_{G1} - \ell_{G2} \qquad (4\text{-}2)$$

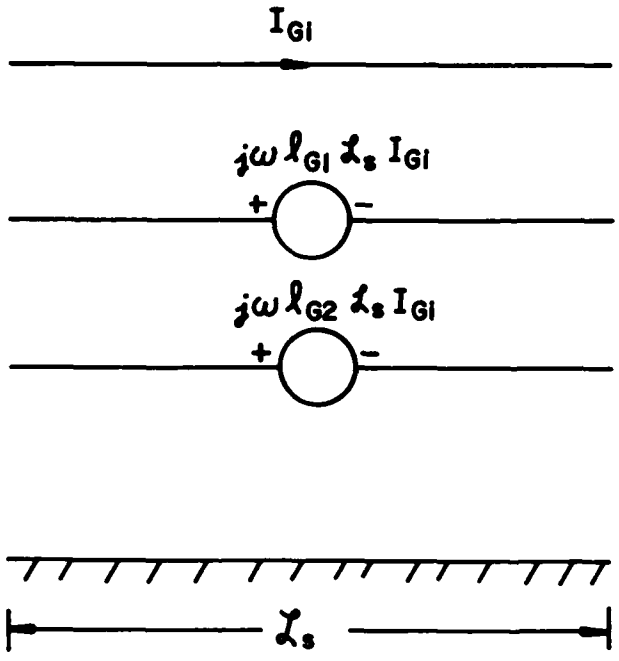
I_{G1}
$j\omega l_{G1} \mathcal{L}_s I_{G1}$
+
−
$j\omega l_{G2} \mathcal{L}_s I_{G1}$
+
−
$\mathcal{L}_s$

Fig. 4-3

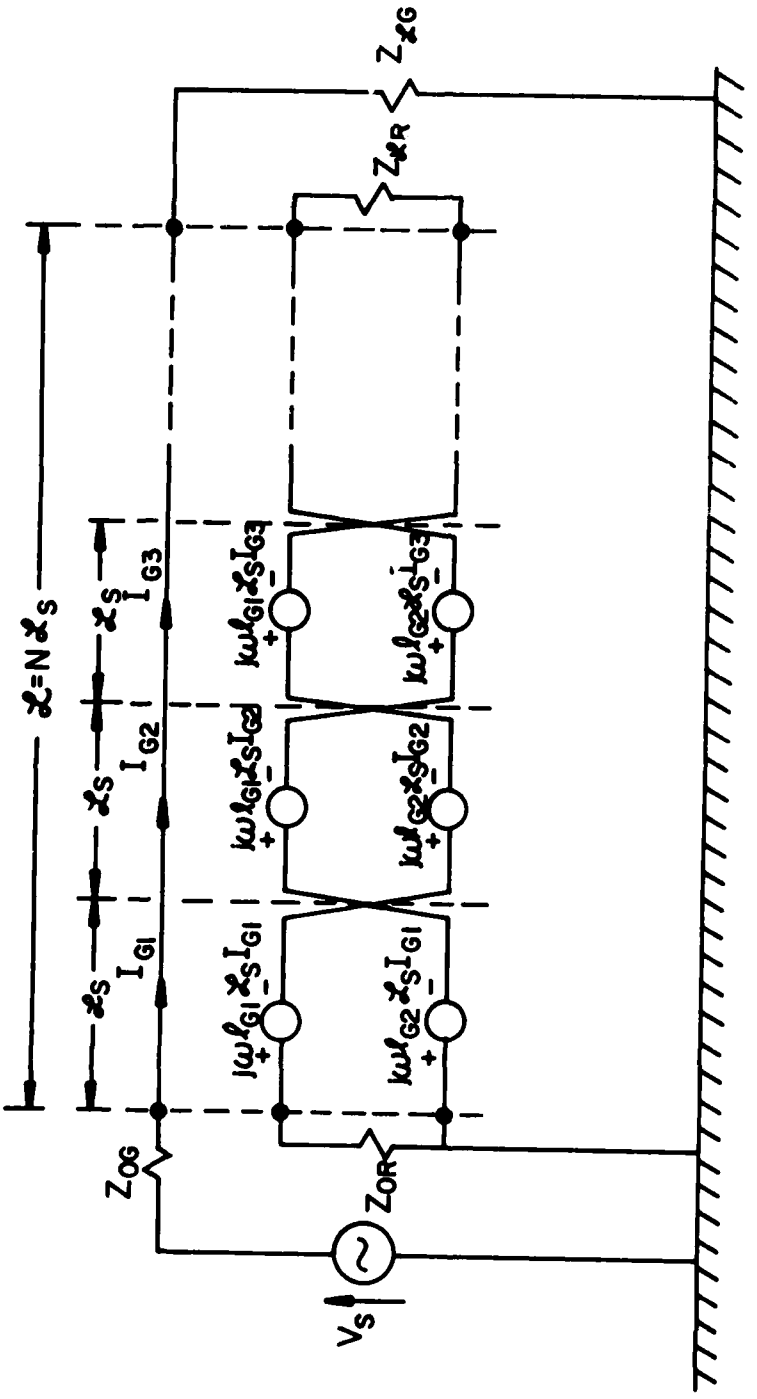
$Z_{\ell G}$
$Z_{\ell R}$
$\ell = N\ell_s$
ℓ_s
ℓ_s
ℓ_s
I_{G3}
I_{G2}
I_{G1}
$j\omega l_{G1}\ell_s I_{G3}$
$j\omega l_{G2}\ell_s I_{G3}$
$j\omega l_{G1}\ell_s I_{G2}$
$j\omega l_{G2}\ell_s I_{G2}$
$j\omega l_{G1}\ell_s I_{G1}$
$j\omega l_{G2}\ell_s I_{G1}$
Z_{OG}
Z_{OR}
V_s

Fig. 4-4

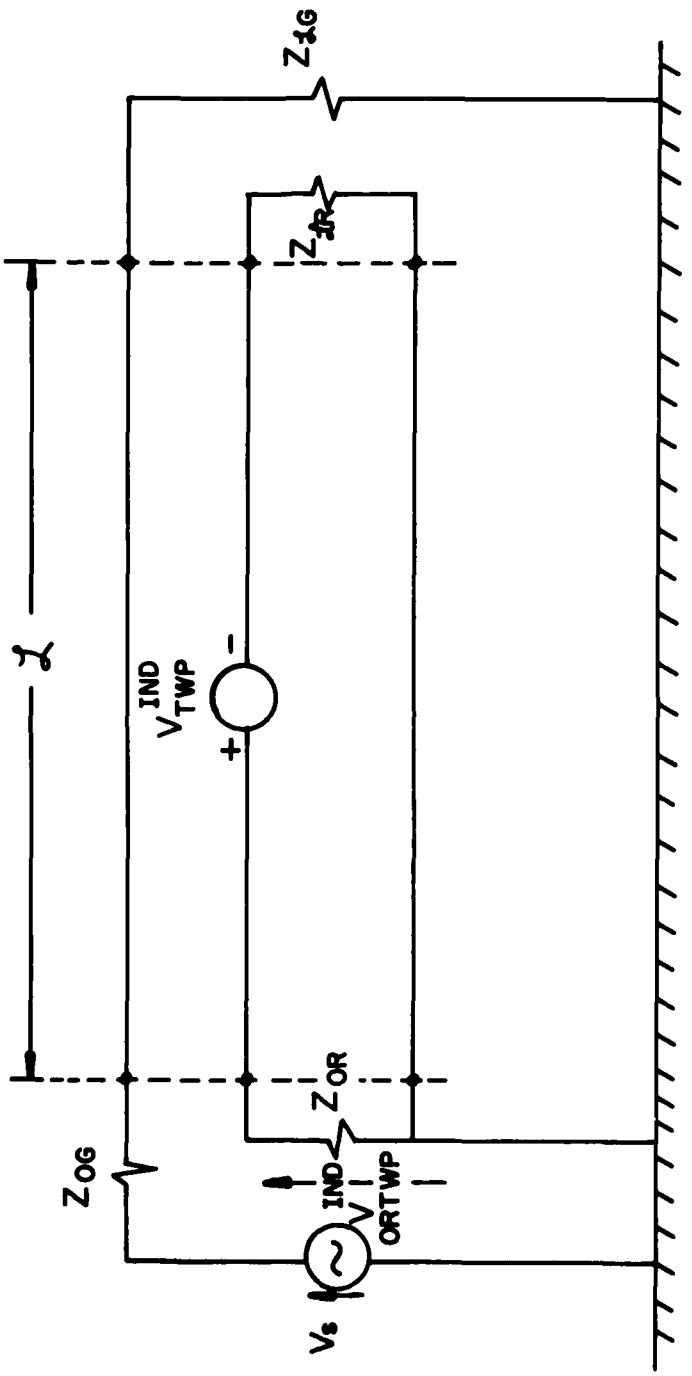

Fig. 4-5

$$XI_{TWP} = \{I_{G1} - I_{G2} + I_{G3} - \ldots\} \qquad (4-3)$$

The portion of the received voltage due to inductive coupling, V^{IND}_{0RTWP}, becomes from Fig. 4-5

$$V^{IND}_{0RTWP} = \left(\frac{Z_{0R}}{Z_{0R} + Z_{\ell R}}\right) V^{IND}_{TWP} \qquad (4-4)$$

$$= \left(\frac{Z_{0R}}{Z_{0R} + Z_{\ell R}}\right) j\omega \mathcal{L}_s \ell_m (XI_{TWP})$$

4.2.2 The Straight Wire Pair

In deriving the inductive coupling for the straight wire pair configuration, one can cascade sections of Fig. 4-3 giving the circuit of Fig. 4-6. The representative induced voltage sources for the inductive coupling of Fig. 4-6 would again simplify as shown in Fig. 4-7 where,

$$V^{IND}_{SWP} = j\omega \mathcal{L}_s (\ell_{G1} I_{G1} + \ell_{G2} I_{G2} + \ldots - \ell_{G2} I_{G2} - \ell_{G1} I_{G1})$$

$$= j\omega \mathcal{L}_s (\ell_{G1} - \ell_{G2}) \{I_{G1} + I_{G2} + \ldots\} \qquad (4-5)$$

$$= j\omega \mathcal{L}_s \ell_m (XI_{SWP})$$

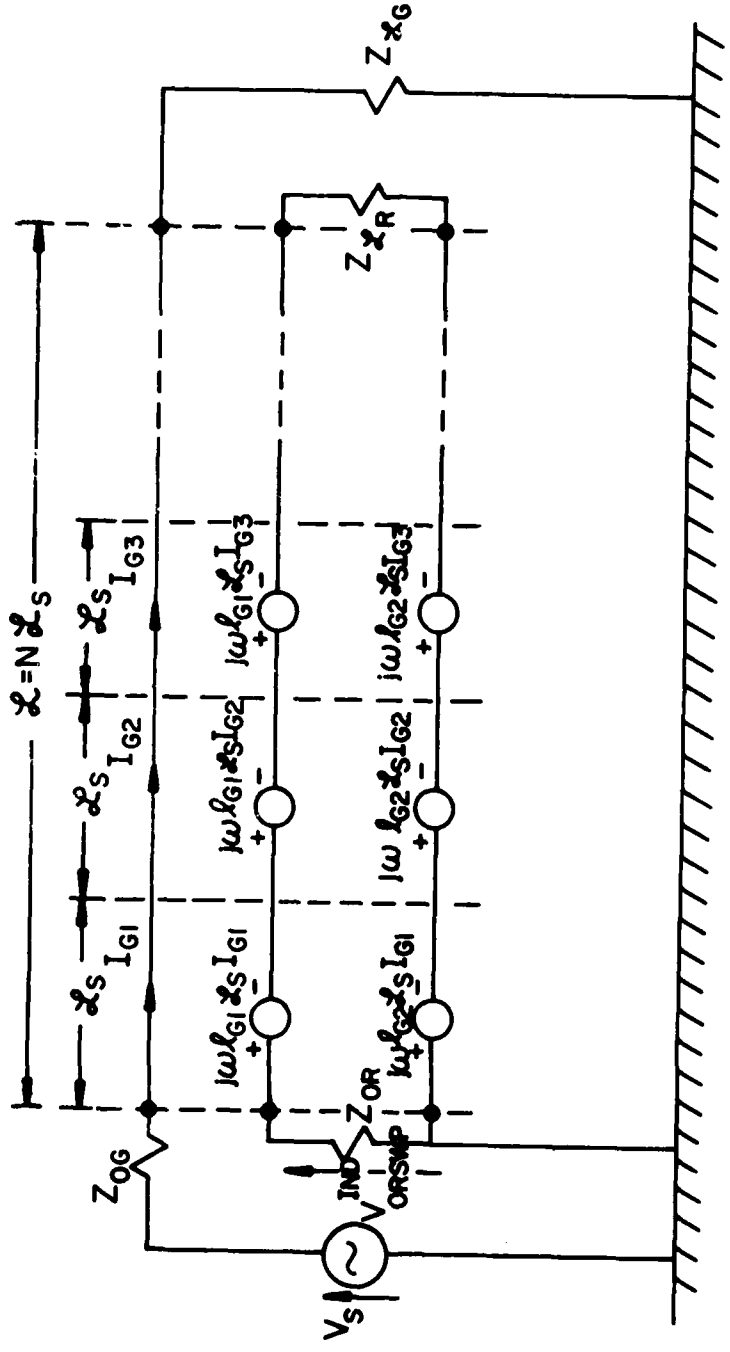
Z_{ℓ_G}
Z_{ℓ_R}
$\ell = N\ell_S$
ℓ_S
I_{G3}
I_{G2}
I_{G1}
$j\omega l_{G1}\ell_S I_{G3}$
$j\omega l_{G1}\ell_S I_{G2}$
$j\omega l_{G2}\ell_S I_{G3}$
$j\omega l_{G1}\ell_S I_{G1}$
$j\omega l_{G2}\ell_S I_{G2}$
$j\omega l_{G2}\ell_S I_{G1}$
Z_{OR}
Z_{OG}
IND
ORSWP
V_S

Fig. 4-6

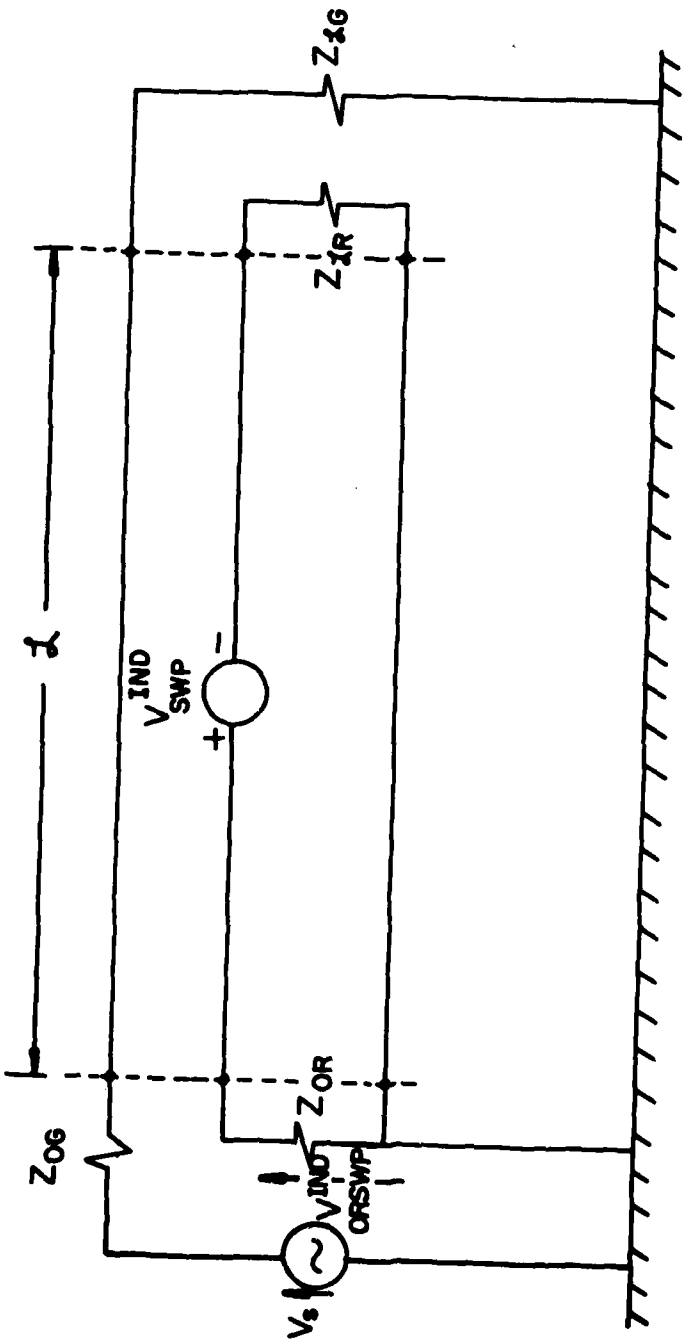

Fig. 4-7

and

$$XI_{SWP} = I_{G1} + I_{G2} + \cdots \tag{4-6}$$

Therefore the inductive coupling transfer ratio, V^{IND}_{0RSWP}, for the straight wire pair is

$$V^{IND}_{0RSWP} = \left(\frac{Z_{0R}}{Z_{0R} + Z_{\ell R}}\right) V^{IND}_{SWP} \tag{4-7}$$

$$= \left(\frac{Z_{0R}}{Z_{0R} + Z_{\ell R}}\right) j\omega \ell_s \ell_m (XI_{SWP})$$

4.2.3 Comparison of the Inductive Coupling Models

In comparing the inductive coupling models for the twisted wire pair configuration in (4-4) and the straight wire pair configuration in (4-7), we observe that the only difference is in the terms XI_{TWP} and XI_{SWP}. The term XI_{SWP} given in (4-6) is the sum of the generator currents I_{G1}, I_{G2}, ---whereas the term XI_{TWP} given in (4-3) is the sum of the currents in the odd numbered generator segments, I_{G1}, I_{G3}, --- minus the sum of the currents in the even numbered generator segments, I_{G2}, I_{G4}, ---. If the line is very short, electrically, one would expect that $I_{G1} = I_{G2} = I_{G3} = \cdots = I_{GN}$. Consequently, for this case, XI_{TWP} would be the current in one segment for an odd number of twisted pair loops and zero

for an even number of loops. Therefore for an even number of loops in the twisted pair, the inductive coupling is zero. This is intuitively satisfying since the traditional explanation of twisted pair coupling discussed in Chapter I reaches the same conclusion.

For the straight wire pair case and an electrically short line, $XI_{SWP} = NI_G$ where I_G is the current in any section of the generator line. Substituting this into (4-7) we observe that the term $j\omega \mathcal{L} \ell_m$ (XI_{SWP}) becomes $j\omega(\ell_m N \mathcal{L}_s) I_G$ and $\ell_m N \mathcal{L}_s$ is the total mutual inductance between the two circuits. This is again an intuitively satisfying result.

4.3 Capacitive Coupling

4.3.1 The Twisted Wire Pair

The capacitive coupling components for each section of the twisted wire pair receptor shown in Fig. 4-1 can be represented as shown in Fig. 4-8, where the capacitive components of coupling are represented as current sources for each receptor wire [2]. We again assume that each loop is electrically very short and therefore the voltage of a generator wire section, V_{G_i}, is independent of position along that section. This result is an extension of the single wire low frequency model discussed in Chapter I and the items c_{G1} and c_{G2} are the mutual capacitances between the single generator wire and each of the receptor wires (See Section 2.3 and 4.5). Applying

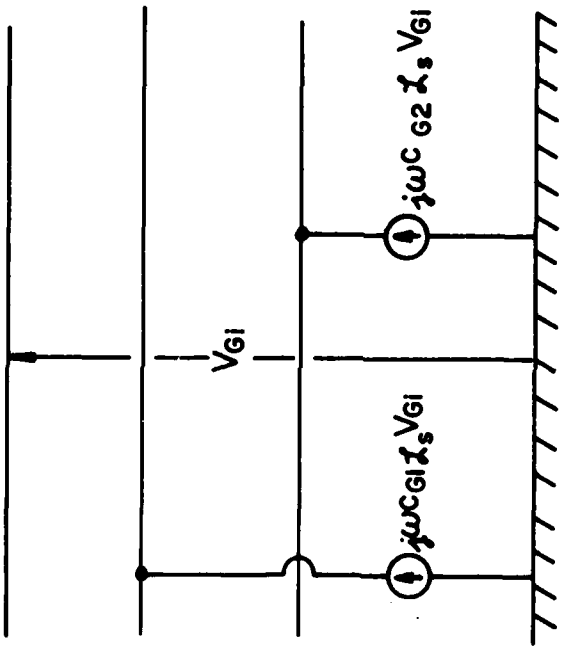

Fig. 4-8

this to the circuit of Fig. 4-1, the result would be a cascade of sections containing current sources as shown in Fig. 4-9. If the receptor circuit of Fig. 4-9 is "untwisted" the result would be the circuit of Fig. 4-10, where V^{CAP}_{0RTWP} would represent the portion of the received voltage due to capacitive coupling. Note in Fig. 4-10, that the short circuit introduced by grounding one end of the twisted wire pair configuration effectively shorts out certain of the current sources. Therefore V^{CAP}_{0RTWP} becomes,

$$V^{CAP}_{0RTWP} = \left(\frac{Z_{0R} Z_{\ell R}}{Z_{0R} + Z_{\ell R}}\right) j\omega \ell_s (c_{G1} V_{G1} + c_{G2} V_{G2} + \ldots) \quad (4\text{-}8)$$

Since the pair of wires in the receptor circuit are separated only by their insulations and are therefore very close together, one would reasonably expect that

$$c_{G1} \cong c_{G2} \quad (4\text{-}9)$$

Substituting (4-9) into (4-8) we obtain

$$V^{CAP}_{0RTWP} = \left(\frac{Z_{0R} Z_{\ell R}}{Z_{0R} + Z_{\ell R}}\right) j\omega \ell_s c_{G1} (V_{G1} + V_{G2} + \ldots) \quad (4\text{-}10)$$

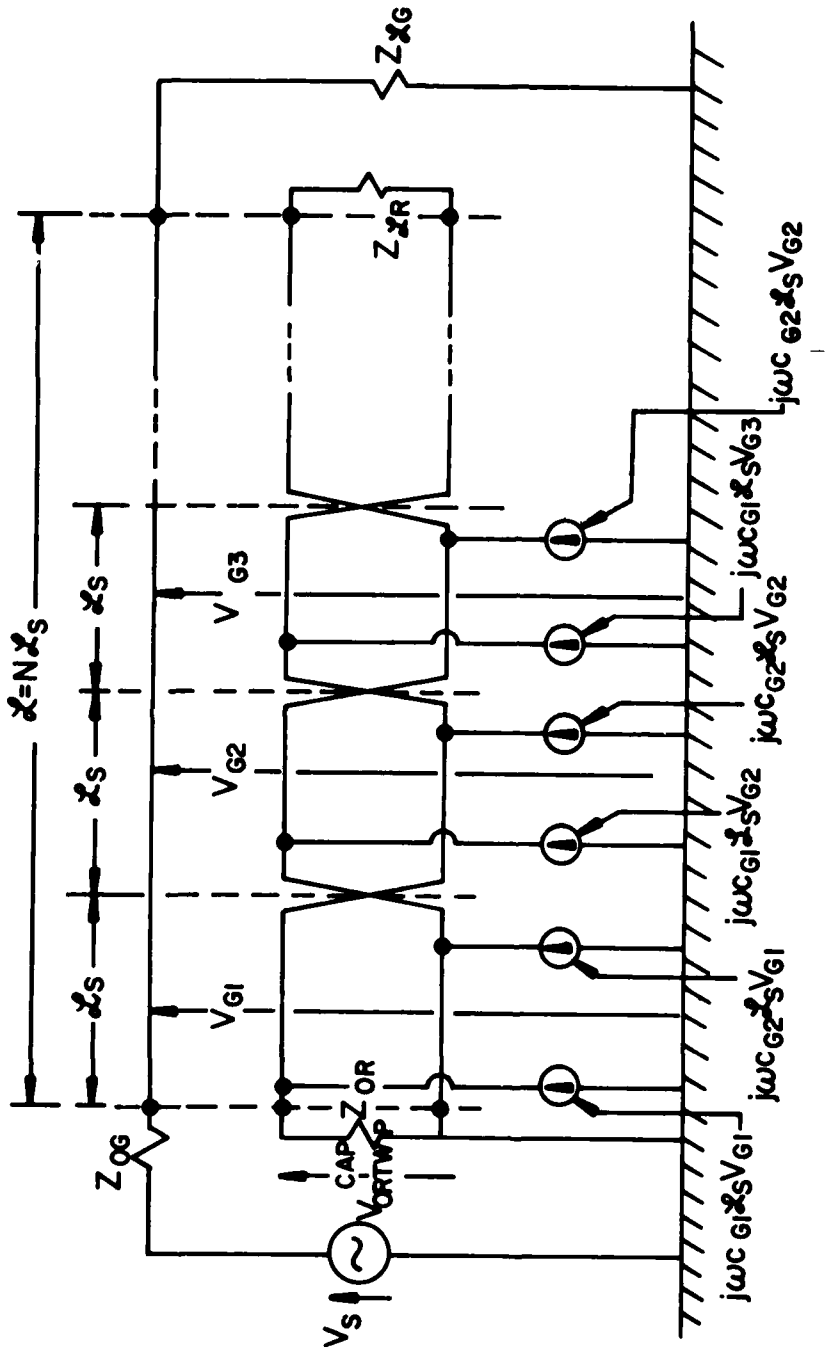
$Z_{\ell G}$
$Z_{\ell R}$
$\ell = N\ell_S$
ℓ_S
ℓ_S
ℓ_S
V_{G3}
V_{G2}
V_{GI}
Z_{OR}
Z_{OG}
CAP
ORTWP
V_S
$j\omega C_{G2}\ell_S V_{G2}$
$j\omega C_{GI}\ell_S V_{G3}$
$j\omega C_{G2}\ell_S V_{G2}$
$j\omega C_{GI}\ell_S V_{G2}$
$j\omega C_{G2}\ell_S V_{GI}$
$j\omega C_{GI}\ell_S V_{GI}$

Fig. 4 - 9

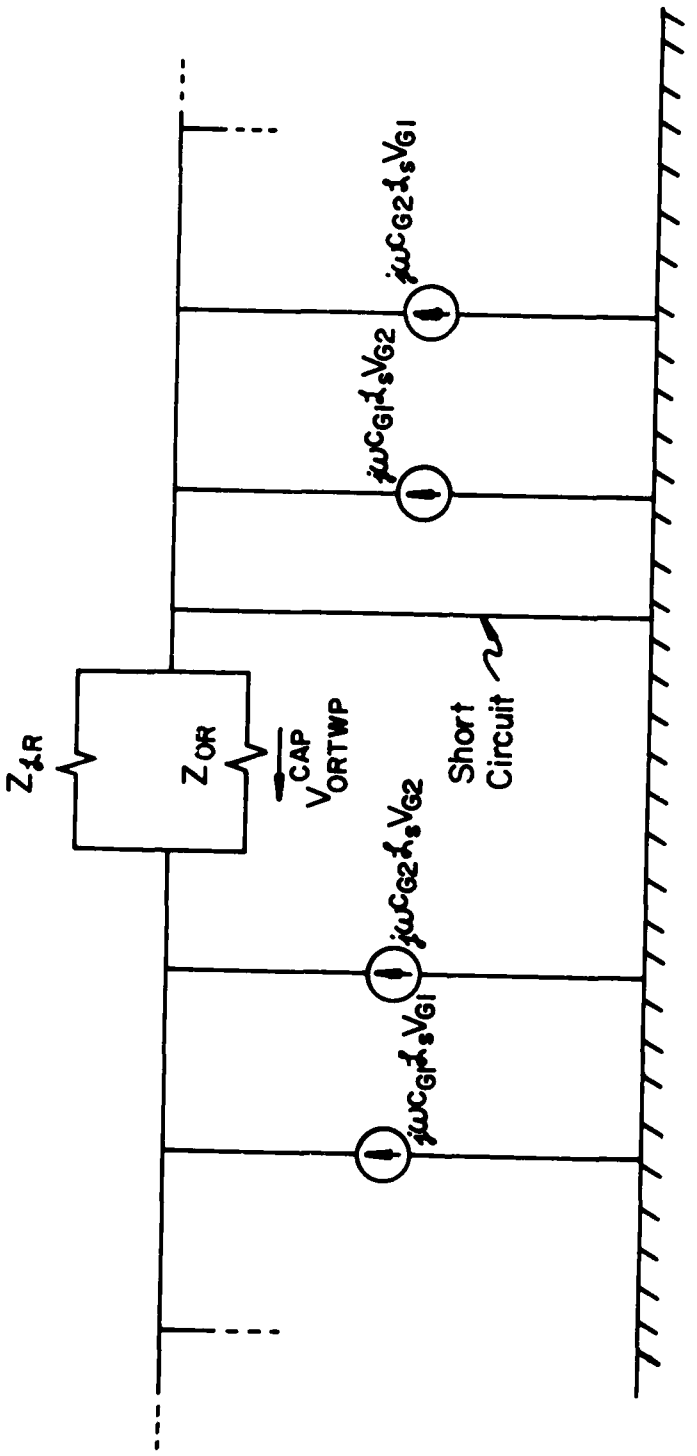
Z_{1R}
Z_{OR}
V_{ORTWP}^{CAP}
Short Circuit
$j\omega C_{G2} A_s V_{G2}$
$j\omega C_{G1} A_s V_{G1}$
$j\omega C_{G1} A_s V_{G2}$
$j\omega C_{G2} A_s V_{G1}$

Fig. 4 - 10

$$= \left(\frac{Z_{0R} Z_{\ell R}}{Z_{0R} + Z_{\ell R}}\right) \cdots$$

where,

$$XV_{TWP} = (V_{G1} \cdots$$

4.3.2 The Straight Wire Pair

In developing the model for the straight wire receptor a cascade of sections shown in Fig. 4-11. These components of capacitive coupling are identified as shown in Fig. 4-12 where,

$$V_{0RSWP}^{CAP} = \left(\frac{Z_{0R} Z_{\ell R}}{Z_{0R} + Z_{\ell R}}\right) j\omega \cdots$$

$$= \left(\frac{Z_{0R} Z_{\ell R}}{Z_{0R} + Z_{\ell R}}\right) j\omega f_s C_{G1} (XV_{SWP}$$

and where

$$XV_{SWP} = (V_{G1} + V_{G2} \cdots$$

4.3.3 Comparison of the Capacitive Coupling

Note that the results of equations ... are the same as those for the twisted wire pair in equation ...

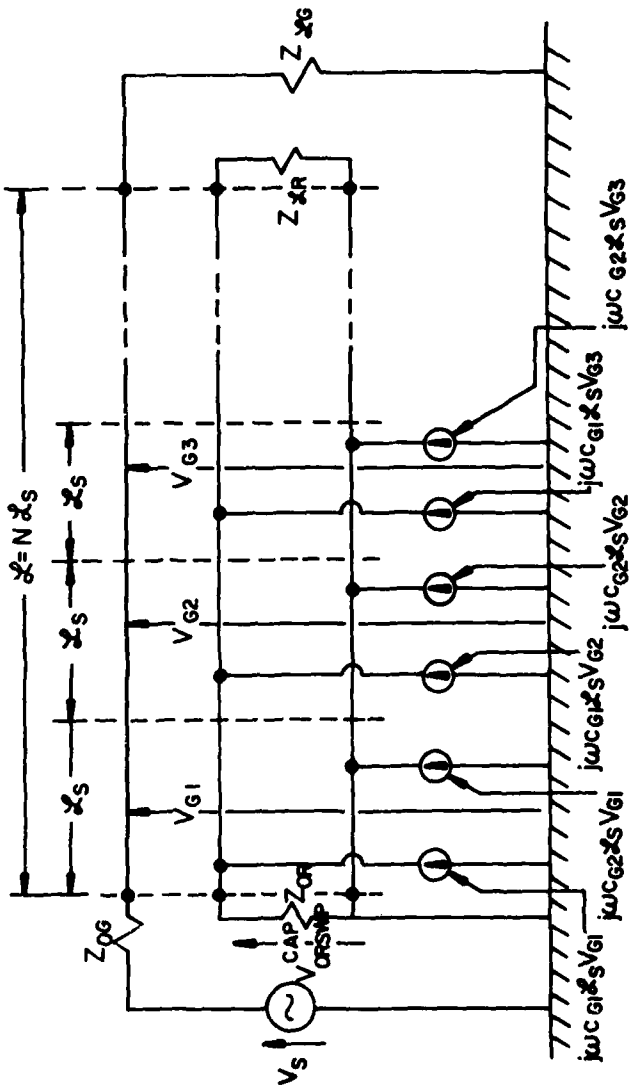
$Z_{\Delta G}$
$Z_{\Delta R}$
$\ell = N\ell_S$
ℓ_S
ℓ_S
ℓ_S
V_{G3}
V_{G2}
V_{G1}
Z_{OG}
Z_{OR}
CAP OR SWP
V_S
$j\omega C_{G2}\ell_S V_{G3}$
$j\omega C_{G1}\ell_S V_{G3}$
$j\omega C_{G2}\ell_S V_{G2}$
$j\omega C_{G1}\ell_S V_{G2}$
$j\omega C_{G2}\ell_S V_{G1}$
$j\omega C_{G1}\ell_S V_{G1}$

Fig. 4-11

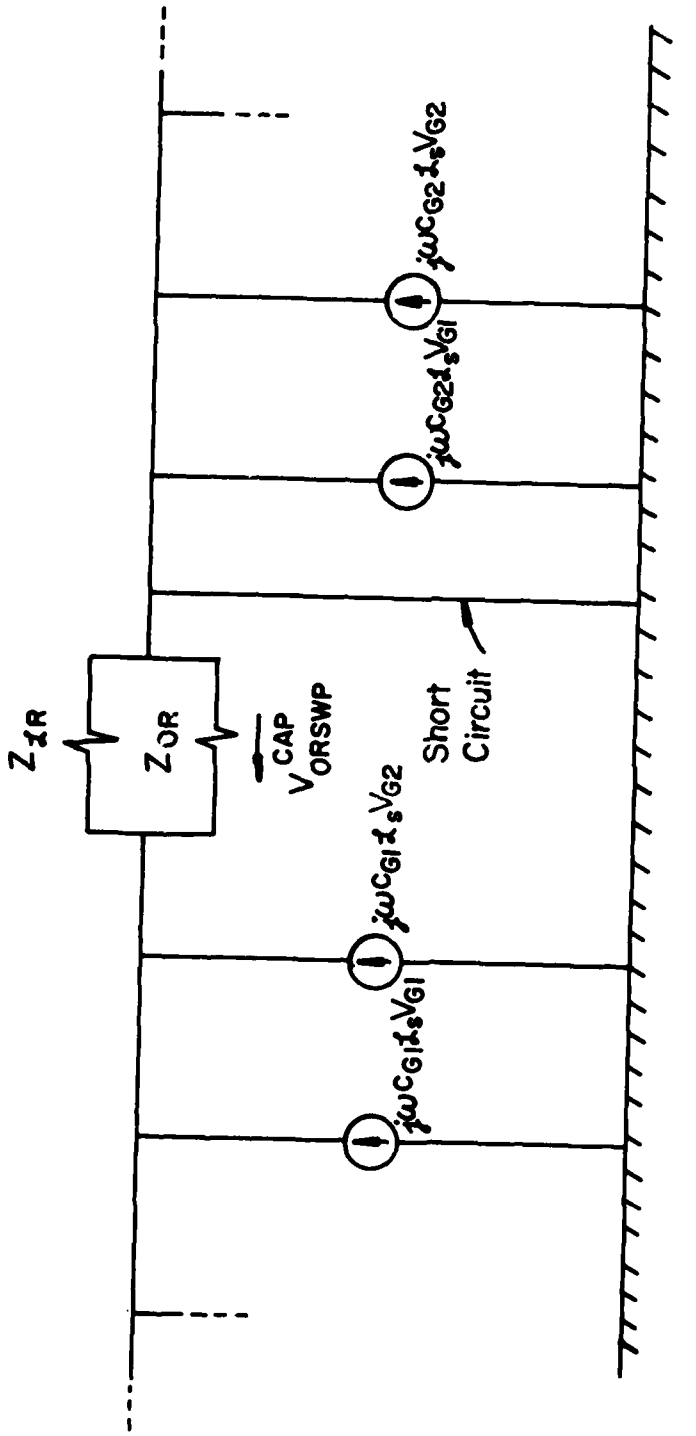
Z_{fR}
Z_{OR}
V_{ORSWP}^{CAP}
Short Circuit
$j\omega C_{G1} f_s V_{G2}$
$j\omega C_{G1} f_s V_{G1}$
$j\omega C_{G2} f_s V_{G1}$
$j\omega C_{G2} f_s V_{G2}$

Fig. 4-12

(4-11) if we assume that $c_{G1} \cong c_{G2}$ as in (4-9). Therefore the capacitive coupling contributions are the same for the twisted wire pair and the straight wire pair configurations.

4.4 Generator Circuit Currents and Voltages

The generator circuit segment voltages, V_{G_i}, and currents, I_{G_i}, will, theoretically, depend upon whether the receptor circuit is a twisted wire pair or a straight wire pair. However, we have implicitly assumed in the preceeding derivations that the generator and receptor circuits are to some degree "weakly coupled" so that the receptor circuit has a negligible or secondary effect on the generator circuit. On the basis of this observation, we will therefore assume that the segment voltages, V_{G_i}, and currents, I_{G_i}, may be computed by considering only the isolated single wire generator circuit. In this case, the segment voltages and currents are independent of the type of receptor circuit.

Furthermore, we will assume that the line, and therefore each segment of length ℓ_s, is electrically short. With this assumption, we may reasonably approximate the segment voltages and currents as

$$I_{G1} = I_{G2} = \cdots = I_{GN} = \frac{V_s}{(Z_{\ell G} + Z_{0G})} \qquad (4\text{-}14)$$

$$V_{G1} = V_{G2} = \cdots = V_{GN} = V_s \left(\frac{Z_{\ell G}}{Z_{\ell G} + Z_{0G}}\right) \tag{4-15}$$

4.5 The Mutual Inductances and Capacitances of the Segments

One final calculation remains; the determination of the segment mutual inductance, ℓ_m, and mutual capacitance, c_{G1} (or c_{G2}).

The segment mutual inductance, ℓ_m, is given by

$$\ell_m = \ell_{G1} - \ell_{G2} \tag{4-16}$$

In Chapter II, the per-unit-length inductance matrix is given by

$$\underset{\sim}{L} = \begin{bmatrix} \ell_{GG} & \ell_{G1} & \ell_{G2} \\ \ell_{G1} & \ell_{11} & \ell_{12} \\ \ell_{G2} & \ell_{12} & \ell_{22} \end{bmatrix} \tag{4-17}$$

where ℓ_{G1} and ℓ_{G2} are given in (2-27d) and (2-27e) as (See Fig. 3-3)

$$\ell_{G1} = 10^{-7} \ell n \left[1 + \frac{4h(h + \Delta h)}{d^2 + \Delta h^2}\right] \tag{4-18}$$

$$\ell_{G2} = 10^{-7} \ell n \left[1 + \frac{4h(h - \Delta h)}{d^2 + \Delta h^2} \right] \tag{4-19}$$

Therefore ℓ_m becomes

$$\ell_m = \ell_{G1} - \ell_{G2}$$

$$= 10^{-7} \ell n \left[\frac{d^2 + \Delta h^2 + 4h^2 + 4h\Delta h}{d^2 + \Delta h^2 + 4h^2 - 4h\Delta h} \right] \tag{4-20}$$

The per-unit-length capacitance matrix $\underset{\sim}{C}$ is found from $\underset{\sim}{L}$ (via the assumption of a homogeneous medium) as

$$\underset{\sim}{C} = \mu_v \epsilon_v \underset{\sim}{L}^{-1} \tag{4-21}$$

$$= \begin{bmatrix} (c_{GG} + c_{G1} + c_{G2}) & -c_{G1} & -c_{G2} \\ -c_{G1} & (c_{11} + c_{G1} + c_{12}) & -c_{12} \\ -c_{G2} & -c_{12} & (c_{22} + c_{G2} + c_{12}) \end{bmatrix}$$

Expanding this result, we obtain,

$$c_{G1} = \mu_v \epsilon_v \frac{(\ell_{G2}\ell_{12} - \ell_{G1}\ell_{22})}{|\underset{\sim}{L}|} \tag{4-22}$$

$$c_{G2} = \mu_v \epsilon_v \frac{(\ell_{G1}\ell_{12} - \ell_{11}\ell_{G2})}{|\underset{\sim}{L}|} \tag{4-23}$$

where $|\underset{\sim}{L}|$ is the determinant of $\underset{\sim}{L}$. From this result, if we assume

$$\ell_{G1} \cong \ell_{G2} \tag{4-24}$$

$$\ell_{11} \cong \ell_{22} \tag{4-25}$$

then clearly $c_{G1} = c_{G2}$. In the computed results, we have chosen c_{G1} to be used in the capacitive coupling model as shown in (4-10) and (4-12).

4.6 The Total Coupling Equation

Combining the results in Sections 4.2, 4.3, and 4.4 we obtain the following results for the received voltage V_{0R};

Twisted Wire Pair:

$$|V_{0R}|_{N\ odd} = \underbrace{|V^{IND}_{0RTWP}|}_{\text{one loop}} + |V^{CAP}_{0RTWP}| \tag{4-26}$$

$$= \left| \frac{Z_{0R}}{(Z_{0R} + Z_{\ell R})} j\omega \ell_s \ell_m \frac{V_s}{(Z_{\ell G} + Z_{0G})} \right|$$

$$+ \left| \frac{Z_{0R} Z_{\ell R}}{(Z_{0R} + Z_{\ell R})} j\omega \ell_s c_{G1} N V_s \frac{Z_{\ell G}}{(Z_{\ell G} + Z_{0G})} \right|$$

$$|V_{0R}|_{N \text{ even}} = \cancel{|V_{0RTWP}^{IND}|}^{0} + |V_{0RTWP}^{CAP}| \qquad (4\text{-}27)$$

$$= \left| \frac{Z_{0R} Z_{\ell R}}{(Z_{0R} + Z_{\ell R})} j\omega \ell_s c_{G1} N V_s \frac{Z_{\ell G}}{(Z_{\ell G} + Z_{0G})} \right|$$

Straight Wire Pair:

$$|V_{0R}| = |V_{0RSWP}^{IND}| + |V_{0RSWP}^{CAP}| \qquad (4\text{-}28)$$

$$= \left| \frac{Z_{0R}}{(Z_{0R} + Z_{\ell R})} j\omega \ell_s \ell_m N \frac{V_s}{(Z_{\ell G} + Z_{0G})} \right|$$

$$+ \left| \frac{Z_{0R} Z_{\ell R}}{(Z_{0R} + Z_{\ell R})} j\omega \ell_s c_{G1} N V_s \frac{Z_{\ell G}}{(Z_{\ell R} + Z_{0G})} \right|$$

4.7 The Coupling Model for Other Excitation Configurations

In the previous model derivations of this chapter, the voltage excitation source, V_s, was attached to the single wire circuit as shown in Fig. 4-1 and Fig. 2-2. The excitation may, however, be

connected to the twisted pair or straight wire pair (which becomes the generator circuit for this situation) as shown in Fig. 4-13 and Fig. 2-15. In this case, we are interested in determining the voltage at either end of the single wire (which becomes the receptor circuit for this situation).

4.7.1 Inductive Coupling

Again we assume that the line is electrically short and determine the equivalent voltage induced in each segment of the receptor circuit (the single wire) by the flux associated with the current in each corresponding segment of the generator circuit (the twisted wire pair or straight wire pair). The net flux passing between the single wire and the ground plane is now due to the currents in each of the two wires comprising the twisted wire pair or straight wire pair generator circuit as shown in Fig. 4-14. In Fig. 4-14, we have assumed that the currents in the two wires of the generator circuit for this segment, I_{G_i}, are equal and oppositely directed. This is based on the assumption that the line (and therefore each segment) is electrically short. This net flux is

$$\phi_i = \ell_{G1} \mathcal{L}_s I_{Gi} - \ell_{G2} \mathcal{L}_s I_{Gi} \qquad (2\text{-}29)$$

$$= (\ell_{G1} - \ell_{G2}) \mathcal{L}_s I_{Gi}$$

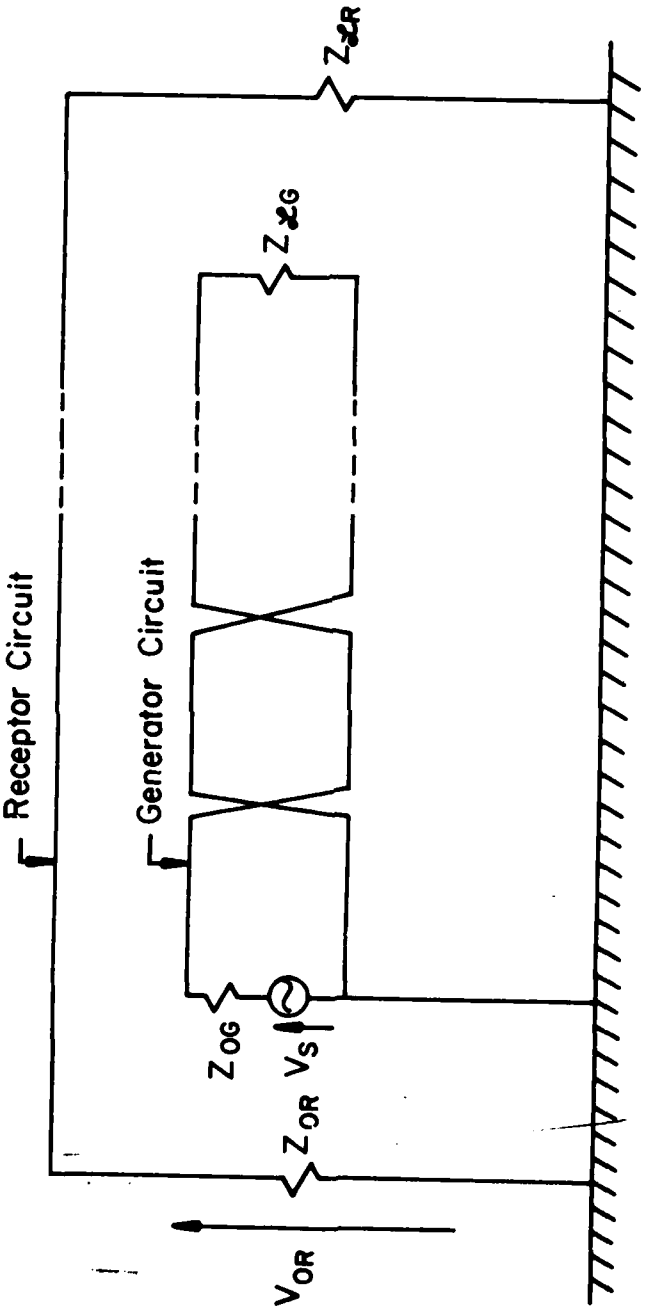

Fig. 4-13

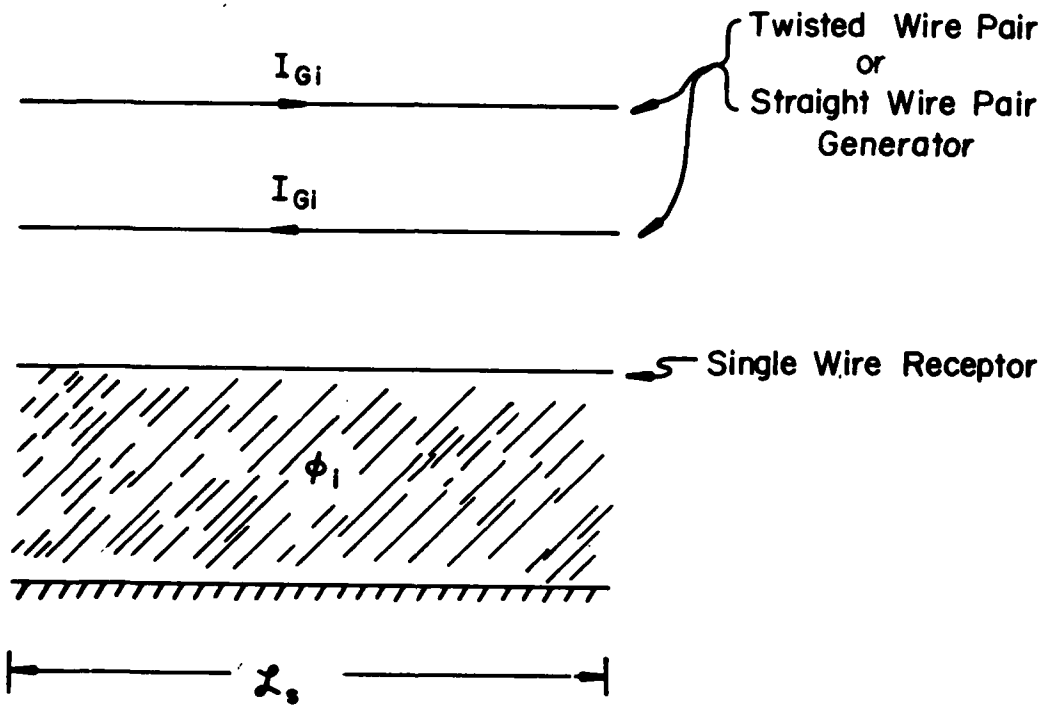
Twisted Wire Pair
or
Straight Wire Pair
Generator
I_{Gi}
I_{Gi}
Single Wire Receptor
ϕ_1
ℓ_s

Fig. 4 - 14

where ℓ_{G1} (ℓ_{G2}) is the mutual inductance between the upper (lower) wire of the twisted wire pair or straight wire pair and the single wire. Clearly ℓ_{G1} and ℓ_{G2} are the same as for the situation in which the excitation, V_s, is attached to the single wire as in Fig. 2-2. The equivalent circuit for the single wire receptor circuit is shown in Fig. 4-15. From this result we obtain

$$V_{0RTWP}^{IND} = \left(\frac{Z_{0R}}{Z_{0R} + Z_{\mathcal{L}R}}\right) j\omega \mathcal{L}_s \ell_m (I_{G1} - I_{G2} + I_{G3} - \ldots) \qquad (4\text{-}30a)$$

and

$$V_{0RSWP}^{IND} = \left(\frac{Z_{0R}}{Z_{0R} + Z_{\mathcal{L}R}}\right) j\omega \mathcal{L}_s \ell_m (I_{G1} + I_{G2} + I_{G3} + \ldots) \qquad (4\text{-}30b)$$

Again we assume that the line is electrically short and approximate the segment currents, I_{G_i}, as

$$I_{G1} = I_{G2} = \ldots = I_{GN} = \left(\frac{V_s}{Z_{0G} + Z_{\mathcal{L}G}}\right) \qquad (4\text{-}31)$$

4.7.2 Capacitive Coupling

The capacitive coupling model for the twisted wire pair generator circuit configuration is shown in Fig. 4-16. The segment voltages V_{bi} and V_{ai} for an electrically short line are approximated as

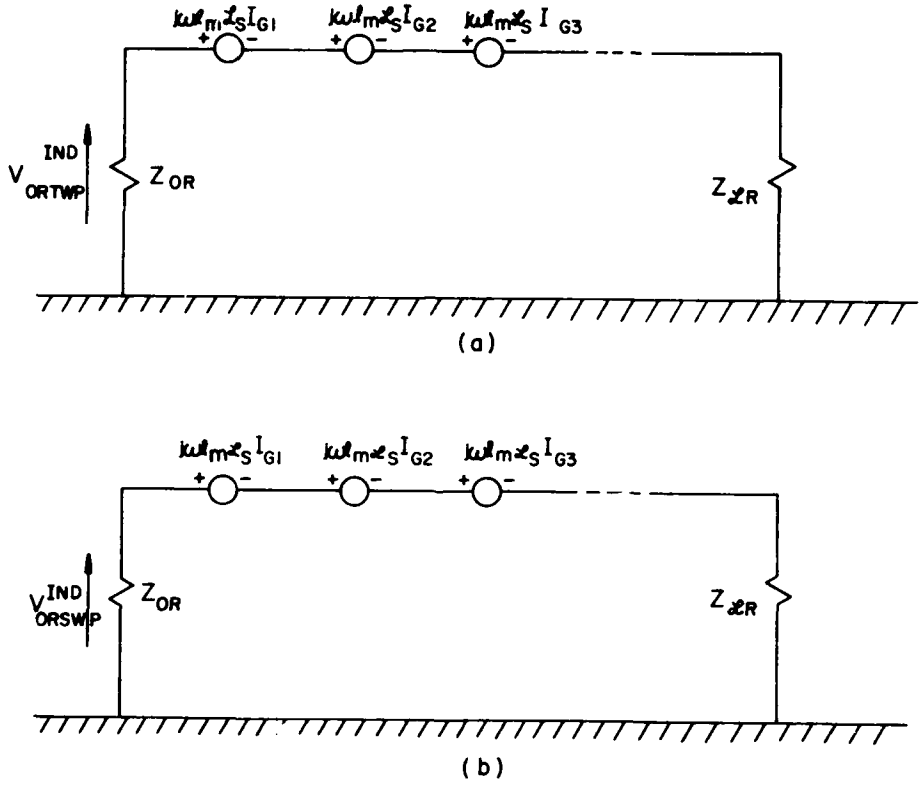
$\omega\ell_{m1}\ell_s I_{G1}$
$\omega\ell_{m2}\ell_s I_{G2}$
$\omega\ell_{m3}\ell_s I_{G3}$
V^{IND}_{ORTWP}
Z_{OR}
$Z_{\ell R}$
(a)
$\omega\ell_{m1}\ell_s I_{G1}$
$\omega\ell_{m2}\ell_s I_{G2}$
$\omega\ell_{m3}\ell_s I_{G3}$
V^{IND}_{ORSWP}
Z_{OR}
$Z_{\ell R}$
(b)

Fig. 4-15

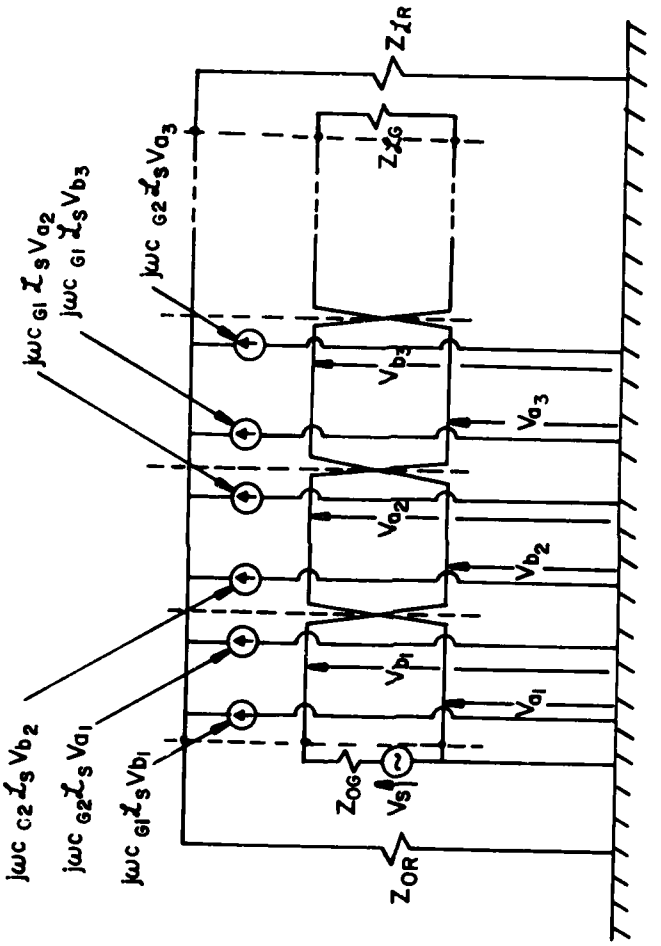
Z_{LR}
Z_{LG}
$jwC_{G2}\mathcal{L}_s V_{a3}$
$jwC_{G1}\mathcal{L}_s V_{b3}$
$jwC_{G1}\mathcal{L}_s V_{a2}$
V_{b3}
V_{a3}
V_{a2}
V_{b2}
V_{b1}
V_{a1}
$jwC_{G2}\mathcal{L}_s V_{b2}$
$jwC_{G2}\mathcal{L}_s V_{a1}$
$jwC_{G1}\mathcal{L}_s V_{b1}$
Z_{OG}
V_s
Z_{OR}

Fig. 4-16

$$V_{b1} = V_{b2} = V_{b3} \cdots \quad V_{bN}$$

and

$$V_{a1} = V_{a2} = V_{a3} \cdots \quad V_{aN}$$

Consequently, the capacitive coupling model

$$V_{0RTWP}^{CAP} = \left(\frac{Z_{0R}Z_{\ell R}}{Z_{0R} + Z_{\ell R}}\right) j\omega \ell_s$$

$$= \left(\frac{Z_{0R}Z_{\ell R}}{Z_{0R} + Z_{\ell R}}\right) j\omega$$

where we have assumed that $c_{G1} = c_{G2}$ and these

are identical to those for the situation in which the

attached to the single wire. The capacitive

straight wire pair generator configuration

to (4-34).

4.7.3 The Total Coupling Model

The magnitude of the total

sum of the magnitudes of the inductive and

tributions. The results are:

Twisted Wire Pair:

$$|V_{0R}|_{N\ odd} = |\underbrace{V^{IND}_{0RTWP}}_{\text{one loop}}| + |V^{CAP}_{0RTWP}| \qquad (4\text{-}35)$$

$$= \left|\frac{Z_{0R}}{(Z_{0R} + Z_{\mathcal{L}R})}\, j\omega \mathcal{L}_s \ell_m \frac{V_s}{(Z_{\mathcal{L}G} + Z_{0G})}\right|$$

$$+ \left|\frac{Z_{0R} Z_{\mathcal{L}R}}{(Z_{0R} + Z_{\mathcal{L}R})}\, j\omega \mathcal{L}_s c_{G1}\, N\, V_s \frac{Z_{\mathcal{L}G}}{(Z_{\mathcal{L}G} + Z_{0G})}\right|$$

$$|V_{0R}|_{N\ even} = |\overset{\searrow\ 0}{V^{IND}_{0RTWP}}| + |V^{CAP}_{0RTWP}| \qquad (4\text{-}36)$$

$$= \left|\frac{Z_{0R} Z_{\mathcal{L}R}}{(Z_{0R} + Z_{\mathcal{L}R})}\, j\omega \mathcal{L}_s c_{G1}\, N\, V_s \frac{Z_{\mathcal{L}G}}{(Z_{\mathcal{L}G} + Z_{0G})}\right|$$

Straight Wire Pair:

$$|V_{0R}| = |V^{IND}_{0RSWP}| + |V^{CAP}_{0RSWP}| \qquad (4\text{-}37)$$

$$= \left|\frac{Z_{0R}}{(Z_{0R} + Z_{\mathcal{L}R})}\, j\omega \mathcal{L}_s \ell_m N \frac{V_s}{(Z_{\mathcal{L}G} + Z_{0G})}\right|$$

$$+ \left|\frac{Z_{0R} Z_{\mathcal{L}R}}{(Z_{0R} + Z_{\mathcal{L}R})}\, j\omega \mathcal{L}_s c_{G1} N\, V_s \frac{Z_{\mathcal{L}G}}{(Z_{\mathcal{L}G} + Z_{0G})}\right|$$

Comparing these results to those for the situation in which the excitation, V_s, is attached to the single wire (See (4-26), (4-27) and (4-28)) we observe that the coupling equations are identical. Therefore one model represents both the situations in Fig. 2-2 and those in Fig. 2-15. Furthermore this implies that the coupling will be the same for the two corresponding situations of Fig. 2-2 and Fig. 2-15 if the corresponding loads on the circuits are the same.

4.8 Prediction Accuracies of the Low Frequency Model

The predictions of the low frequency model for the cases in Fig. 3-4 are compared with the predictions of the chain parameter model in Appendix C. Since the chain parameter model was compared to experimental results in Chapter III and found to yield accurate predictions, experimental results will not be plotted on these graphs. The predictions of both models will be shown for an odd number of loops (N = 225) and an even number of loops (N = 226). In each case, the length of each segment, ℓ_s, was obtained by dividing the total line length, ℓ, by the total number of loops, N. In Appendix C, the excitation and load impedances will be comprised of the following cases:

$$V_1 = 0,\ V_2 = 1,\ R_{01} = 0,\ R_{\ell 1} = R_{02} = R_{\ell 2} = R$$

$$V_1 = 1,\ V_2 = 0,\ R_{02} = 0,\ R_{\ell 2} = R_{01} = R_{\ell 1} = R$$

Six values for R will be used;

1 KΩ, 50Ω, 25Ω, 10Ω, 5Ω, 1Ω and circuit separations of 2 cm and Touching will be investigated. A cross reference of the figure numbers and the configurations they represent is given in Table III.

In these results, the effect of having an odd number of loops as opposed to an even number in the twisted wire pair is only significant for 5Ω and 1Ω loads. For the 1Ω load situation and 2 cm separation, an odd number of loops (N = 225) provides approximately 30 db more coupling than an even number (N = 226) at the lower frequencies. For all cases investigated, the low frequency model not only predicts this difference (within 1 db accuracy) but also predicts with remarkable accuracy (typically within 1 db) the straight wire pair and twisted pair results of the chain parameter model. This rather astonishing accuracy of the simple low frequency model suggests that the separation of the coupling into capacitive and inductive coupling contributions is valid. Note also that the results for $V_1 = 1$, $V_2 = 0$ and $V_1 = 0$, $V_2 = 1$ for corresponding load impendances are identical. This was evident in the low frequency model and provides a further indication of the validity of this model.

TABLE III

Circuit Separation	V_1 (volts)	V_2 (volts)	R01 (Ω)	R02 (Ω)	RL1 (Ω)	RL2 (Ω)	Fig.
Touching	1	0	0	1K	1K	1K	C-1
Touching	1	0	0	50	50	50	C-2
Touching	1	0	0	25	25	25	C-3
Touching	1	0	0	10	10	10	C-4
Touching	1	0	0	5	5	5	C-5
Touching	1	0	0	1	1	1	C-6
Touching	0	1	1K	0	1K	1K	C-7
Touching	0	1	50	0	50	50	C-8
Touching	0	1	25	0	25	25	C-9
Touching	0	1	10	0	10	10	C-10
Touching	0	1	5	0	5	5	C-11
Touching	0	1	1	0	1	1	C-12

TABLE III (continued)

Circuit Separation	V_1(volts)	V_2(volts)	R01(Ω)	R02(Ω)	RL1(Ω)	RL2(Ω)	Fig.
2 cm	1	0	0	1K	1K	1K	C-13
2 cm	1	0	0	50	50	50	C-14
2 cm	1	0	0	25	25	25	C-15
2 cm	1	0	0	10	10	10	C-16
2 cm	1	0	0	5	5	5	C-17
2 cm	1	0	0	1	1	1	C-18
2 cm	0	1	1K	1K	1K	1K	C-19
2 cm	0	1	50	50	50	50	C-20
2 cm	0	1	25	25	25	25	C-21
2 cm	0	1	10	10	10	10	C-22
2 cm	0	1	5	5	5	5	C-23
2 cm	0	1	1	1	1	1	C-24

4.9 Further Observations Based on the Low Frequency Model

It was determined in the previous Section that the low frequency model provides predictions that are virtually identical to the chain parameter model when the line is sufficiently short, electrically. The low frequency model is significant not only for its ability to provide these accurate predictions with very little computational effort but also for its ability to explain the twisted pair coupling phenomena as the following will show.

The ability of the low frequency model to explain numerous aspects of the twisted pair coupling phenomena is a direct result of our separation of the total coupling into capacitive and inductive contributions. Recall that the capacitive coupling contribution for the twisted pair configuration was identical to the capacitive coupling contribution for the straight wire pair configuration. Yet we know from our computed and experimental results that twisting the wire pairs reduces the coupling for low impedance loads and has virtually no effect for high impedance loads. Clearly, if the low frequency model is to explain these results, the effect of the twist must lie in the inductive coupling contribution. The difference in the inductive coupling contributions for the twisted wire pair and straight wire pair configurations is dramatically illustrated by observing the equations for these

contributions given in (4-26), (4-27) and (4-28). From these equations we may form the ratios

$$\frac{|V_{0RSWP}^{IND}|}{|V_{0RTWP}^{IND}|_{N\ odd}} = N \tag{4-38}$$

$$\frac{|V_{0RSWP}^{IND}|}{|V_{0RTWP}^{IND}|_{N\ even}} = \infty \tag{4-39}$$

For an odd number of loops in the twisted pair, the twist reduces the inductive coupling over the straight wire pair by a factor of N. For an even number of loops in the twisted pair, the twist reduces the inductive coupling to zero. This points out an interesting aspect of twisted pair coupling. Although the inductive coupling for an even number of loops is reduced to zero, the total coupling is the sum of the inductive and capacitive coupling contributions and the capacitive coupling is not zero. Therefore even though the twist reduces the inductive coupling, the capacitive coupling contribution provides a "floor" which limits the net reduction in total coupling! Therefore the total coupling is no less than the larger of the capacitive and inductive coupling contributions.

To illustrate this, Tables IV, V and VI show the values of the capacitive and inductive coupling contributions for $V_1 = 1$, $V_2 = 0$, $R_{01} = 0$, $R_{\ell 1} = R_{02} = R_{\ell 2} = R$ and 2 cm circuit separation where R takes on three values, 1000Ω , 50Ω , 1Ω . For R = 1Ω in Table IV, we observe that for the straight wire pair, the total coupling is inductive; the capacitive coupling is below this by a factor of 75 db. However for the twisted wire pair cases, for an even number of loops, the total coupling is limited by the capacitive contribution. For an odd number of loops, the inductive contribution is considerably larger than the capacitive contribution; on the order of 30 db!

For R = 50Ω in Table V, both contributions are of the same order of magnitude for the straight wire pair. For the twisted wire pair and an even number of loops the coupling is capacitive whereas for an odd number of loops the capacitive coupling is on the order of 40 db larger than the inductive component.

For R = 1KΩ in Table VI, the capacitive component dominates the total coupling for the straight wire pair which is on the order of 45 db larger than the inductive component. The capacitive coupling also dominates for an odd number of loops in the twisted wire pairs; being 90 db larger than the inductive component. The total coupling is

TABLE IV

Circuit Separation: 2 cm

$R_{01} = 0$ $R_{\ell 1} = 1\Omega$

$R_{02} = 1\Omega$ $R_{\ell 2} = 1\Omega$

		Twisted Wire Pair				Straight Wire Pair			
		Low Frequency Model			CPM*	Low Frequency Model			CPM*
No. of Loops	Freq(Hz)	CAP(V)	IND(V)	Total(V)	Total(V)	CAP(V)	IND(V)	Total(V)	Total(V)
even	1K	2.09E-8	0	2.09E-8	1.93E-8	2.09E-8	9.91E-5	9.91E-5	9.91E-5
even	5K	1.04E-7	0	1.04E-7	9.65E-8	1.04E-7	4.96E-4	4.96E-4	4.91E-4
even	10K	2.09E-7	0	2.09E-7	1.95E-7	2.09E-7	9.91E-4	9.91E-4	9.54E-4
even	50K	1.04E-6	0	1.04E-6	1.16E-6	1.04E-6	4.96E-3	4.96E-3	2.71E-3
even	100K	2.09E-6	0	2.09E-6	2.88E-6	2.09E-6	9.91E-3	9.91E-3	2.63E-3
even	500K	1.04E-5	0	1.04E-5	1.88E-5	1.04E-5	4.96E-2	4.96E-2	8.28E-4
even	1M	2.09E-5	0	2.09E-5	3.84E-5	2.09E-5	9.91E-2	9.91E-2	3.94E-4
even	5M	1.04E-4	0	1.04E-4	2.63E-4	1.04E-4	4.96E-1	4.96E-1	1.92E-3
even	10M	2.09E-4	0	2.09E-4	5.90E-3	2.09E-4	9.91E-1	9.91E-1	5.47E-4

* Chain Parameter Model

TABLE IV (cont'd)

Circuit Separation: 2 cm

$R_{01} = 0$ $R_{\ell 1} = 1\Omega$

$R_{02} = 1\Omega$ $R_{\ell 2} = 1\Omega$

		Twisted Wire Pair				Straight Wire Pair			
		Low Frequency Model			CPM*	Low Frequency Model			CPM*
No. of Loops	Freq(Hz)	CAP(V)	IND(V)	Total(V)	Total(V)	CAP(V)	IND(V)	Total(V)	Total(V)
odd	1K	2.09E-8	4.41E-7	4.61E-7	4.60E-7	2.09E-8	9.91E-5	9.91E-5	9.91E-5
odd	5K	1.04E-7	2.20E-6	2.31E-6	2.28E-6	1.04E-7	4.96E-4	4.96E-4	4.91E-4
odd	10K	2.09E-7	4.41E-6	4.61E-6	4.41E-6	2.09E-7	9.91E-4	9.91E-4	9.54E-4
odd	50K	1.04E-6	2.20E-5	2.31E-5	1.20E-5	1.04E-6	4.96E-3	4.96E-3	2.71E-3
odd	100K	2.09E-6	4.41E-5	4.61E-5	1.01E-5	2.09E-6	9.91E-3	9.91E-3	2.63E-3
odd	500K	1.04E-5	2.20E-4	2.31E-4	1.52E-5	1.04E-5	4.96E-2	4.96E-2	8.28E-4
odd	1M	2.09E-5	4.41E-4	4.61E-4	3.65E-5	2.09E-5	9.91E-2	9.91E-2	3.94E-4
odd	5M	1.04E-4	2.20E-3	2.31E-3	2.09E-4	1.04E-4	4.96E-1	4.96E-1	1.24E-4
odd	10M	2.09E-4	4.41E-3	4.61E-3	5.90E-4	2.09E-4	9.91E-1	9.91E-1	5.46E-4

*Chain Parameter Model

TABLE V

Circuit Separation: 2 cm

$R_{01} = 0$ $R_{\ell 1} = 50\,\Omega$

$R_{02} = 50\,\Omega$ $R_{\ell 2} = 50\,\Omega$

		Twisted Wire Pair				Twisted Wire Pair			
		Low Frequency Model			CPM*	Low Frequency Model			CPM*
No. of Loops	Freq(Hz)	CAP(V)	IND(V)	Total(V)	Total(V)	CAP(V)	IND(V)	Total(V)	Total(V)
even	1K	1.04E-6	0	1.04E-6	9.62E-7	1.04E-6	1.98E-6	3.03E-6	3.03E-6
even	5K	5.22E-6	0	5.22E-6	4.81E-6	5.22E-6	9.91E-6	1.51E-5	1.51E-5
even	10K	1.04E-5	0	1.04E-5	9.63E-5	1.04E-5	1.98E-5	3.03E-5	3.03E-5
even	50K	5.22E-5	0	5.22E-5	4.81E-5	5.22E-5	9.91E-5	1.51E-4	1.51E-4
even	100K	1.04E-4	0	1.04E-4	9.63E-5	1.04E-4	1.98E-4	3.03E-4	3.02E-4
even	500K	5.22E-4	0	5.22E-4	4.86E-4	5.22E-4	9.91E-4	1.51E-3	1.45E-3
even	1 M	1.04E-3	0	1.04E-3	1.00E-3	1.04E-3	1.98E-3	3.03E-3	2.60E-3
even	5 M	5.22E-3	0	5.22E-3	7.80E-3	5.22E-3	9.91E-3	1.51E-2	6.72E-3
even	10 M	1.04E-2	0	1.04E-2	2.63E-2	1.04E-2	1.98E-2	3.03E-2	2.46E-2

* Chain Parameter Model

TABLE V (cont'd)

Circuit Separation: 2 cm

$R_{01} = 0$ $R_{\ell 1} = 50\,\Omega$

$R_{02} = 50\,\Omega$ $R_{\ell 2} = 50\,\Omega$

		Twisted Wire Pair				Straight Wire Pair			
		Low Frequency Model			CPM*	Low Frequency Model			CPM*
No. of Loops	Freq(Hz)	CAP(V)	IND(V)	Total(V)	Total(V)	CAP(V)	IND(V)	Total(V)	Total(V)
odd	1K	1.04E-6	8.81E-9	1.05E-6	9.72E-7	1.04E-6	1.98E-6	3.03E-6	3.03E-6
odd	5K	5.22E-6	4.41E-8	5.26E-6	4.86E-6	5.22E-6	9.91E-6	1.51E-5	1.51E-5
odd	10K	1.04E-5	8.81E-8	1.05E-5	9.72E-6	1.04E-5	1.98E-5	3.03E-5	3.03E-5
odd	50K	5.22E-5	4.41E-7	5.26E-5	4.86E-5	5.22E-5	9.91E-5	1.51E-4	1.51E-4
odd	100K	1.04E-4	8.81E-7	1.05E-4	9.72E-5	1.04E-4	1.98E-4	3.03E-4	3.02E-4
odd	500K	5.22E-4	4.41E-6	5.26E-4	4.90E-4	5.22E-4	9.91E-4	1.51E-3	1.45E-3
odd	1M	1.04E-3	8.81E-6	1.05E-3	1.01E-3	1.04E-3	1.98E-3	3.03E-3	2.60E-3
odd	5M	5.22E-3	4.41E-5	5.26E-3	7.79E-3	5.22E-3	9.91E-3	1.51E-2	6.72E-3
odd	10M	1.04E-2	8.81E-5	1.05E-2	2.63E-2	1.04E-2	1.98E-2	3.03E-2	2.46E-2

* Chain Parameter Model

TABLE VI

Circuit Separation: 2 cm

$R_{01} = 0$ $R_{\ell 1} = 1K\Omega$

$R_{02} = 1K\Omega$ $R_{\ell 2} = 1K\Omega$

		Twisted Wire Pair				Straight Wire Pair			
		Low Frequency Model			CPM*	Low Frequency Mocel			CPM*
No. of Loops	Freq(Hz)	CAP(V)	IND(V)	Total(V)	Total(V)	CAP(V)	IND(V)	Total(V)	Total(V)
even	1K	2.09E-5	0	2.09E-5	1.93E-5	2.09E-5	9.91E-8	2.10E-5	2.10E-5
even	5K	1.04E-4	0	1.04E-4	9.62E-5	1.04E-4	4.96E-7	1.05E-4	1.05E-4
even	10K	2.09E-4	0	2.09E-4	1.93E-4	2.09E-4	9.91E-7	2.10E-4	2.10E-4
even	50K	1.04E-3	0	1.04E-3	9.62E-4	1.04E-3	4.96E-6	1.05E-3	1.05E-3
even	100K	2.09E-3	0	2.09E-3	1.92E-3	2.09E-3	9.91E-6	2.10E-3	2.10E-3
even	500K	1.04E-2	0	1.04E-2	9.49E-3	1.04E-2	4.96E-5	1.05E-2	1.03E-2
even	1M	2.09E-2	0	2.09E-2	1.82E-2	2.09E-2	9.91E-5	2.10E-2	1.99E-2
even	5M	1.04E-1	0	1.04E-1	4.87E-2	1.04E-1	4.96E-4	1.05E-1	5.36E-2
even	10M	2.09E-1	0	2.09E-1	5.56E-2	2.09E-1	9.91E-4	2.10E-1	6.14E-2

*Chain Parameter Model

TABLE VI (cont'd)

Circuit Separation: 2 cm

R_{01} = 0 $R_{\ell 1}$ = 1KΩ

R_{02} = 1KΩ $R_{\ell 2}$ = 1KΩ

		Twisted Wire Pair				Straight Wire Pair			
		Low Frequency Model			CPM*	Low Frequency Model			CPM*
No. of Loops	Freq(Hz)	CAP(V)	IND(V)	Total(V)	Total(V)	CAP(V)	IND(V)	Total(V)	Total(V)
odd	1K	2.09E-5	4.41E-10	2.09E-5	1.93E-5	2.09E-5	9.91E-8	2.10E-5	2.10E-5
odd	5K	1.04E-4	2.20E-9	1.04E-4	9.63E-5	1.04E-4	4.96E-7	1.05E-4	1.05E-4
odd	10K	2.09E-4	4.41E-9	2.09E-4	1.93E-4	2.09E-4	9.91E-7	2.10E-4	2.10E-4
odd	50K	1.04E-3	2.20E-8	1.04E-3	9.63E-4	1.04E-3	4.96E-6	1.05E-3	1.05E-3
odd	100K	2.09E-3	4.41E-8	2.09E-3	1.93E-3	2.09E-3	9.91E-6	2.10E-3	2.10E-3
[illegible]	[illegible]	[illegible]	[illegible]	[illegible]	[illegible]	[illegible]	[illegible]	[illegible]	[illegible]
[illegible]	[illegible]	[illegible]	[illegible]	[illegible]	[illegible]	[illegible]	[illegible]	[illegible]	[illegible]
[illegible]	[illegible]	[illegible]	[illegible]	[illegible]	[illegible]	[illegible]	[illegible]	[illegible]	[illegible]

purely capacitive for the twisted wire pair with an even number of loops.

Thus we have shown cases involving twisted wire pairs in which the capacitive coupling dominated the inductive coupling and cases in which the inductive coupling dominated the capacitive coupling. The fact that the low frequency model predicted each of these cases with extraordinary accuracy should provide strong evidence to indicate that the individual equations for the capacitive and inductive contributions are both correct.

4.10 Balanced Load Configurations

All of the previous single wire, twisted wire pair, and straight wire pair configurations are commonly termed as "unbalanced". Quite often, an attempt is made to "balance" the loads with either center tapped transformers or dual input-dual output operational amplifiers. This "balanced" load configuration for the twisted wire pair is shown in Fig. 4-17, and is supposedly used to further reduce the coupling over that attainable with the unbalanced case. Therefore, since this configuration is such a popular choice over the "unbalanced" configurations, we will investigate this twisted wire pair circuit configuration using the same approach as discussed for the unbalanced cases

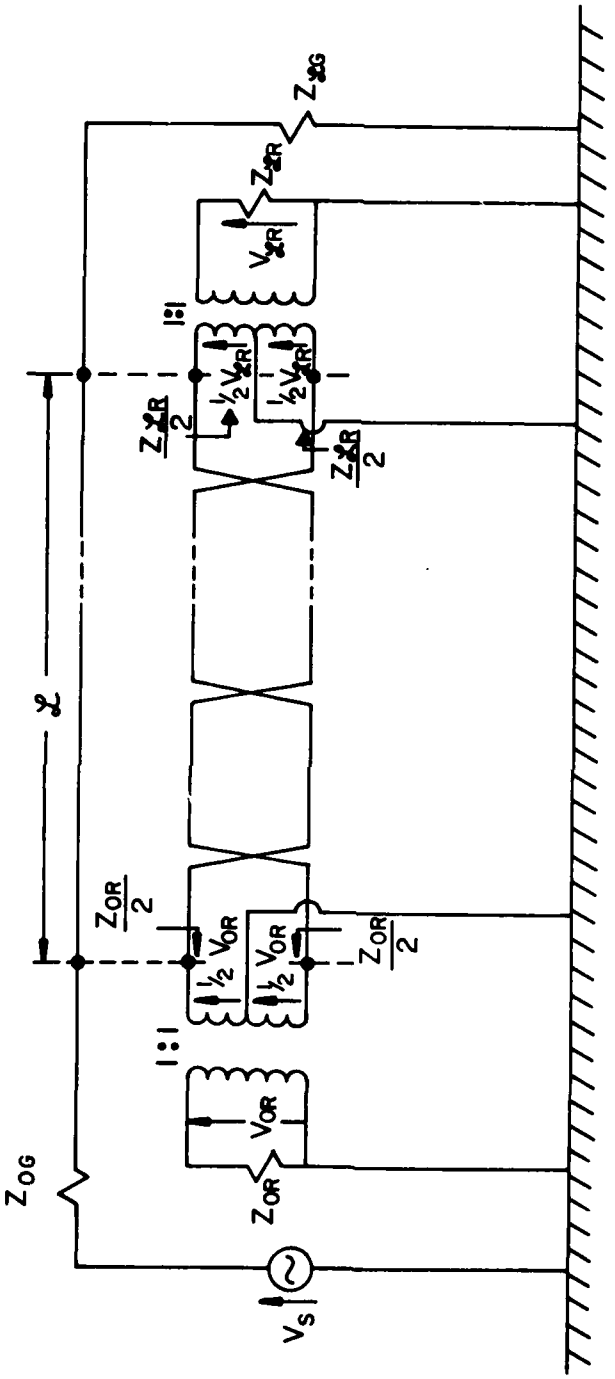

Fig. 4-17

in which the chain parameter model and a low frequency model will be derived.

Note that the balanced load configuration for the twisted wire pair of Fig. 4-17 can be reduced for modeling purposes to that of Fig. 4-18. Obviously the overall chain parameter matrix for this balanced load configuration will be the same as for the unbalanced configuration developed in Chapter II. The difference in the chain parameter model will be in the terminal network equations. The terminal network equations for the balanced load configurations are developed in the same manner as in Chapter II and the result is easily seen to be

$$\underline{V}(0) = \underline{V} - \underset{\sim}{Z}_0 \underline{I}(0) \tag{4-40a}$$

$$\underline{I}(\mathcal{L}) = \underset{\sim}{Y}_{\mathcal{L}} \underline{V}(\mathcal{L}) \tag{4-40b}$$

where

$$\underline{V}(0) = \begin{bmatrix} V_G(0) \\ V_{R1}(0) \\ V_{R2}(0) \end{bmatrix} \qquad \underline{V}(\mathcal{L}) = \begin{bmatrix} V_G(\mathcal{L}) \\ V_{R1}(\mathcal{L}) \\ V_{R2}(\mathcal{L}) \end{bmatrix} \qquad \underline{V} = \begin{bmatrix} V_s \\ 0 \\ 0 \end{bmatrix}$$

$$\underline{I}(0) = \begin{bmatrix} I_G(0) \\ I_{R1}(0) \\ I_{R2}(0) \end{bmatrix} \qquad \underline{I}(\mathcal{L}) = \begin{bmatrix} I_G(\mathcal{L}) \\ I_{R1}(\mathcal{L}) \\ I_{R2}(\mathcal{L}) \end{bmatrix} \tag{4-41}$$

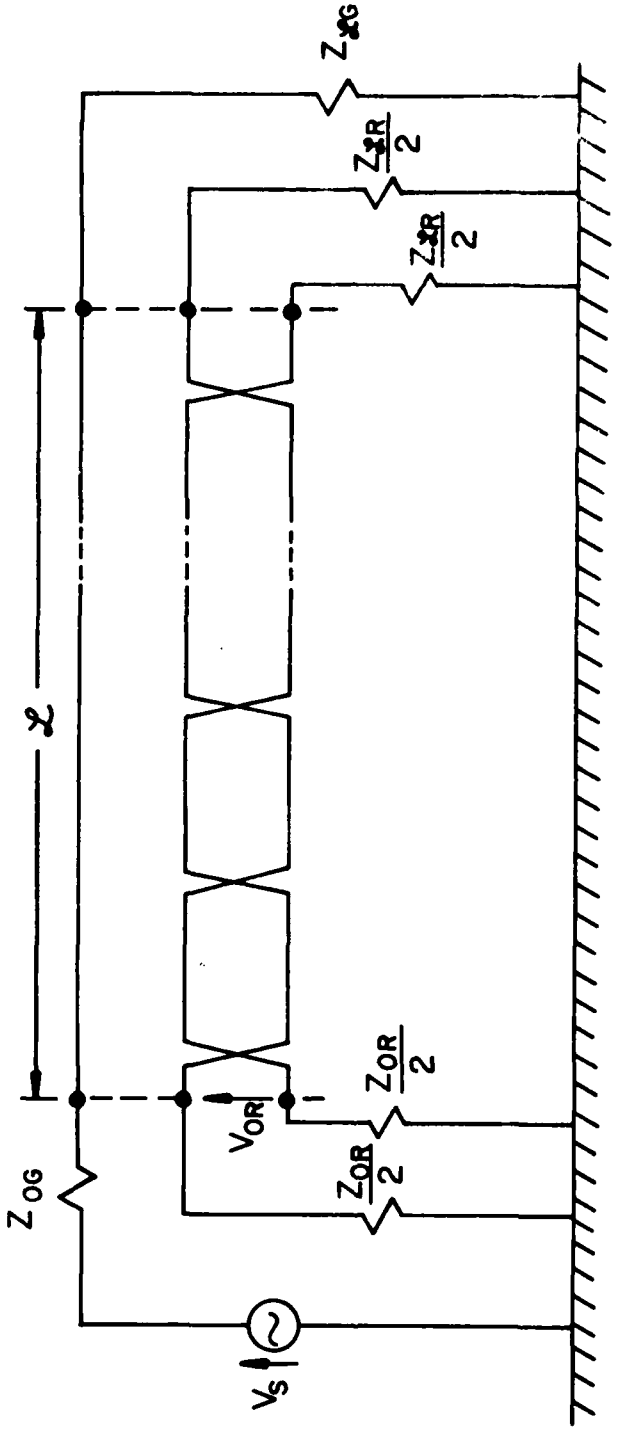

Fig. 4-18

$$\underset{\sim}{Z}_0 = \begin{bmatrix} Z_{0G} & 0 & 0 \\ 0 & \frac{Z_{0R}}{2} & 0 \\ 0 & 0 & \frac{Z_{0R}}{2} \end{bmatrix} \qquad \underset{\sim}{Y}_{\ell} = \begin{bmatrix} \frac{1}{Z_{\ell G}} & 0 & 0 \\ 0 & \frac{2}{Z_{\ell R}} & 0 \\ 0 & 0 & \frac{2}{Z_{\ell R}} \end{bmatrix}$$

Note that the only difference in these equations and those developed for the unbalanced load configurations in equations (2-29) and (2-30) is on $\underset{\sim}{Z}_0$ and $\underset{\sim}{Y}_{\ell}$. Therefore, the chain parameter model for the balanced load configuration can be obtained using a similar formulation to that of the unbalanced case.

In developing the low frequency model of the balanced load configuration, one can again model the inductive and capacitive components separately as was done in Sections 4-2 and 4-3, where Fig. 4-19 shows the resulting circuit models. If the circuits are simplified as was done in Sections 4-2 and 4-3 the result would be as shown in Fig. 4-20. From these circuits we obtain,

$$V_{0RTWP}^{IND} = \frac{Z_{0R}}{(Z_{0R} + Z_{\ell R})} = j\omega \ell_s \{\ell_{G1}(I_{G1} + I_{G3} + \ldots)$$

$$+ \ell_{G2}(I_{G2} + I_{G4} + \ldots)\}$$

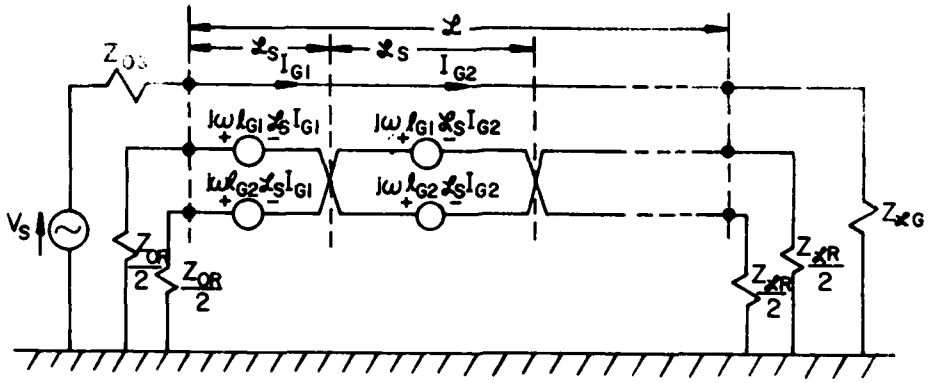
$\mathcal{L}$
$\mathcal{L}_S$
$\mathcal{L}_S$
I_{G1}
I_{G2}
Z_{OG}
$j\omega l_{G1}\mathcal{L}_S I_{G1}$
$j\omega l_{G1}\mathcal{L}_S I_{G2}$
$j\omega l_{G2}\mathcal{L}_S I_{G1}$
$j\omega l_{G2}\mathcal{L}_S I_{G2}$
V_S
$\frac{Z_{OR}}{2}$
$\frac{Z_{OR}}{2}$
$Z_{\mathcal{L}G}$
$\frac{Z_{\mathcal{L}R}}{2}$
$\frac{Z_{\mathcal{L}R}}{2}$

(a)

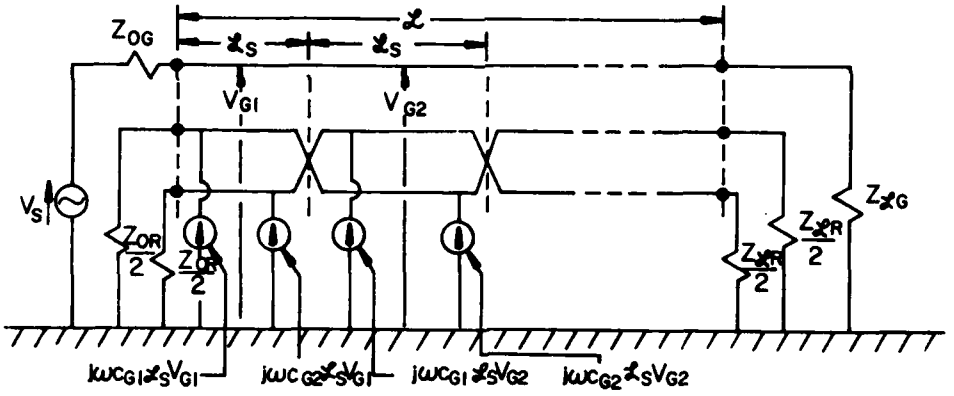
$\mathcal{L}$
$\mathcal{L}_S$
$\mathcal{L}_S$
Z_{OG}
V_{G1}
V_{G2}
V_S
$\frac{Z_{OR}}{2}$
$\frac{Z_{OR}}{2}$
$Z_{\mathcal{L}G}$
$\frac{Z_{\mathcal{L}R}}{2}$
$\frac{Z_{\mathcal{L}R}}{2}$
$j\omega C_{G1}\mathcal{L}_S V_{G1}$
$j\omega C_{G2}\mathcal{L}_S V_{G1}$
$j\omega C_{G1}\mathcal{L}_S V_{G2}$
$j\omega C_{G2}\mathcal{L}_S V_{G2}$

(b)

Fig. 4 -19

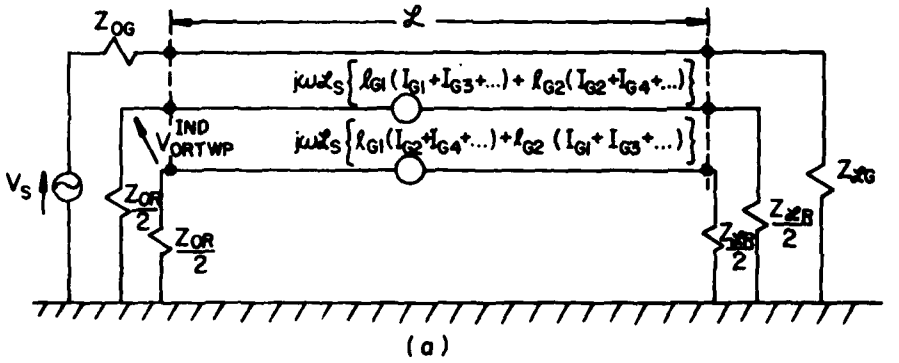
Z_{OG}
ℓ
$j\omega\ell_S\{\ell_{G1}(I_{G1}+I_{G3}+\ldots)+\ell_{G2}(I_{G2}+I_{G4}+\ldots)\}$
IND
V_{ORTWP}
$j\omega\ell_S\{\ell_{G1}(I_{G2}+I_{G4}+\ldots)+\ell_{G2}(I_{G1}+I_{G3}+\ldots)\}$
V_S
$\frac{Z_{OR}}{2}$
$\frac{Z_{OR}}{2}$
$\frac{Z_{\ell R}}{2}$
$\frac{Z_{\ell R}}{2}$
$Z_{\ell G}$

(a)

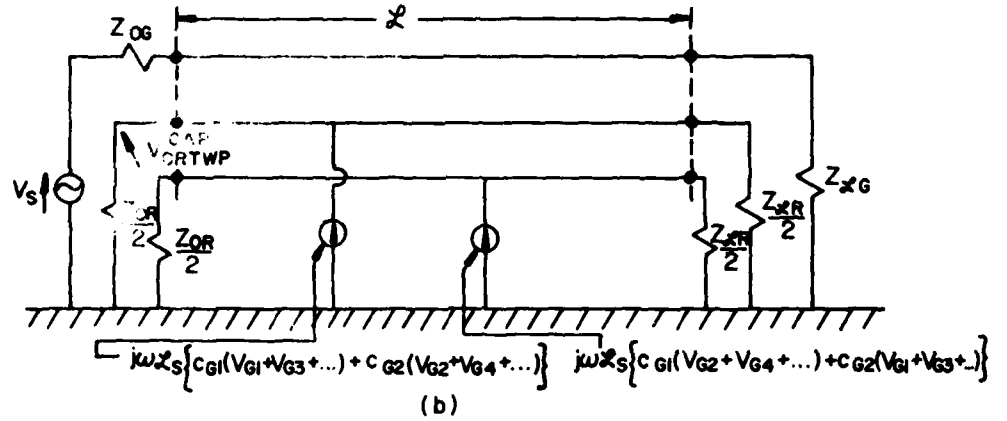
Z_{OG}
ℓ
CAP
V_{ORTWP}
V_S
$\frac{Z_{OR}}{2}$
$\frac{Z_{OR}}{2}$
$\frac{Z_{\ell R}}{2}$
$\frac{Z_{\ell R}}{2}$
$Z_{\ell G}$
$j\omega\ell_S\{C_{G1}(V_{G1}+V_{G3}+\ldots)+C_{G2}(V_{G2}+V_{G4}+\ldots)\}$
$j\omega\ell_S\{C_{G1}(V_{G2}+V_{G4}+\ldots)+C_{G2}(V_{G1}+V_{G3}+\ldots)\}$

(b)

Fig. 4-20

$$- \left(\frac{Z_{0R}}{Z_{0R} + Z_{\ell R}}\right) j\omega \ell_s \{\ell_{G1}(I_{G2} + I_{G4} + \ldots) + \ell_{G2}(I_{G1} + I_{G3} + \ldots)\}$$

$$= \left(\frac{Z_{0R}}{Z_{0R} + Z_{\ell R}}\right) j\omega \ell_s (\ell_{G1} - \ell_{G2}) \{I_{G1} - I_{G2} + I_{G3} - \ldots\}$$

$$= \left(\frac{Z_{0R}}{Z_{0R} + Z_{\ell R}}\right) j\omega \ell_s \ell_m XI_{TWP} \qquad (4\text{-}42)$$

and

$$V_{0RTWP}^{CAP} = \frac{1}{2} \left(\frac{Z_{0R} Z_{\ell R}}{Z_{0R} + Z_{\ell R}}\right) j\omega \ell_s \{c_{G1}(V_{G1} + V_{G3} + \ldots) + c_{G2} (V_{G2} + V_{G4} + \ldots)\}$$

$$- \frac{1}{2} \left(\frac{Z_{0R} Z_{\ell R}}{Z_{0R} + Z_{\ell R}}\right) j\omega \ell_s \{c_{G1}(V_{G2} + V_{G4} + \ldots) + c_{G2} (V_{G2} + V_{G4} + \ldots)\}$$

$$= \frac{1}{2} \left(\frac{Z_{0R} Z_{\ell R}}{Z_{0R} + Z_{\ell R}}\right) j\omega \ell_s (c_{G1} - c_{G2}) \{V_{G1} - V_{G2} + V_{G3} - \ldots\} \qquad (4\text{-}43)$$

The inductive coupling contribution for the balanced load configuration is the same as for the unbalanced case as shown in equations (4-4) and (4-42). The capacitive coupling for the balanced load con-

figuration is dramatically different from that of the unbalanced as shown in equations (4-10) and (4-43). Note that if $c_{G1} \cong c_{G2}$ as reasoned in equation (4-9) that equation (4-43) will equal zero! Thus there is a canceling effect in the capacitive coupling when the balanced load configuration is used. This canceling effect can be seen when Fig. 4-10 is compared to Fig. 4-20(b), where it is apparent that there is no short circuit present in the circuit of Figs. 4-20(b) as there is in Fig. 4-10 in which the short circuit does not allow the current sources on the right of the circuit of Fig. 4-10 to cancel with th[illegible]on the left of the circuit. This is an amazing result since one can now lower the capacitive floor of the twisted wire pair configuration for the unbalanced case by balancing the load. One could similarly develop the low frequency model for the SWP balanced load configuration. The results would obviously be the same as for the straight wire pair unbalanced load configuration in the inductive contribution and the capacitive coupling contribution would be zero.

In order to verify the low frequency model results for the balanced load twisted wire pair configuration, we will again compare the low frequency model predictions to those of the chain parameter model for the equal load cases. Tables VII, VIII, and IX show comparisons of the total coupling calculated using the low frequency model and using

TABLE VII

Circuit Separation: 2 cm

$R_{01} = 0$ $R_{\ell 1} = 1\Omega$

$R_{02} = 1\Omega$ $R_{\ell 2} = 1\Omega$

		Twisted Wire Pair				Straight Wire Pair			
		Low Frequency Model			CPM*	Low Frequency Model			CPM*
No. of Loops	Freq(Hz)	CAP(V)	IND(V)	Total(V)	Total(V)	CAP(V)	IND(V)	Total(V)	Total(V)
even	1K	0	0	0	3.75E-13	0	9.91E-5	9.91E-5	9.90E-5
even	5K	0	0	0	9.22E-12	0	4.96E-4	4.96E-4	4.85E-4
even	10K	0	0	0	3.52E-11	0	9.91E-4	9.91E-4	9.12E-4
even	50K	0	0	0	4.98E-10	0	4.96E-3	4.96E-3	2.17E-3
even	100K	0	0	0	1.22E-9	0	9.91E-3	9.91E-3	2.04E-3
even	500K	0	0	0	7.13E-9	0	4.96E-2	4.96E-2	6.51E-4
even	1 M	0	0	0	1.44E-8	0	9.91E-2	9.91E-2	3.32E-4
even	5 M	0	0	0	7.22E-8	0	4.96E-1	4.96E-1	6.15E-5
even	10 M	0	0	0	1.44E-7	0	9.91E-1	9.91E-1	2.19E-5

* Chain Parameter Model

TABLE VII (cont'd)

Circuit Separation: 2 cm

$R_{01} = 0$ $R_{\ell 1} = 1\Omega$

$R_{02} = 1\Omega$ $R_{\ell 2} = 1\Omega$

		Twisted Wire Pair				Straight Wire Pair			
		Low Frequency Model			CPM*	Low Frequency Model			CPM*
No. of Loops	Freq(Hz)	CAP(V)	IND(V)	Total(V)	Total(V)	CAP(V)	IND(V)	Total(V)	Total(V)
odd	1K	0	4.41E-7	4.41E-7	4.40E-7	0	9.91E-5	9.91E-5	9.90E-5
odd	5K	0	2.20E-6	2.20E-6	2.15E-6	0	4.96E-4	4.96E-4	4.85E-4
odd	10K	0	4.41E-6	4.41E-6	4.05E-6	0	9.91E-4	9.91E-4	9.12E-4
odd	50K	0	2.20E-5	2.20E-5	9.62E-6	0	4.96E-3	4.96E-3	2.17E-3
odd	100K	0	4.41E-5	4.41E-5	9.07E-6	0	9.91E-3	9.91E-3	2.04E-3
odd	500K	0	2.20E-4	2.20E-4	2.89E-6	0	4.96E-2	4.96E-2	6.51E-4
odd	1M	0	4.41E-4	4.41E-4	1.47E-6	0	9.91E-2	9.91E-2	3.32E-4
odd	5M	0	2.20E-3	2.20E-3	2.51E-7	0	4.96E-1	4.96E-1	6.15E-5
odd	10M	0	4.41E-3	4.41E-3	6.35E-8	0	9.91E-1	9.91E-1	2.19E-5

* Chain Parameter Model

TABLE VIII

Circuit Separation: 2 cm

$R_{01} = 0$ $R_{\ell 1} = 50\,\Omega$

$R_{02} = 50\,\Omega$ $R_{\ell 2} = 50\,\Omega$

		Twisted Wire Pair				Straight Wire Pair			
		Low Frequency Model			CPM*	Low Frequency Model			CPM*
No. of Loops	Freq(Hz)	CAP(V)	IND(V)	Total(V)	Total(V)	CAP(V)	IND(V)	Total(V)	Total(V)
even	1K	0	0	0	3.76E-13	0	1.98E-6	1.98E-6	2.06E-6
even	5K	0	0	0	9.39E-12	0	9.91E-6	9.91E-6	1.03E-6
even	10K	0	0	0	3.76E-11	0	1.98E-5	1.98E-5	2.06E-5
even	50K	0	0	0	9.38E-10	0	9.91E-5	9.91E-5	1.03E-4
even	100K	0	0	0	3.75E-9	0	1.98E-4	1.98E-4	2.06E-4
even	500K	0	0	0	8.79E-8	0	9.91E-4	9.91E-4	9.51E-4
even	1M	0	0	0	3.06E-7	0	1.98E-3	1.98E-3	1.59E-3
even	5M	0	0	0	3.07E-6	0	9.91E-3	9.91E-3	2.06E-3
even	10M	0	0	0	6.84E-6	0	1.98E-2	1.98E-2	1.19E-3

* Chain Parameter Model

TABLE VIII (cont'd)

Circuit Separation: 2 cm

$R_{01} = 0$ $R_{\ell 1} = 50\,\Omega$

$R_{02} = 50\,\Omega$ $R_{\ell 2} = 50\,\Omega$

		Twisted Wire Pair				Straight Wire Pair			
		Low Frequency Model			CPM*	Low Frequency Model			CPM*
No. of Loops	Freq(Hz)	CAP(V)	IND(V)	Total(V)	Total(V)	CAP(V)	IND(V)	Total(V)	Total(V)
odd	1K	0	8.81E-9	8.81E-9	9.17E-9	0	1.98E-6	1.98E-6	2.06E-6
odd	5K	0	4.41E-8	4.41E-8	4.59E-8	0	9.91E-6	9.91E-6	1.03E-5
odd	10K	0	8.81E-8	8.81E-8	9.17E-8	0	1.98E-5	1.98E-5	2.06E-5
odd	50K	0	4.41E-7	4.41E-7	4.58E-7	0	9.91E-5	9.91E-5	1.03E-4
odd	100K	0	8.81E-7	8.81E-7	9.14E-7	0	1.98E-4	1.98E-4	2.06E-4
odd	500K	0	4.41E-6	4.41E-6	4.22E-6	0	9.91E-4	9.91E-4	9.51E-4
odd	1M	0	8.81E-6	8.81E-6	7.06E-6	0	1.98E-3	1.98E-3	1.59E-3
odd	5M	0	4.41E-5	4.41E-5	8.38E-6	0	9.91E-3	9.91E-3	2.06E-3
odd	10M	0	8.81E-5	8.81E-5	3.46E-6	0	1.98E-2	1.98E-2	1.19E-3

*Chain Parameter Model

TABLE IX

Circuit Separation: 2 cm

$R_{01} = 0$ $R_{\ell 1} = 1K\Omega$

$R_{02} = 1K\Omega$ $R_{\ell 2} = 1K\Omega$

		Twisted Wire Pair				Straight Wire Pair			
		Low Frequency Model			CPM*	Low Frequency Model			CPM*
No. of Loops	Freq(Hz)	CAP(V)	IND(V)	Total(V)	Total(V)	CAP(V)	IND(V)	Total(V)	Total(V)
even	1K	0	0	0	3.76E-13	0	9.91R-8	9.91E-8	1.73E-6
even	5K	0	0	0	9.39E-12	0	4.96E-7	4.96E-7	8.65E-6
even	10K	0	0	0	3.76E-11	0	9.91E-7	9.91E-7	1.73E-5
even	50K	0	0	0	9.39E-10	0	4.96E-6	4.96E-6	8.65E-5
even	100K	0	0	0	3.76E-9	0	9.91E-6	9.91E-6	1.73E-4
even	500K	0	0	0	9.39E-8	0	4.96E-5	4.96E-5	8.65E-4
even	1M	0	0	0	3.76E-7	0	9.91E-5	9.91E-5	1.73E-3

TABLE IX (cont'd)

Circuit Separation: 2 cm

R_{01} = 0 $R_{\ell 1}$ = 1KΩ

R_{02} = 1KΩ $R_{\ell 2}$ = 1KΩ

		Twisted Wire Pair				Straight Wire Pair			
		Low Frequency Model			CPM*	Low Frequency Model			CPM*
No. of Loops	Freq(Hz)	CAP(V)	IND(V)	Total(V)	Total(V)	CAP(V)	IND(V)	Total(V)	Total(V)
odd	1K	0	4.41E-10	4.41E-10	7.69E-9	0	9.91E-8	9.91E-8	1.73E-4
odd	5K	0	2.20E-9	2.20E-9	3.85E-8	0	4.96E-7	4.96E-7	8.65E-6
odd	10K	0	4.41E-9	4.41E-9	7.69E-8	0	9.91E-7	9.91E-7	1.73E-5
odd	50K	0	2.20E-8	2.20E-8	3.85E-7	0	4.96E-6	4.96E-6	8.65E-5
odd	100K	0	4.41E-8	4.41E-8	7.69E-7	0	9.91E-6	9.91E-6	1.73E-4
odd	500K	0	2.20E-7	2.20E-7	3.80E-6	0	4.96E-5	4.96E-5	8.57E-4
odd	1M	0	4.41E-7	4.41E-7	7.38E-6	0	9.91E-5	9.91E-5	1.67E-3
odd	5M	0	2.20E-6	2.20E-6	2.11E-5	0	4.96E-4	4.96E-4	5.17E-3
odd	10M	0	4.41E-6	4.41E-6	2.11E-5	0	9.91E-4	9.91E-4	7.26E-3

* Chain Parameter Model

the chain parameter model for both the twisted wire pair and straight wire pair configurations.

Note in these tables for the twisted wire pair configuration that for an even number of loops, the total coupling for the low frequency model is equal to zero whereas the chain parameter model results are negligible or very near zero. For an odd number of loops and low frequencies the low frequency model and the chain parameter model both show almost the same total coupling, which has been found to be purely inductive in the balanced load configuration since the capacitive coupling is essentially zero.

Note also in these tables that the low frequency model compares very well with the chain parameter model in predicting straight wire pair coupling. Thus once again, the low frequency model proves to be accurate in computing total coupling, not only for unbalanced but also balanced load configurations.

V. SUMMARY

In reviewing the results of this work, there are many conclusions to be emphasized. Therefore, the results are listed in statement form under the following categories;

(1) Accuracy of the Chain Parameter Model Predictions

(a) The chain parameter models for the single wire, straight wire pair, and twisted wire pair configurations accurately predict the corresponding coupling.

(b) For "high" impedance loads both the single wire model and straight wire pair model predict twisted wire pair coupling very well.

(c) For "low" impedance loads neither the single wire model nor the straight wire pair model do well in predicting twisted wire pair coupling.

(d) The twisted wire pair model predicts twisted wire pair coupling very well for both "high" and "low" impedance loads.

(2) Comparison of the Effectiveness of the Three Circuit Configurations in Reducing Crosstalk

(a) For "high" impedance loads, the single wire, the straight wire

pair, and twisted wire pair configurations all give the same amount of coupling (i.e. the transfer ratios for each circuit configuration are approximately the same).

(b) For "low" impedance loads, the twisted wire pair configuration is the most effective in reducing crosstalk, followed by the straight wire pair configuration and then by the single wire configuration.

(3) Comparison of the Low Frequency Model Predictions

(a) The low frequency models for the straight wire pair and twisted wire configurations, accurately predict the corresponding circuit configuration coupling for both the balanced and unbalanced load configurations.

(b) The low frequency model is easier to conceptually model than that of the chain parameter model (i.e., software development is simpler.)

(c) The actual computation time for the low frequency model is much less than that of the chain parameter model since the mathematics modeling is proportionally less (verified from actual usage).

(d) Since in actual practice the circuit configurations are not as modeled but more of a random configuration (such as in random cable bundles) the low frequency model is much more attractive to use since it accurately predicts coupling, but also is much more efficient computationally than the chain parameter model.

(4) Low Frequency Model Implications

(a) The low frequency model shows that the inductive coupling component is zero for an even number of twists in the twisted wire pair configuration, and is equivalent to that in only one loop for an odd number of loops.

(b) The low frequency model shows that there is a capacitive "floor" on coupling for the unbalanced load configurations.

Although twisting of wire pairs has proven to reduce inductive coupling, this capacitive "floor" may limit the total reduction in coupling, therefore the twisting may have no effect.

(c) The low frequency model shows that the capacitive "floor" on coupling seen in the unbalanced load configuration is reduced in the balanced load configurations.

The objective of this work was to quantitatively predict coupling to twisted wire pairs. This was achieved by developing two models, the chain parameter model and the low frequency model. The chain parameter model was found to be very accurate for all frequency ranges except the standing wave region where the results, although not as accurate as lower frequencies, still tend to follow the experimental results. Generally speaking, the low frequency model proved to be as accurate as the chain parameter model for frequencies such that the

line is electrically short, e.g., when the line length is less than $1/20\,\lambda$. The low frequency model was found to be more appealing since not only was it simpler to derive but led to more insight into the components of coupling.

APPENDIX A

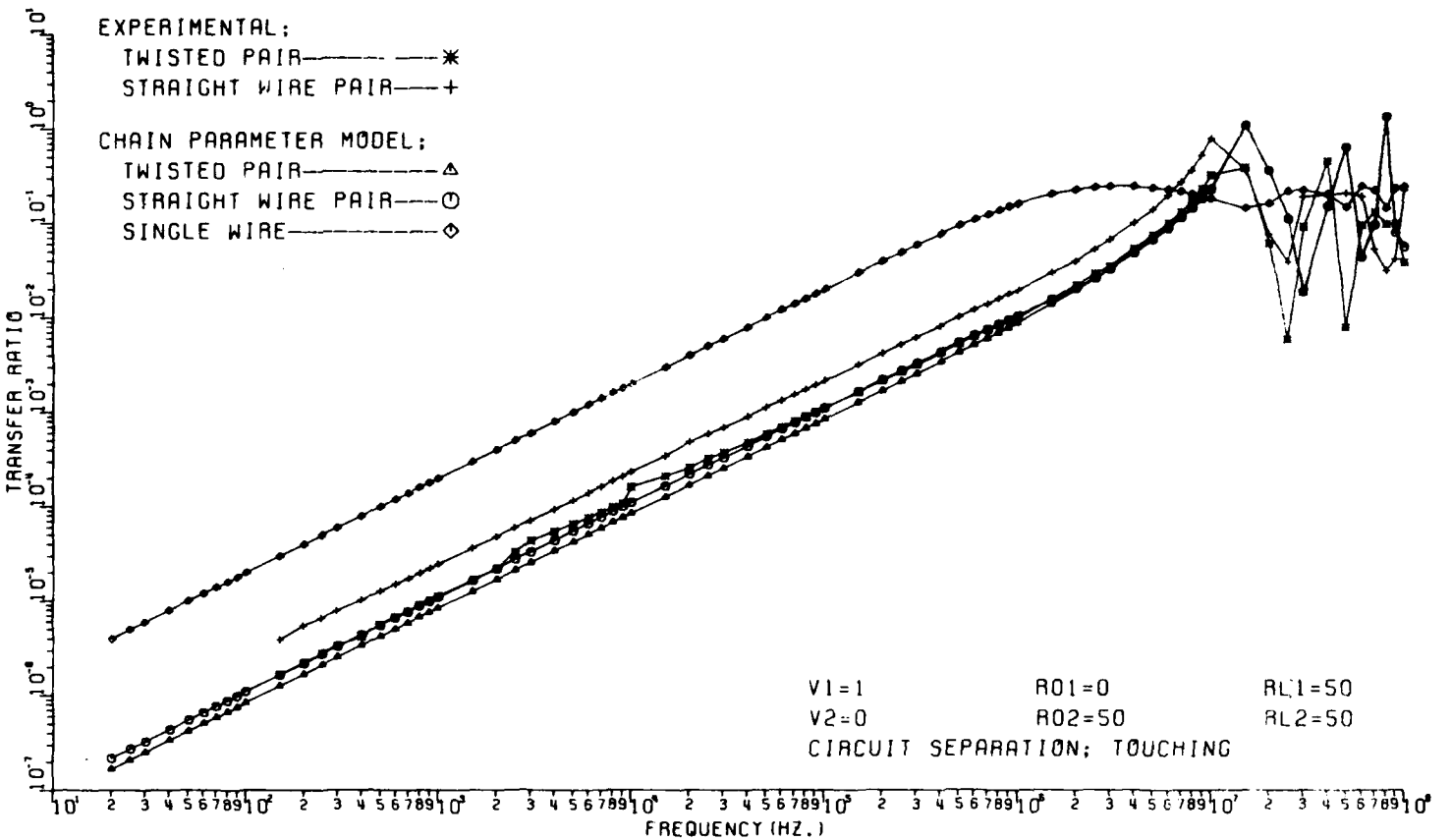
EXPERIMENTAL;
TWISTED PAIR
STRAIGHT WIRE PAIR
CHAIN PARAMETER MODEL;
TWISTED PAIR
STRAIGHT WIRE PAIR
SINGLE WIRE
TRANSFER RATIO
FREQUENCY (HZ.)
V1=1
V2=0
R01=0
R02=50
RL1=50
RL2=50
CIRCUIT SEPARATION; TOUCHING

Fig. A-1

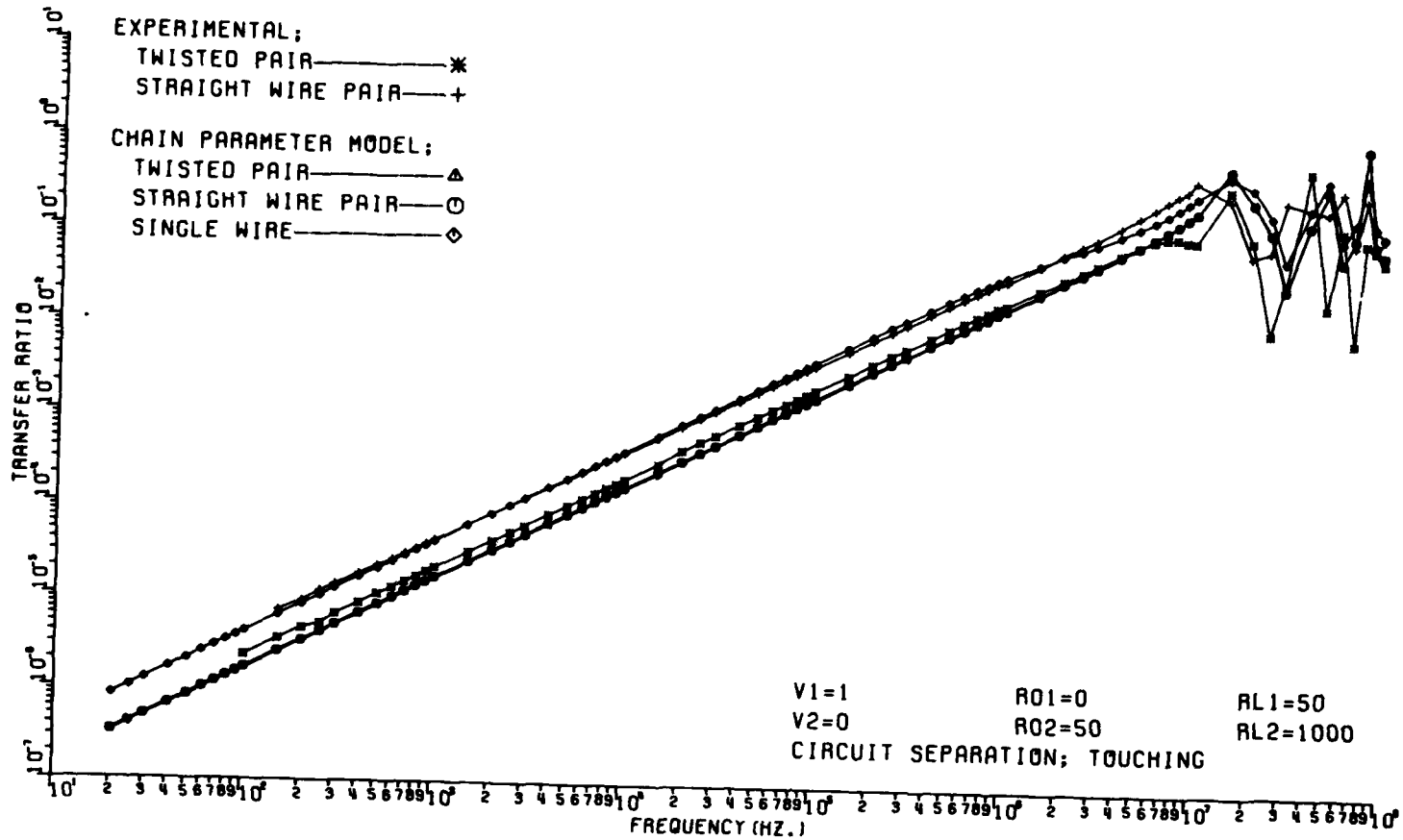
EXPERIMENTAL;
TWISTED PAIR
STRAIGHT WIRE PAIR
CHAIN PARAMETER MODEL;
TWISTED PAIR
STRAIGHT WIRE PAIR
SINGLE WIRE
TRANSFER RATIO
FREQUENCY (HZ.)
V1=1
V2=0
R01=0
R02=50
RL1=50
RL2=1000
CIRCUIT SEPARATION; TOUCHING

Fig. A-2

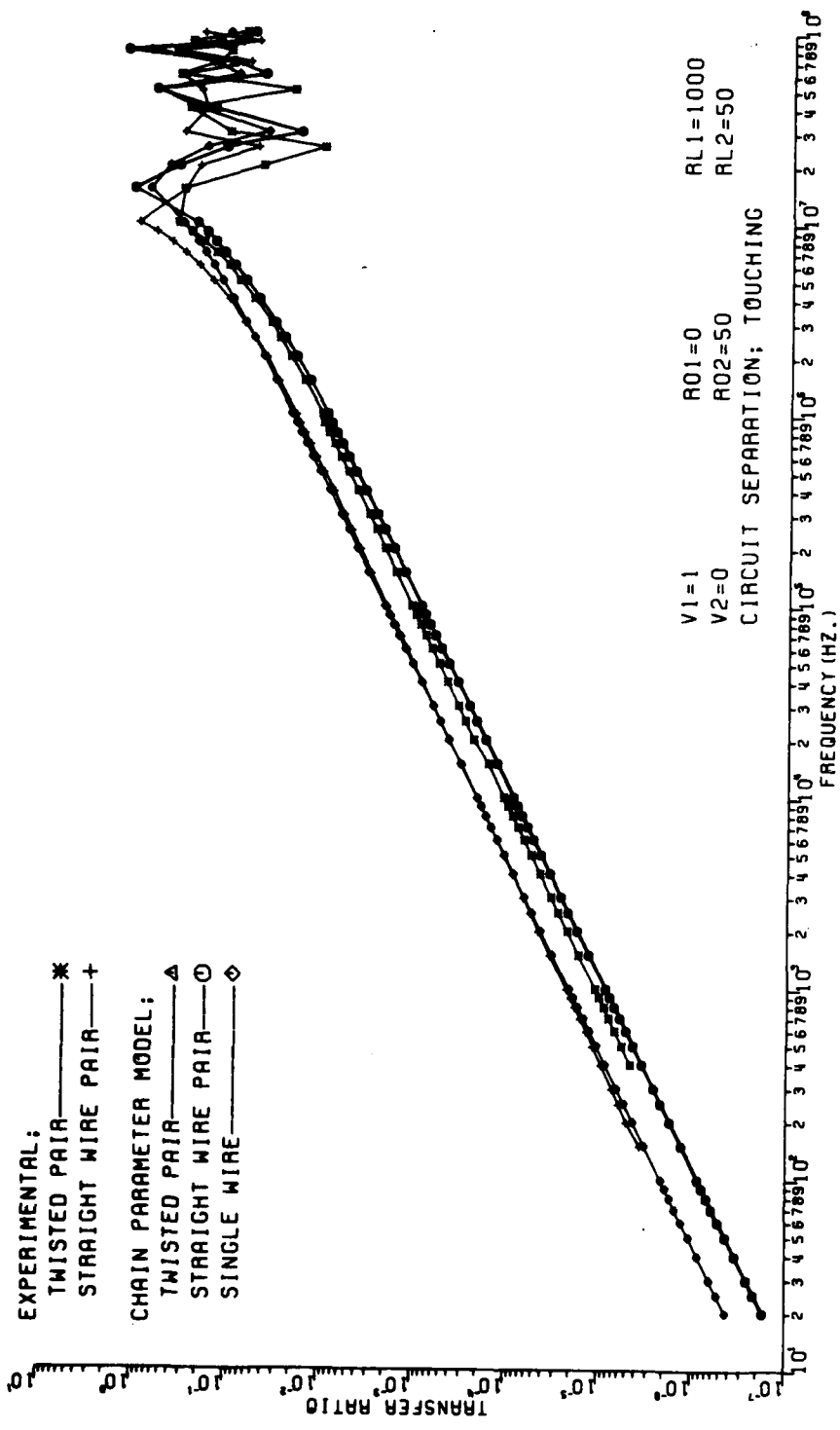
EXPERIMENTAL:
TWISTED PAIR
STRAIGHT WIRE PAIR
CHAIN PARAMETER MODEL:
TWISTED PAIR
STRAIGHT WIRE PAIR
SINGLE WIRE
TRANSFER RATIO
FREQUENCY (HZ.)
V1=1
V2=0
RO1=0
RO2=50
RL1=1000
RL2=50
CIRCUIT SEPARATION; TOUCHING

Fig. A-3

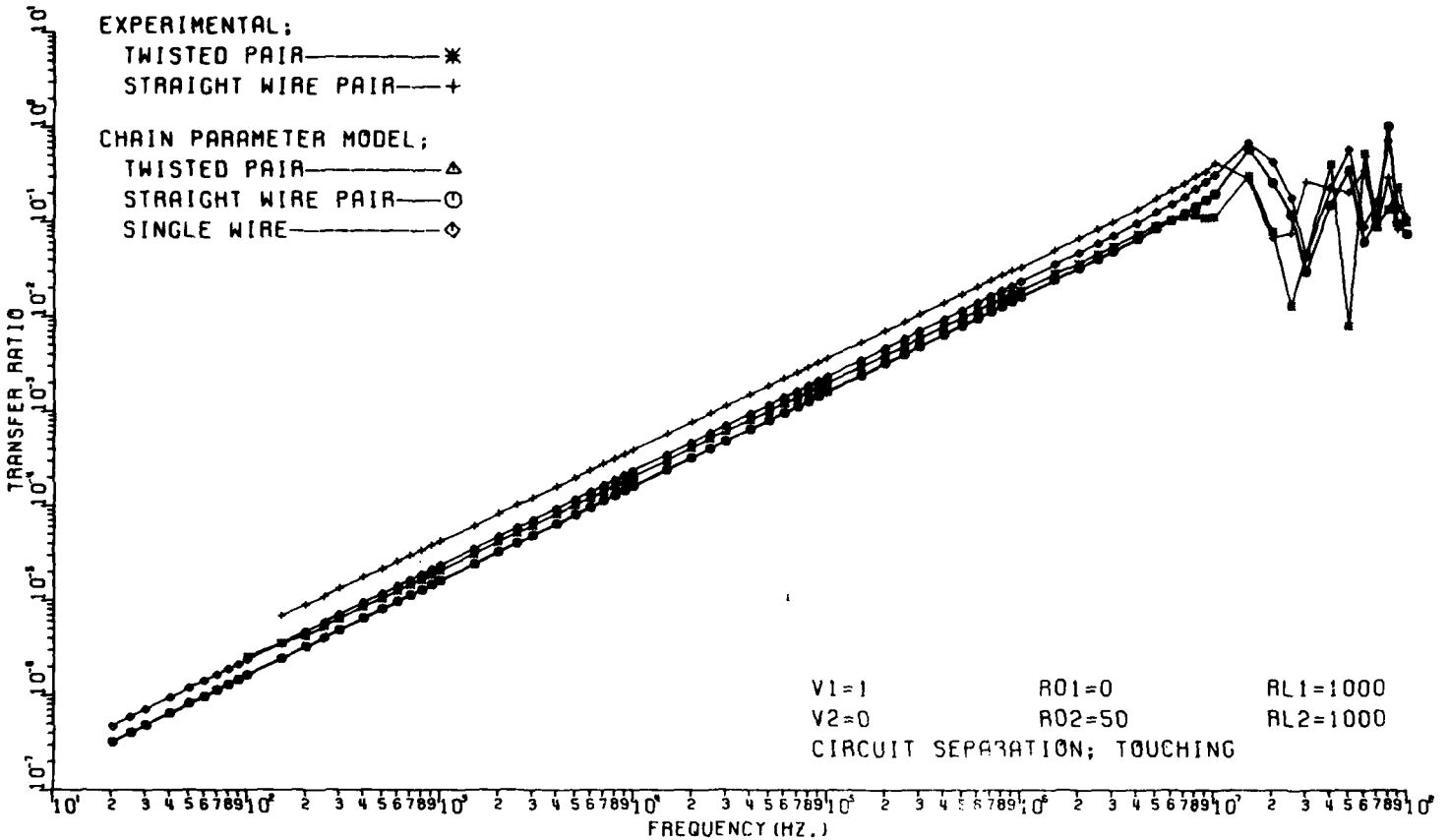
EXPERIMENTAL;
TWISTED PAIR
STRAIGHT WIRE PAIR
CHAIN PARAMETER MODEL;
TWISTED PAIR
STRAIGHT WIRE PAIR
SINGLE WIRE
TRANSFER RATIO
FREQUENCY (HZ.)
V1=1
R01=0
RL1=1000
V2=0
R02=50
RL2=1000
CIRCUIT SEPARATION; TOUCHING

Fig. A-4

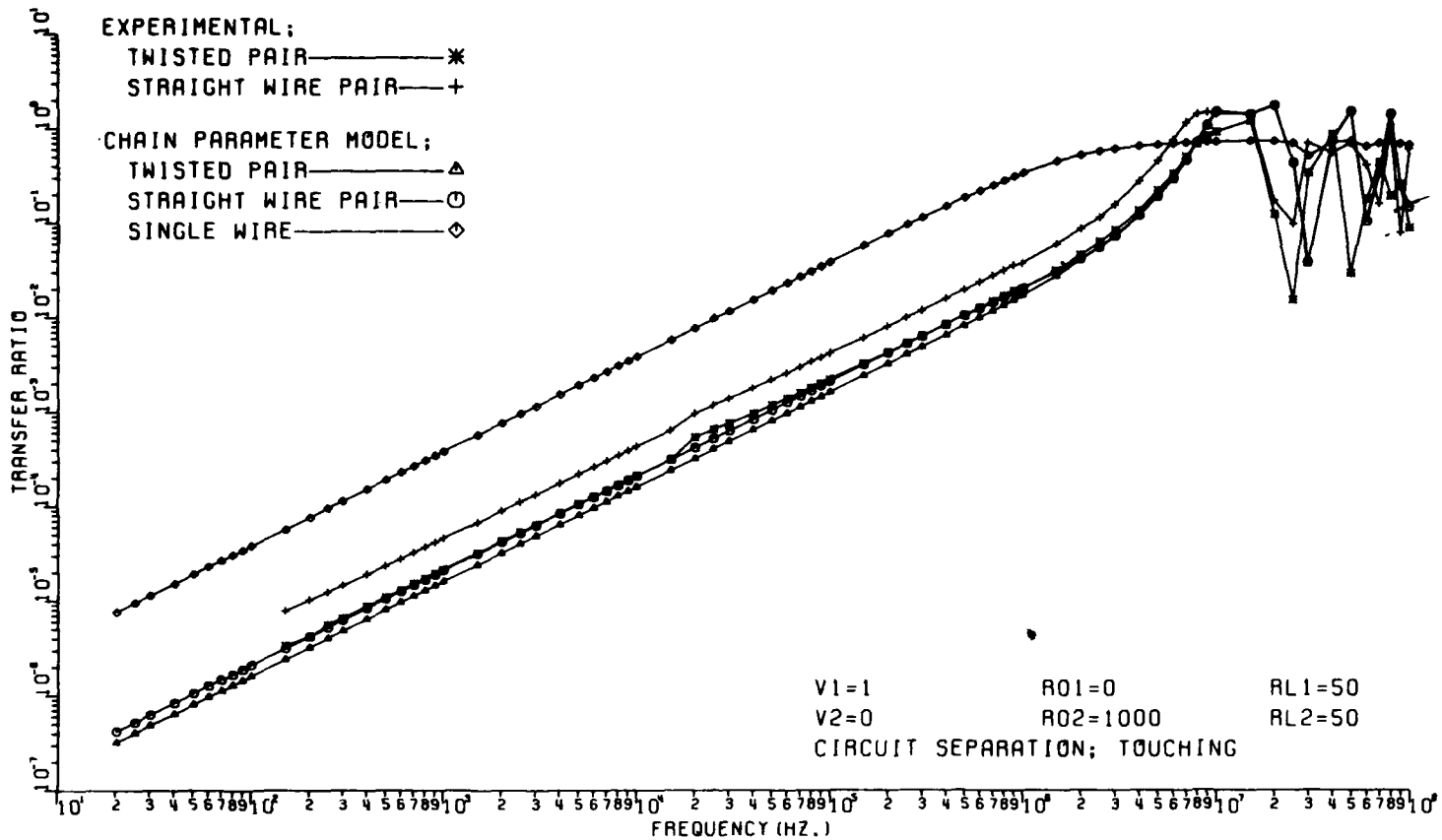
EXPERIMENTAL;
TWISTED PAIR
STRAIGHT WIRE PAIR
CHAIN PARAMETER MODEL;
TWISTED PAIR
STRAIGHT WIRE PAIR
SINGLE WIRE
TRANSFER RATIO
FREQUENCY (HZ.)
V1=1
R01=0
RL1=50
V2=0
R02=1000
RL2=50
CIRCUIT SEPARATION; TOUCHING

Fig. A-5

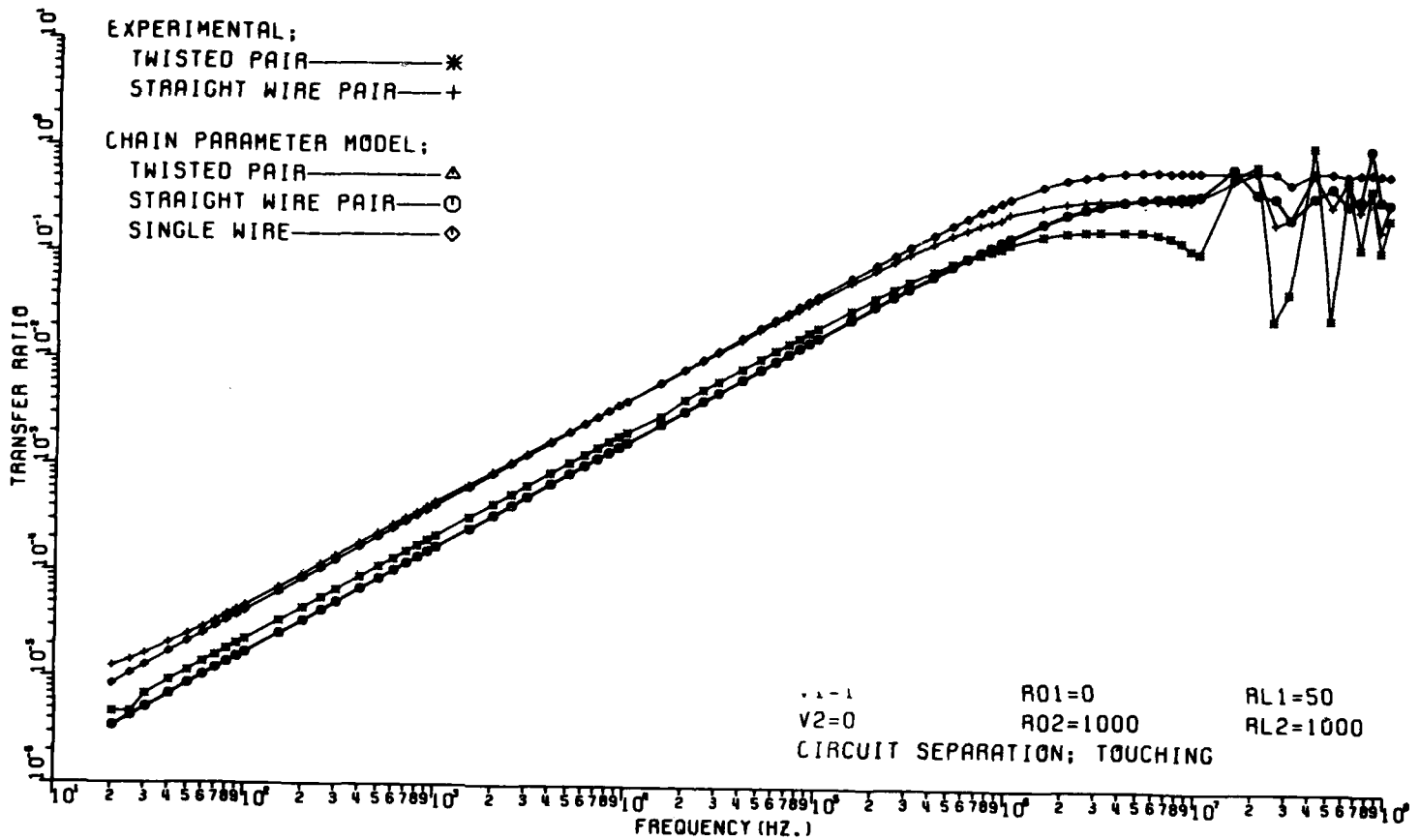
EXPERIMENTAL;
TWISTED PAIR
STRAIGHT WIRE PAIR
CHAIN PARAMETER MODEL;
TWISTED PAIR
STRAIGHT WIRE PAIR
SINGLE WIRE
TRANSFER RATIO
FREQUENCY (HZ.)
R01=0
RL1=50
V2=0
R02=1000
RL2=1000
CIRCUIT SEPARATION; TOUCHING

Fig. A-6

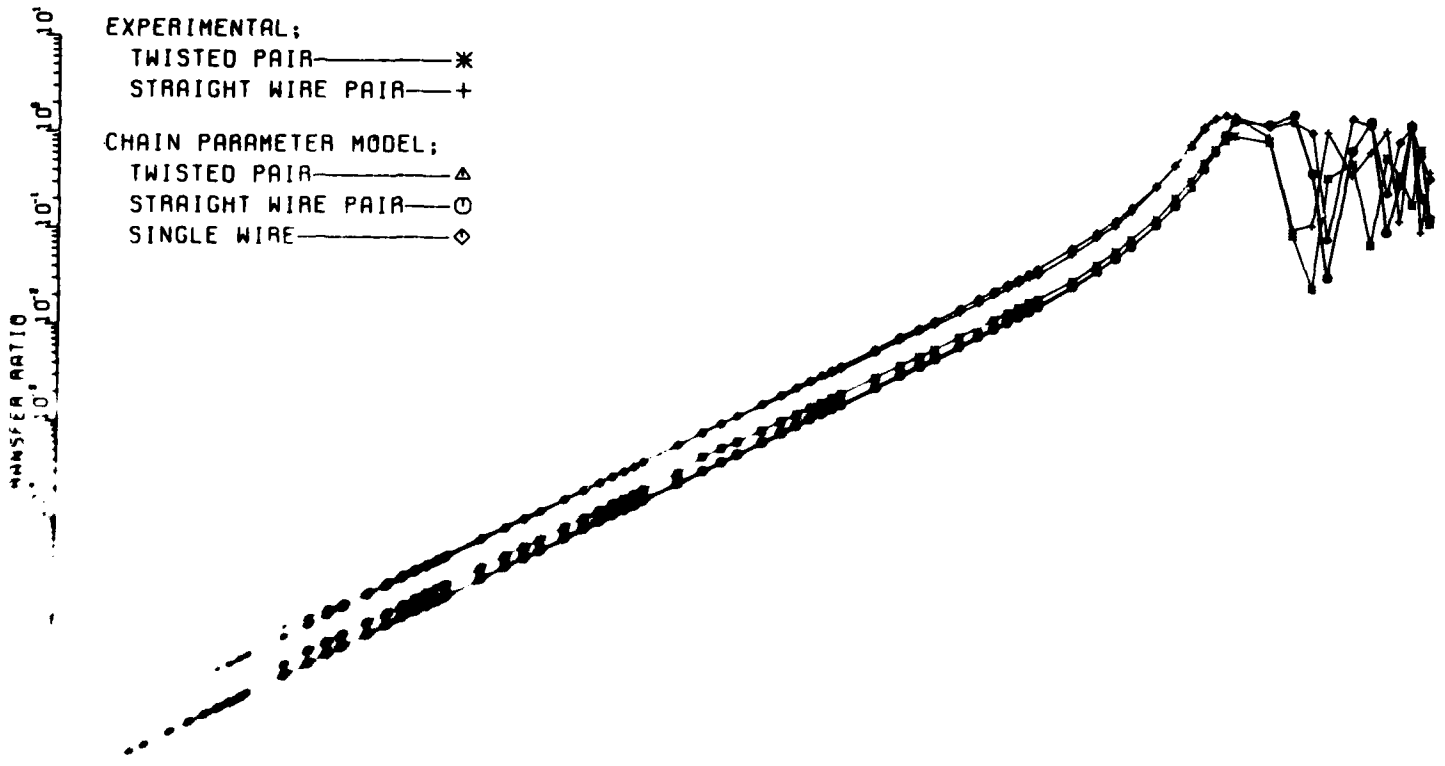
EXPERIMENTAL;
TWISTED PAIR
STRAIGHT WIRE PAIR
CHAIN PARAMETER MODEL;
TWISTED PAIR
STRAIGHT WIRE PAIR
SINGLE WIRE
TRANSFER RATIO
10^{0}
10^{-1}
10^{-2}
10^{-3}

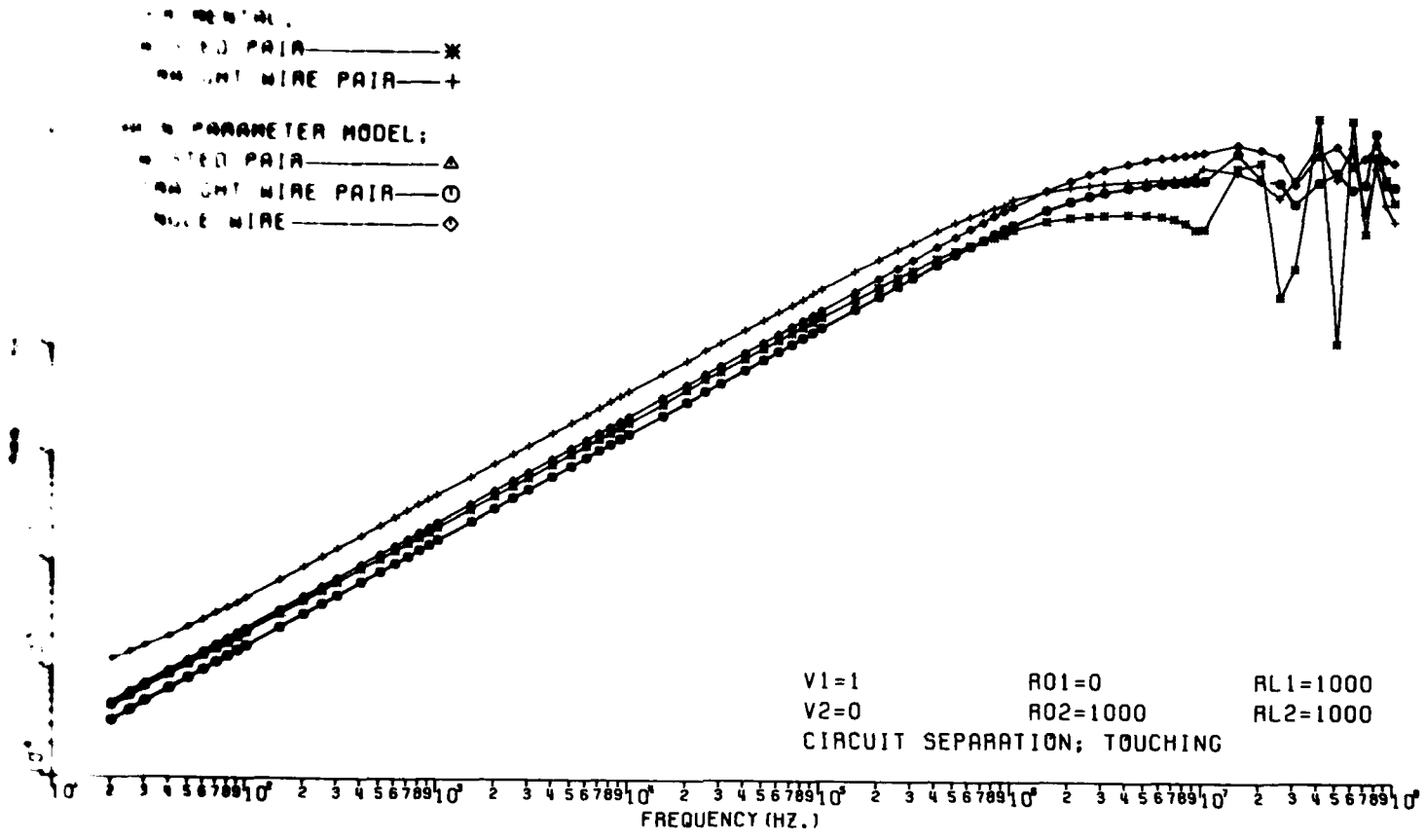
PAIR
WIRE PAIR
PARAMETER MODEL:
PAIR
WIRE PAIR
WIRE
V1=1
V2=0
R01=0
R02=1000
RL1=1000
RL2=1000
CIRCUIT SEPARATION; TOUCHING
FREQUENCY (HZ.)

Fig. A-8

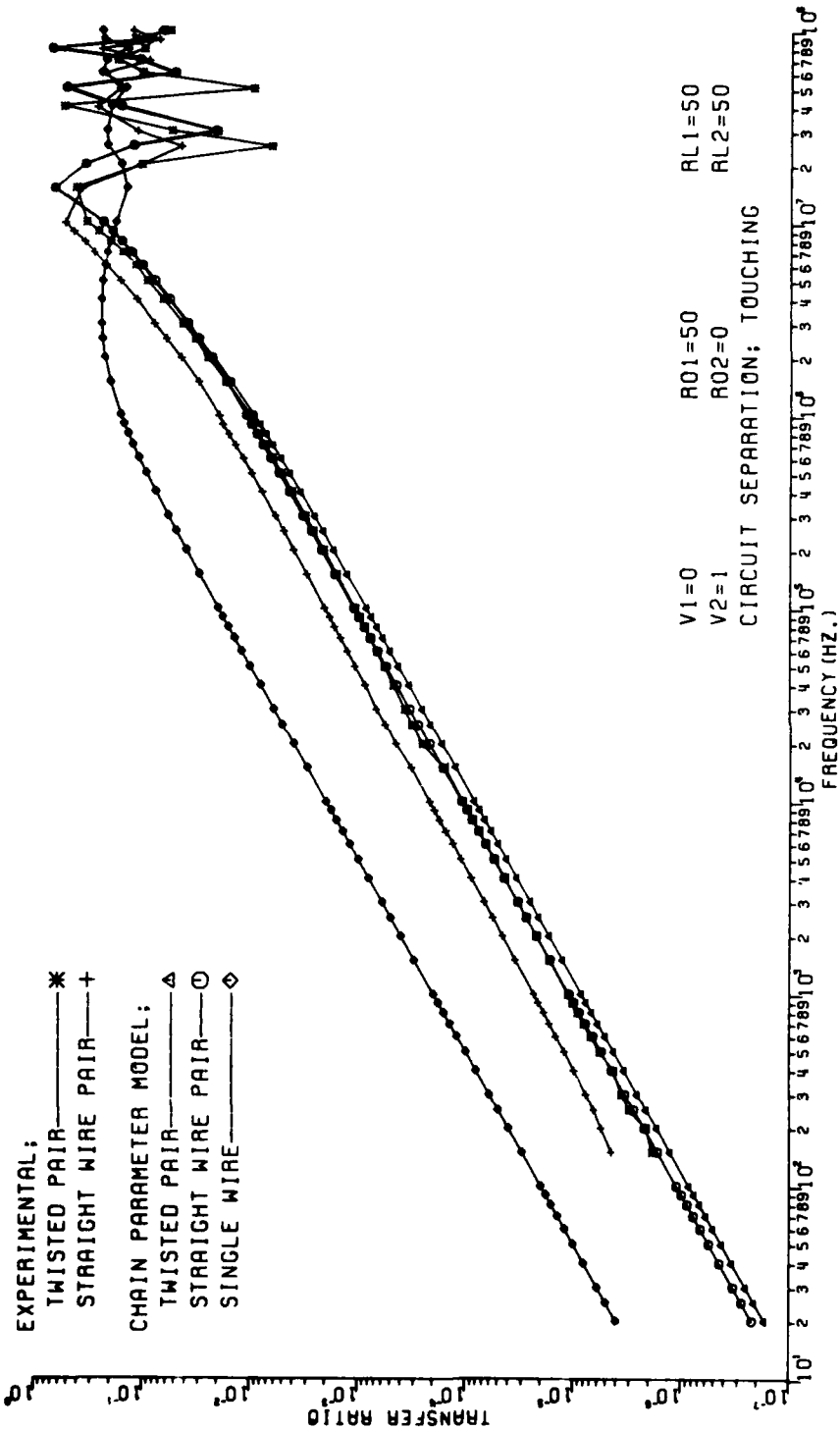
EXPERIMENTAL;
TWISTED PAIR
STRAIGHT WIRE PAIR
CHAIN PARAMETER MODEL;
TWISTED PAIR
STRAIGHT WIRE PAIR
SINGLE WIRE
TRANSFER RATIO
FREQUENCY (HZ.)
V1=0
V2=1
CIRCUIT SEPARATION; TOUCHING
R01=50
R02=0
RL1=50
RL2=50

Fig. A-9

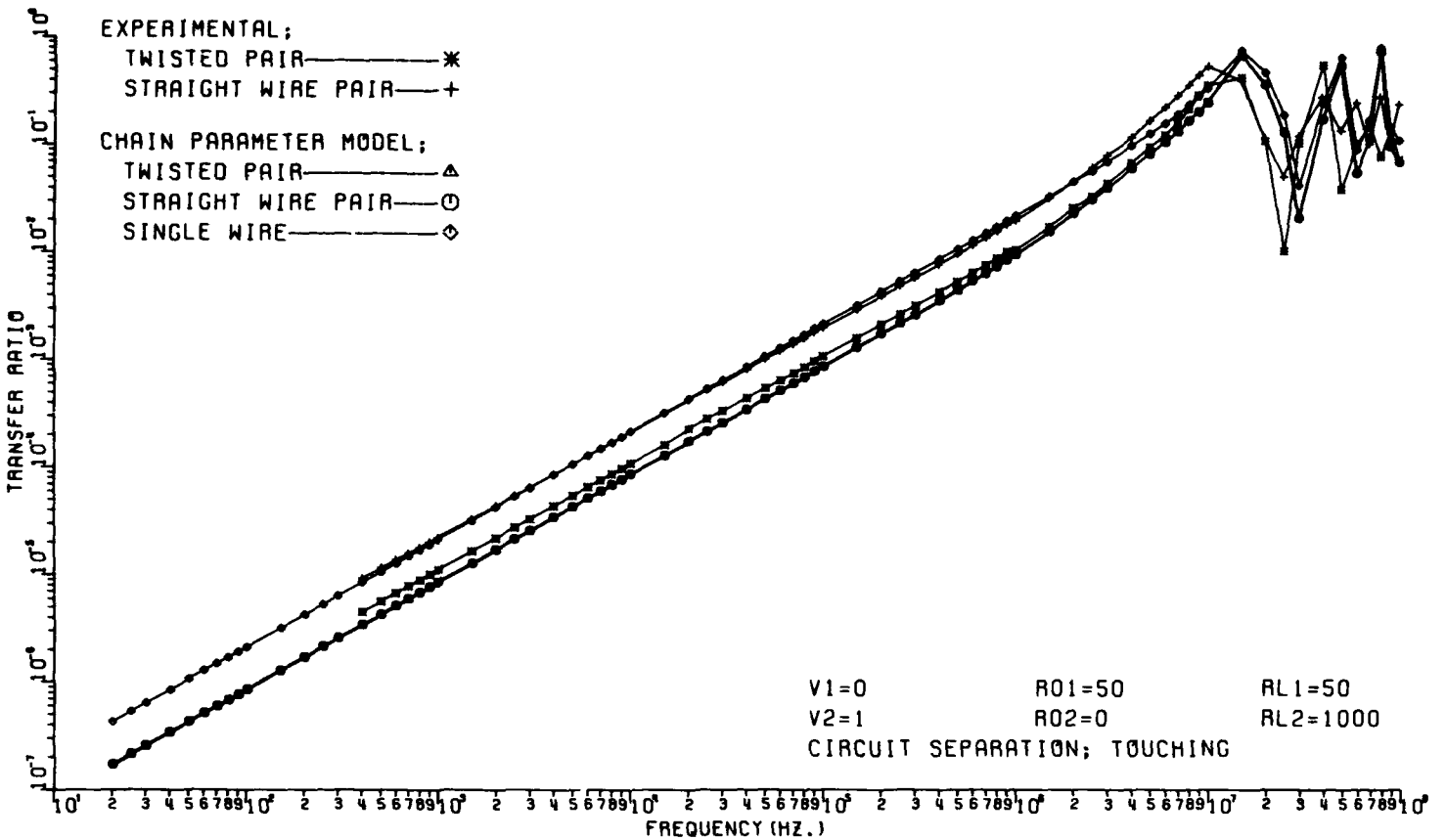
EXPERIMENTAL;
TWISTED PAIR
STRAIGHT WIRE PAIR
CHAIN PARAMETER MODEL;
TWISTED PAIR
STRAIGHT WIRE PAIR
SINGLE WIRE
TRANSFER RATIO
FREQUENCY (HZ.)
V1=0
V2=1
R01=50
R02=0
RL1=50
RL2=1000
CIRCUIT SEPARATION; TOUCHING

Fig. A-10

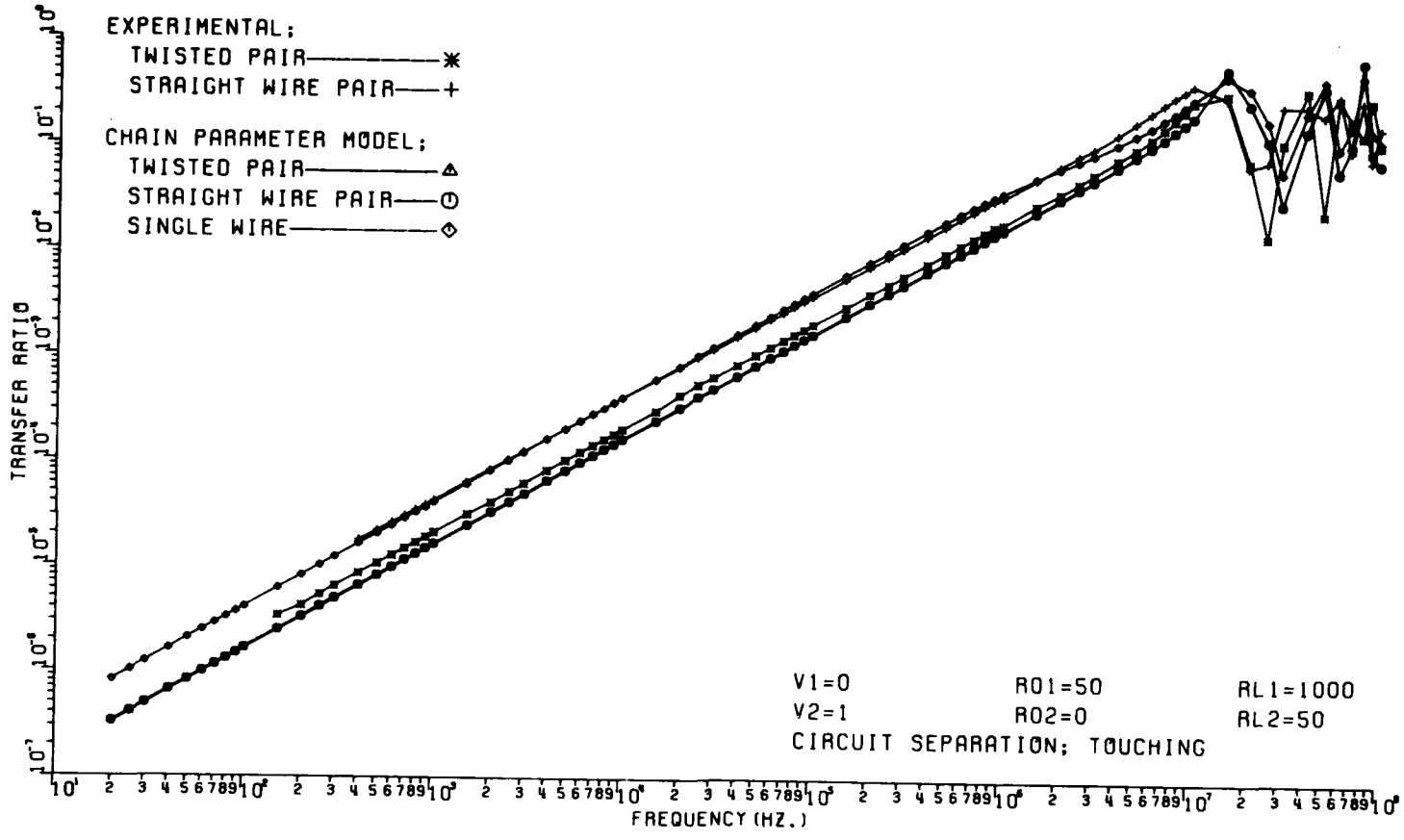
EXPERIMENTAL;
TWISTED PAIR
STRAIGHT WIRE PAIR
CHAIN PARAMETER MODEL;
TWISTED PAIR
STRAIGHT WIRE PAIR
SINGLE WIRE
TRANSFER RATIO
FREQUENCY (HZ.)
V1=0
V2=1
R01=50
R02=0
RL1=1000
RL2=50
CIRCUIT SEPARATION; TOUCHING

Fig. A-11

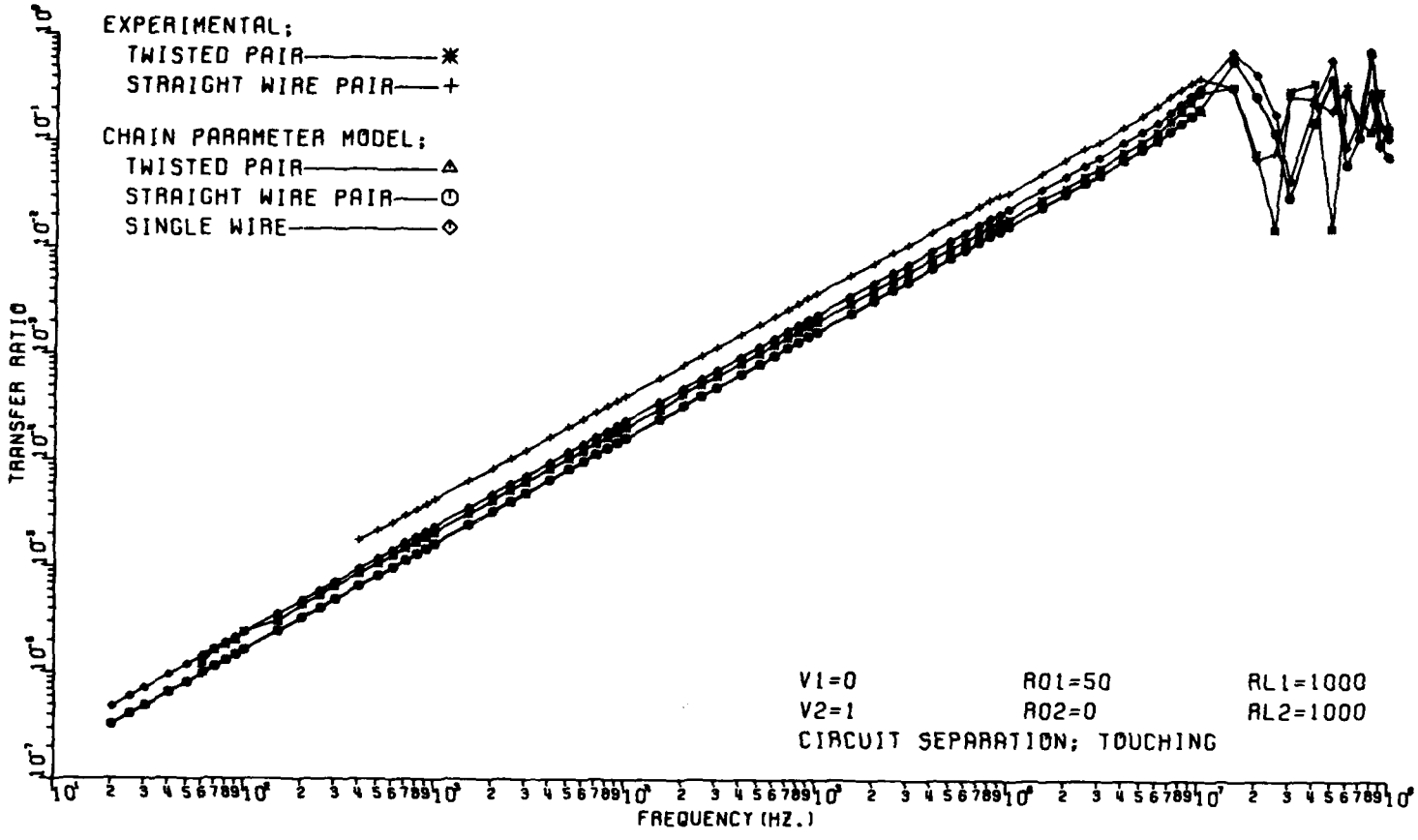
EXPERIMENTAL;
TWISTED PAIR
STRAIGHT WIRE PAIR
CHAIN PARAMETER MODEL;
TWISTED PAIR
STRAIGHT WIRE PAIR
SINGLE WIRE
TRANSFER RATIO
FREQUENCY (HZ.)
V1=0
V2=1
R01=50
R02=0
RL1=1000
RL2=1000
CIRCUIT SEPARATION; TOUCHING

Fig. A-12

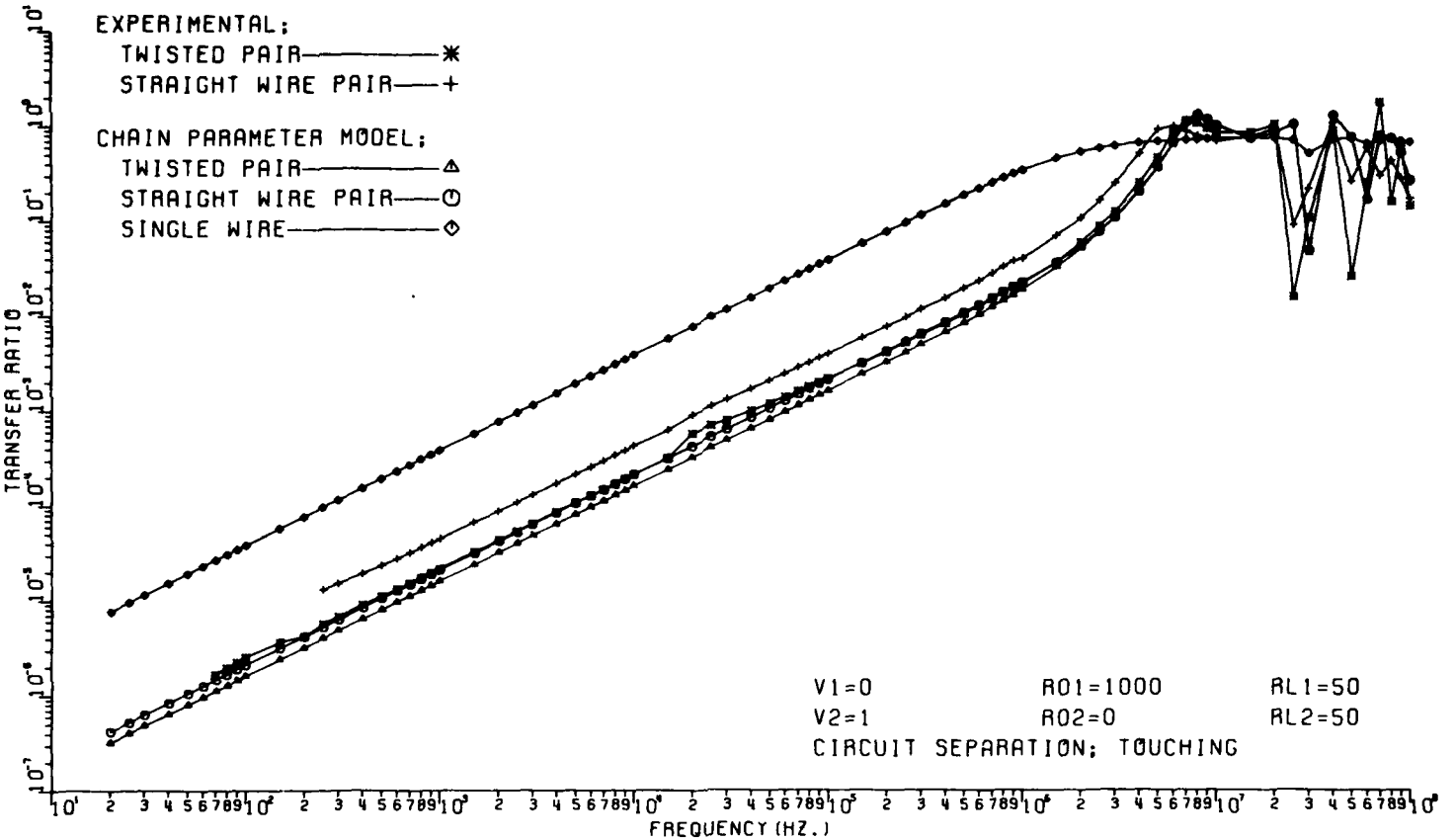
EXPERIMENTAL;
TWISTED PAIR
STRAIGHT WIRE PAIR
CHAIN PARAMETER MODEL;
TWISTED PAIR
STRAIGHT WIRE PAIR
SINGLE WIRE
TRANSFER RATIO
FREQUENCY (HZ.)
V1=0
V2=1
R01=1000
R02=0
RL1=50
RL2=50
CIRCUIT SEPARATION; TOUCHING

Fig. A-13

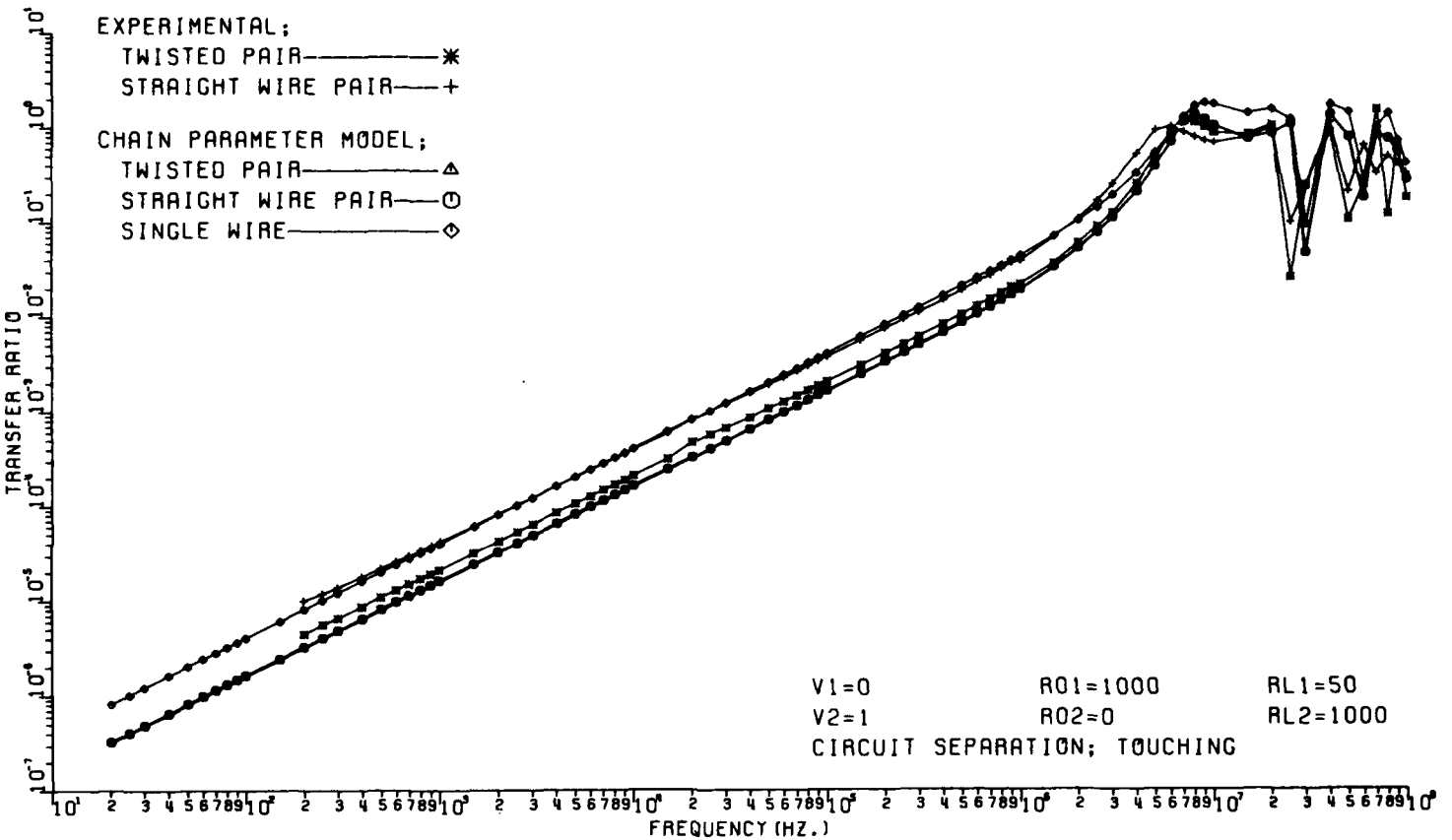
EXPERIMENTAL;
TWISTED PAIR
STRAIGHT WIRE PAIR
CHAIN PARAMETER MODEL;
TWISTED PAIR
STRAIGHT WIRE PAIR
SINGLE WIRE
TRANSFER RATIO
FREQUENCY (HZ.)
V1=0
R01=1000
RL1=50
V2=1
R02=0
RL2=1000
CIRCUIT SEPARATION; TOUCHING

Fig. A-14

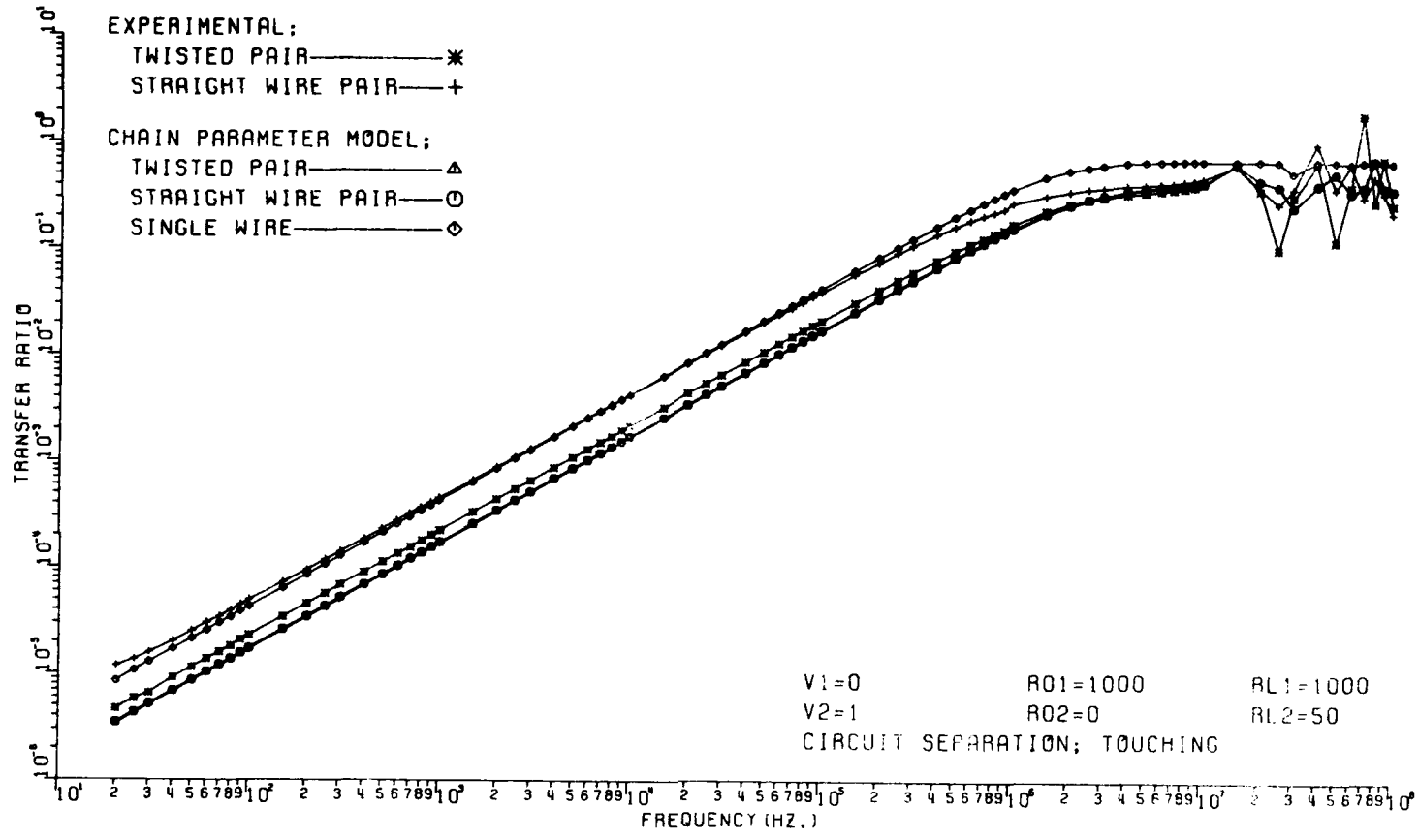
EXPERIMENTAL:
TWISTED PAIR
STRAIGHT WIRE PAIR
CHAIN PARAMETER MODEL;
TWISTED PAIR
STRAIGHT WIRE PAIR
SINGLE WIRE
TRANSFER RATIO
FREQUENCY (HZ.)
V1=0
V2=1
R01=1000
R02=0
RL1=1000
RL2=50
CIRCUIT SEPARATION; TOUCHING

Fig. A-15

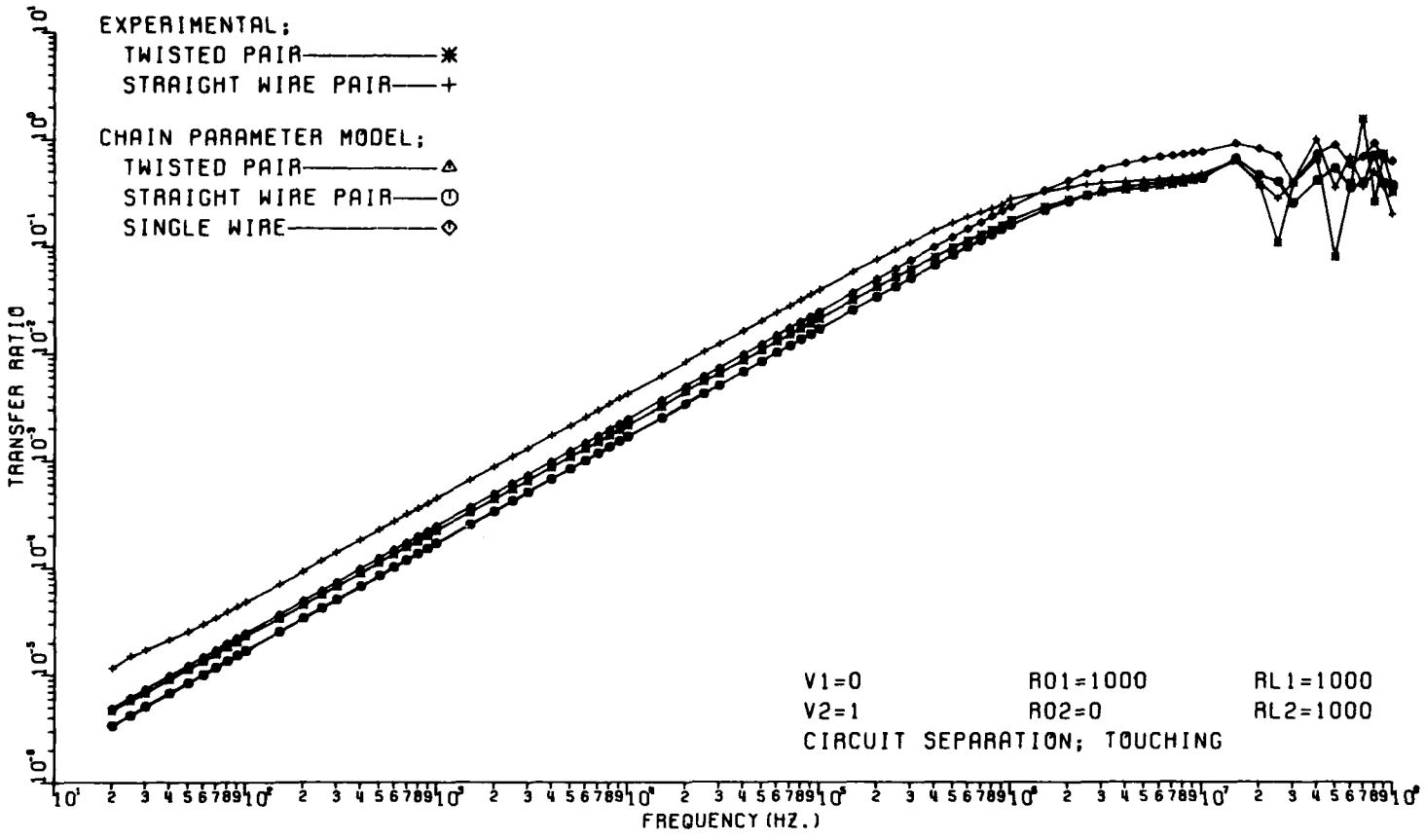
EXPERIMENTAL;
TWISTED PAIR
STRAIGHT WIRE PAIR
CHAIN PARAMETER MODEL;
TWISTED PAIR
STRAIGHT WIRE PAIR
SINGLE WIRE
TRANSFER RATIO
FREQUENCY (HZ.)
V1=0
V2=1
R01=1000
R02=0
RL1=1000
RL2=1000
CIRCUIT SEPARATION; TOUCHING

Fig. A-16

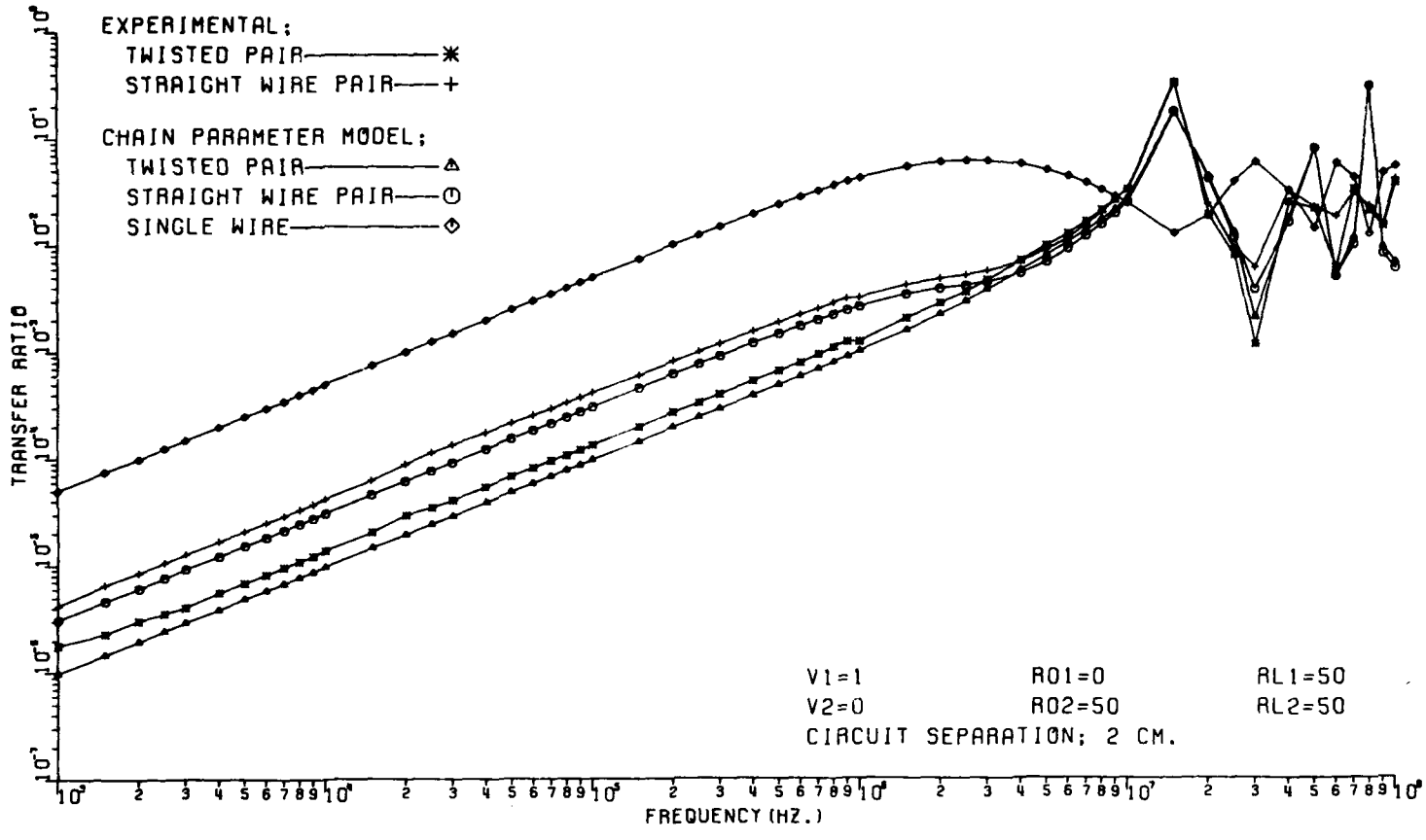
EXPERIMENTAL;
TWISTED PAIR
STRAIGHT WIRE PAIR
CHAIN PARAMETER MODEL;
TWISTED PAIR
STRAIGHT WIRE PAIR
SINGLE WIRE
TRANSFER RATIO
FREQUENCY (HZ.)
V1=1
V2=0
R01=0
R02=50
RL1=50
RL2=50
CIRCUIT SEPARATION; 2 CM.

Fig. A-17

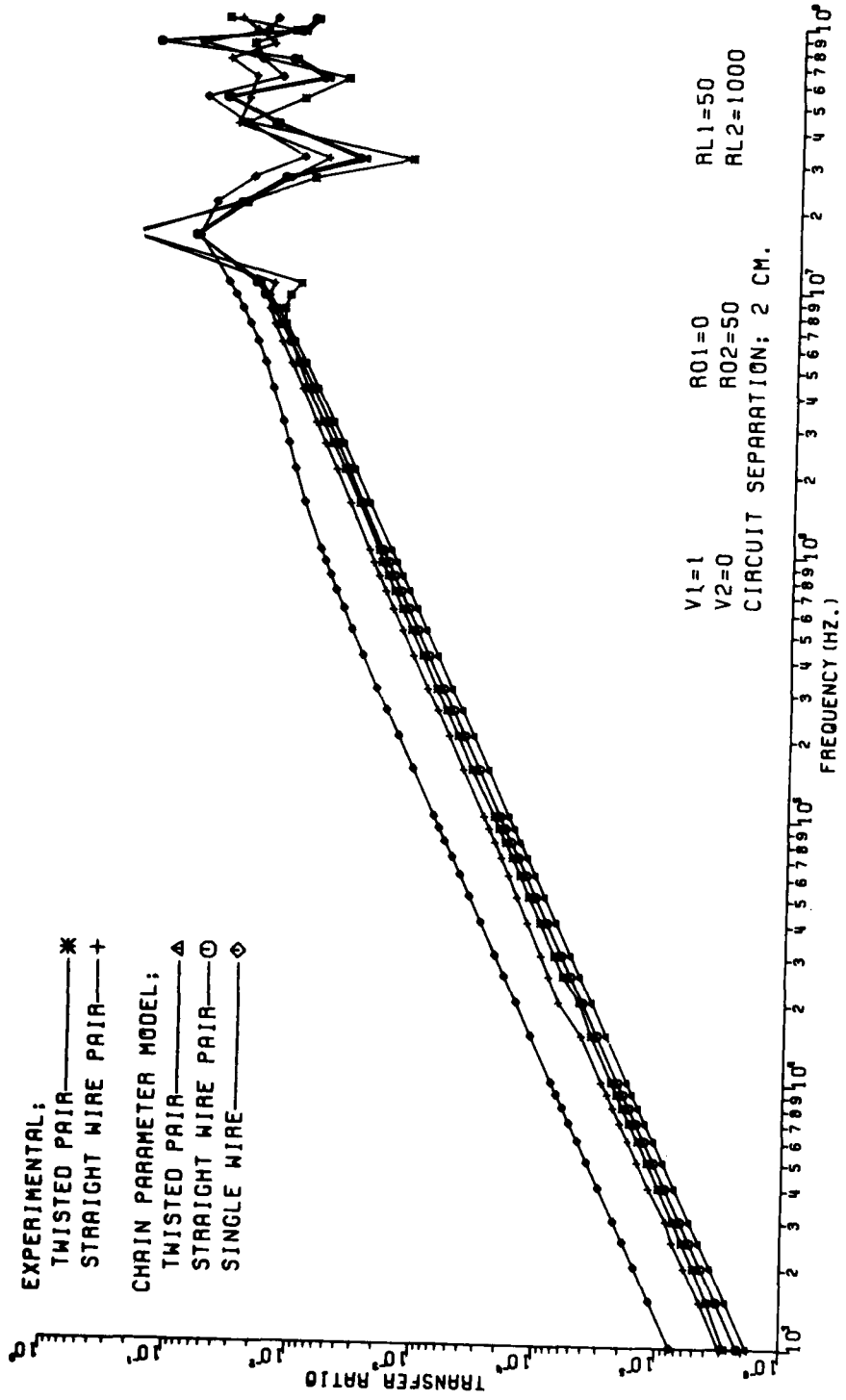
EXPERIMENTAL:
TWISTED PAIR
STRAIGHT WIRE PAIR
CHAIN PARAMETER MODEL:
TWISTED PAIR
STRAIGHT WIRE PAIR
SINGLE WIRE
TRANSFER RATIO
FREQUENCY (HZ.)
V1=1
V2=0
RO1=0
RO2=50
RL1=50
RL2=1000
CIRCUIT SEPARATION: 2 CM.

Fig. A-18

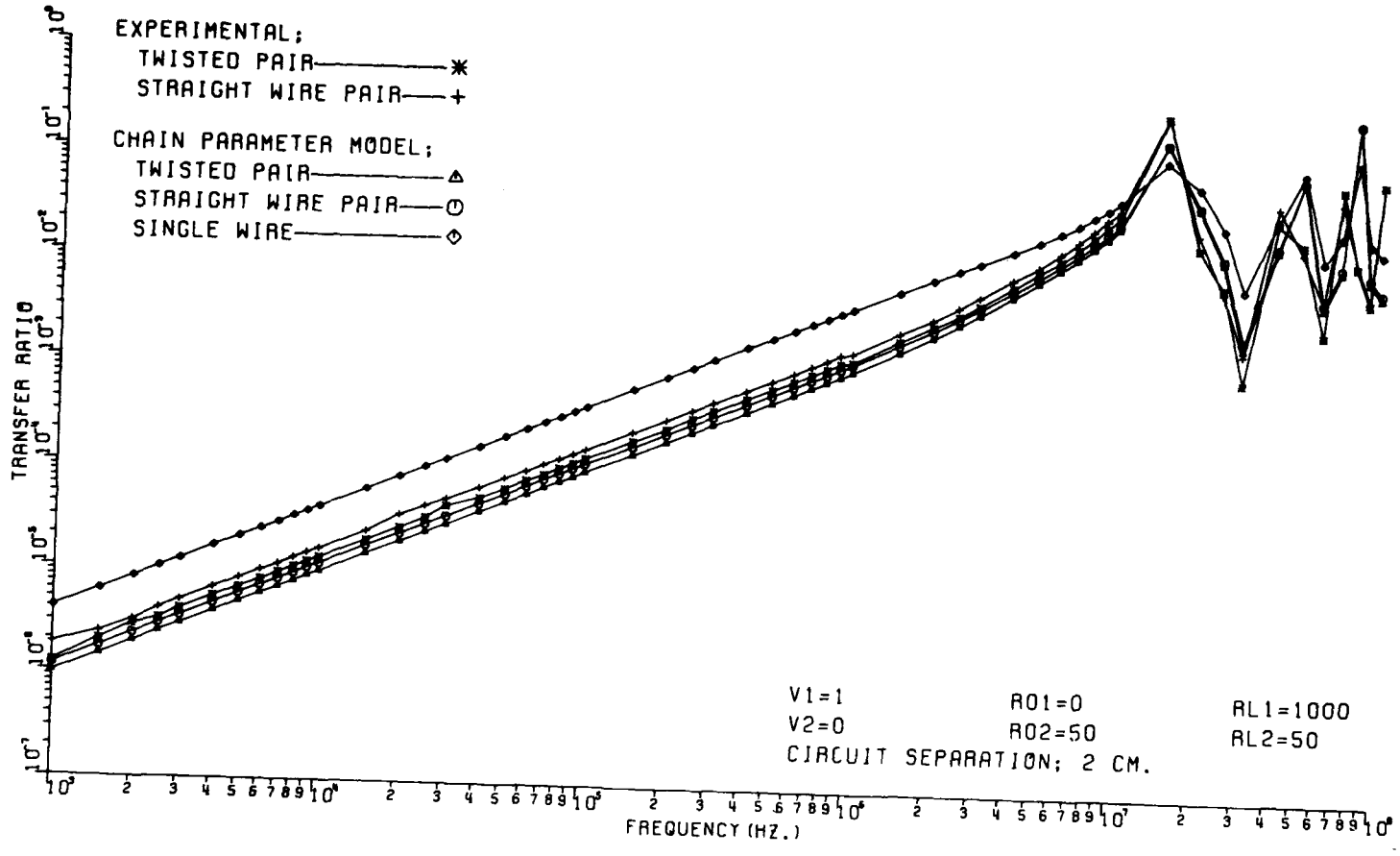
EXPERIMENTAL;
TWISTED PAIR
STRAIGHT WIRE PAIR
CHAIN PARAMETER MODEL;
TWISTED PAIR
STRAIGHT WIRE PAIR
SINGLE WIRE
TRANSFER RATIO
FREQUENCY (HZ.)
V1=1
V2=0
R01=0
R02=50
RL1=1000
RL2=50
CIRCUIT SEPARATION; 2 CM.

Fig. A-19

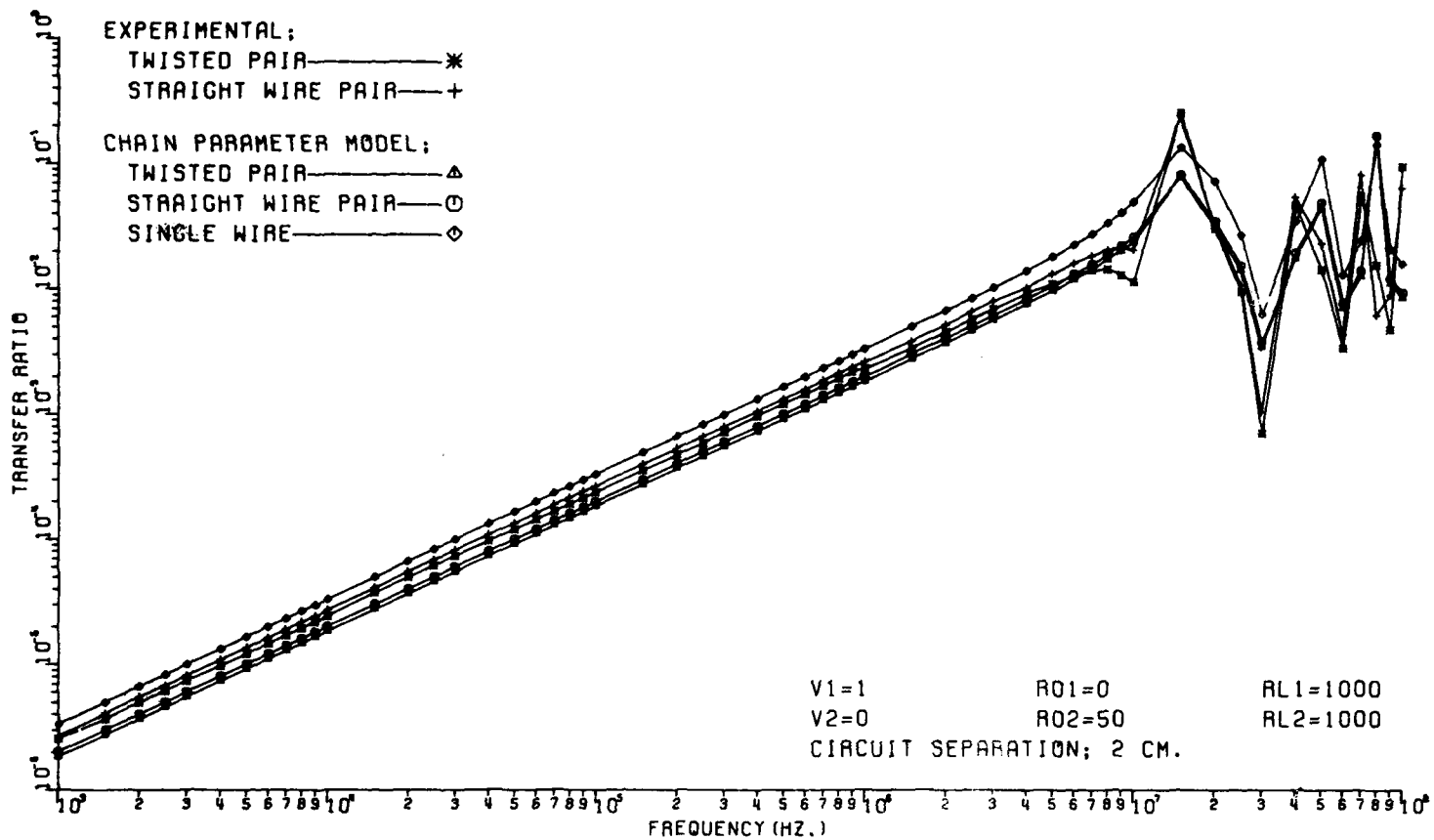
EXPERIMENTAL;
TWISTED PAIR
STRAIGHT WIRE PAIR
CHAIN PARAMETER MODEL;
TWISTED PAIR
STRAIGHT WIRE PAIR
SINGLE WIRE
TRANSFER RATIO
FREQUENCY (HZ.)
V1=1
V2=0
RO1=0
RO2=50
RL1=1000
RL2=1000
CIRCUIT SEPARATION; 2 CM.

Fig. A-20

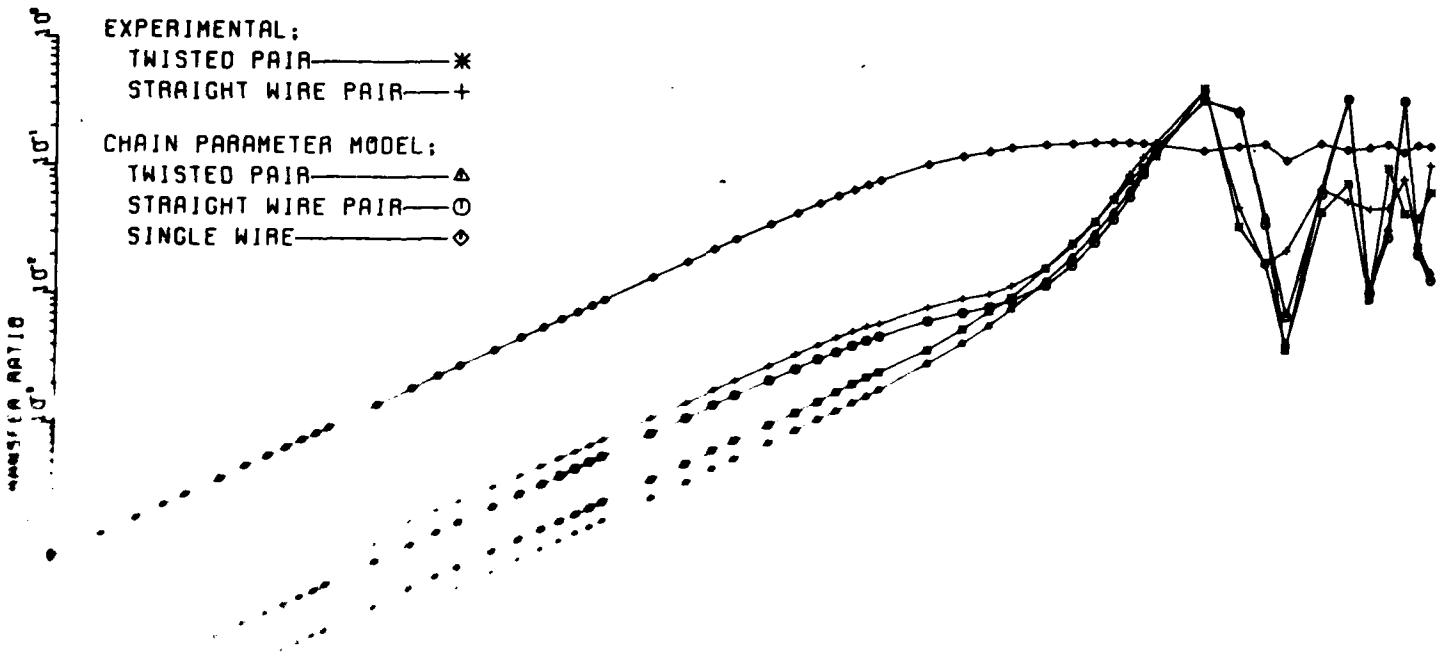
EXPERIMENTAL:
TWISTED PAIR
STRAIGHT WIRE PAIR
CHAIN PARAMETER MODEL:
TWISTED PAIR
STRAIGHT WIRE PAIR
SINGLE WIRE

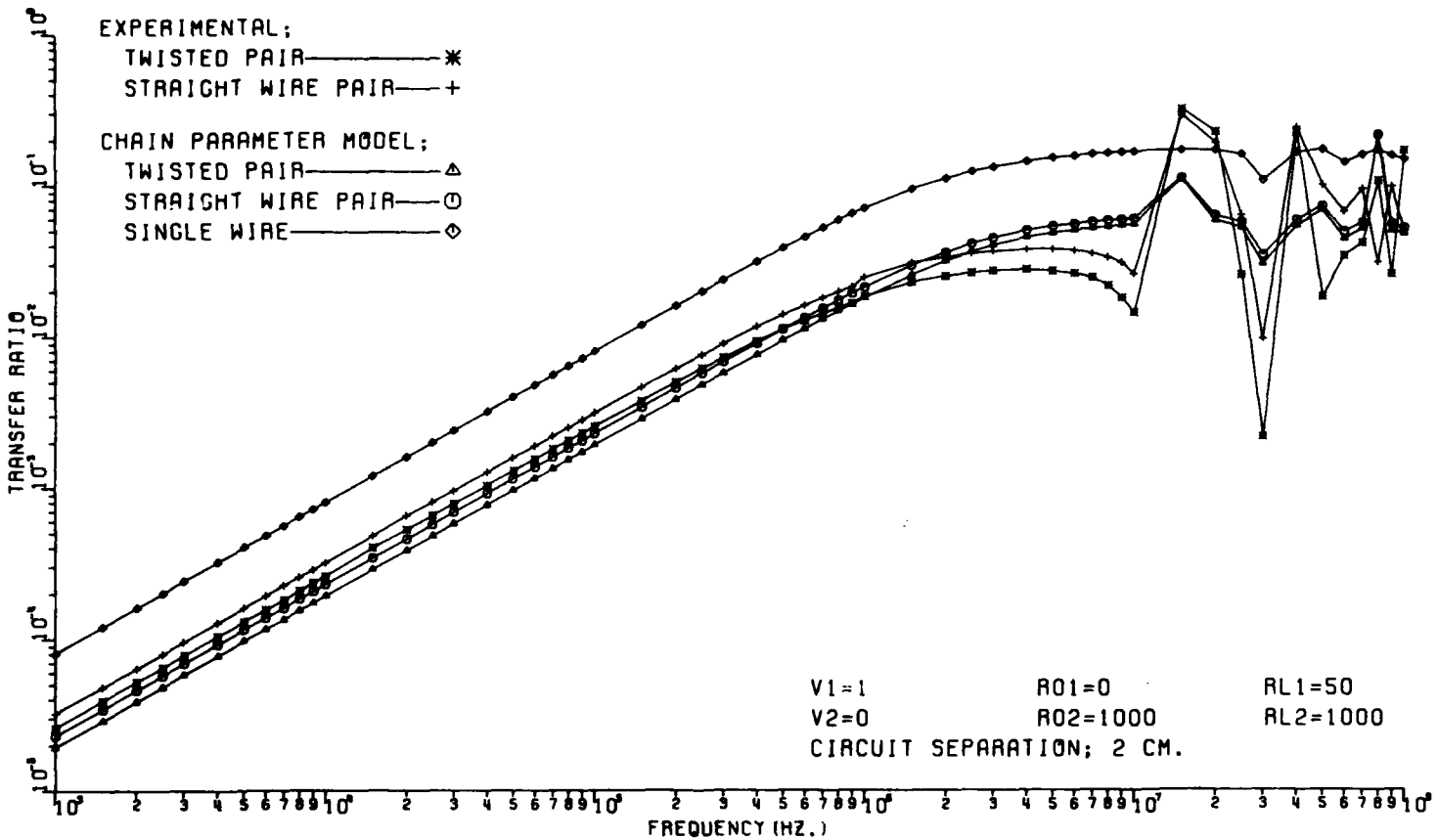
EXPERIMENTAL;
TWISTED PAIR
STRAIGHT WIRE PAIR
CHAIN PARAMETER MODEL;
TWISTED PAIR
STRAIGHT WIRE PAIR
SINGLE WIRE
TRANSFER RATIO
FREQUENCY (HZ.)
V1=1
V2=0
R01=0
R02=1000
RL1=50
RL2=1000
CIRCUIT SEPARATION; 2 CM.

Fig. A-22

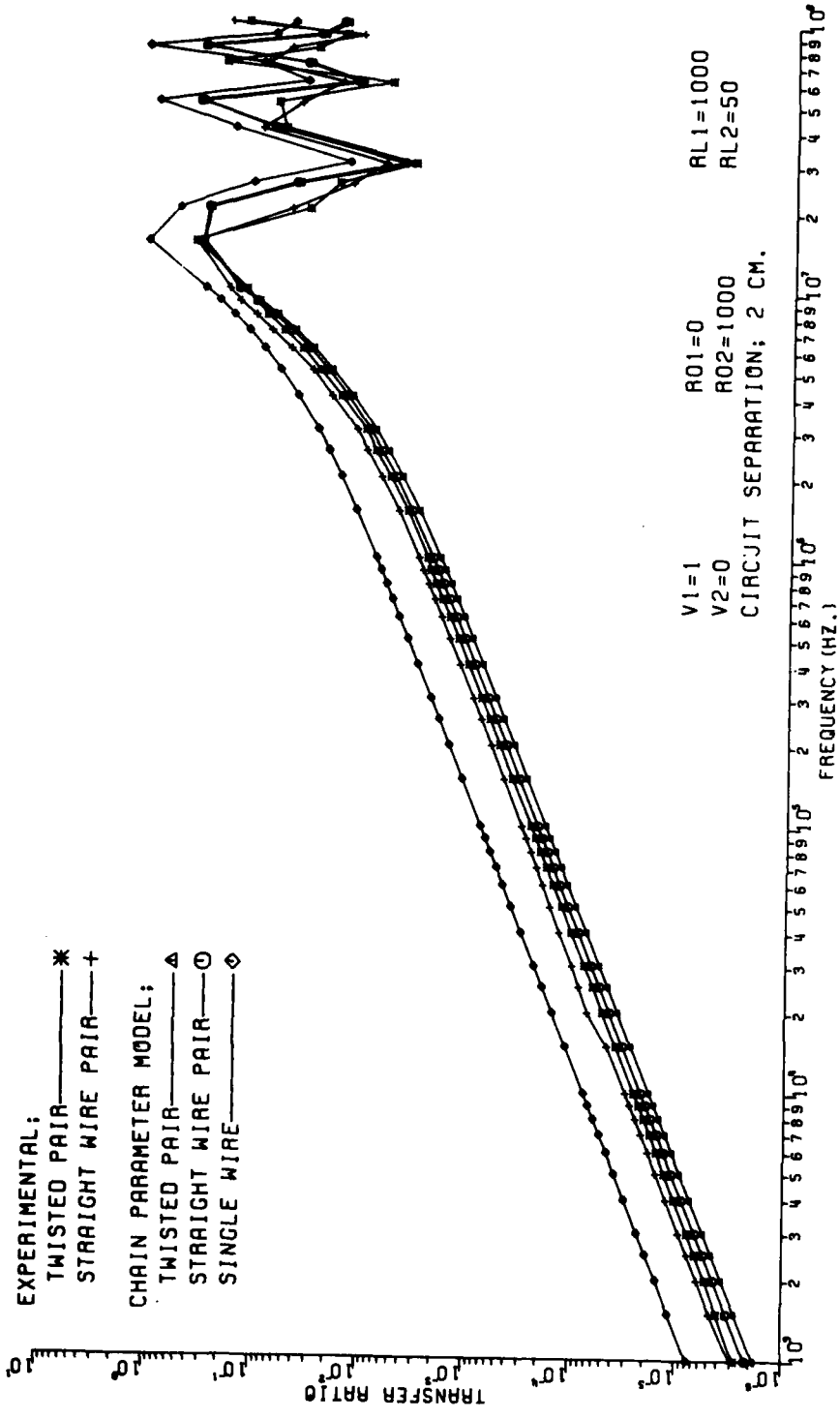
EXPERIMENTAL:
TWISTED PAIR
STRAIGHT WIRE PAIR
CHAIN PARAMETER MODEL:
TWISTED PAIR
STRAIGHT WIRE PAIR
SINGLE WIRE
TRANSFER RATIO
FREQUENCY (HZ.)
V1=1
V2=0
R01=0
R02=1000
RL1=1000
RL2=50
CIRCUIT SEPARATION: 2 CM.

Fig. A-23

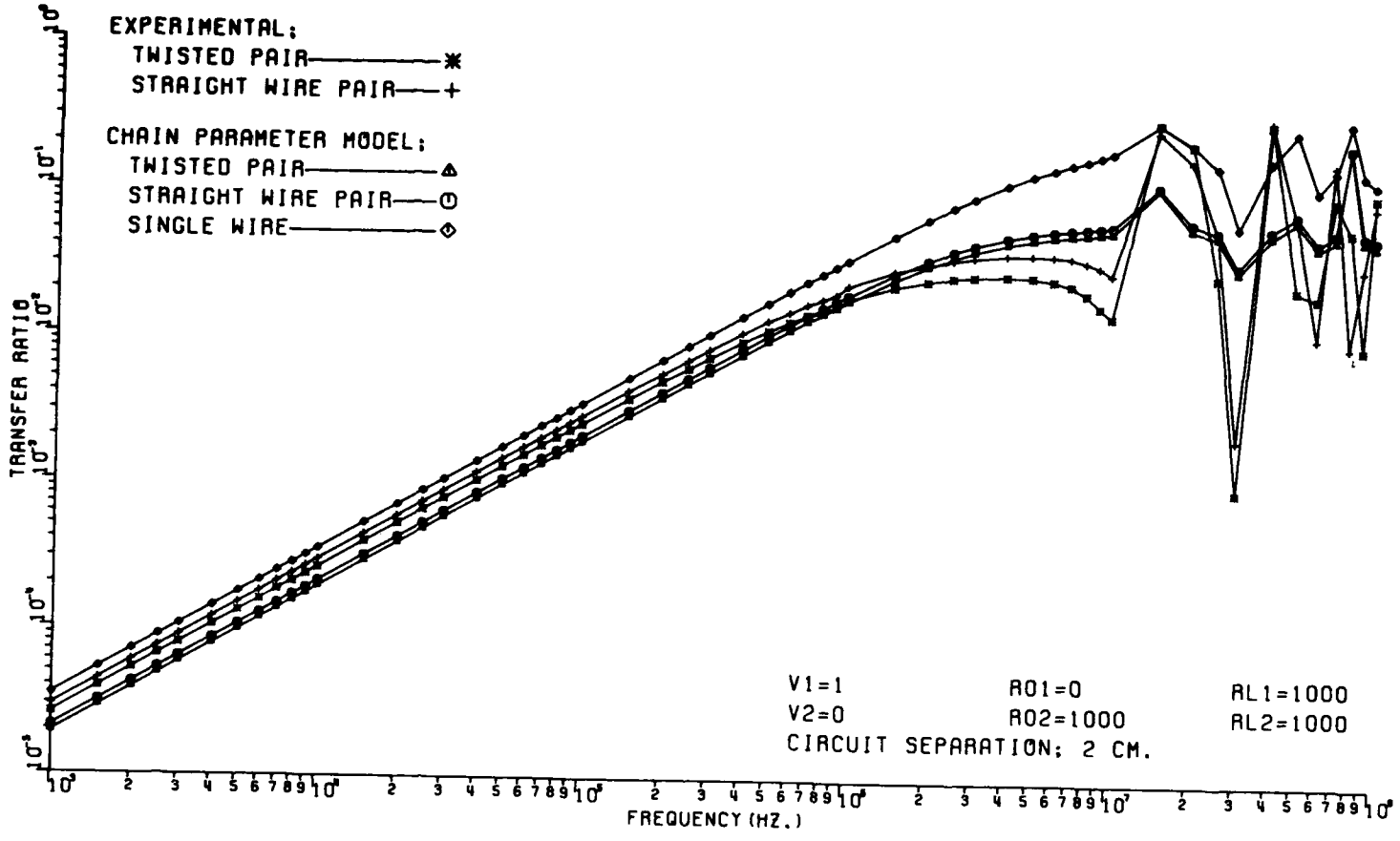
EXPERIMENTAL:
TWISTED PAIR
STRAIGHT WIRE PAIR
CHAIN PARAMETER MODEL:
TWISTED PAIR
STRAIGHT WIRE PAIR
SINGLE WIRE
TRANSFER RATIO
FREQUENCY (HZ.)
V1=1
V2=0
R01=0
R02=1000
RL1=1000
RL2=1000
CIRCUIT SEPARATION: 2 CM.

Fig. A-24

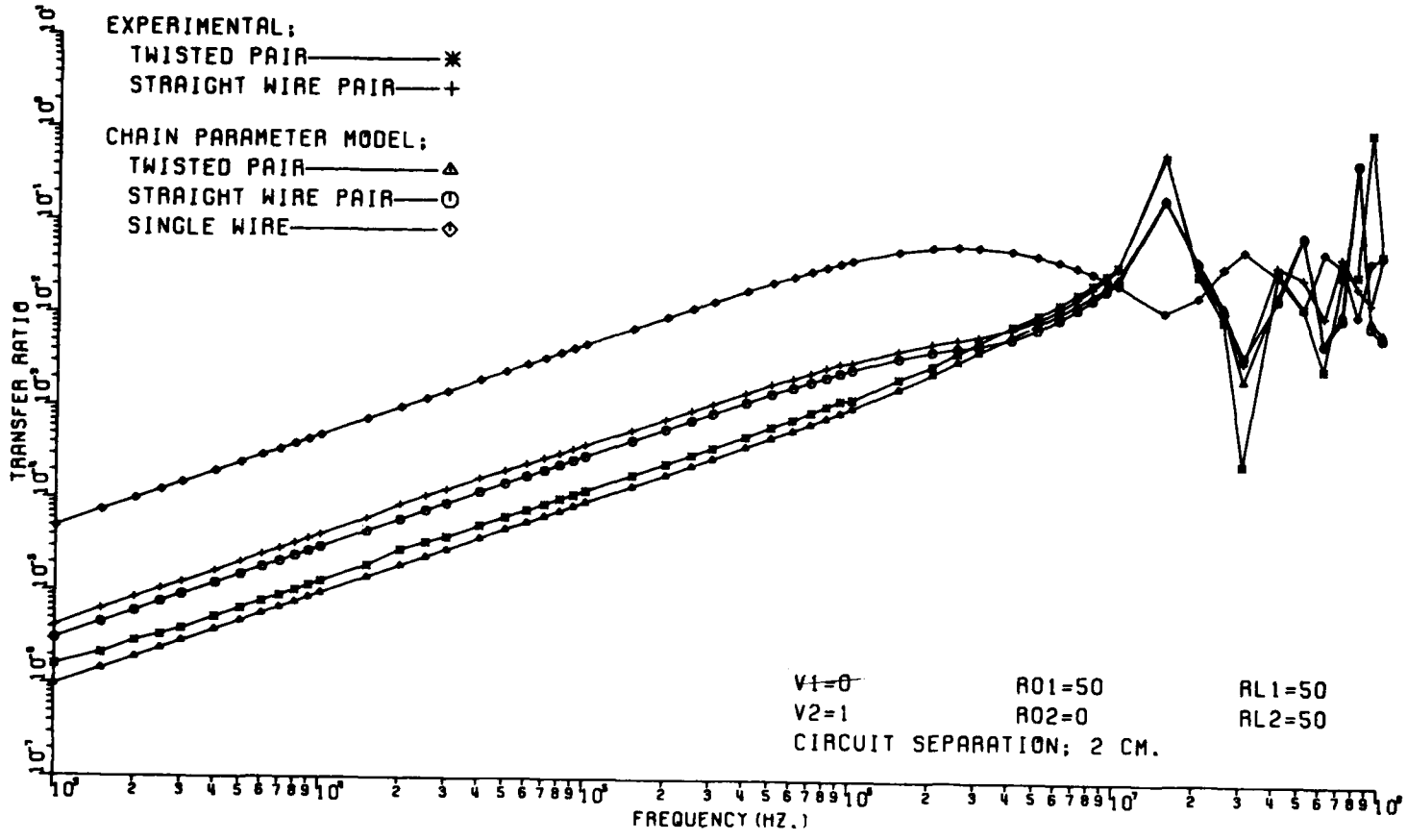
EXPERIMENTAL:
TWISTED PAIR
STRAIGHT WIRE PAIR
CHAIN PARAMETER MODEL:
TWISTED PAIR
STRAIGHT WIRE PAIR
SINGLE WIRE
TRANSFER RATIO
FREQUENCY (HZ.)
V1=0
V2=1
RO1=50
RO2=0
RL1=50
RL2=50
CIRCUIT SEPARATION; 2 CM.

Fig. A-25

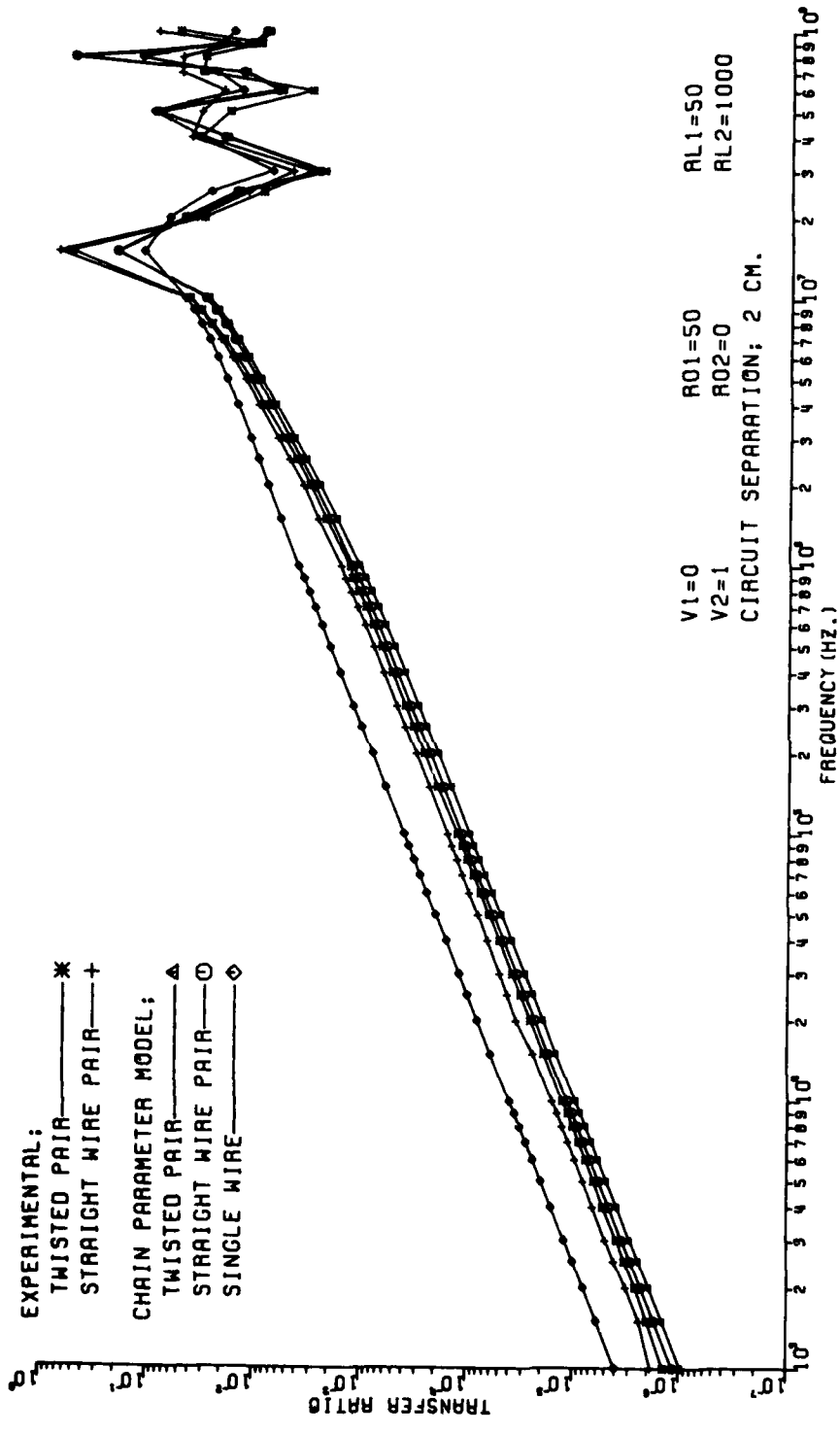
EXPERIMENTAL;
TWISTED PAIR
STRAIGHT WIRE PAIR
CHAIN PARAMETER MODEL;
TWISTED PAIR
STRAIGHT WIRE PAIR
SINGLE WIRE
TRANSFER RATIO
FREQUENCY (HZ.)
V1=0
V2=1
RO1=50
RO2=0
RL1=50
RL2=1000
CIRCUIT SEPARATION; 2 CM.

Fig. A-26

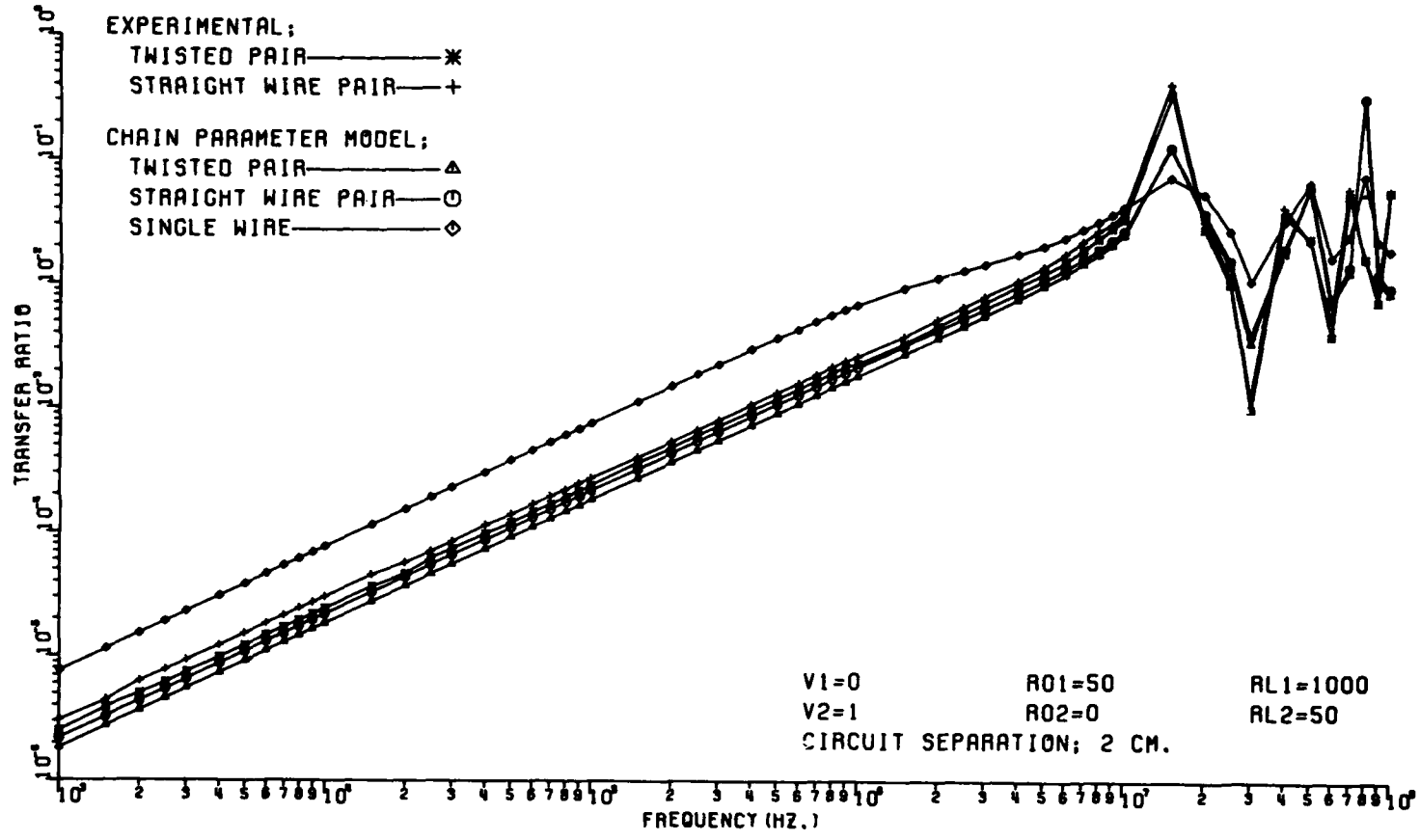
EXPERIMENTAL;
TWISTED PAIR
STRAIGHT WIRE PAIR
CHAIN PARAMETER MODEL;
TWISTED PAIR
STRAIGHT WIRE PAIR
SINGLE WIRE
TRANSFER RATIO
FREQUENCY (HZ.)
V1=0
V2=1
R01=50
R02=0
RL1=1000
RL2=50
CIRCUIT SEPARATION; 2 CM.

Fig. A-27

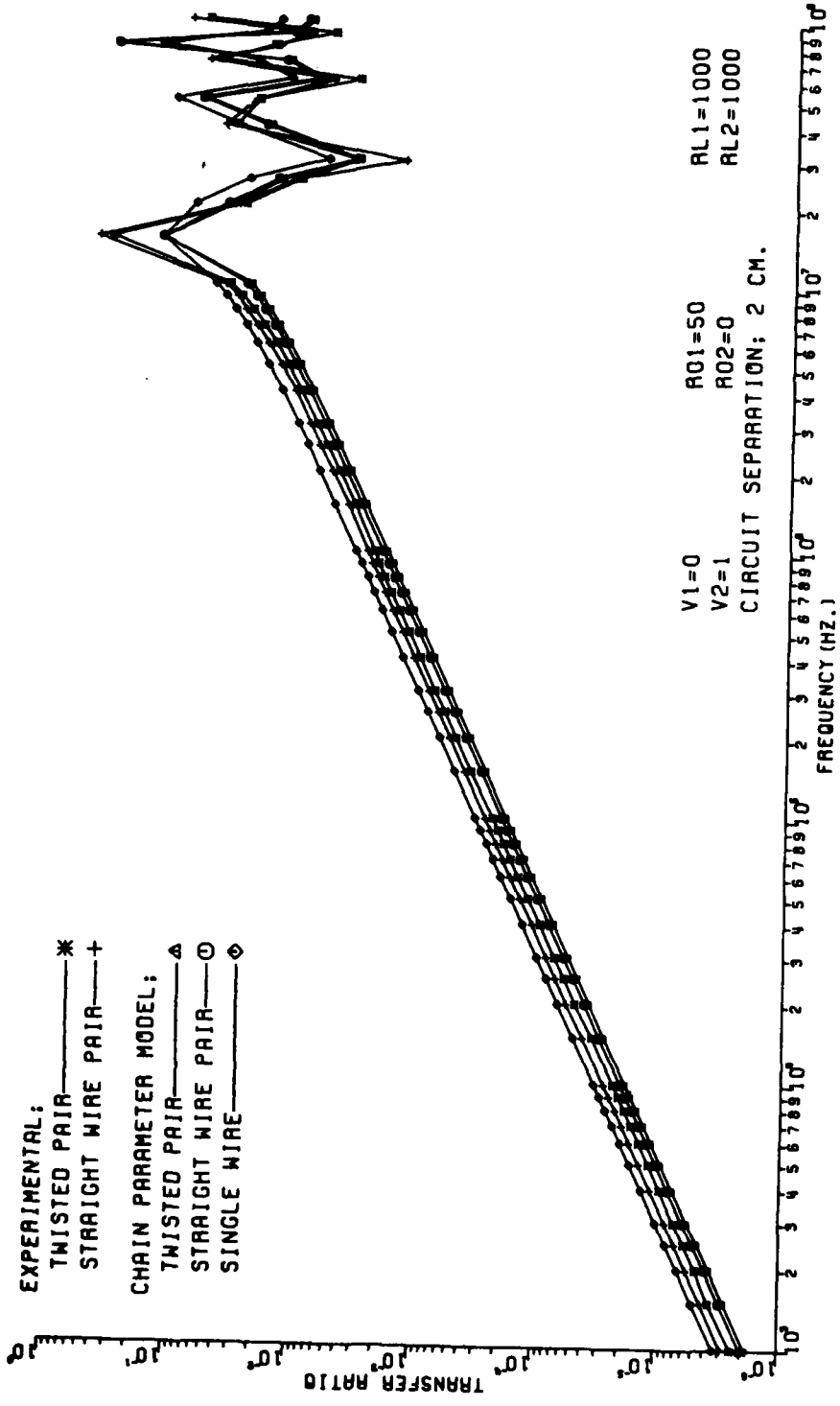
EXPERIMENTAL:
TWISTED PAIR
STRAIGHT WIRE PAIR
CHAIN PARAMETER MODEL:
TWISTED PAIR
STRAIGHT WIRE PAIR
SINGLE WIRE
TRANSFER RATIO
FREQUENCY (HZ.)
V1=0
V2=1
RO1=50
RO2=0
RL1=1000
RL2=1000
CIRCUIT SEPARATION; 2 CM.

Fig. A-28

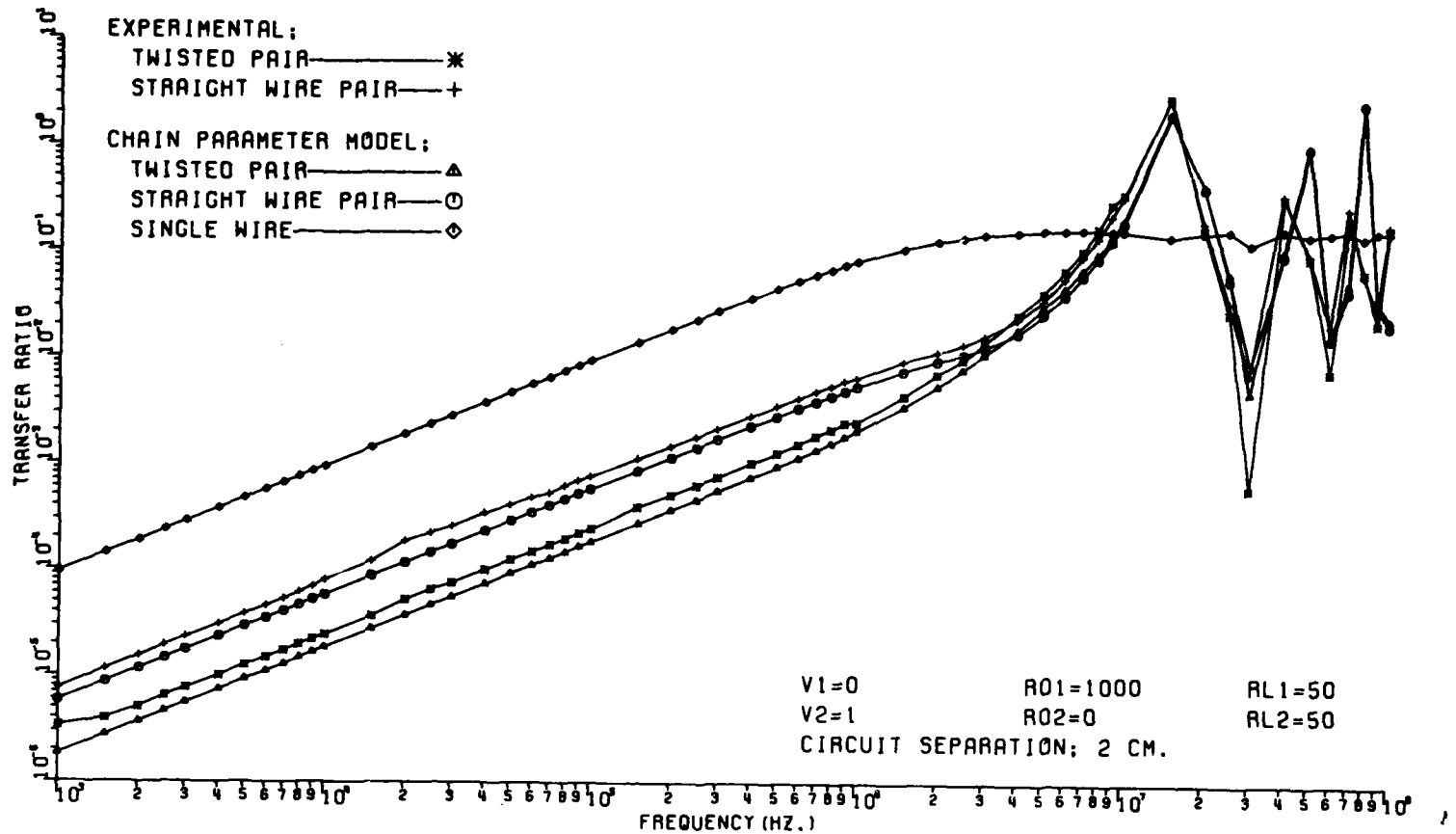
EXPERIMENTAL:
TWISTED PAIR
STRAIGHT WIRE PAIR
CHAIN PARAMETER MODEL:
TWISTED PAIR
STRAIGHT WIRE PAIR
SINGLE WIRE
TRANSFER RATIO
FREQUENCY (HZ.)
V1=0
V2=1
R01=1000
R02=0
RL1=50
RL2=50
CIRCUIT SEPARATION; 2 CM.

Fig. A-29

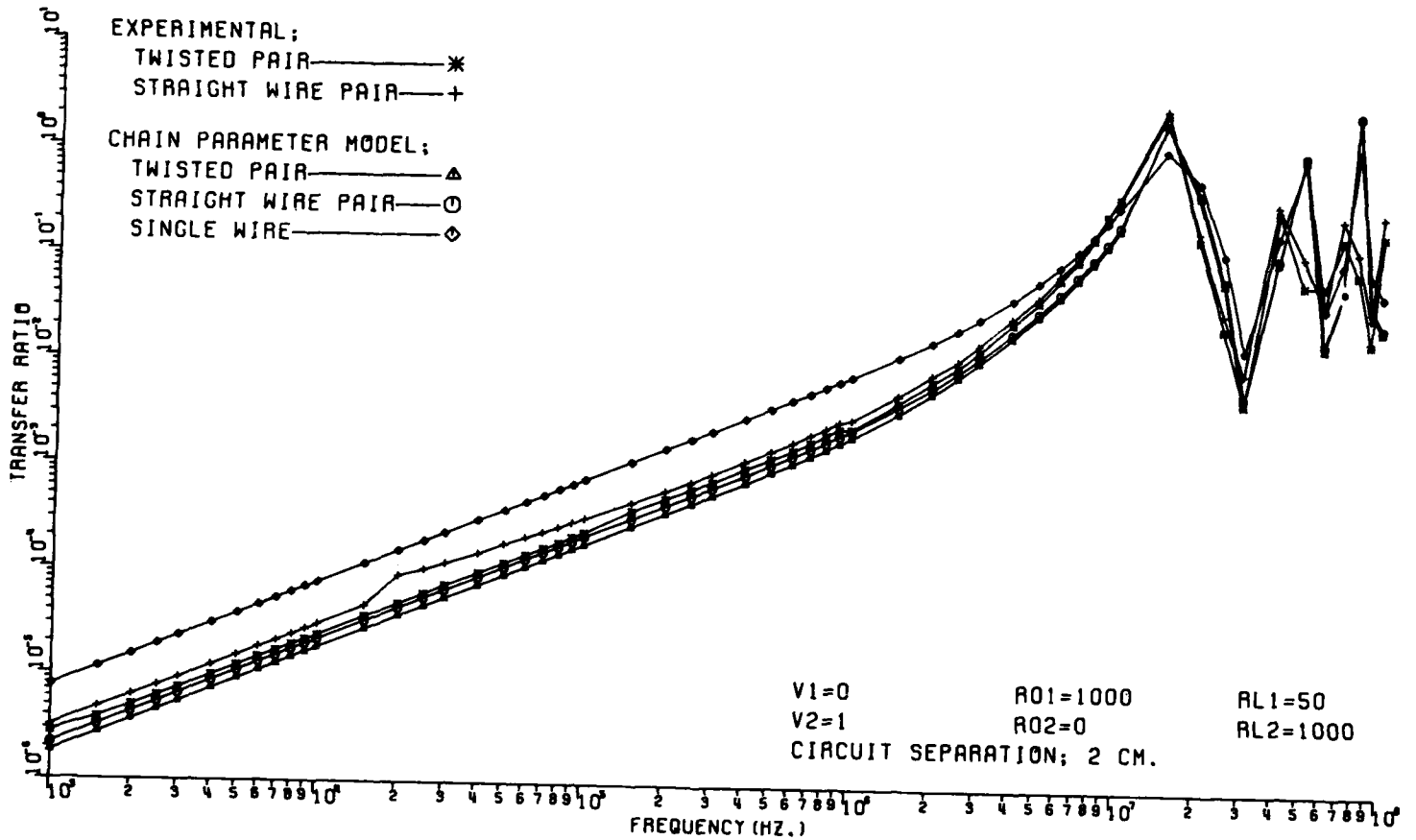
EXPERIMENTAL;
TWISTED PAIR
STRAIGHT WIRE PAIR
CHAIN PARAMETER MODEL;
TWISTED PAIR
STRAIGHT WIRE PAIR
SINGLE WIRE
TRANSFER RATIO
FREQUENCY (HZ.)
V1=0
V2=1
RO1=1000
RO2=0
RL1=50
RL2=1000
CIRCUIT SEPARATION; 2 CM.

Fig. A-30

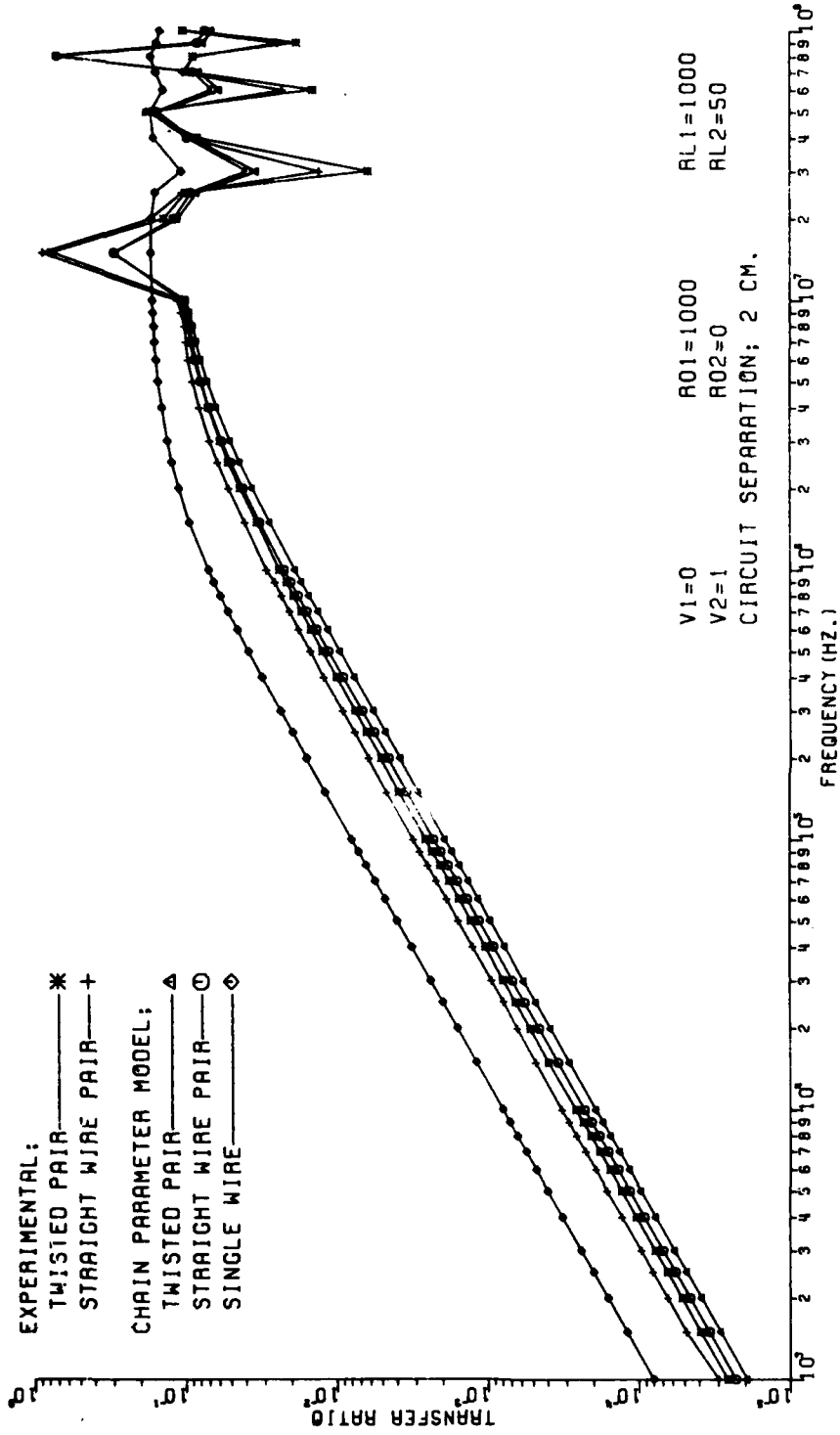
EXPERIMENTAL:
TWISTED PAIR
STRAIGHT WIRE PAIR
CHAIN PARAMETER MODEL;
TWISTED PAIR
STRAIGHT WIRE PAIR
SINGLE WIRE
TRANSFER RATIO
FREQUENCY (HZ.)
V1=0
V2=1
RO1=1000
RO2=0
RL1=1000
RL2=50
CIRCUIT SEPARATION; 2 CM.

Fig. A-31

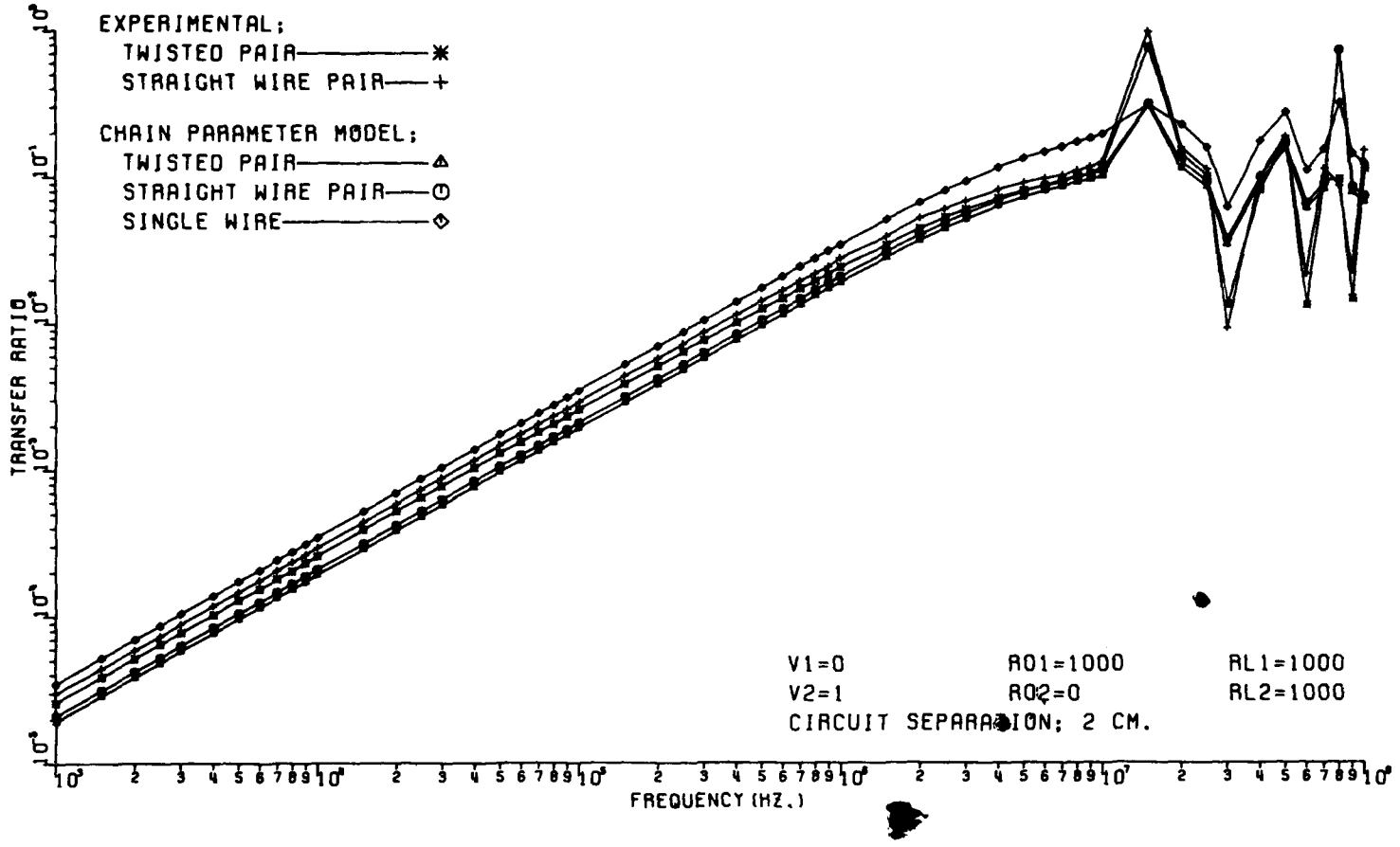
EXPERIMENTAL;
TWISTED PAIR
STRAIGHT WIRE PAIR
CHAIN PARAMETER MODEL;
TWISTED PAIR
STRAIGHT WIRE PAIR
SINGLE WIRE
TRANSFER RATIO
FREQUENCY (HZ.)
V1=0
V2=1
RO1=1000
RO2=0
RL1=1000
RL2=1000
CIRCUIT SEPARATION; 2 CM.

Fig. A-32

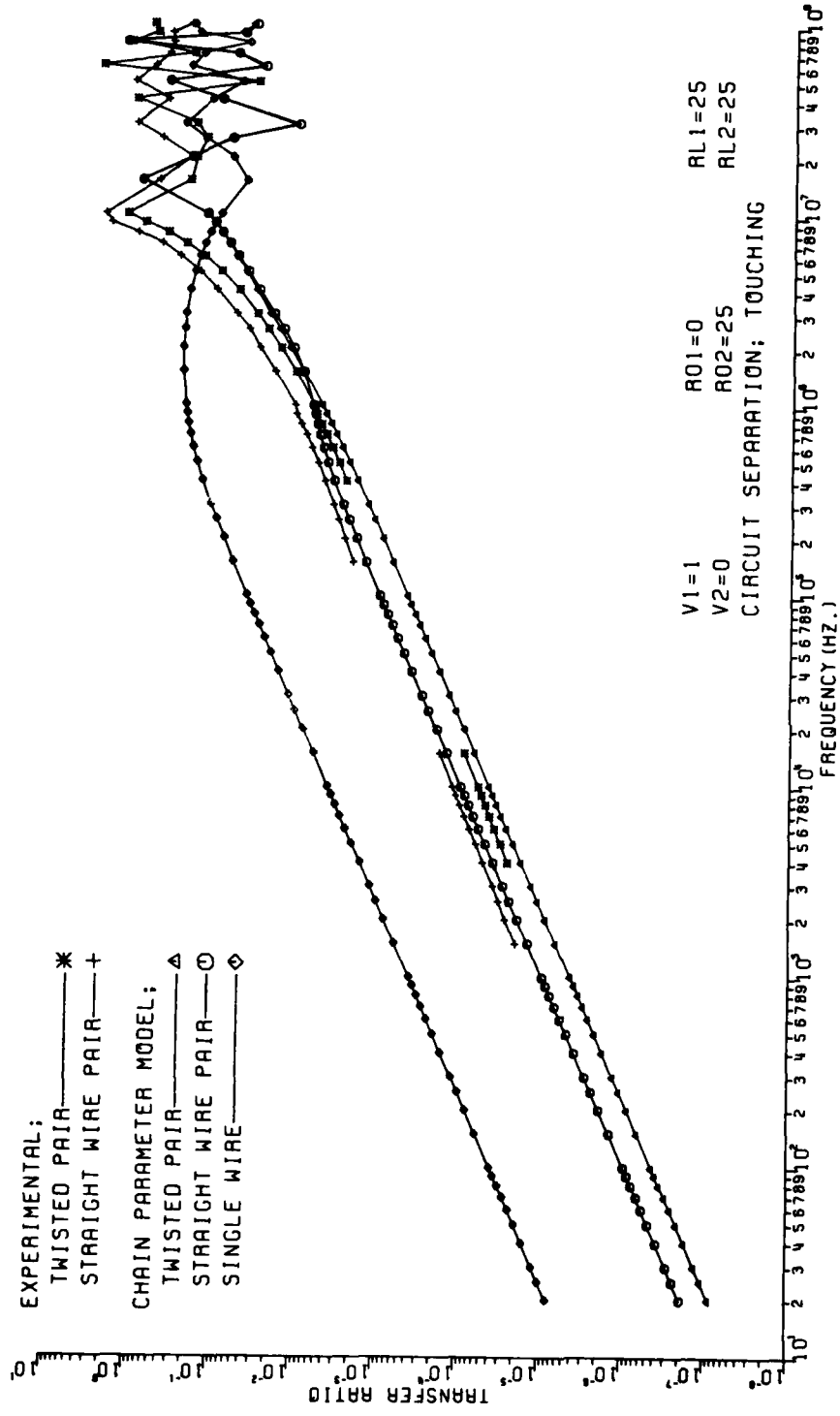
EXPERIMENTAL;
TWISTED PAIR
STRAIGHT WIRE PAIR
CHAIN PARAMETER MODEL;
TWISTED PAIR
STRAIGHT WIRE PAIR
SINGLE WIRE
TRANSFER RATIO
FREQUENCY (HZ.)
V1=1
V2=0
CIRCUIT SEPARATION; TOUCHING
RO1=0
RO2=25
RL1=25
RL2=25

Fig. B-1

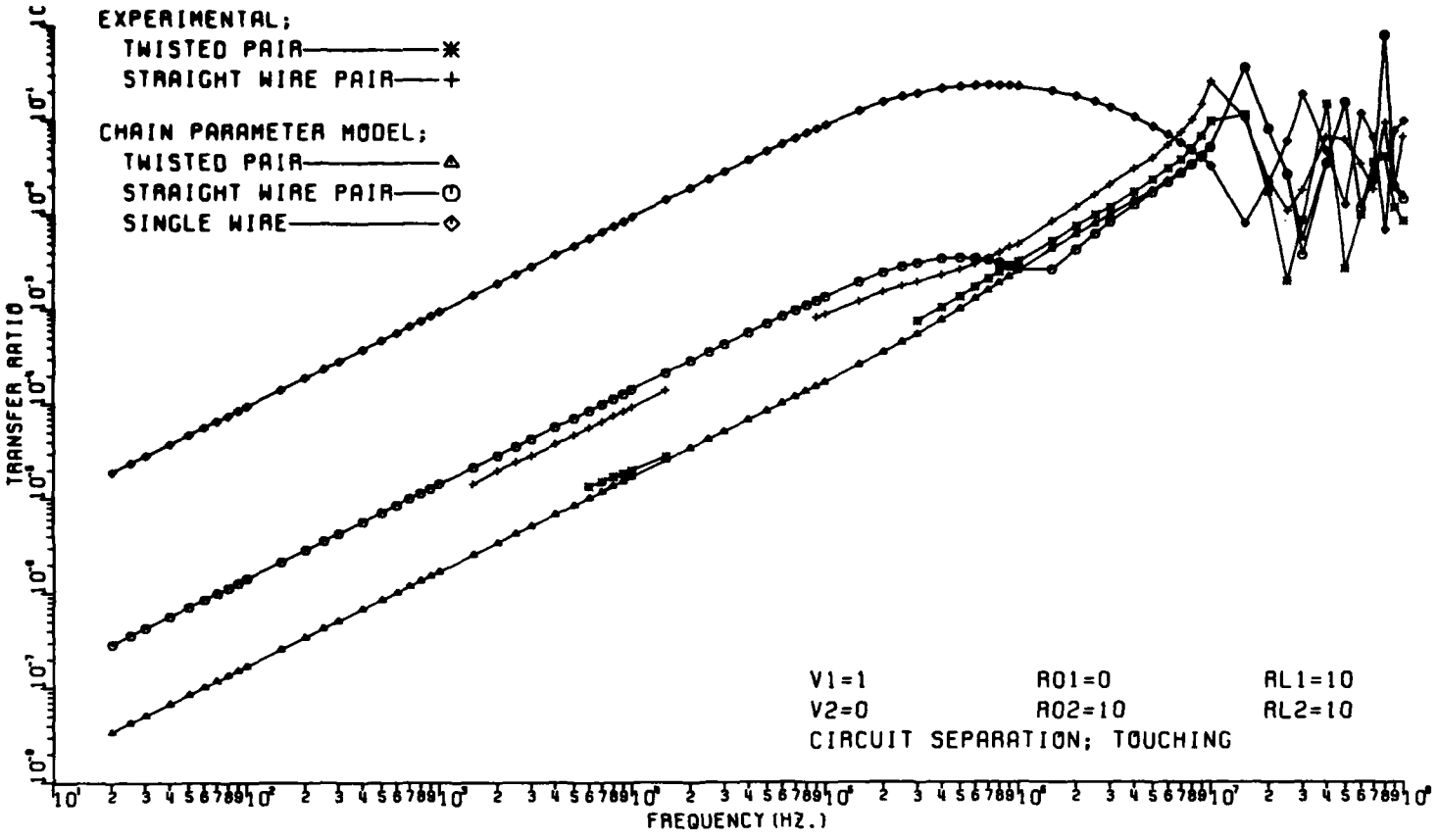
EXPERIMENTAL;
TWISTED PAIR
STRAIGHT WIRE PAIR
CHAIN PARAMETER MODEL;
TWISTED PAIR
STRAIGHT WIRE PAIR
SINGLE WIRE
TRANSFER RATIO
FREQUENCY (HZ.)
V1=1
V2=0
R01=0
R02=10
RL1=10
RL2=10
CIRCUIT SEPARATION; TOUCHING

Fig. B-2

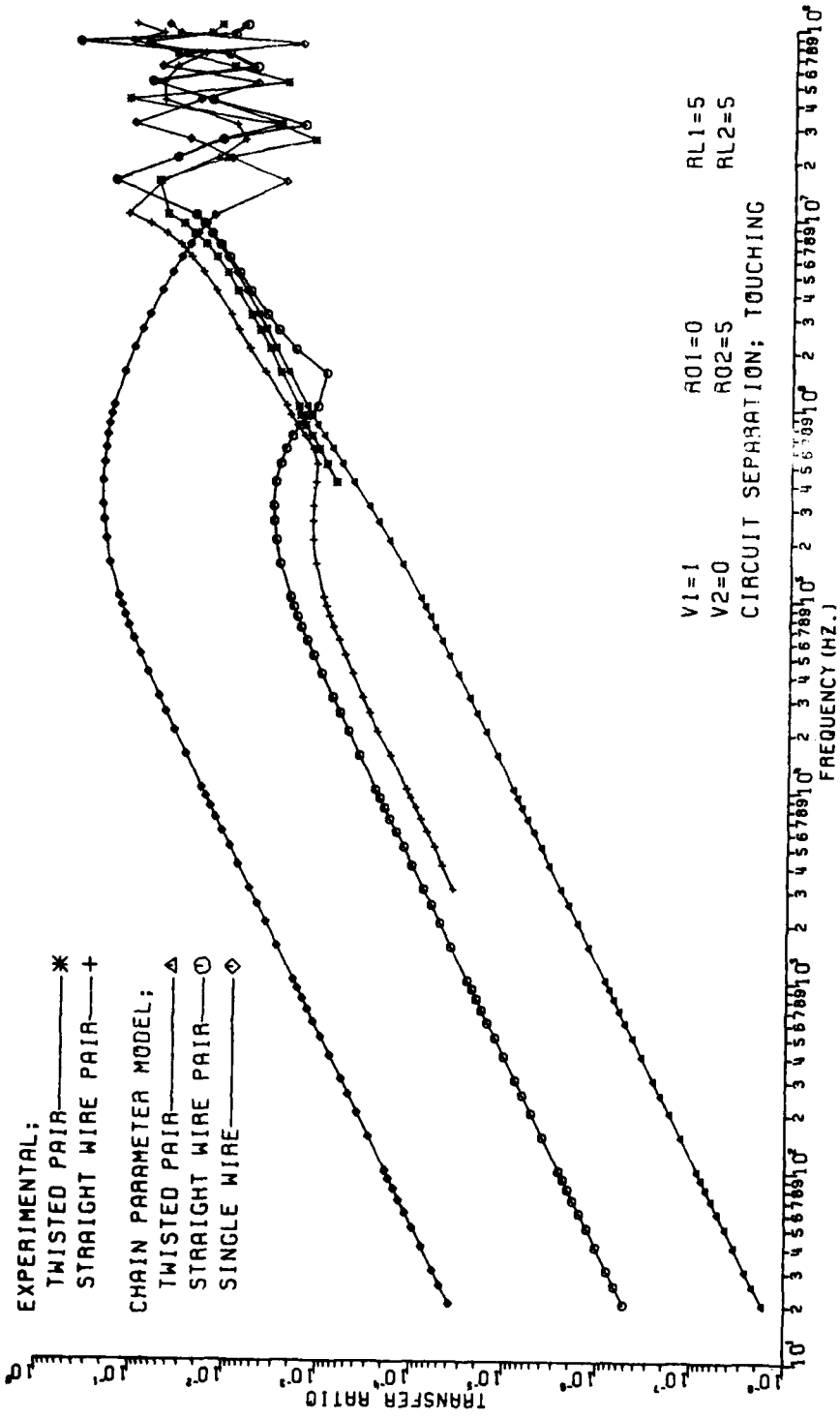
EXPERIMENTAL;
TWISTED PAIR——*
STRAIGHT WIRE PAIR——+
CHAIN PARAMETER MODEL;
TWISTED PAIR——△
STRAIGHT WIRE PAIR——□
SINGLE WIRE——◇
TRANSFER RATIO
FREQUENCY (HZ.)
V1=1
V2=0
RO1=0
RO2=5
RL1=5
RL2=5
CIRCUIT SEPARATION; TOUCHING

Fig. B-3

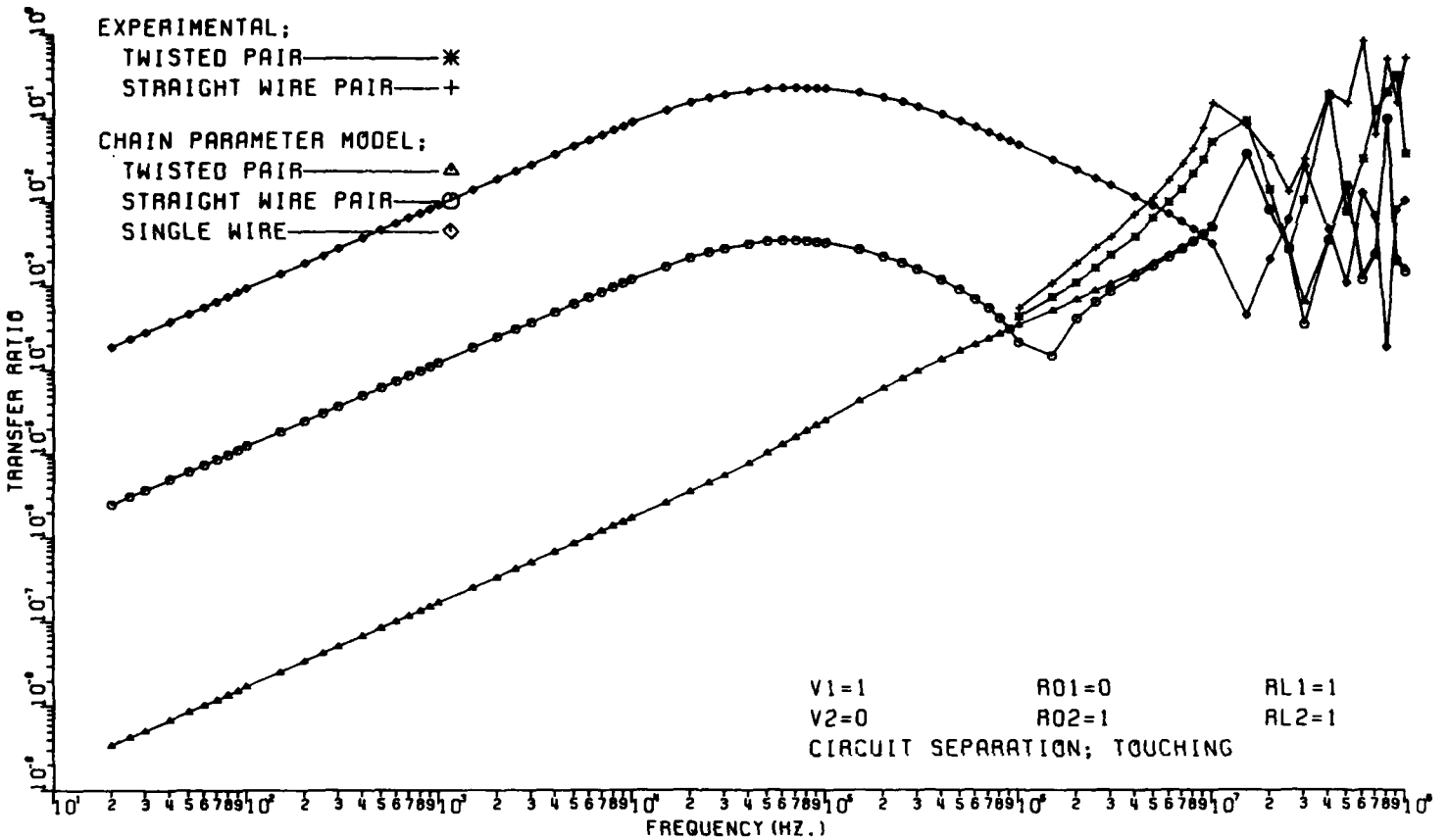
EXPERIMENTAL;
TWISTED PAIR
STRAIGHT WIRE PAIR
CHAIN PARAMETER MODEL;
TWISTED PAIR
STRAIGHT WIRE PAIR
SINGLE WIRE
TRANSFER RATIO
FREQUENCY (HZ.)
V1=1
V2=0
R01=0
R02=1
RL1=1
RL2=1
CIRCUIT SEPARATION; TOUCHING

Fig. B-4

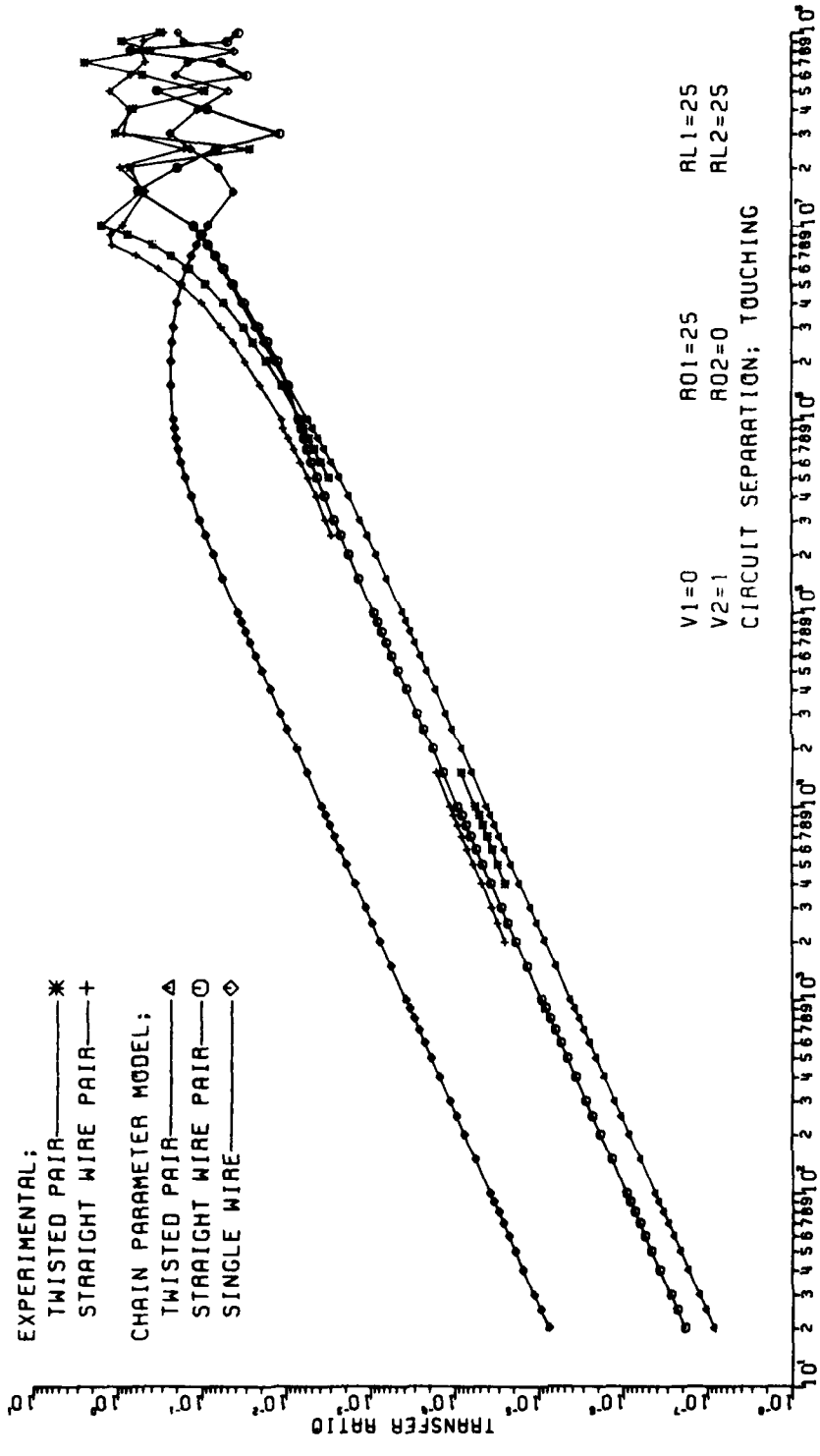
EXPERIMENTAL;
TWISTED PAIR
STRAIGHT WIRE PAIR
CHAIN PARAMETER MODEL;
TWISTED PAIR
STRAIGHT WIRE PAIR
SINGLE WIRE
TRANSFER RATIO
FREQUENCY (HZ.)
V1=0
V2=1
RO1=25
RO2=0
RL1=25
RL2=25
CIRCUIT SEPARATION; TOUCHING

Fig. B-5

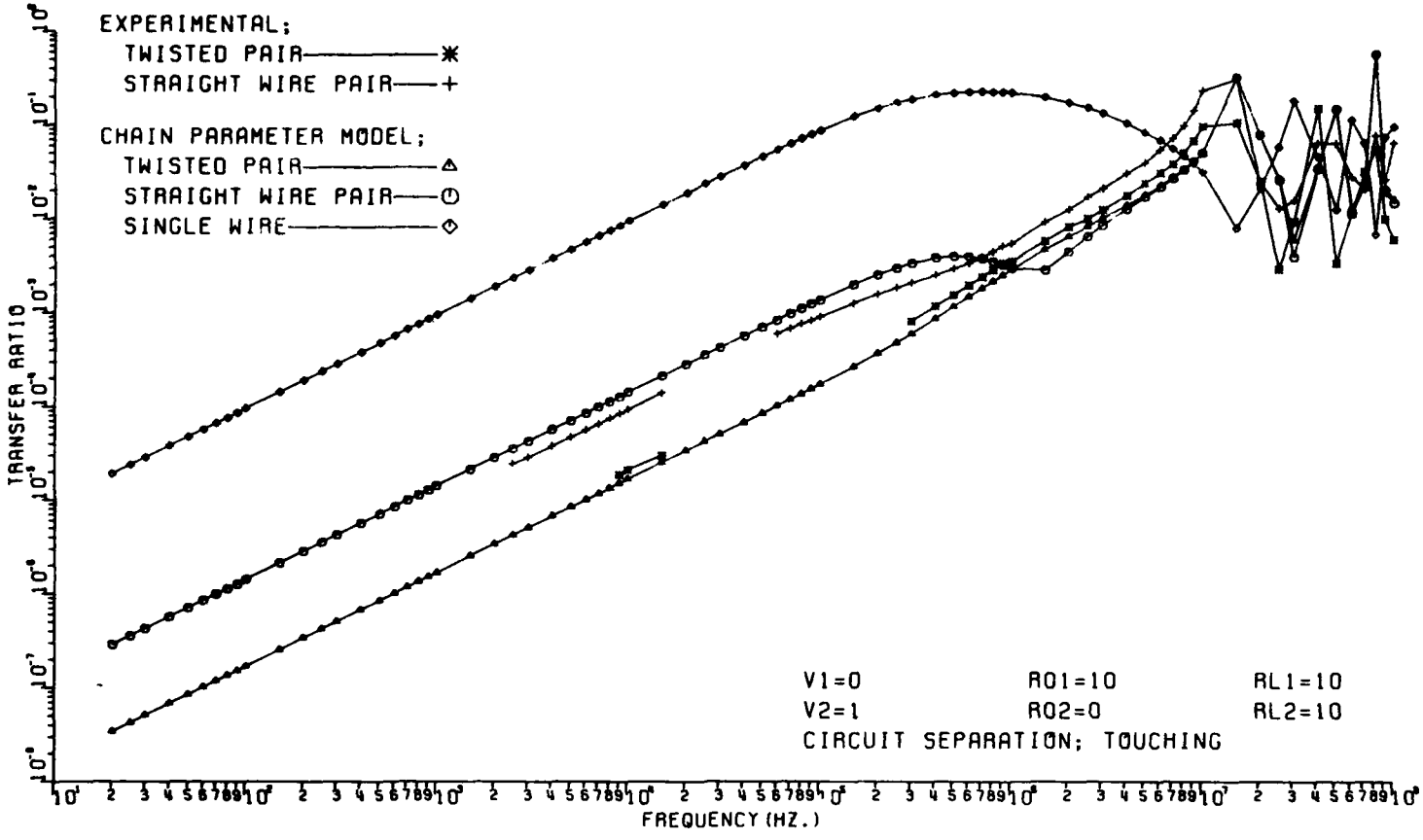
EXPERIMENTAL;
TWISTED PAIR
STRAIGHT WIRE PAIR
CHAIN PARAMETER MODEL;
TWISTED PAIR
STRAIGHT WIRE PAIR
SINGLE WIRE
TRANSFER RATIO
FREQUENCY (HZ.)
V1=0
V2=1
R01=10
R02=0
RL1=10
RL2=10
CIRCUIT SEPARATION; TOUCHING

Fig. B-6

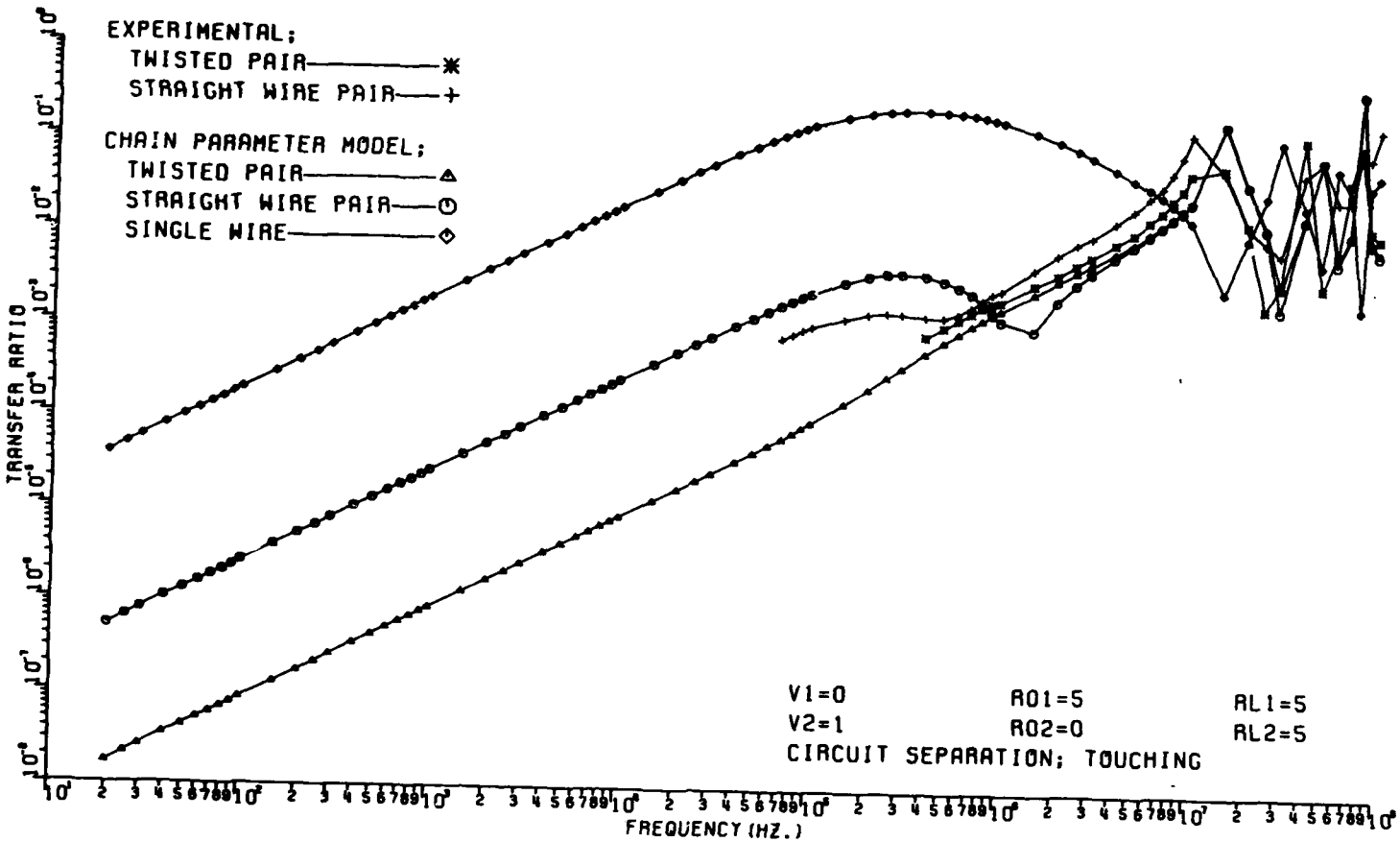
EXPERIMENTAL;
TWISTED PAIR
STRAIGHT WIRE PAIR
CHAIN PARAMETER MODEL;
TWISTED PAIR
STRAIGHT WIRE PAIR
SINGLE WIRE
TRANSFER RATIO
FREQUENCY (HZ.)
V1=0
V2=1
R01=5
R02=0
RL1=5
RL2=5
CIRCUIT SEPARATION; TOUCHING

Fig. B-7

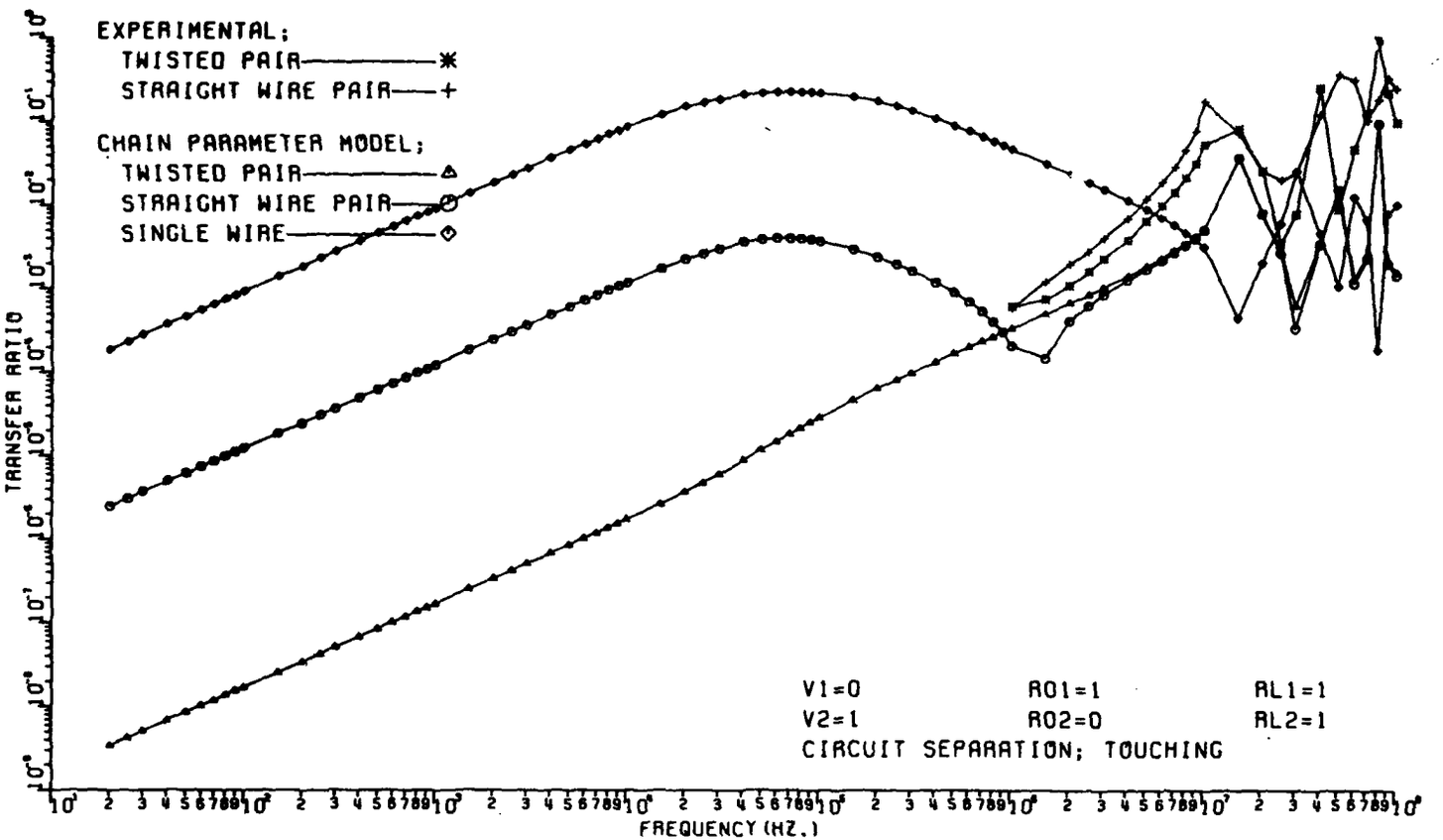
EXPERIMENTAL;
TWISTED PAIR
STRAIGHT WIRE PAIR
CHAIN PARAMETER MODEL;
TWISTED PAIR
STRAIGHT WIRE PAIR
SINGLE WIRE
TRANSFER RATIO
FREQUENCY (HZ.)
V1=0
V2=1
RO1=1
RO2=0
RL1=1
RL2=1
CIRCUIT SEPARATION; TOUCHING

Fig. B-8

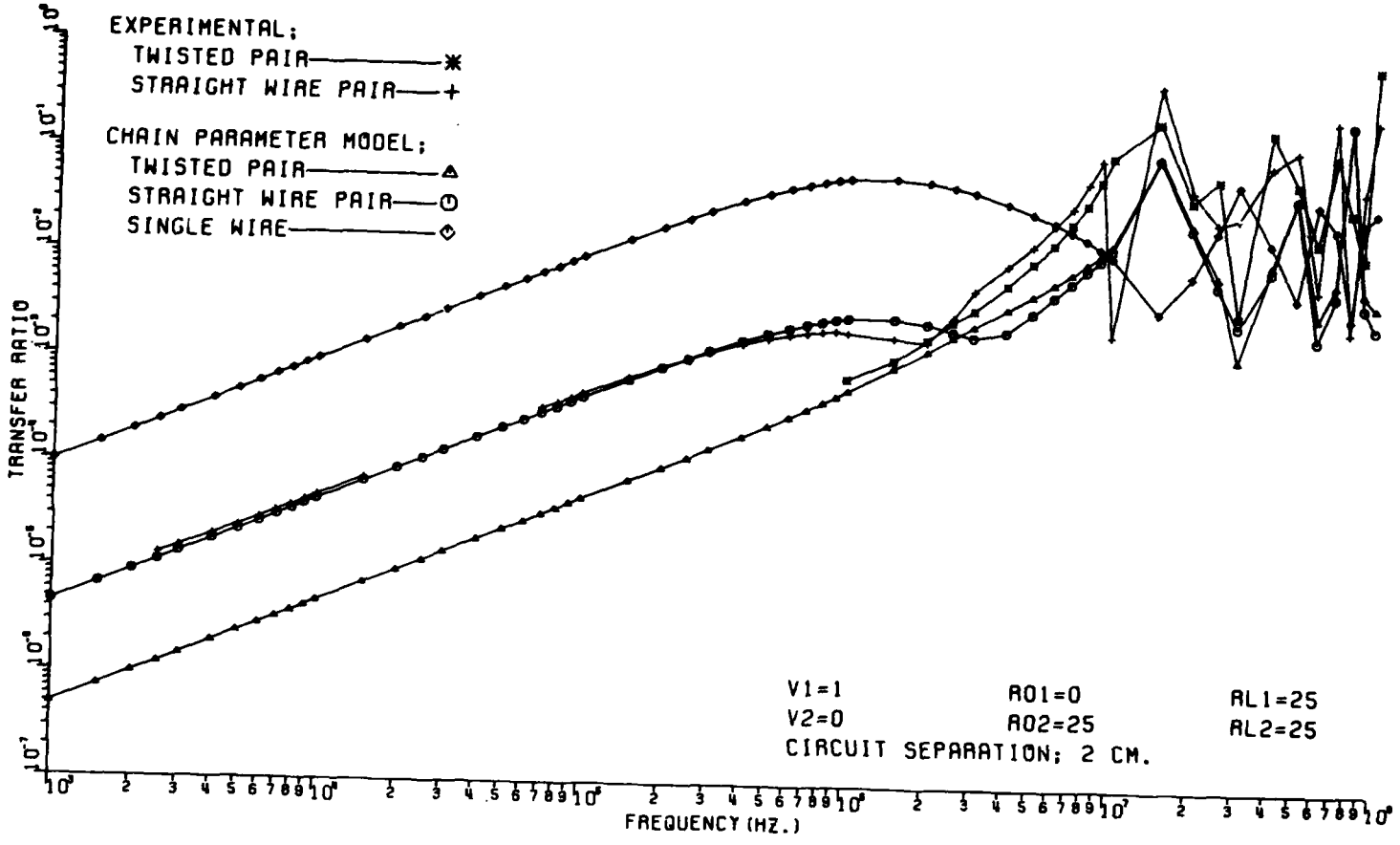
EXPERIMENTAL;
TWISTED PAIR
STRAIGHT WIRE PAIR
CHAIN PARAMETER MODEL;
TWISTED PAIR
STRAIGHT WIRE PAIR
SINGLE WIRE
TRANSFER RATIO
FREQUENCY (HZ.)
V1=1
V2=0
R01=0
R02=25
RL1=25
RL2=25
CIRCUIT SEPARATION; 2 CM.

Fig. B-9

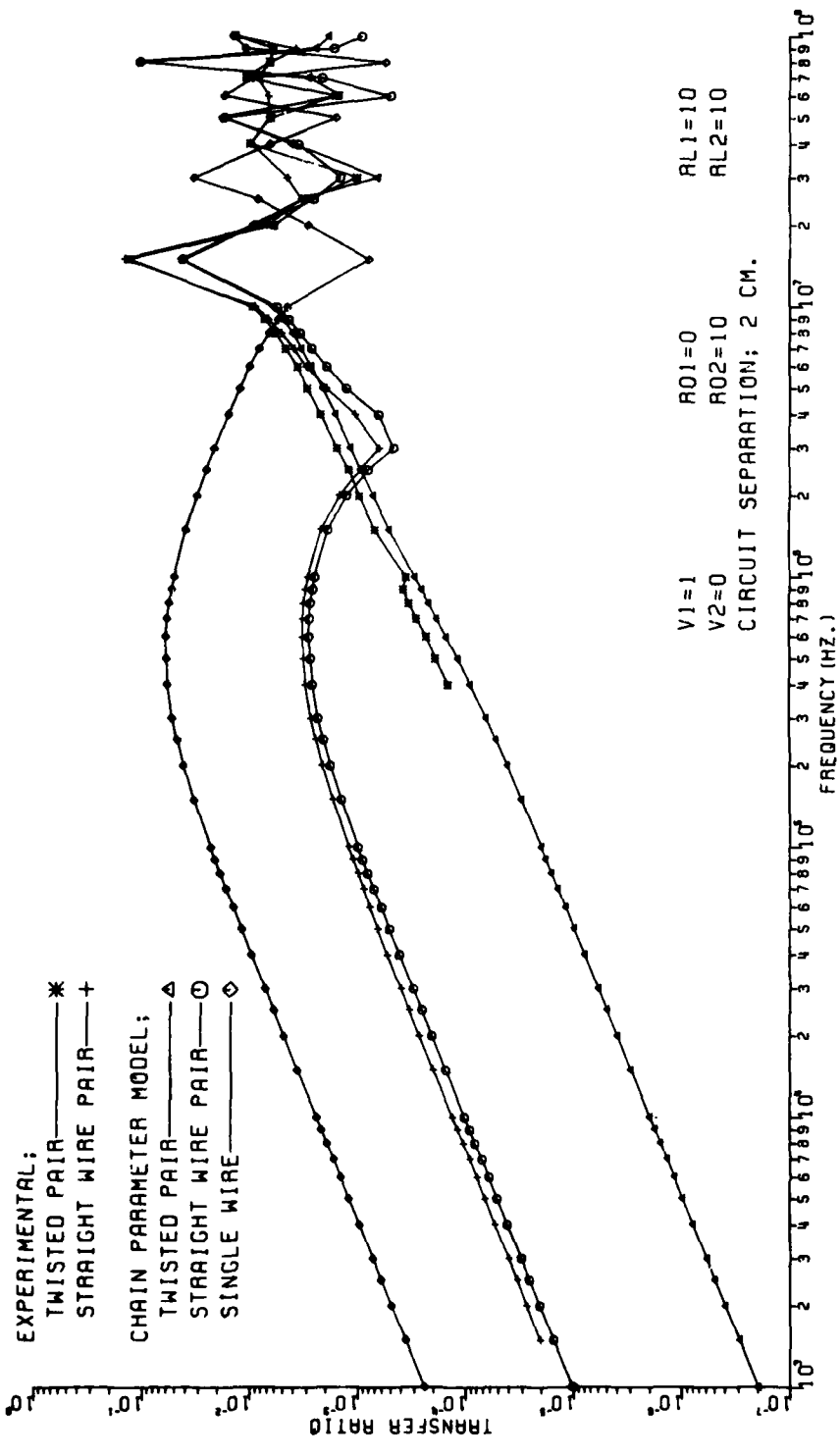
EXPERIMENTAL;
TWISTED PAIR
STRAIGHT WIRE PAIR
CHAIN PARAMETER MODEL;
TWISTED PAIR
STRAIGHT WIRE PAIR
SINGLE WIRE
TRANSFER RATIO
FREQUENCY (HZ.)
V1=1
V2=0
RO1=0
RO2=10
RL1=10
RL2=10
CIRCUIT SEPARATION; 2 CM.

Fig. B-10

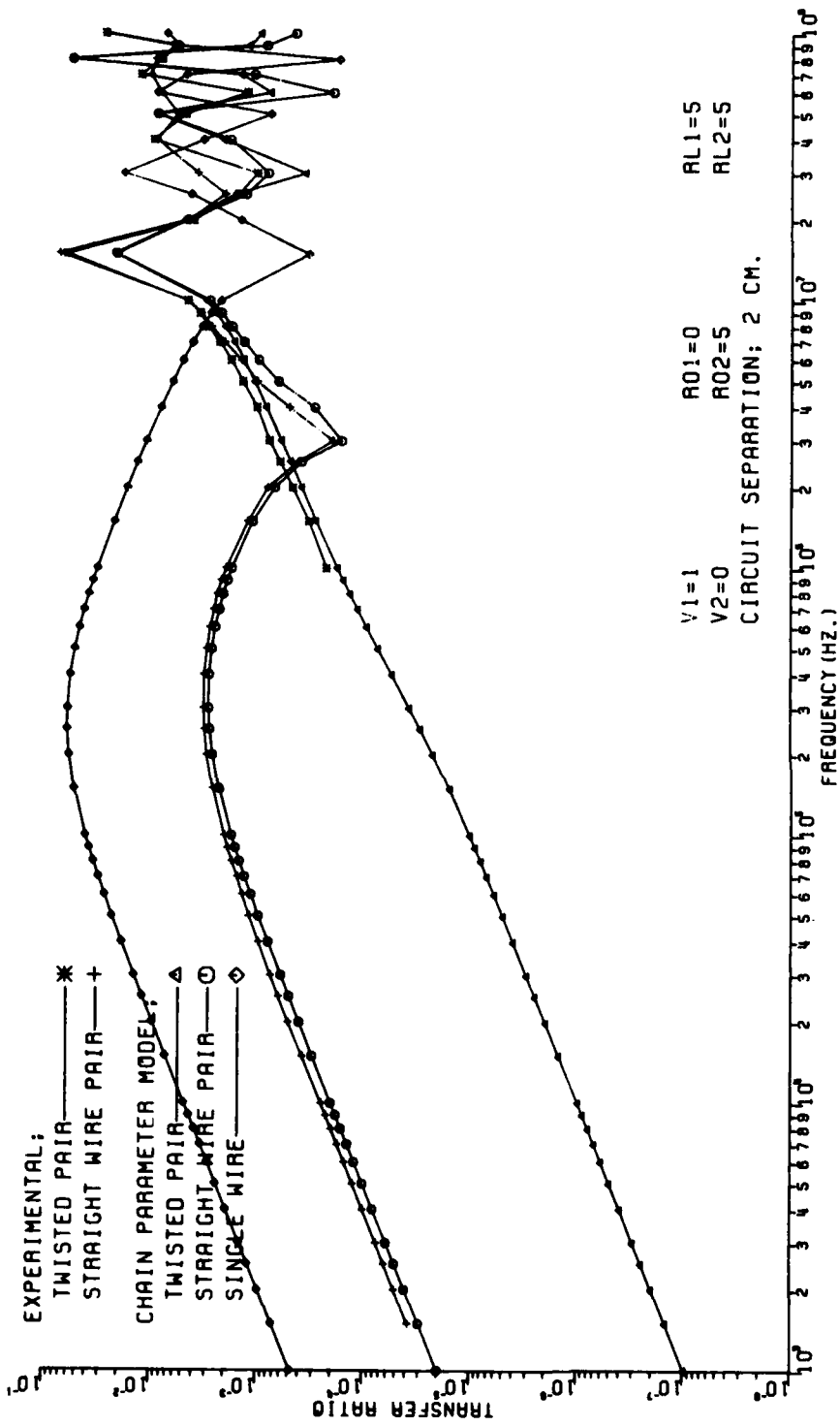
EXPERIMENTAL;
TWISTED PAIR
STRAIGHT WIRE PAIR
CHAIN PARAMETER MODEL;
TWISTED PAIR
STRAIGHT WIRE PAIR
SINGLE WIRE
TRANSFER RATIO
FREQUENCY(HZ.)
V1=1
V2=0
CIRCUIT SEPARATION; 2 CM.
RO1=0
RO2=5
RL1=5
RL2=5

Fig. B-11

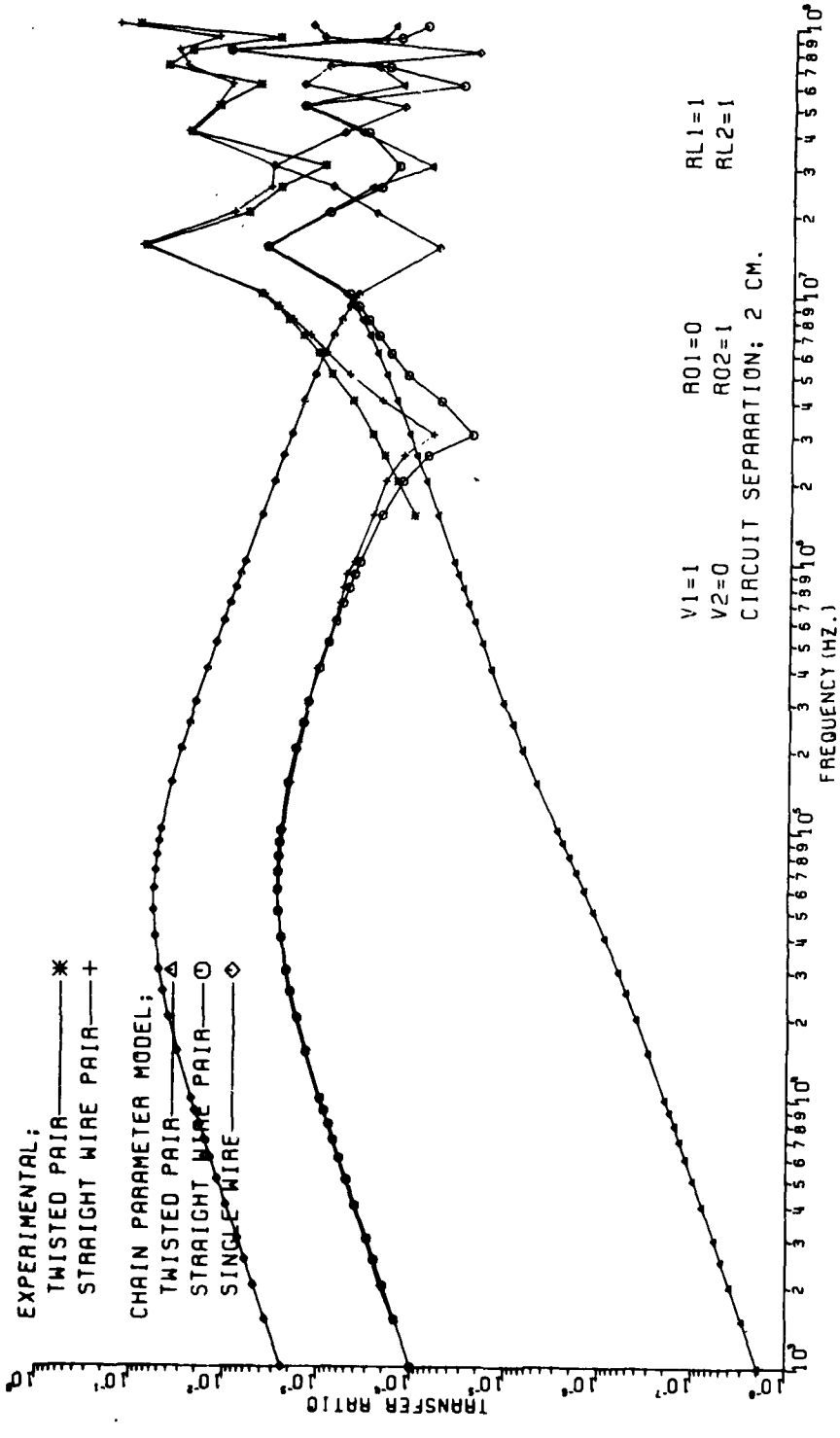
EXPERIMENTAL;
TWISTED PAIR
STRAIGHT WIRE PAIR
CHAIN PARAMETER MODEL;
TWISTED PAIR
STRAIGHT WIRE PAIR
SINGLE WIRE
TRANSFER RATIO
FREQUENCY (HZ.)
V1=1
V2=0
RO1=0
RO2=1
RL1=1
RL2=1
CIRCUIT SEPARATION; 2 CM.

Fig. B-12

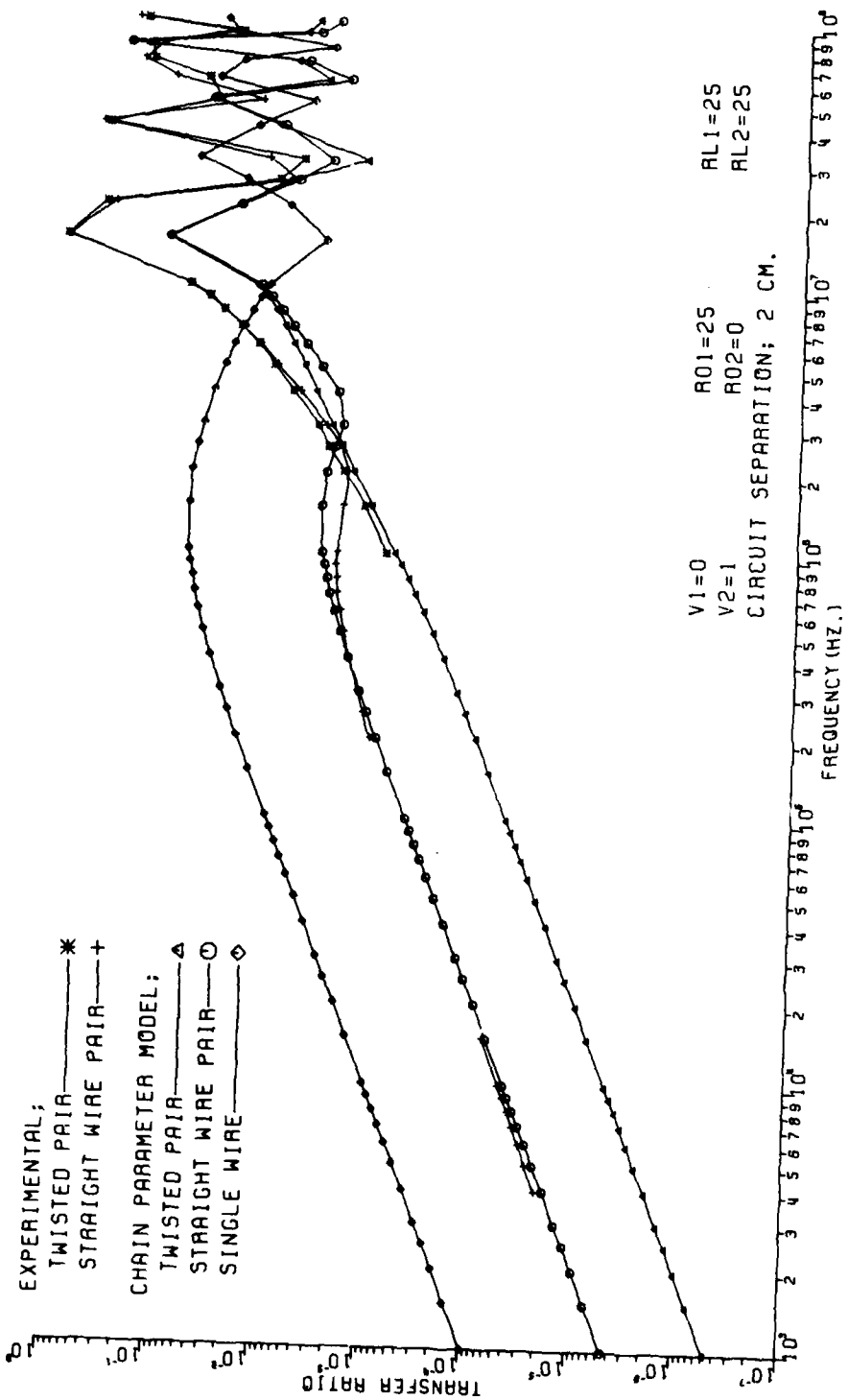
EXPERIMENTAL;
TWISTED PAIR
STRAIGHT WIRE PAIR
CHAIN PARAMETER MODEL;
TWISTED PAIR
STRAIGHT WIRE PAIR
SINGLE WIRE
TRANSFER RATIO
FREQUENCY (HZ.)
V1=0
V2=1
CIRCUIT SEPARATION; 2 CM.
RO1=25
RO2=0
RL1=25
RL2=25

Fig. B-13

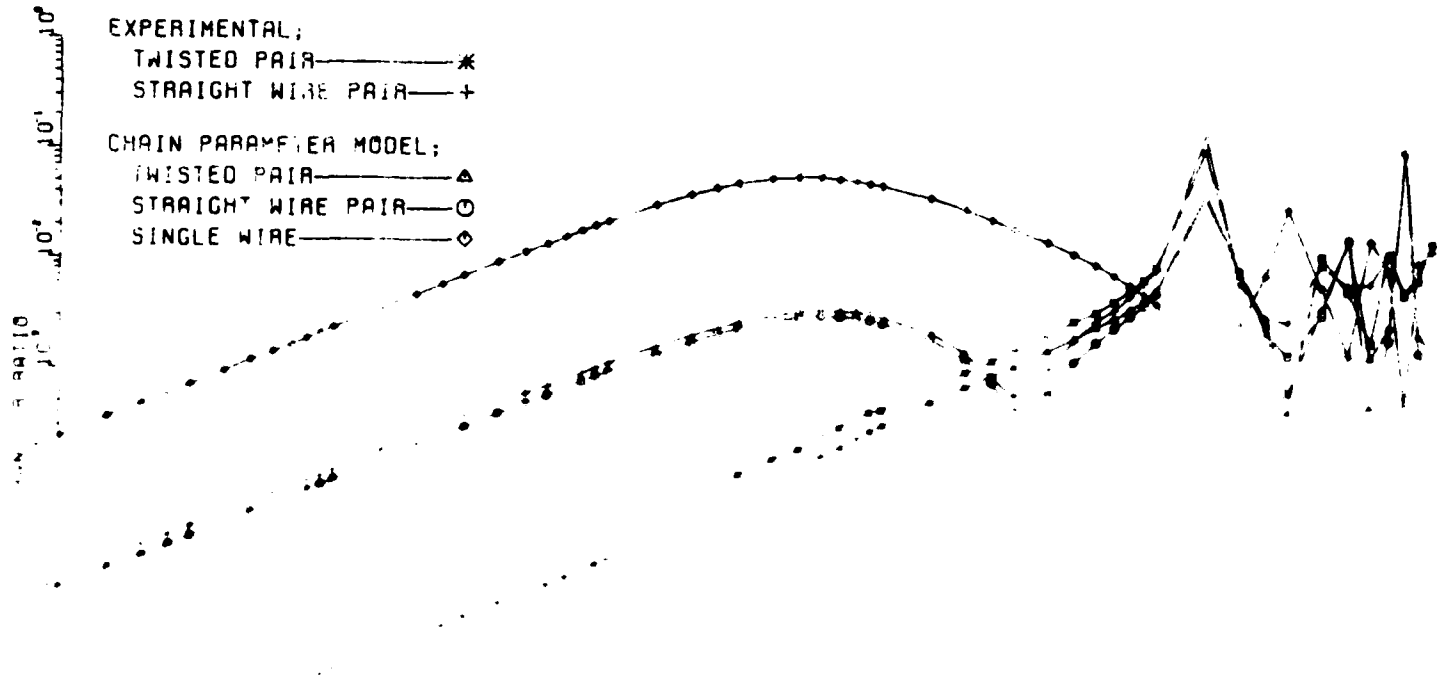
EXPERIMENTAL;
TWISTED PAIR
STRAIGHT WIRE PAIR
CHAIN PARAMETER MODEL;
TWISTED PAIR
STRAIGHT WIRE PAIR
SINGLE WIRE

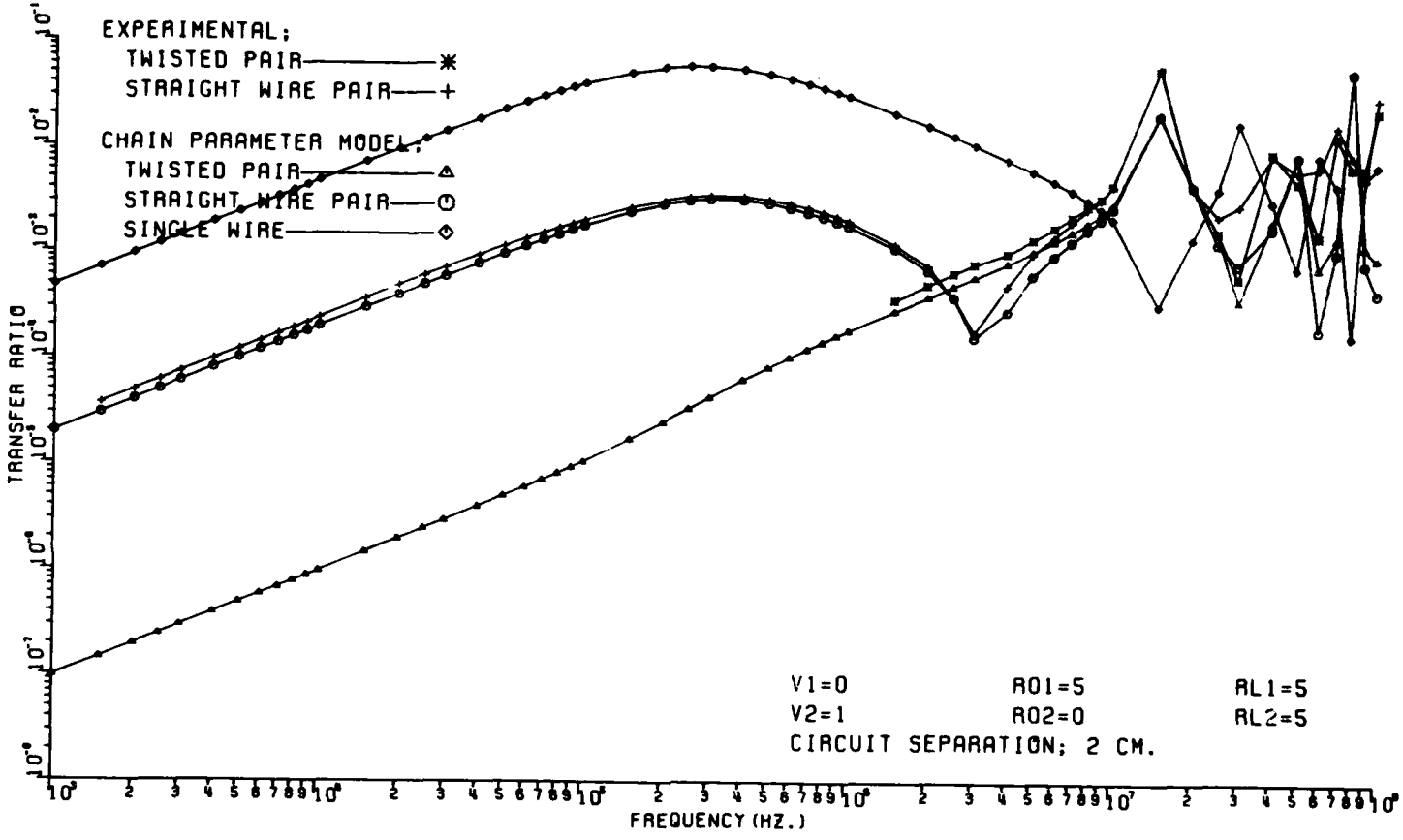
EXPERIMENTAL;
TWISTED PAIR
STRAIGHT WIRE PAIR
CHAIN PARAMETER MODEL;
TWISTED PAIR
STRAIGHT WIRE PAIR
SINGLE WIRE
TRANSFER RATIO
FREQUENCY (HZ.)
V1=0
V2=1
RO1=5
RO2=0
RL1=5
RL2=5
CIRCUIT SEPARATION; 2 CM.

Fig. B-15

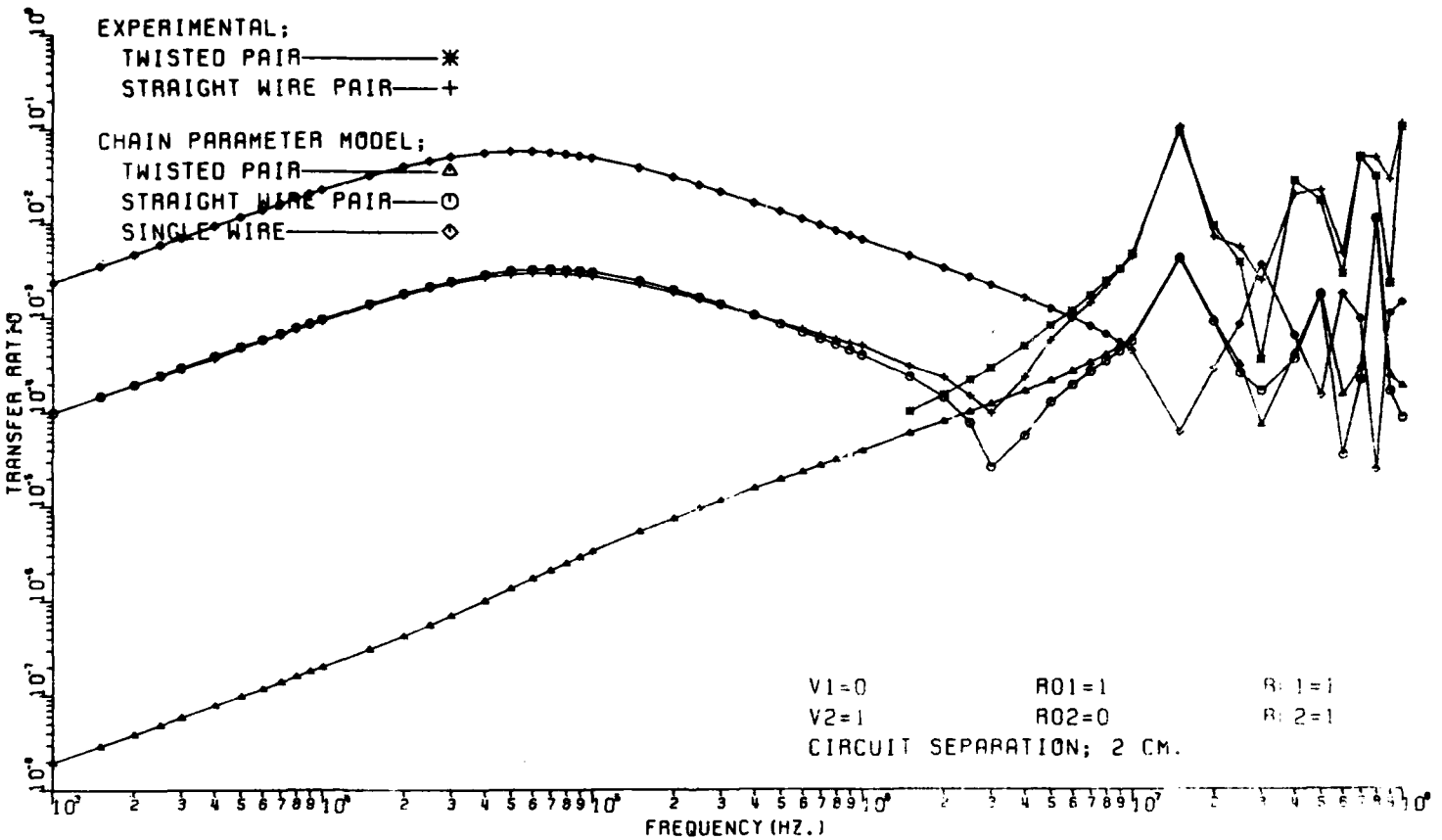
EXPERIMENTAL;
TWISTED PAIR
STRAIGHT WIRE PAIR
CHAIN PARAMETER MODEL;
TWISTED PAIR
STRAIGHT WIRE PAIR
SINGLE WIRE
TRANSFER RATIO
FREQUENCY (HZ.)
V1=0
V2=1
RO1=1
RO2=0
CIRCUIT SEPARATION; 2 CM.

Fig. B-16

APPENDIX C

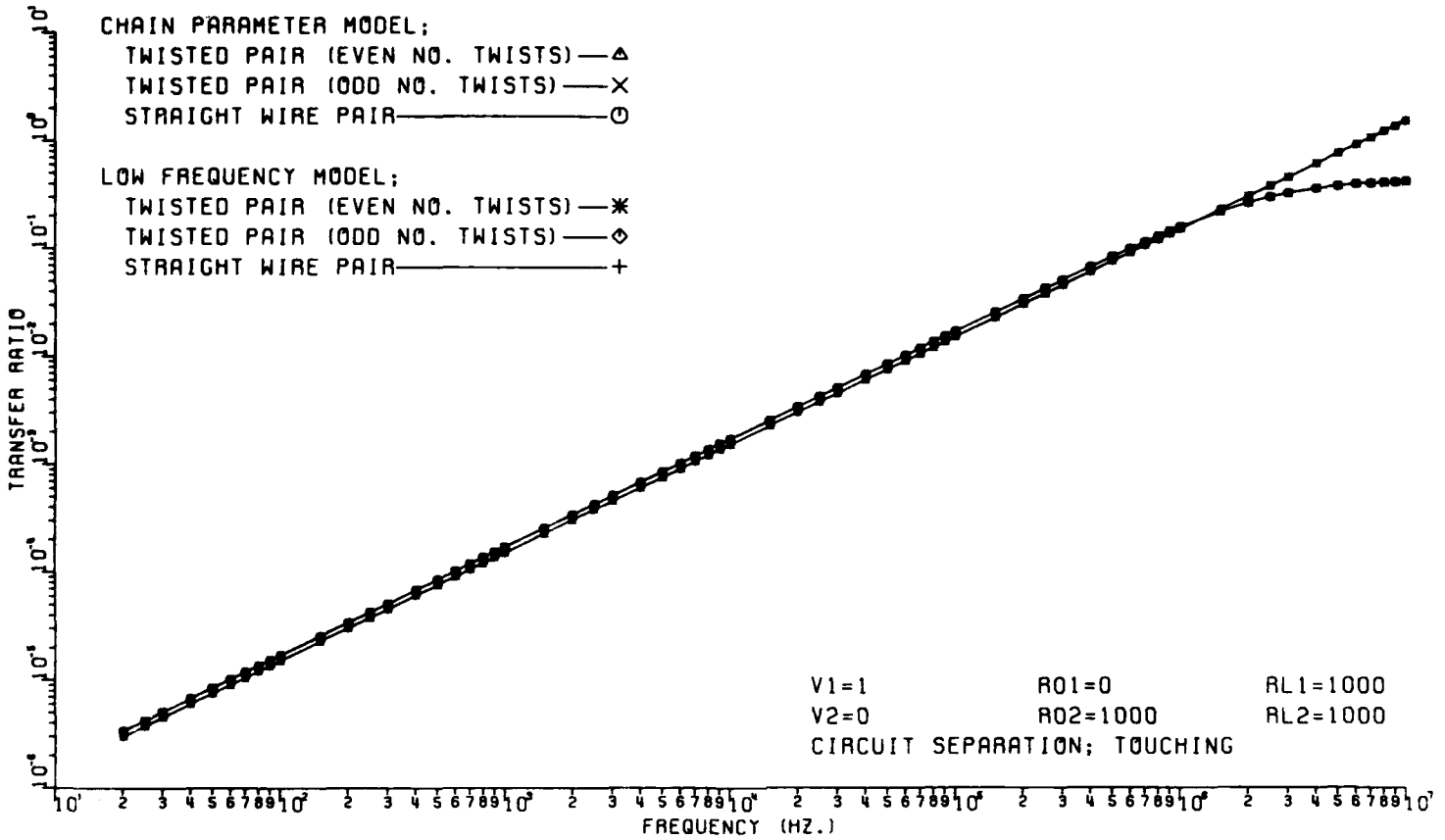
CHAIN PARAMETER MODEL;
TWISTED PAIR (EVEN NO. TWISTS)
TWISTED PAIR (ODD NO. TWISTS)
STRAIGHT WIRE PAIR
LOW FREQUENCY MODEL;
TWISTED PAIR (EVEN NO. TWISTS)
TWISTED PAIR (ODD NO. TWISTS)
STRAIGHT WIRE PAIR
V1=1
R01=0
RL1=1000
V2=0
R02=1000
RL2=1000
CIRCUIT SEPARATION; TOUCHING
TRANSFER RATIO
FREQUENCY (HZ.)

Fig. C-1

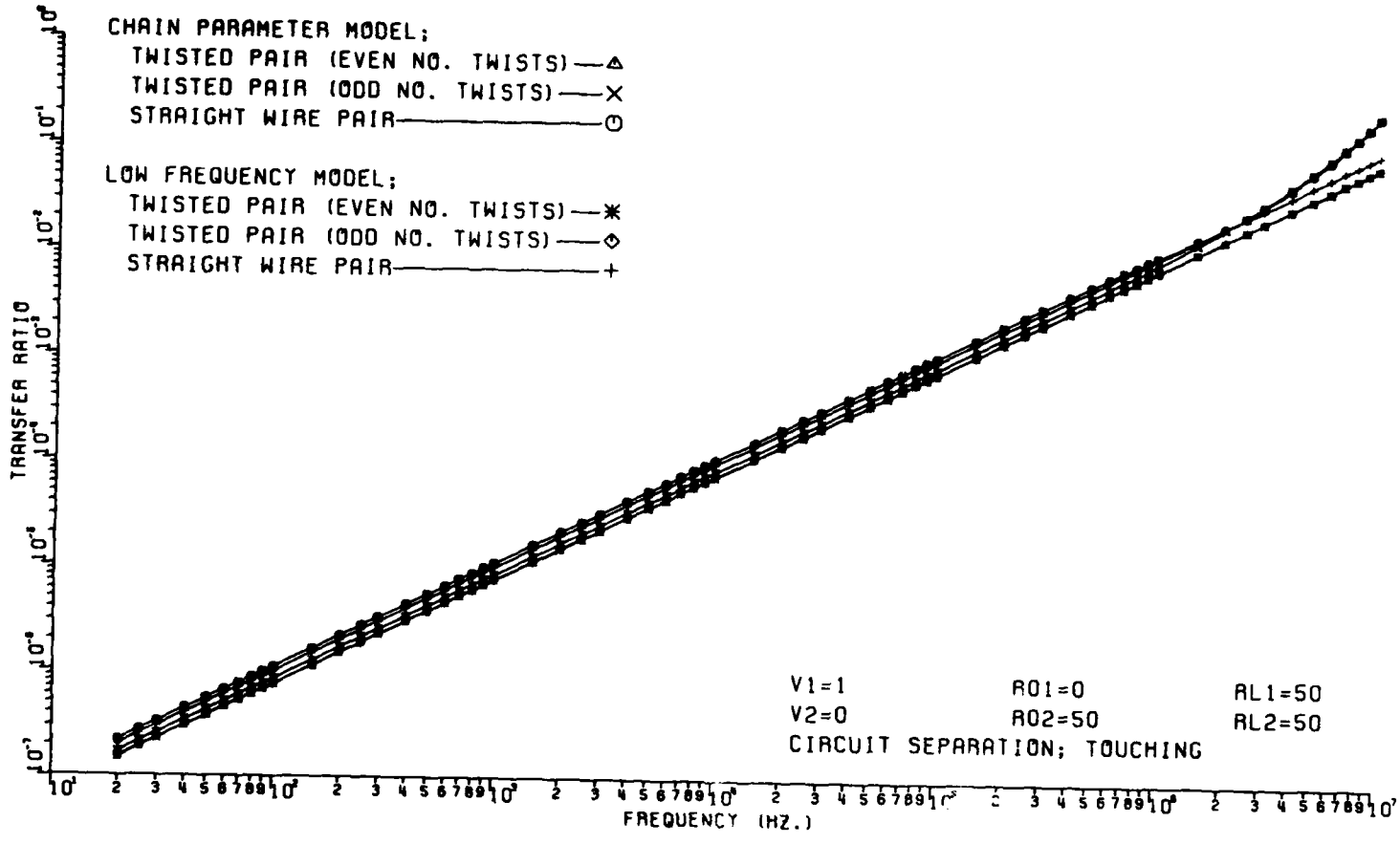
CHAIN PARAMETER MODEL;
TWISTED PAIR (EVEN NO. TWISTS)
TWISTED PAIR (ODD NO. TWISTS)
STRAIGHT WIRE PAIR
LOW FREQUENCY MODEL;
TWISTED PAIR (EVEN NO. TWISTS)
TWISTED PAIR (ODD NO. TWISTS)
STRAIGHT WIRE PAIR
TRANSFER RATIO
FREQUENCY (HZ.)
V1=1
V2=0
R01=0
R02=50
RL1=50
RL2=50
CIRCUIT SEPARATION; TOUCHING

Fig. C-2

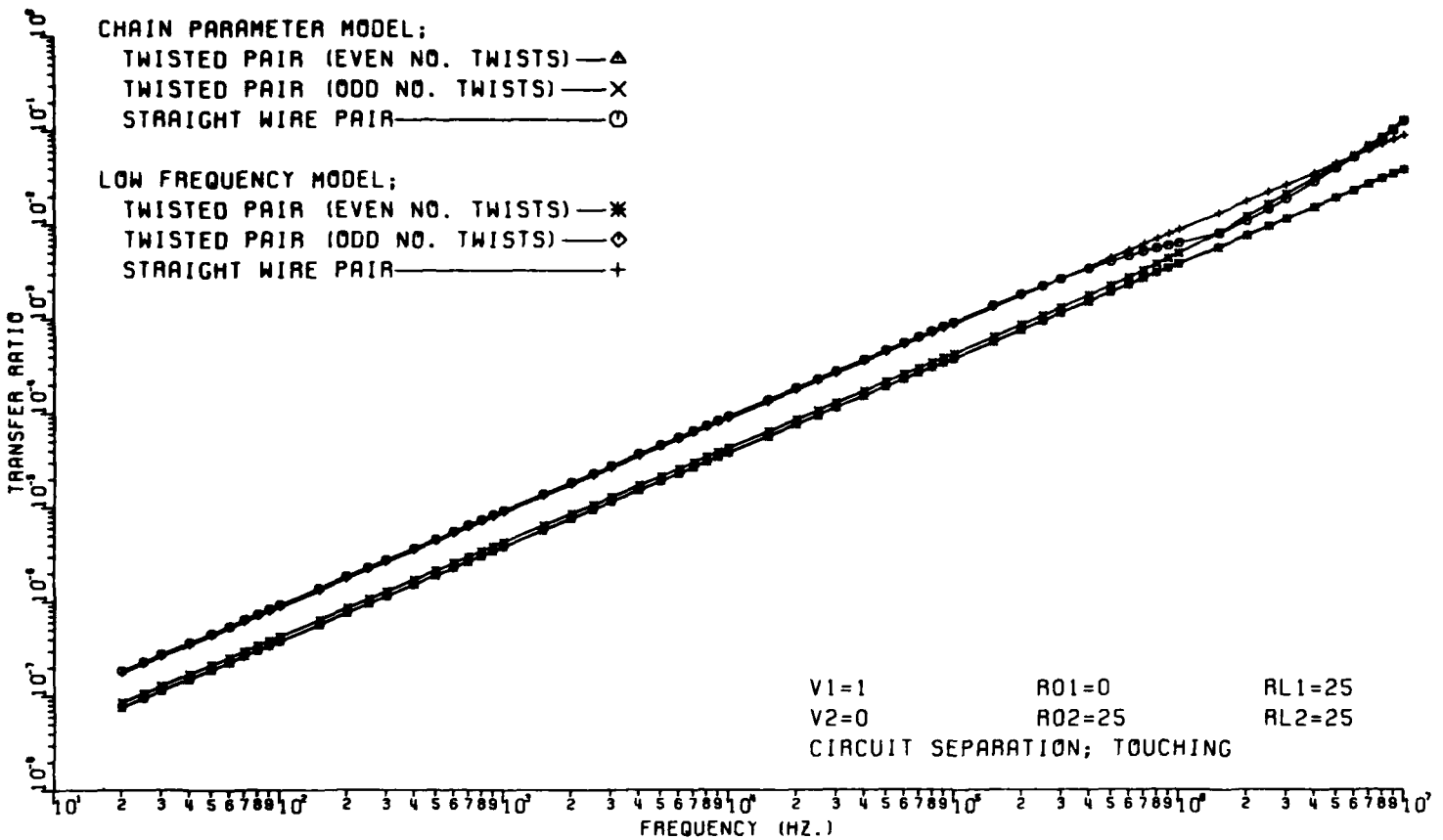
CHAIN PARAMETER MODEL;
TWISTED PAIR (EVEN NO. TWISTS)
TWISTED PAIR (ODD NO. TWISTS)
STRAIGHT WIRE PAIR
LOW FREQUENCY MODEL;
TWISTED PAIR (EVEN NO. TWISTS)
TWISTED PAIR (ODD NO. TWISTS)
STRAIGHT WIRE PAIR
TRANSFER RATIO
FREQUENCY (HZ.)
V1=1
R01=0
RL1=25
V2=0
R02=25
RL2=25
CIRCUIT SEPARATION; TOUCHING

Fig. C-3

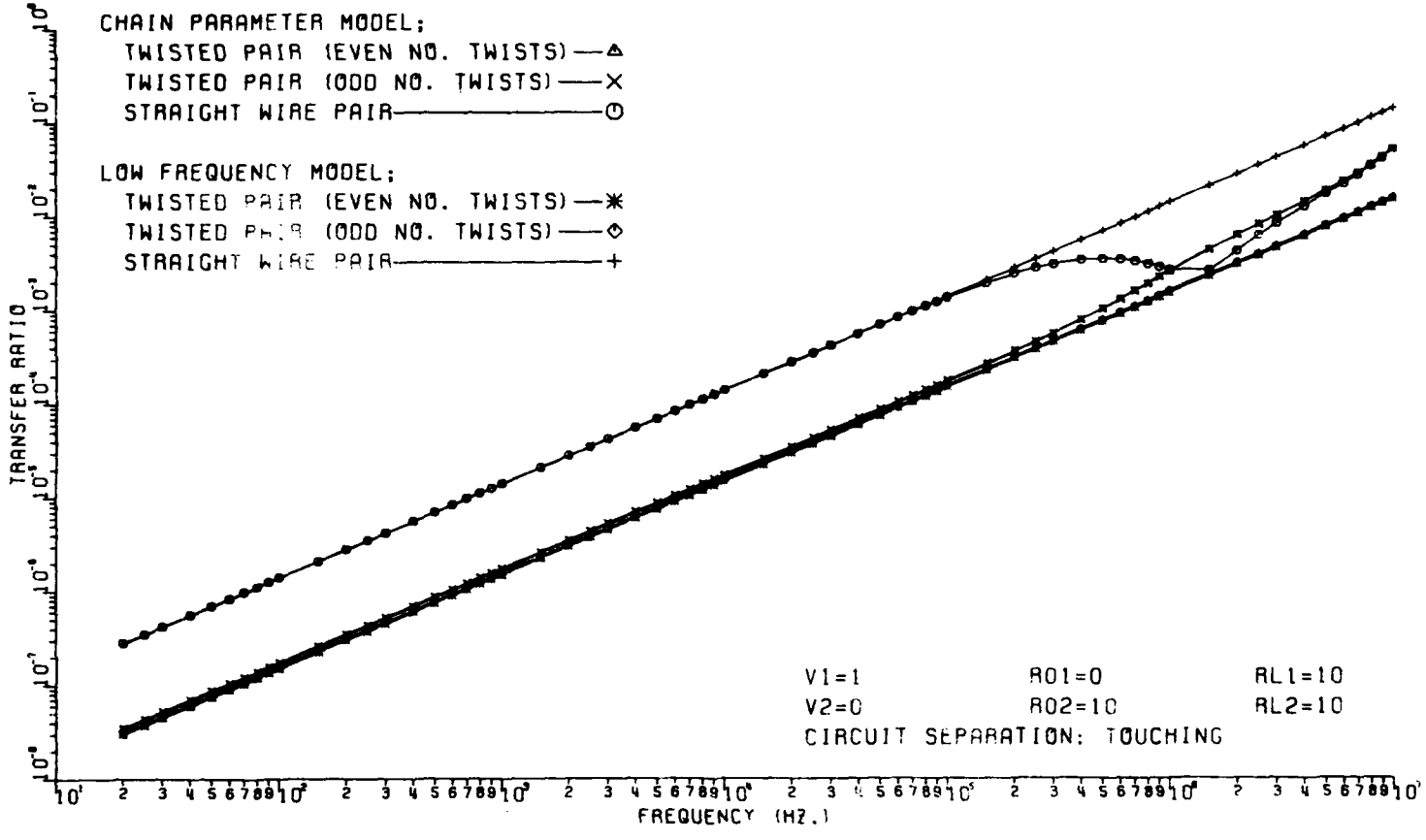
CHAIN PARAMETER MODEL;
TWISTED PAIR (EVEN NO. TWISTS)
TWISTED PAIR (ODD NO. TWISTS)
STRAIGHT WIRE PAIR
LOW FREQUENCY MODEL;
TWISTED PAIR (EVEN NO. TWISTS)
TWISTED PAIR (ODD NO. TWISTS)
STRAIGHT WIRE PAIR
V1=1
R01=0
RL1=10
V2=0
R02=10
RL2=10
CIRCUIT SEPARATION: TOUCHING
TRANSFER RATIO
FREQUENCY (HZ.)

Fig. C-4

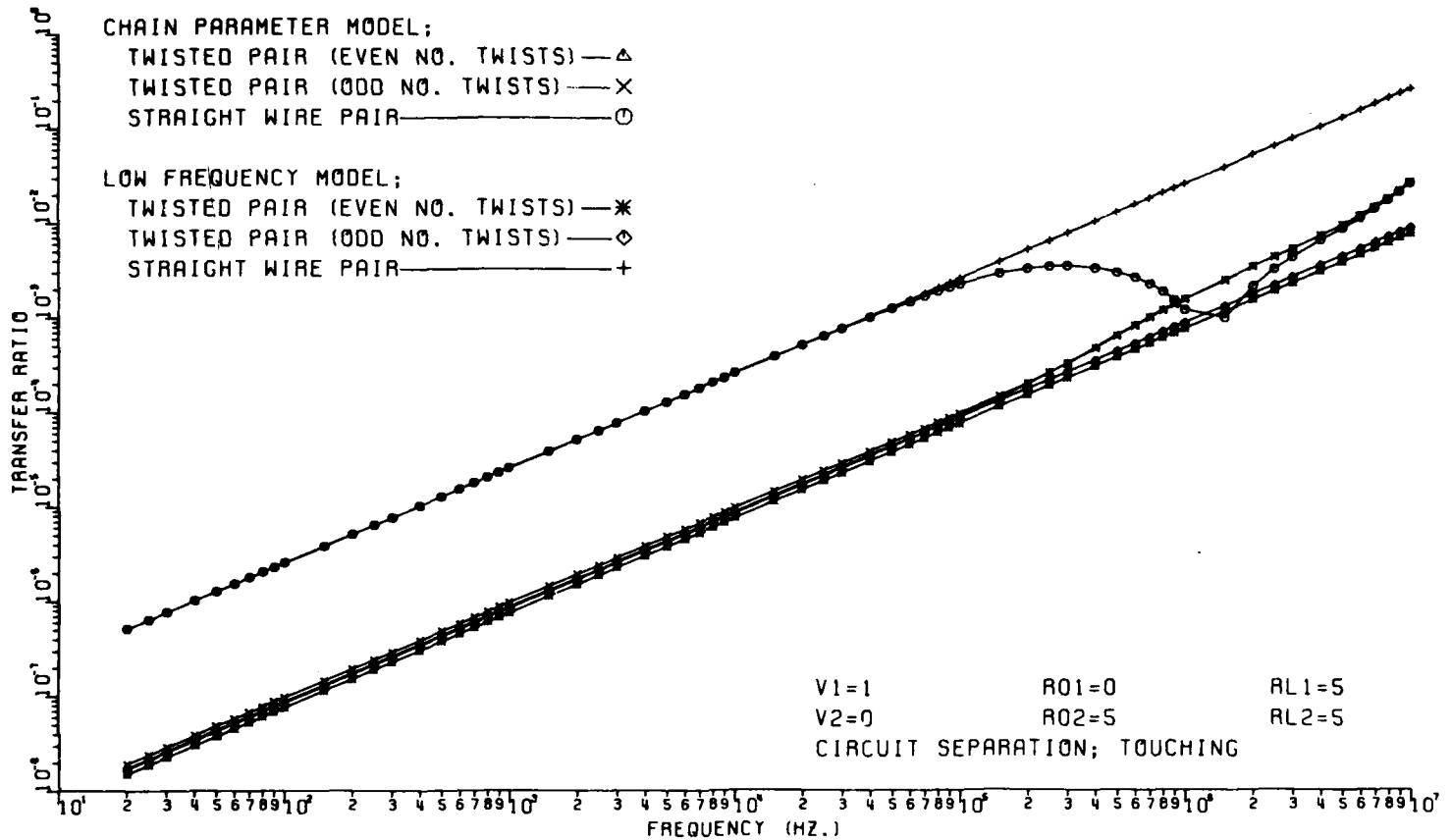
CHAIN PARAMETER MODEL;
TWISTED PAIR (EVEN NO. TWISTS)
TWISTED PAIR (ODD NO. TWISTS)
STRAIGHT WIRE PAIR
LOW FREQUENCY MODEL;
TWISTED PAIR (EVEN NO. TWISTS)
TWISTED PAIR (ODD NO. TWISTS)
STRAIGHT WIRE PAIR
V1=1
V2=0
RO1=0
RO2=5
RL1=5
RL2=5
CIRCUIT SEPARATION; TOUCHING
TRANSFER RATIO
FREQUENCY (HZ.)

Fig. C-5

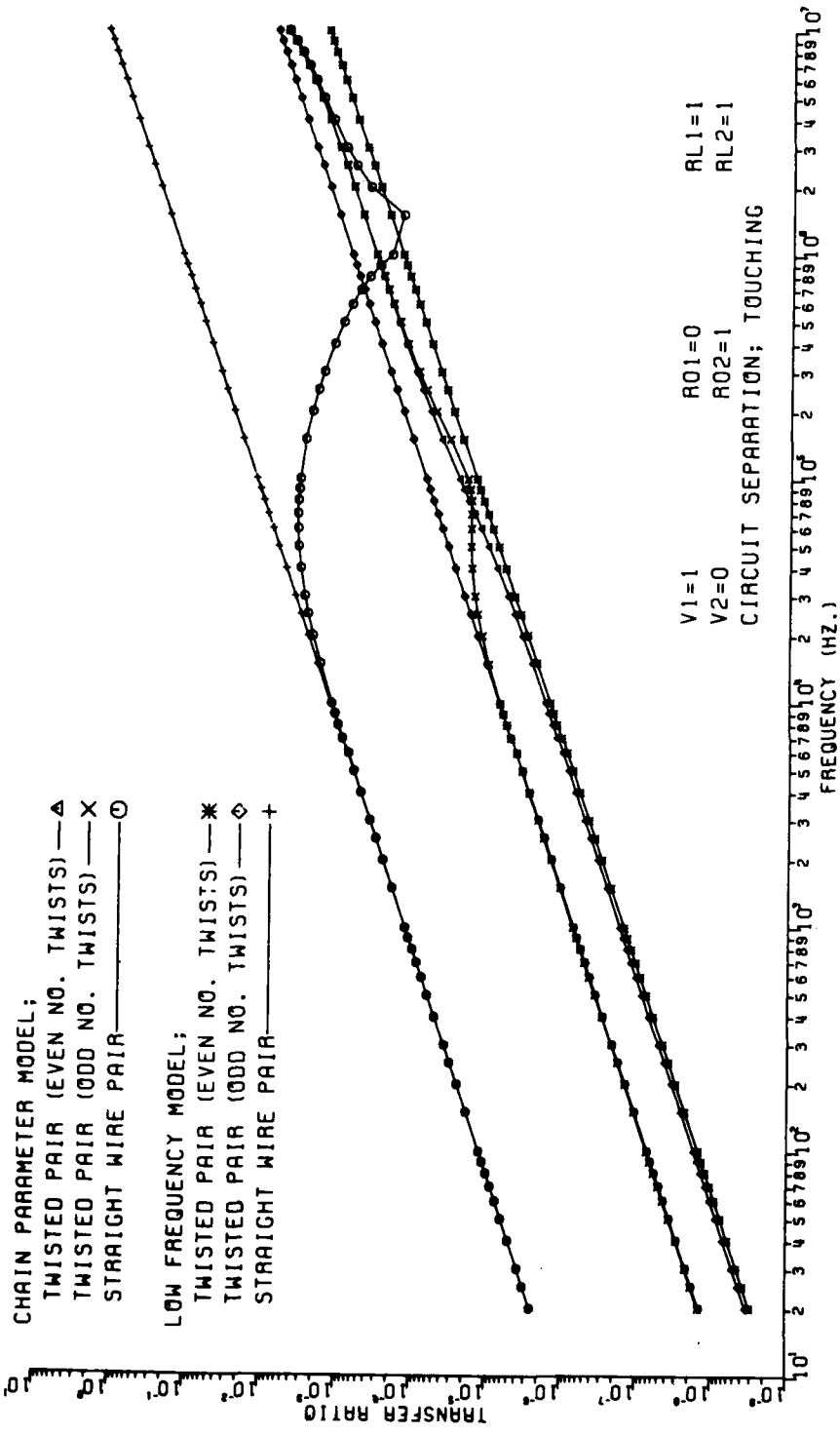
CHAIN PARAMETER MODEL;
TWISTED PAIR (EVEN NO. TWISTS)
TWISTED PAIR (ODD NO. TWISTS)
STRAIGHT WIRE PAIR
LOW FREQUENCY MODEL;
TWISTED PAIR (EVEN NO. TWISTS)
TWISTED PAIR (ODD NO. TWISTS)
STRAIGHT WIRE PAIR
TRANSFER RATIO
FREQUENCY (HZ.)
V1=1
V2=0
RO1=0
RO2=1
RL1=1
RL2=1
CIRCUIT SEPARATION; TOUCHING

Fig. C-6

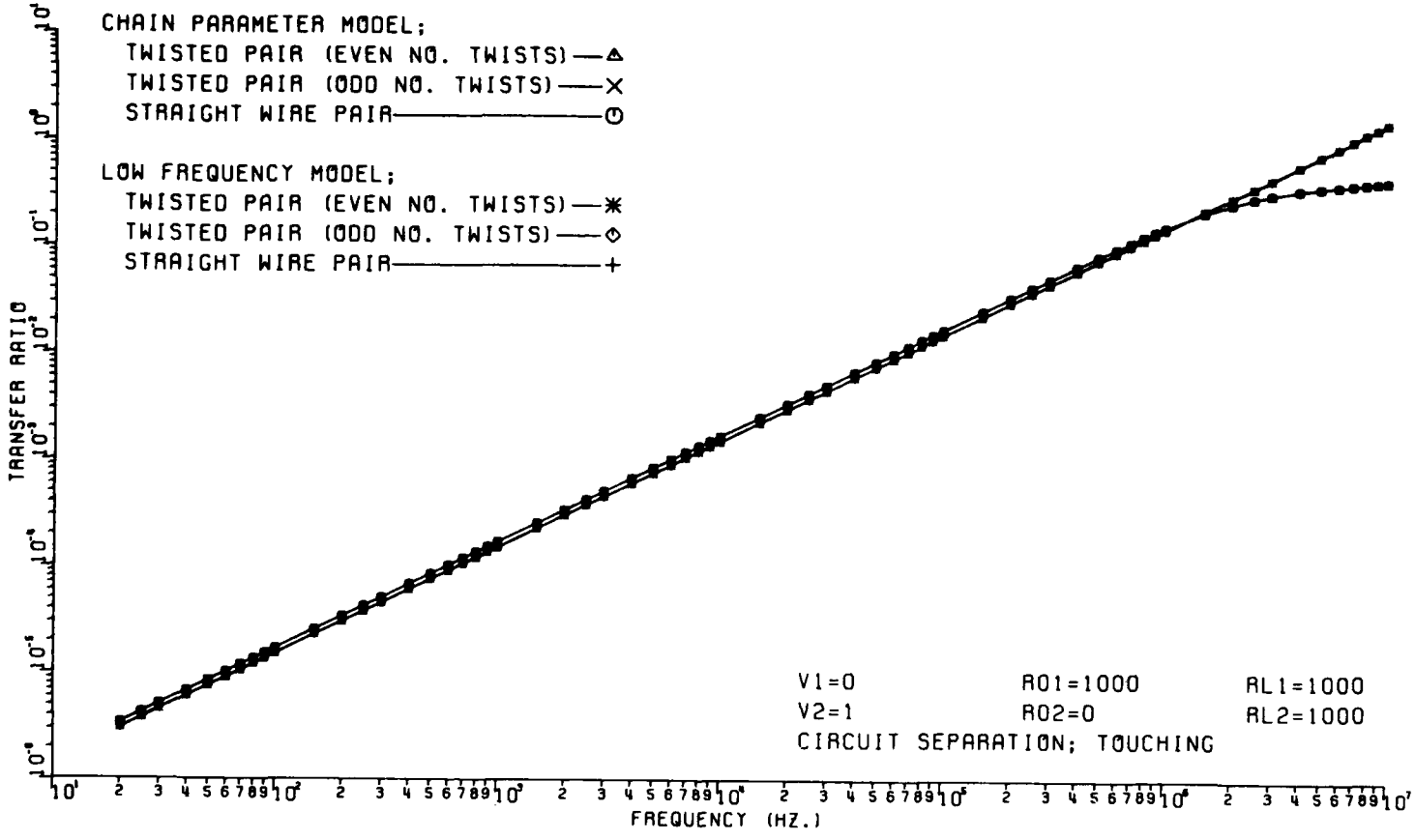
CHAIN PARAMETER MODEL;
TWISTED PAIR (EVEN NO. TWISTS)
TWISTED PAIR (ODD NO. TWISTS)
STRAIGHT WIRE PAIR
LOW FREQUENCY MODEL;
TWISTED PAIR (EVEN NO. TWISTS)
TWISTED PAIR (ODD NO. TWISTS)
STRAIGHT WIRE PAIR
V1=0
V2=1
R01=1000
R02=0
RL1=1000
RL2=1000
CIRCUIT SEPARATION; TOUCHING
TRANSFER RATIO
FREQUENCY (HZ.)

Fig. C-7

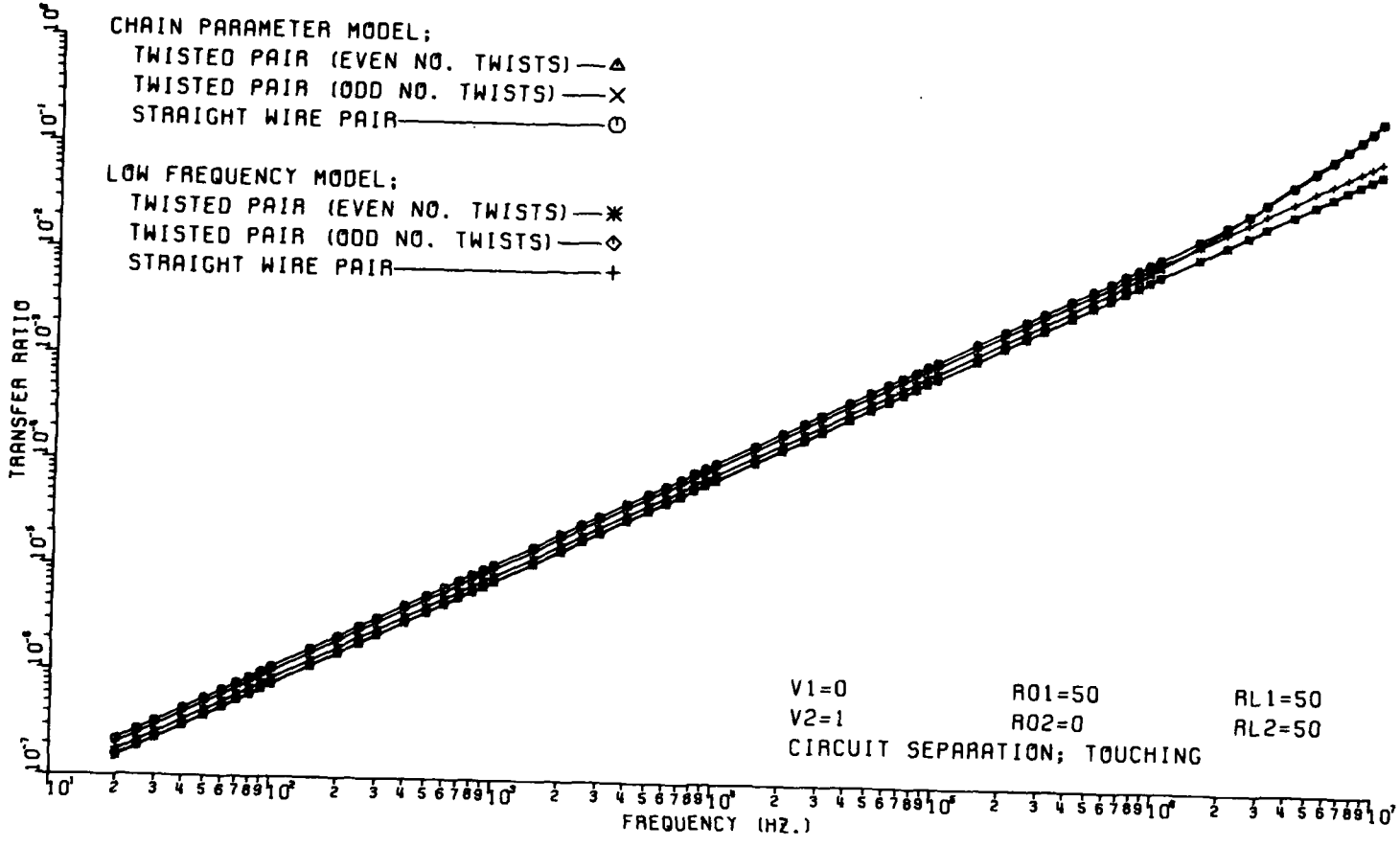
CHAIN PARAMETER MODEL;
TWISTED PAIR (EVEN NO. TWISTS)
TWISTED PAIR (ODD NO. TWISTS)
STRAIGHT WIRE PAIR
LOW FREQUENCY MODEL;
TWISTED PAIR (EVEN NO. TWISTS)
TWISTED PAIR (ODD NO. TWISTS)
STRAIGHT WIRE PAIR
TRANSFER RATIO
FREQUENCY (HZ.)
V1=0
V2=1
R01=50
R02=0
RL1=50
RL2=50
CIRCUIT SEPARATION; TOUCHING

Fig. C-8

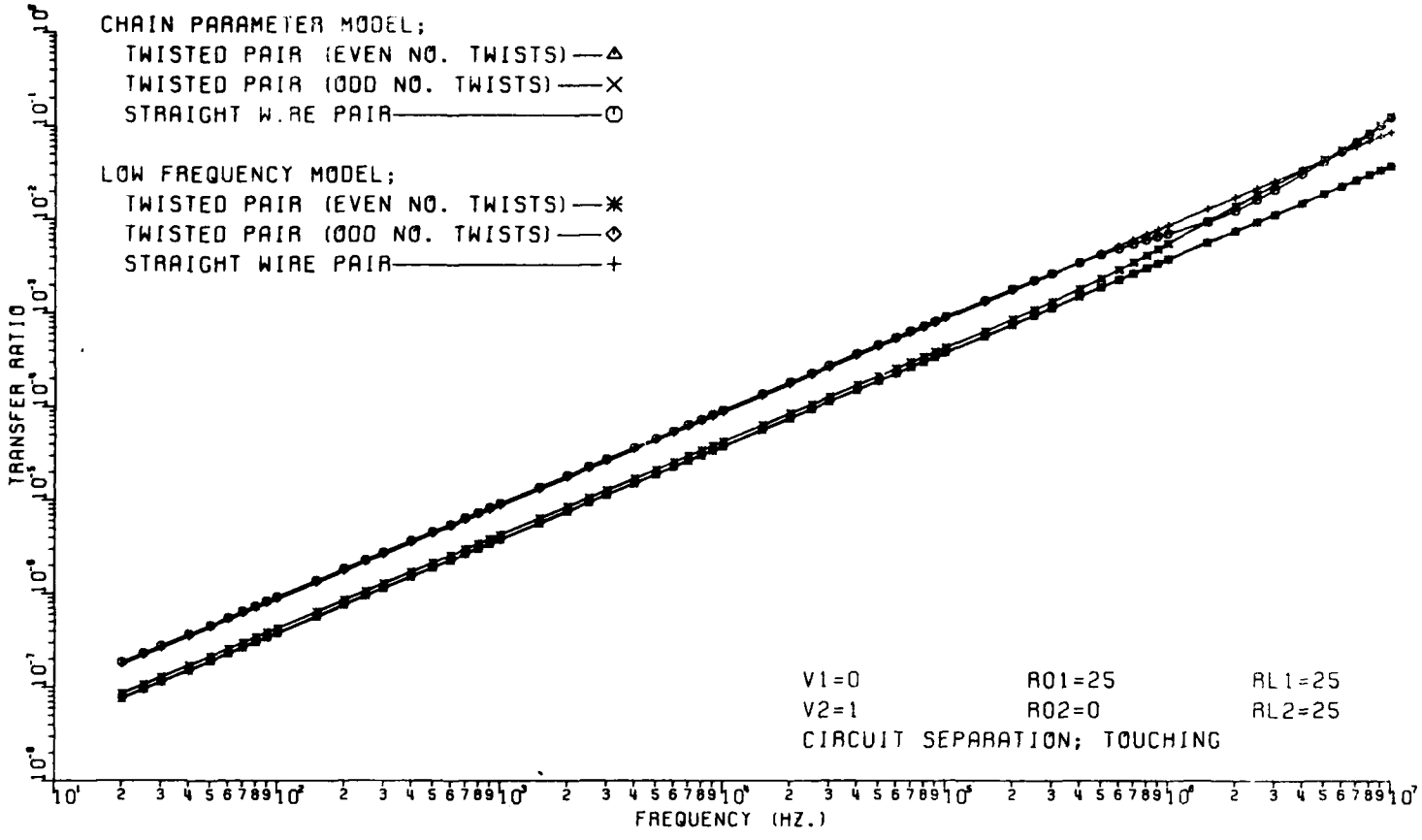
CHAIN PARAMETER MODEL;
TWISTED PAIR (EVEN NO. TWISTS)—Δ
TWISTED PAIR (ODD NO. TWISTS)—X
STRAIGHT WIRE PAIR—O
LOW FREQUENCY MODEL;
TWISTED PAIR (EVEN NO. TWISTS)—✳
TWISTED PAIR (ODD NO. TWISTS)—◇
STRAIGHT WIRE PAIR—+
V1=0
V2=1
RO1=25
RO2=0
RL1=25
RL2=25
CIRCUIT SEPARATION; TOUCHING
TRANSFER RATIO
FREQUENCY (HZ.)

Fig. C-9

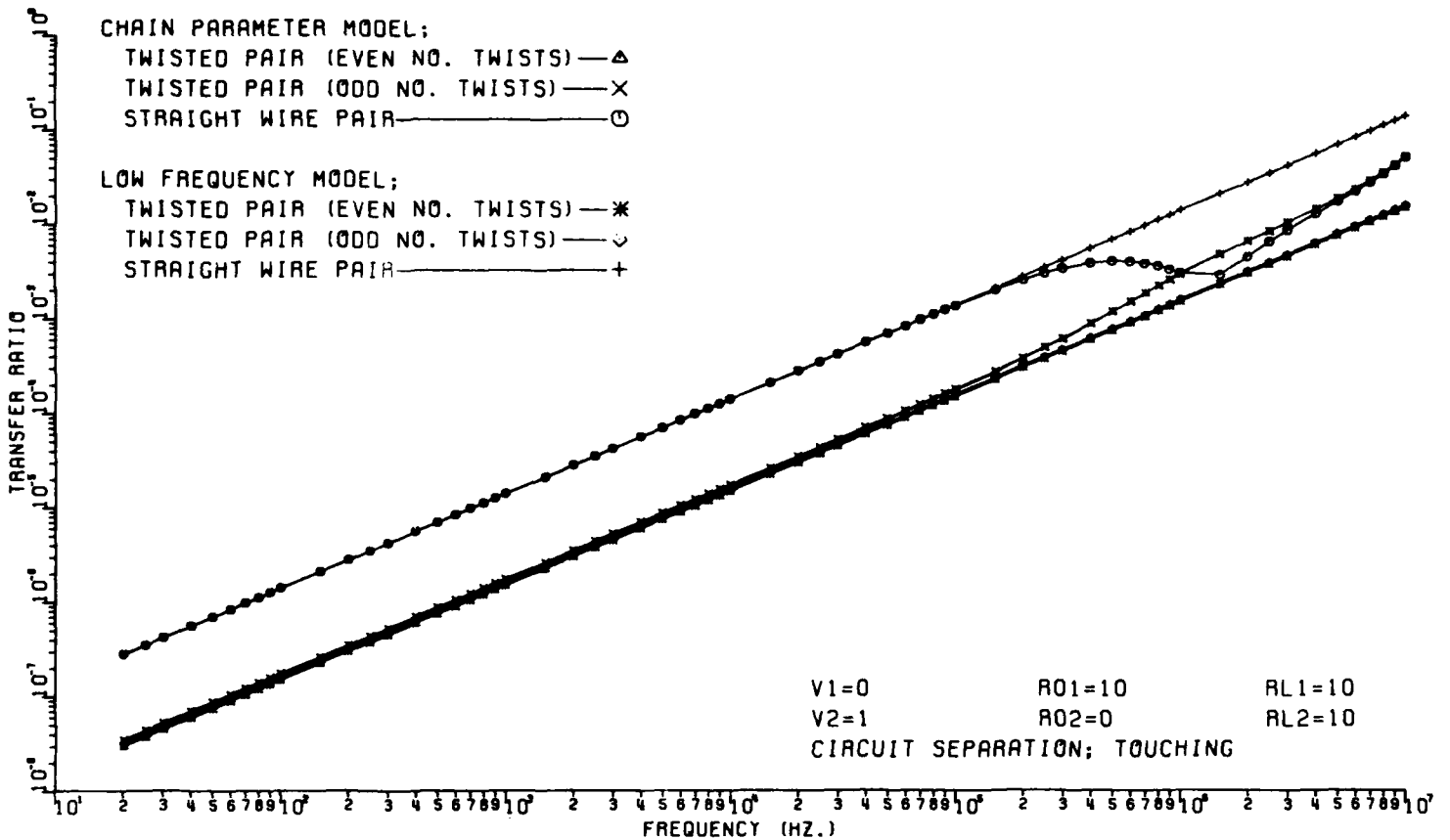
CHAIN PARAMETER MODEL;
TWISTED PAIR (EVEN NO. TWISTS)
TWISTED PAIR (ODD NO. TWISTS)
STRAIGHT WIRE PAIR
LOW FREQUENCY MODEL;
TWISTED PAIR (EVEN NO. TWISTS)
TWISTED PAIR (ODD NO. TWISTS)
STRAIGHT WIRE PAIR
TRANSFER RATIO
FREQUENCY (HZ.)
V1=0
V2=1
RO1=10
RO2=0
RL1=10
RL2=10
CIRCUIT SEPARATION; TOUCHING

Fig. C-10

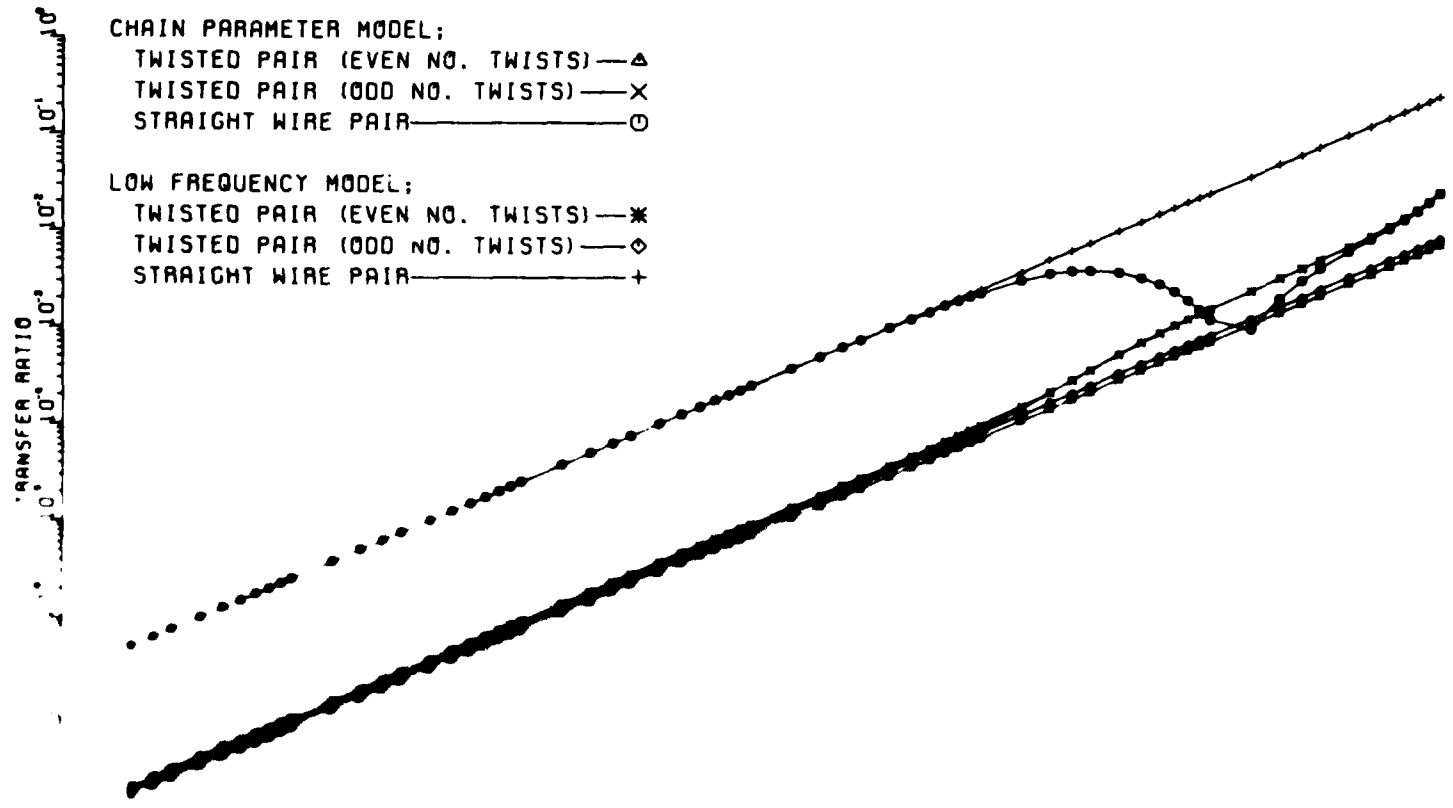
CHAIN PARAMETER MODEL;
TWISTED PAIR (EVEN NO. TWISTS)—Δ
TWISTED PAIR (ODD NO. TWISTS)—X
STRAIGHT WIRE PAIR—O
LOW FREQUENCY MODEL;
TWISTED PAIR (EVEN NO. TWISTS)—✱
TWISTED PAIR (ODD NO. TWISTS)—◇
STRAIGHT WIRE PAIR—+
TRANSFER RATIO
10⁰
10⁻¹
10⁻²
10⁻³
10⁻⁴

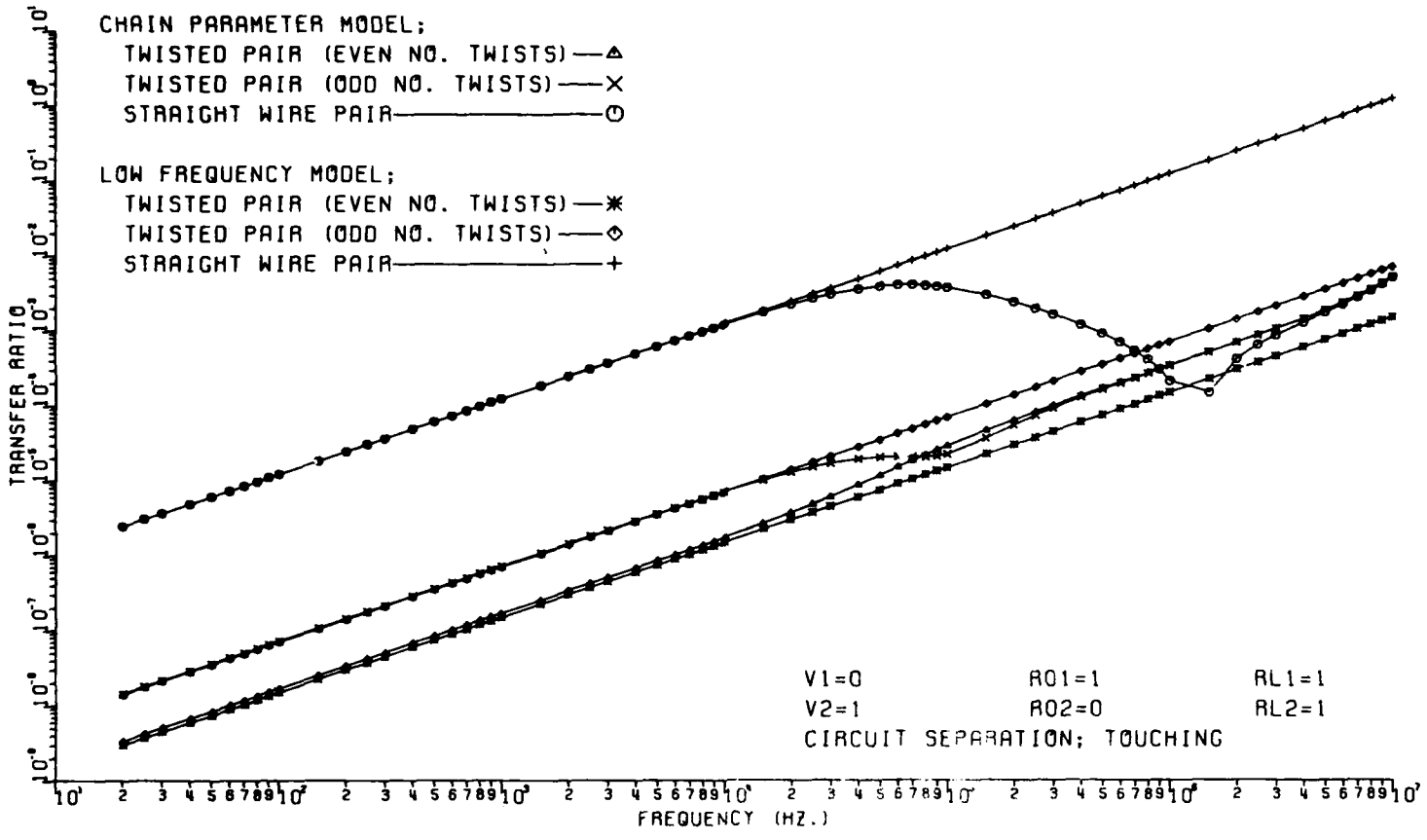
CHAIN PARAMETER MODEL;
TWISTED PAIR (EVEN NO. TWISTS)
TWISTED PAIR (ODD NO. TWISTS)
STRAIGHT WIRE PAIR
LOW FREQUENCY MODEL;
TWISTED PAIR (EVEN NO. TWISTS)
TWISTED PAIR (ODD NO. TWISTS)
STRAIGHT WIRE PAIR
V1=0
V2=1
R01=1
R02=0
RL1=1
RL2=1
CIRCUIT SEPARATION; TOUCHING
TRANSFER RATIO
FREQUENCY (HZ.)

Fig. C-12

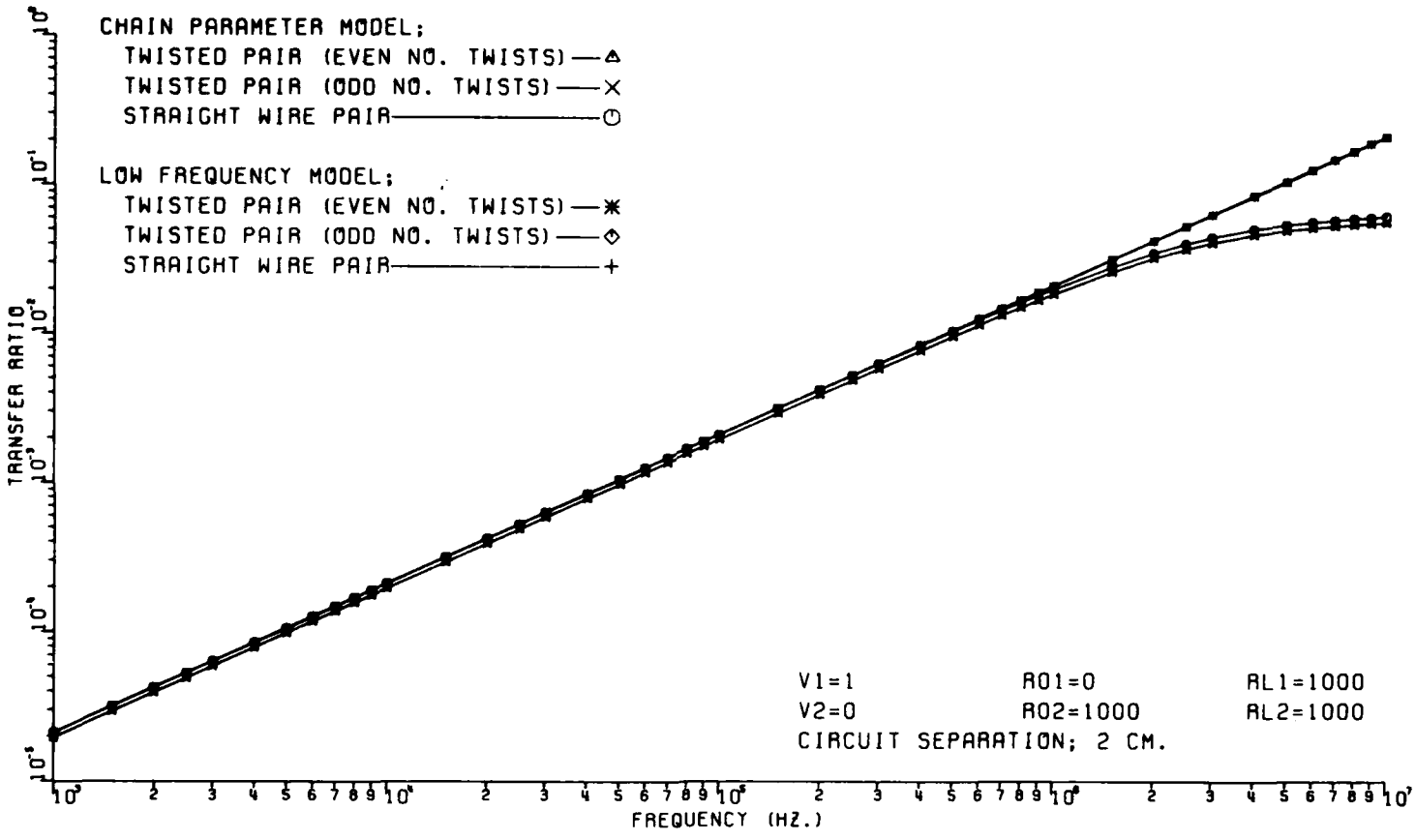
CHAIN PARAMETER MODEL;
TWISTED PAIR (EVEN NO. TWISTS)
TWISTED PAIR (ODD NO. TWISTS)
STRAIGHT WIRE PAIR
LOW FREQUENCY MODEL;
TWISTED PAIR (EVEN NO. TWISTS)
TWISTED PAIR (ODD NO. TWISTS)
STRAIGHT WIRE PAIR
TRANSFER RATIO
FREQUENCY (HZ.)
V1=1
V2=0
R01=0
R02=1000
RL1=1000
RL2=1000
CIRCUIT SEPARATION; 2 CM.

Fig. C-13

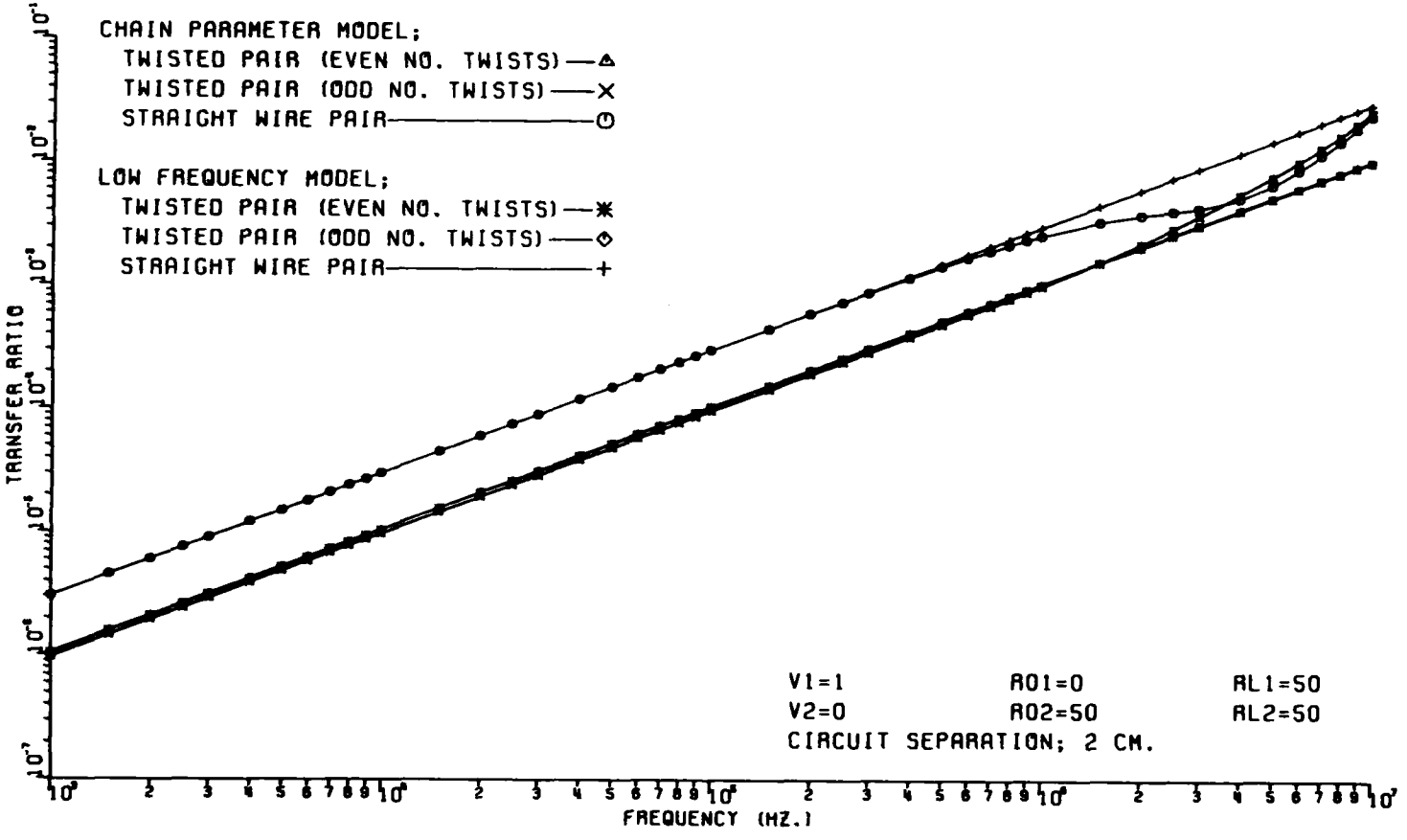
CHAIN PARAMETER MODEL;
TWISTED PAIR (EVEN NO. TWISTS)
TWISTED PAIR (ODD NO. TWISTS)
STRAIGHT WIRE PAIR
LOW FREQUENCY MODEL;
TWISTED PAIR (EVEN NO. TWISTS)
TWISTED PAIR (ODD NO. TWISTS)
STRAIGHT WIRE PAIR
TRANSFER RATIO
FREQUENCY (HZ.)
V1=1
V2=0
R01=0
R02=50
RL1=50
RL2=50
CIRCUIT SEPARATION; 2 CM.

Fig. C-14

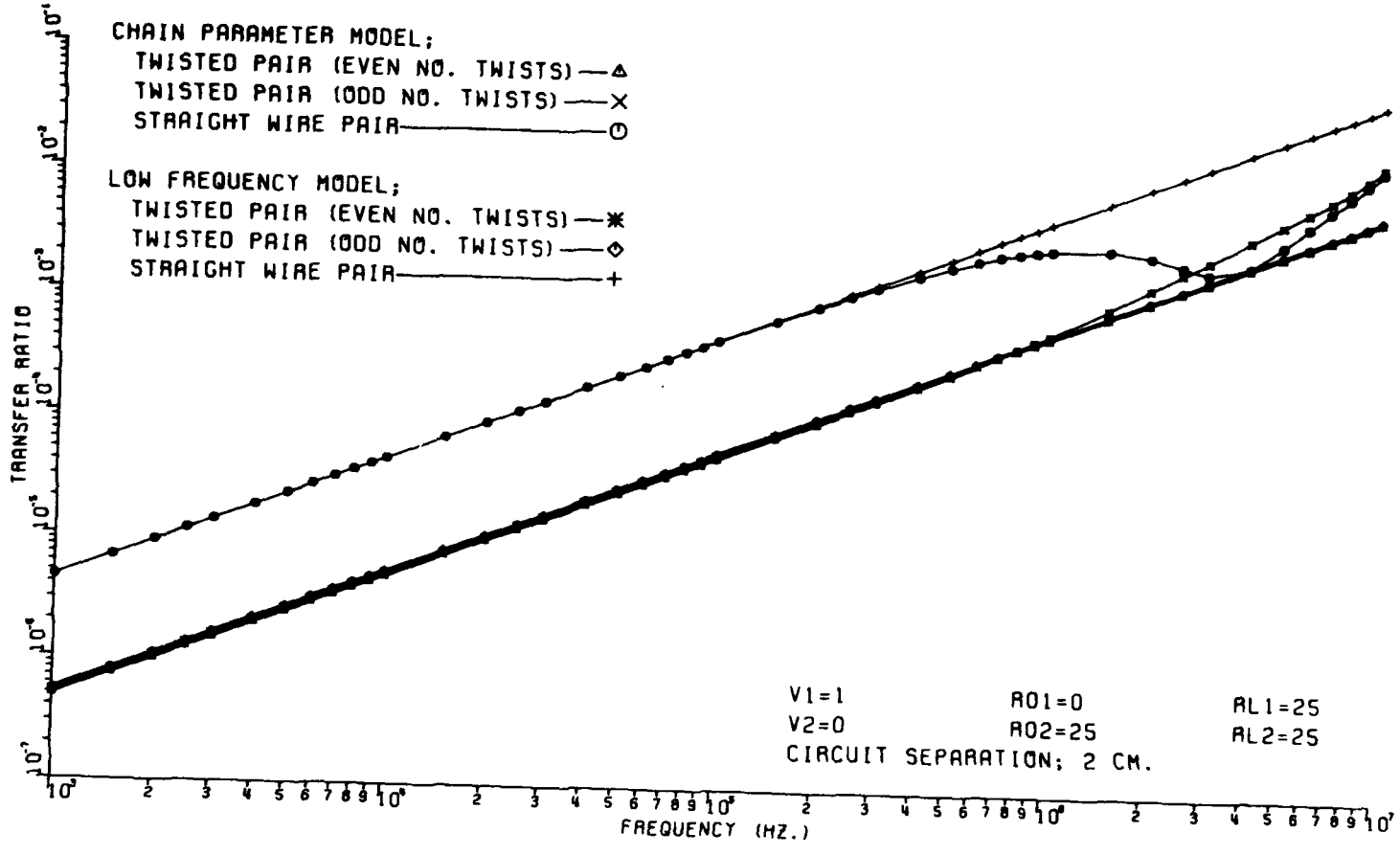
CHAIN PARAMETER MODEL;
TWISTED PAIR (EVEN NO. TWISTS)—△
TWISTED PAIR (ODD NO. TWISTS)—×
STRAIGHT WIRE PAIR—⊙
LOW FREQUENCY MODEL;
TWISTED PAIR (EVEN NO. TWISTS)—✳
TWISTED PAIR (ODD NO. TWISTS)—◇
STRAIGHT WIRE PAIR—+
TRANSFER RATIO
FREQUENCY (HZ.)
V1=1
V2=0
RO1=0
RO2=25
RL1=25
RL2=25
CIRCUIT SEPARATION; 2 CM.

Fig. C-15

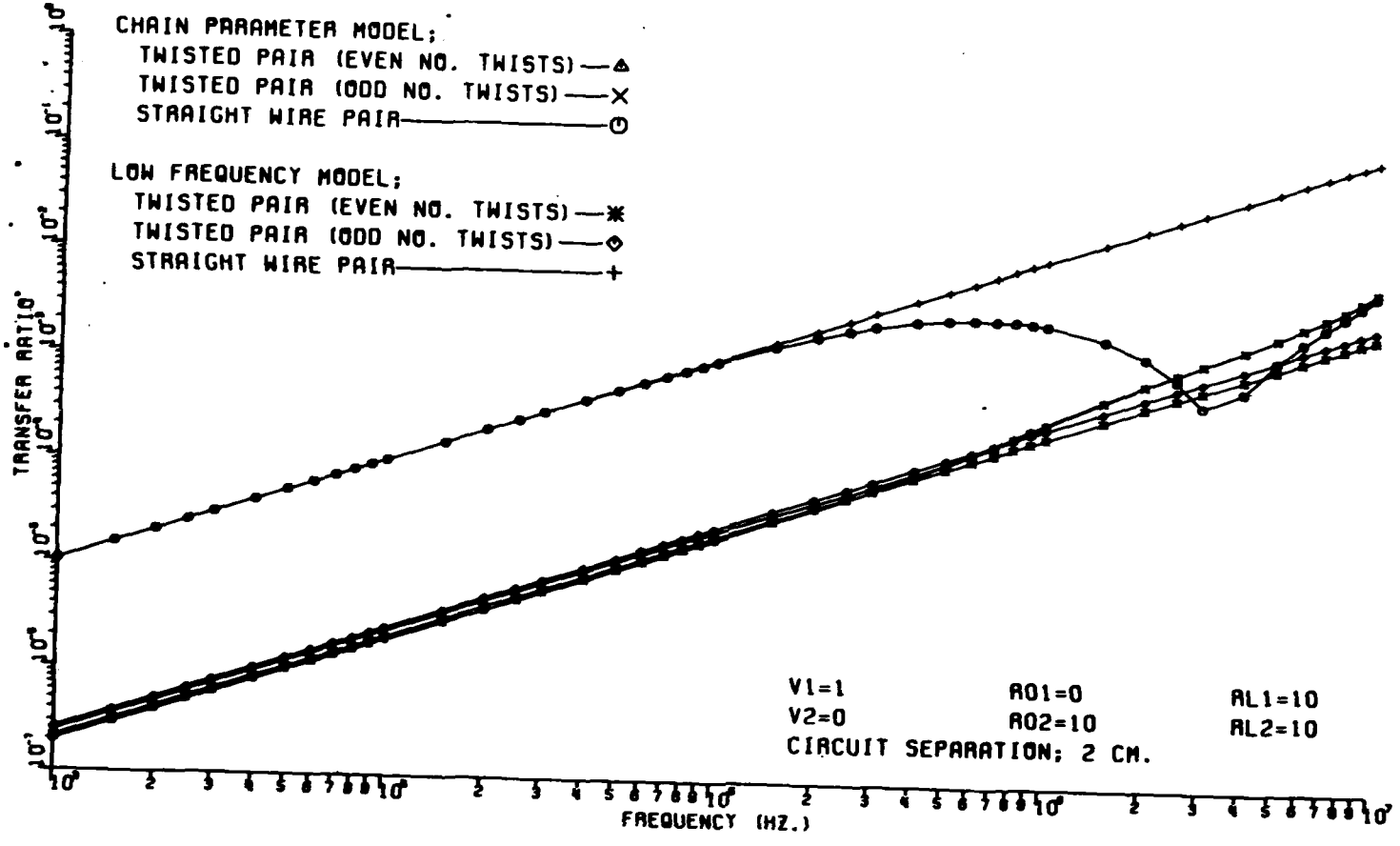
CHAIN PARAMETER MODEL;
TWISTED PAIR (EVEN NO. TWISTS)
TWISTED PAIR (ODD NO. TWISTS)
STRAIGHT WIRE PAIR
LOW FREQUENCY MODEL;
TWISTED PAIR (EVEN NO. TWISTS)
TWISTED PAIR (ODD NO. TWISTS)
STRAIGHT WIRE PAIR
TRANSFER RATIO
FREQUENCY (HZ.)
V1=1
V2=0
RO1=0
RO2=10
RL1=10
RL2=10
CIRCUIT SEPARATION; 2 CM.

Fig. C-16

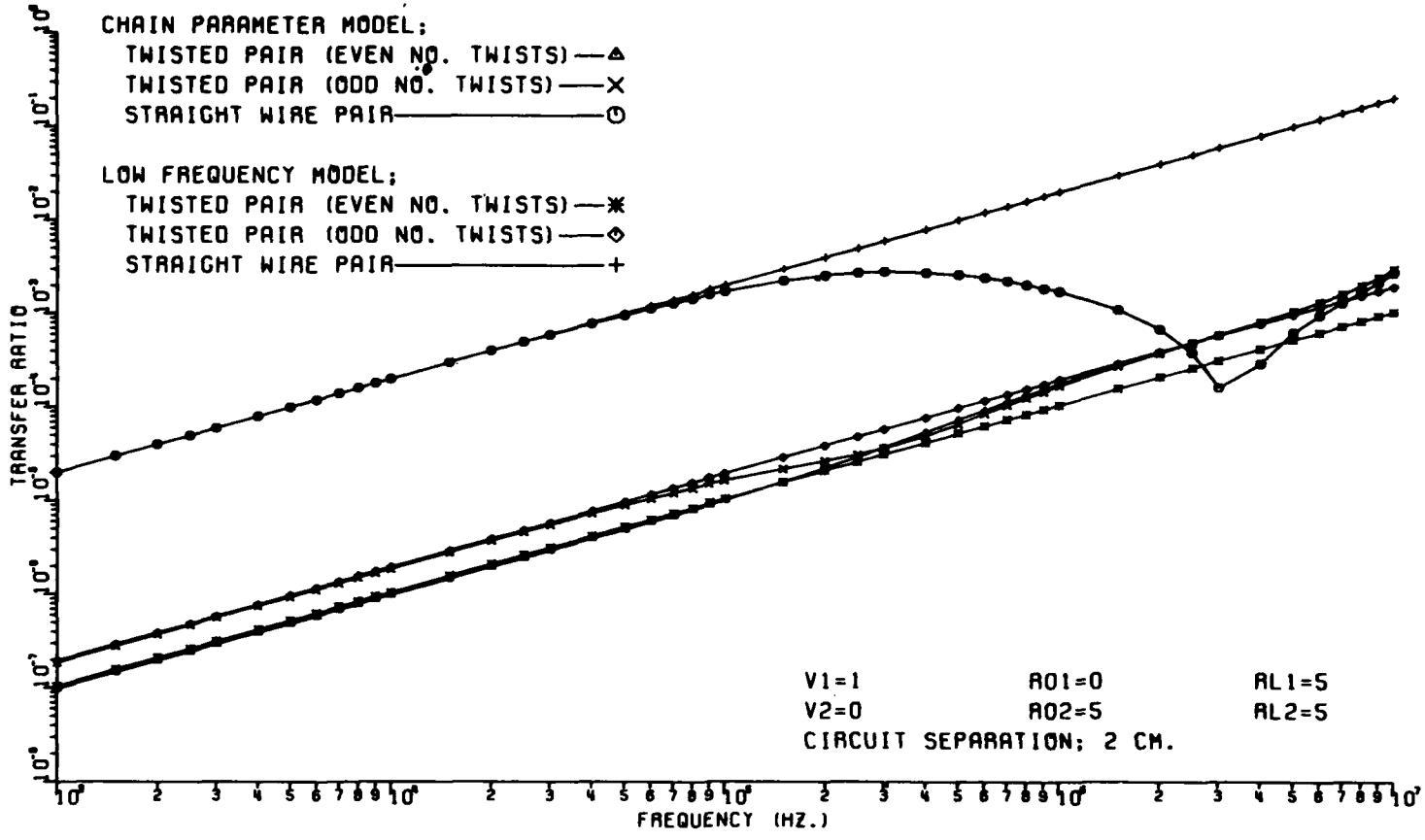
CHAIN PARAMETER MODEL;
TWISTED PAIR (EVEN NO. TWISTS)—△
TWISTED PAIR (ODD NO. TWISTS)—X
STRAIGHT WIRE PAIR—○
LOW FREQUENCY MODEL;
TWISTED PAIR (EVEN NO. TWISTS)—✳
TWISTED PAIR (ODD NO. TWISTS)—◇
STRAIGHT WIRE PAIR—+
TRANSFER RATIO
FREQUENCY (HZ.)
V1=1
V2=0
RO1=0
RO2=5
RL1=5
RL2=5
CIRCUIT SEPARATION; 2 CM.

Fig. C-17

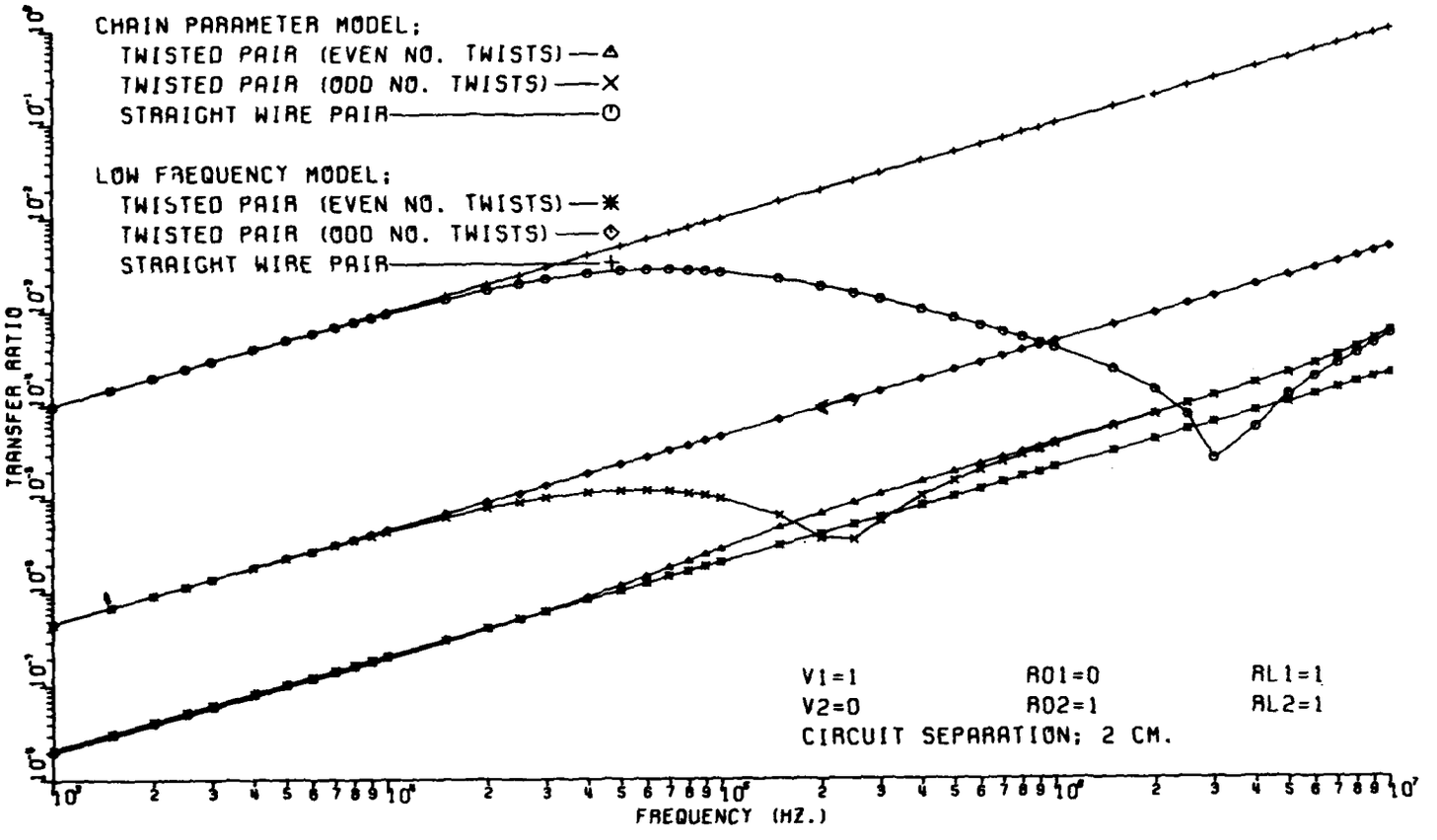
CHAIN PARAMETER MODEL;
TWISTED PAIR (EVEN NO. TWISTS)
TWISTED PAIR (ODD NO. TWISTS)
STRAIGHT WIRE PAIR
LOW FREQUENCY MODEL;
TWISTED PAIR (EVEN NO. TWISTS)
TWISTED PAIR (ODD NO. TWISTS)
STRAIGHT WIRE PAIR
TRANSFER RATIO
FREQUENCY (HZ.)
V1=1
V2=0
R01=0
R02=1
RL1=1
RL2=1
CIRCUIT SEPARATION; 2 CM.

Fig. C-18

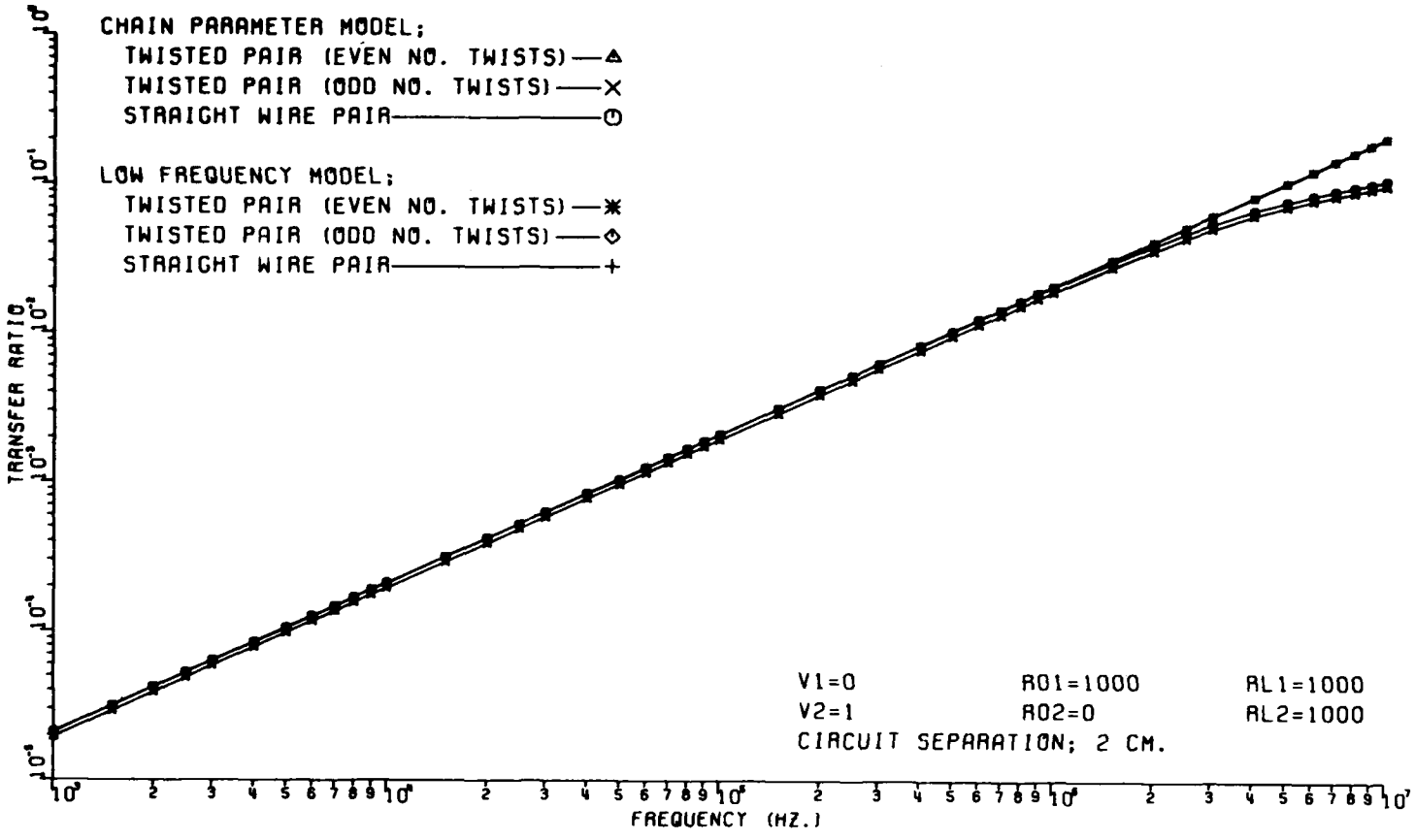
CHAIN PARAMETER MODEL;
TWISTED PAIR (EVEN NO. TWISTS)
TWISTED PAIR (ODD NO. TWISTS)
STRAIGHT WIRE PAIR
LOW FREQUENCY MODEL;
TWISTED PAIR (EVEN NO. TWISTS)
TWISTED PAIR (ODD NO. TWISTS)
STRAIGHT WIRE PAIR
TRANSFER RATIO
FREQUENCY (HZ.)
V1=0
V2=1
R01=1000
R02=0
RL1=1000
RL2=1000
CIRCUIT SEPARATION; 2 CM.

Fig. C-19

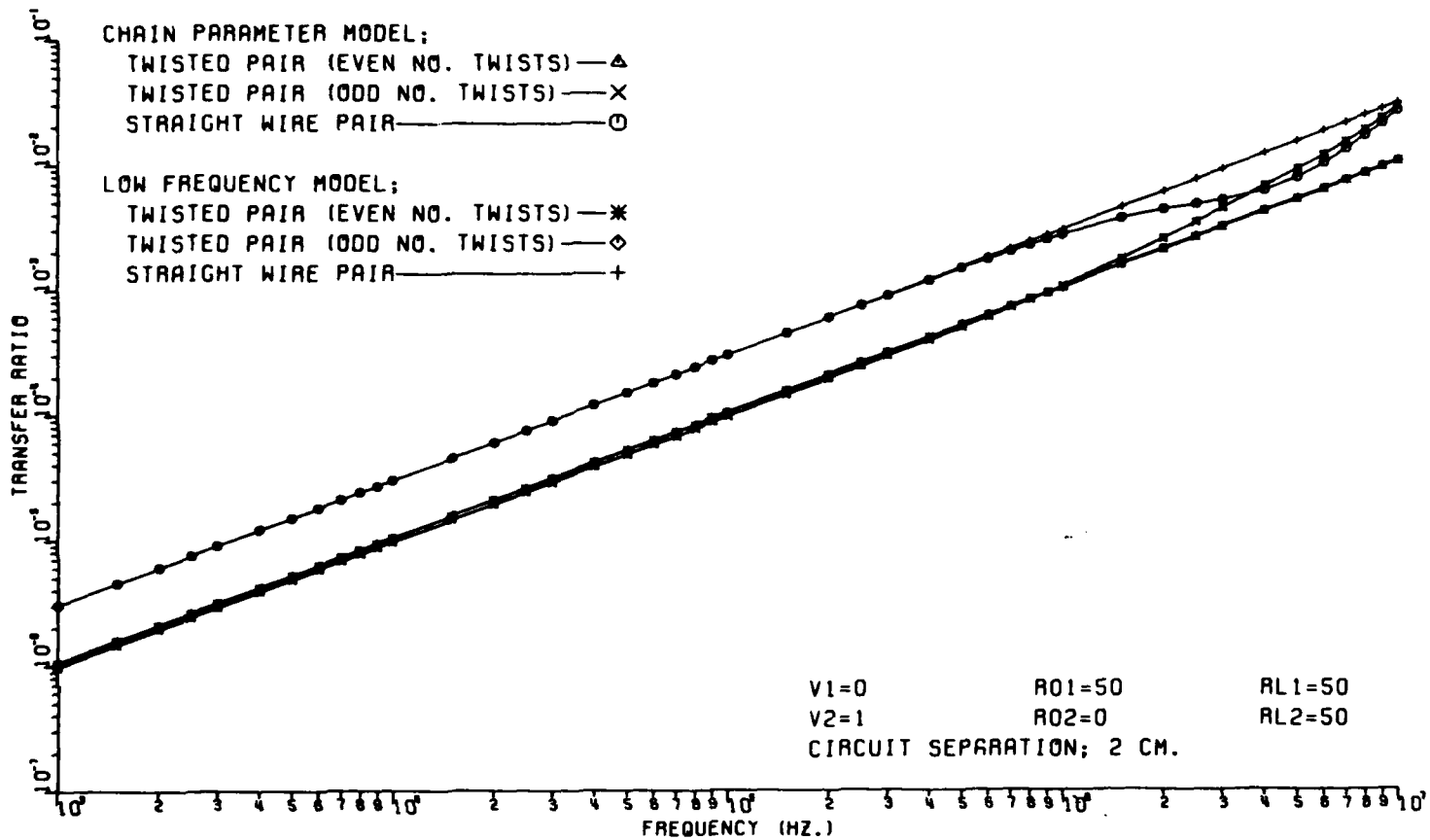
CHAIN PARAMETER MODEL;
TWISTED PAIR (EVEN NO. TWISTS)—△
TWISTED PAIR (ODD NO. TWISTS)—X
STRAIGHT WIRE PAIR——————O
LOW FREQUENCY MODEL;
TWISTED PAIR (EVEN NO. TWISTS)—✳
TWISTED PAIR (ODD NO. TWISTS)—◇
STRAIGHT WIRE PAIR——————+
TRANSFER RATIO
FREQUENCY (HZ.)
V1=0
R01=50
RL1=50
V2=1
R02=0
RL2=50
CIRCUIT SEPARATION; 2 CM.

Fig. C-20

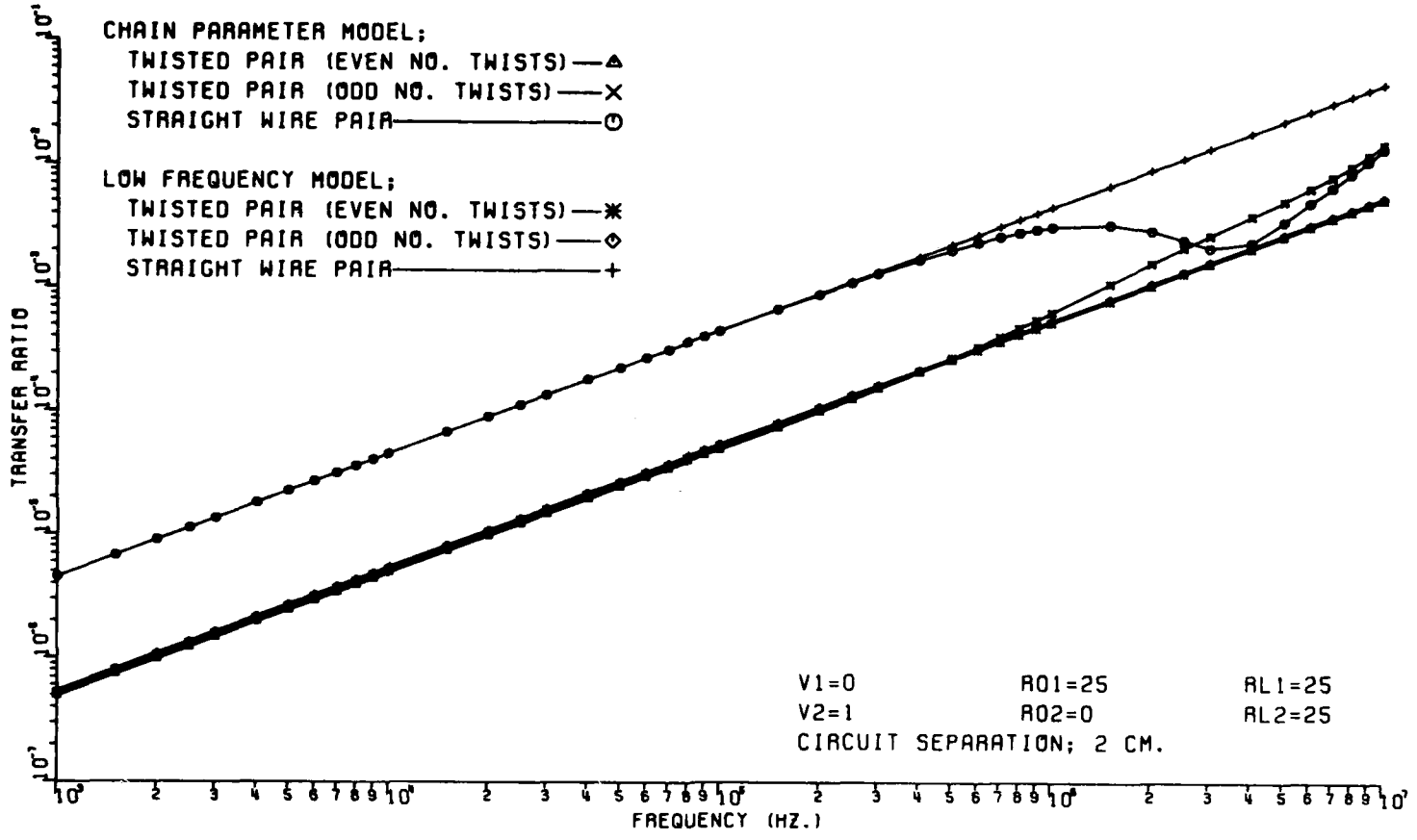
CHAIN PARAMETER MODEL;
TWISTED PAIR (EVEN NO. TWISTS)
TWISTED PAIR (ODD NO. TWISTS)
STRAIGHT WIRE PAIR
LOW FREQUENCY MODEL;
TWISTED PAIR (EVEN NO. TWISTS)
TWISTED PAIR (ODD NO. TWISTS)
STRAIGHT WIRE PAIR
TRANSFER RATIO
FREQUENCY (HZ.)
V1=0
V2=1
R01=25
R02=0
RL1=25
RL2=25
CIRCUIT SEPARATION; 2 CM.

Fig. C-21

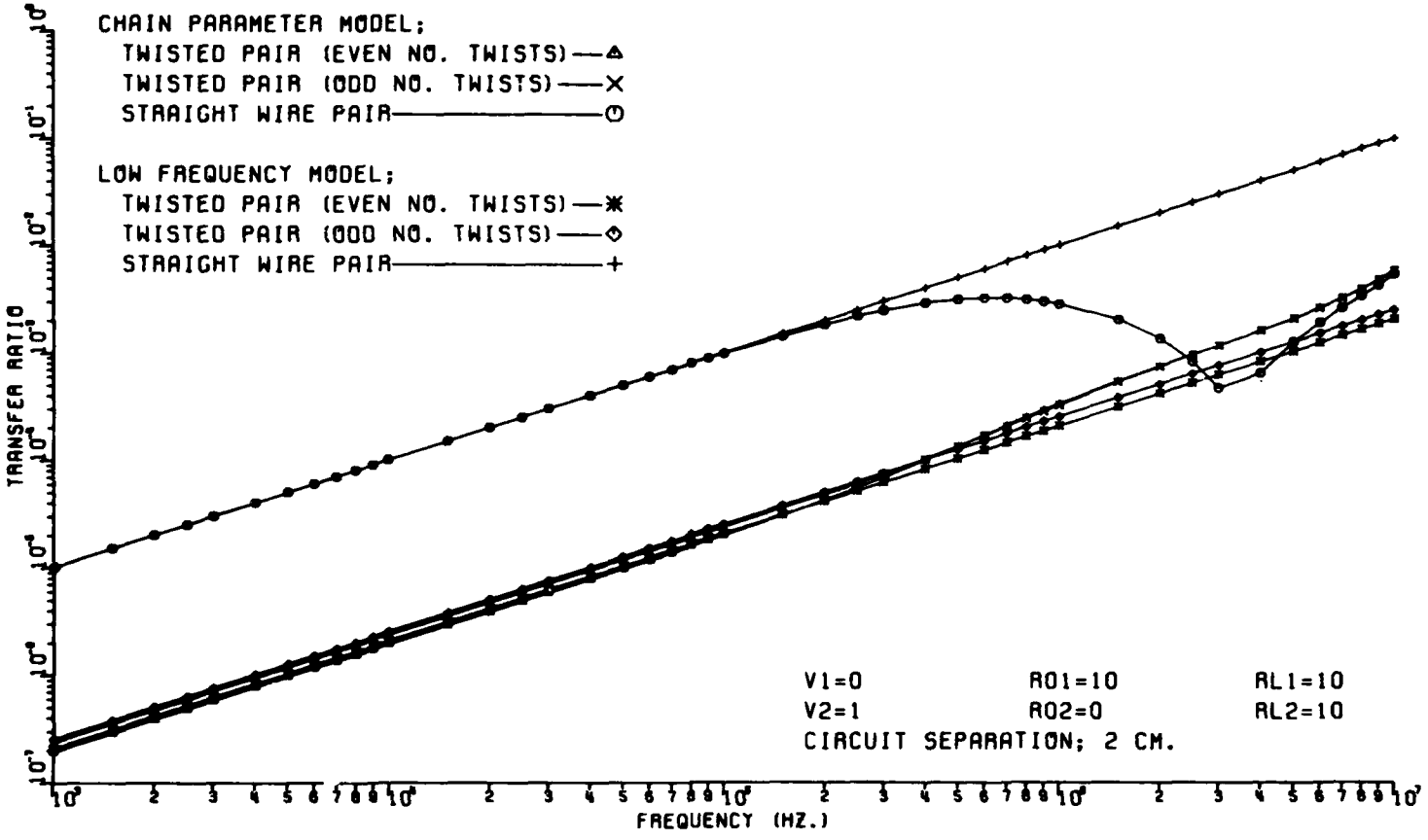
CHAIN PARAMETER MODEL;
TWISTED PAIR (EVEN NO. TWISTS)
TWISTED PAIR (ODD NO. TWISTS)
STRAIGHT WIRE PAIR
LOW FREQUENCY MODEL;
TWISTED PAIR (EVEN NO. TWISTS)
TWISTED PAIR (ODD NO. TWISTS)
STRAIGHT WIRE PAIR
TRANSFER RATIO
FREQUENCY (HZ.)
V1=0
V2=1
R01=10
R02=0
RL1=10
RL2=10
CIRCUIT SEPARATION; 2 CM.

Fig. C-22

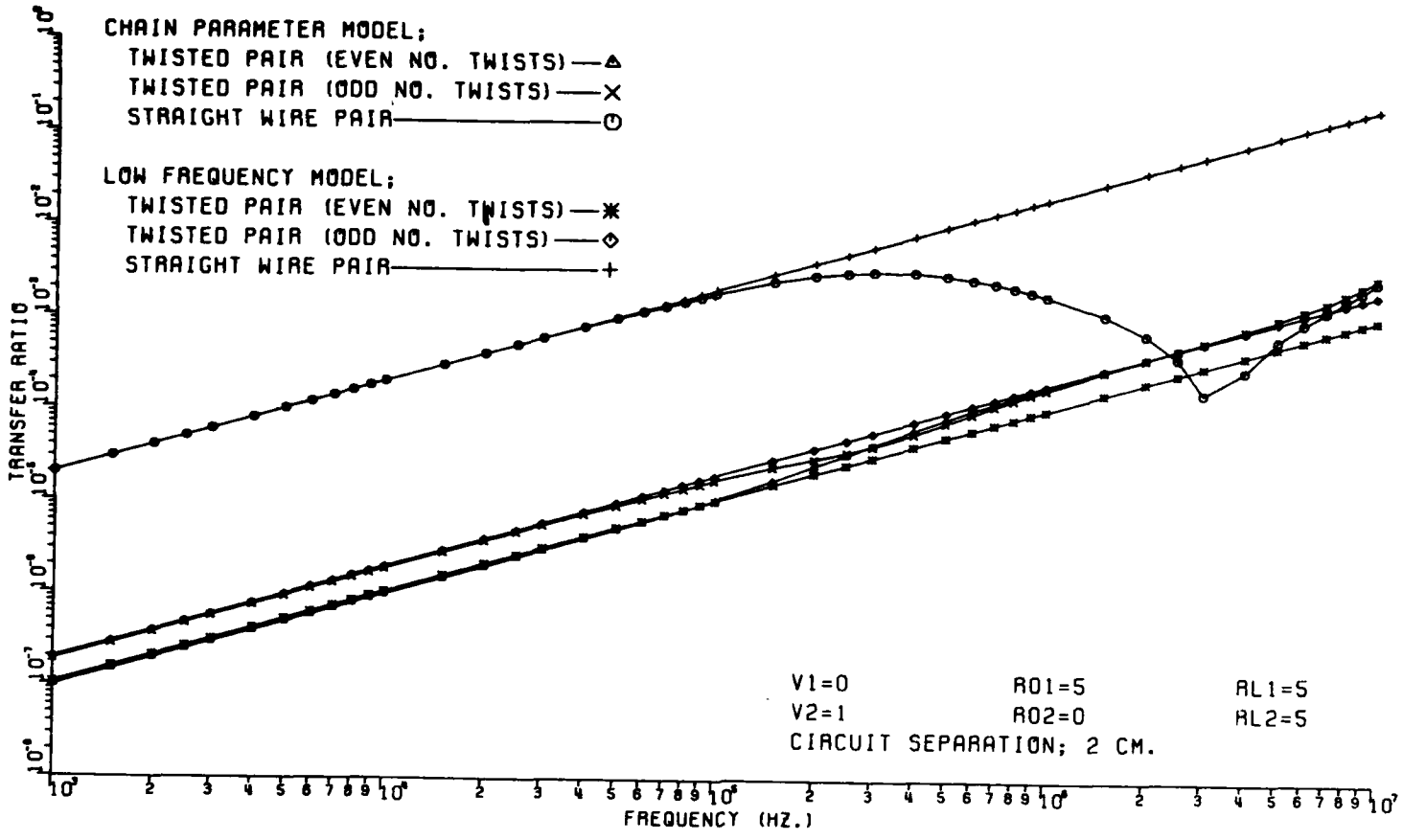
CHAIN PARAMETER MODEL;
TWISTED PAIR (EVEN NO. TWISTS)
TWISTED PAIR (ODD NO. TWISTS)
STRAIGHT WIRE PAIR
LOW FREQUENCY MODEL;
TWISTED PAIR (EVEN NO. TWISTS)
TWISTED PAIR (ODD NO. TWISTS)
STRAIGHT WIRE PAIR
TRANSFER RATIO
FREQUENCY (HZ.)
V1=0
V2=1
RO1=5
RO2=0
RL1=5
RL2=5
CIRCUIT SEPARATION; 2 CM.

Fig. C-23

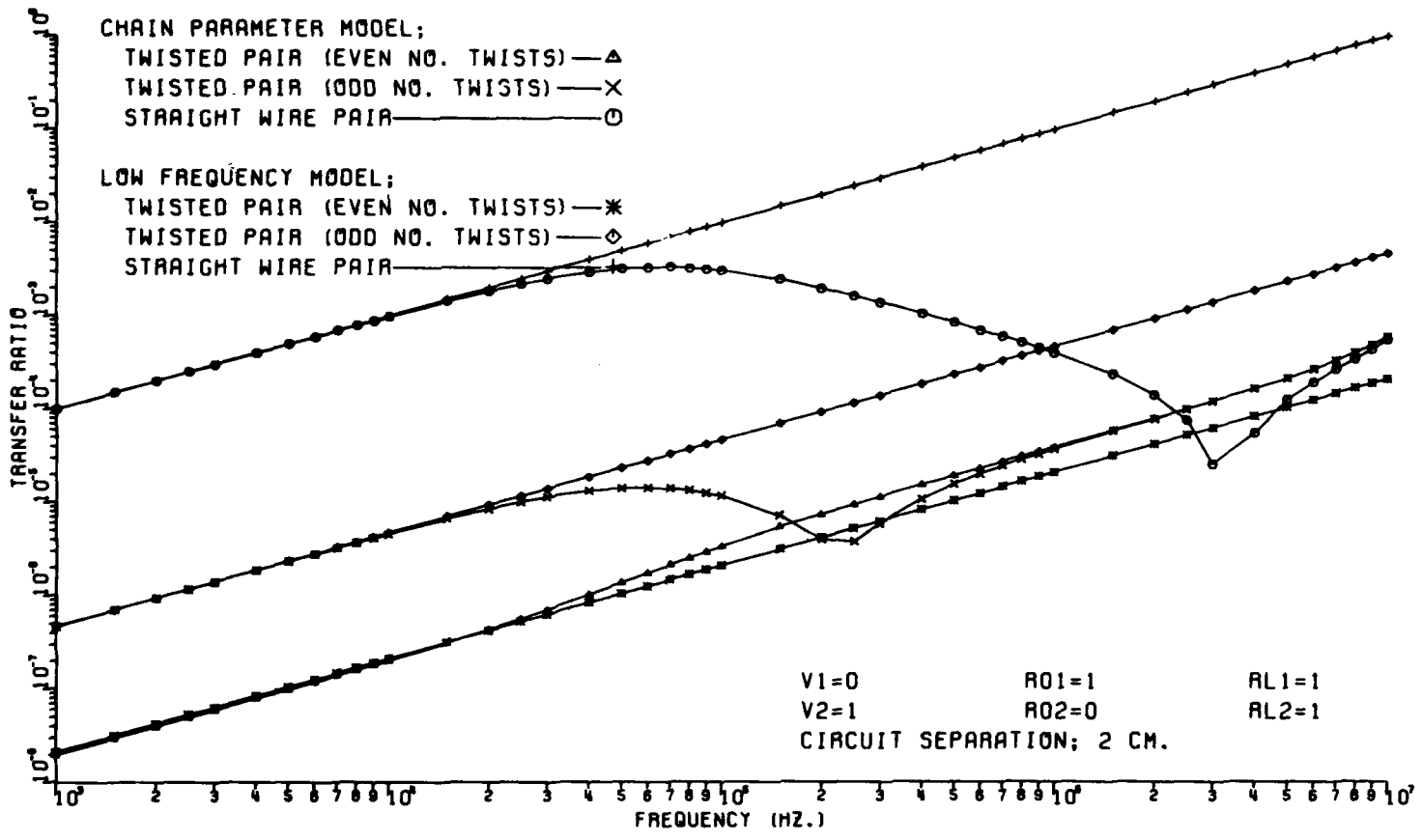
CHAIN PARAMETER MODEL;
TWISTED PAIR (EVEN NO. TWISTS)
TWISTED PAIR (ODD NO. TWISTS)
STRAIGHT WIRE PAIR
LOW FREQUENCY MODEL;
TWISTED PAIR (EVEN NO. TWISTS)
TWISTED PAIR (ODD NO. TWISTS)
STRAIGHT WIRE PAIR
V1=0
V2=1
R01=1
R02=0
RL1=1
RL2=1
CIRCUIT SEPARATION; 2 CM.
TRANSFER RATIO
FREQUENCY (HZ.)

Fig. C-24

BIBLIOGRAPHY

[1] C. R. Paul, Applications of Multiconductor Transmission Line Theory to the Prediction of Cable Coupling, Volume [illegible] conductor Transmission Line Theory. Technical Report Air Development Center, Griffiss AFB, N.Y. [illegible] 101, Volume I, April 1976, (A025028).

[2] C. R. Paul, "Solution of the Transmission Line [illegible] Three-Conductor Lines in Homogeneous Media [illegible] on Electromagnetic Compatibility, accepted [illegible]

[3] G. Barker, E. Gray, and R. M. Showers [illegible] ments Related to Procedures for Measuring System [illegible] ity", Unclassified Proceedings of the Eighth [illegible] ence on E.M.C., 1962.

[4] J. Moser and R. F. Spencer, Jr., Predicting the [illegible] Fields From a Twisted-Pair Cable, IEEE Trans. [illegible] magnetic Compatibility, Volume EMC 10 [illegible] Sept. 1968.

[5] S. Shenfeld, "Magnetic Fields of Twisted Wire Pairs", Trans. on Electromagnetic Compatibility [illegible] No. 4, pp. 164-169, November 1969.

[6] E. N. Protonotarious and O. Wing. Analysis and [illegible] Properties of the General Nonuniform Transmission [illegible] IEEE Trans. on Microwave Theory and Techniques MTT-15, No. 3, pp. 142-150.

[7] M. S. Ghausi and J. J. Kelly, Introduction to Distributed meter Networks. New York: Holt, Rinehart and W[illegible] 1968.

[8] D.R.J. White, Electromagnetic Interference and [illegible] Vol. 3, Electromagnetic Compatibility Control Methods & Techniques, Don White Consultants, Inc., Germantown [illegible] 1973.

[9] C. R. Paul and A. E. Feather, "Computation of the Transmission Line Inductance and Capacitance Matrices from the Generalized Capitance Matrix", IEEE Trans. on Electromagnetic Compatibility, Volume EMC-18, No. 4, pp. 175-183, November 1976.

[10] C. R. Paul, Applications of Multiconductor Transmission Line Theory to the Prediction of Cable Coupling, Volume III, Prediction of Crosstalk in Random Cable Bundles, Technical Report, Rome Air Development Center, Griffiss AFB, NY, RADC-TR-76-101, Volume III, Feb., 1977, A038316.

[11] C. R. Paul, Applications of Multiconductor Transmission Line Theory to the Prediction of Cable Coupling, Volume IV, Prediction of Crosstalk in Ribbon Cables, Technical Report, Rome Air Development Center, Griffiss AFB, NY, RADC-TR-76-101, Volume IV, February 1978.

MISSION
of
Rome Air Development Center

RADC plans and conducts research, exploratory and advanced development programs in command, control, and communications (C^3) activities, and in the C^3 areas of information sciences and intelligence. The principal technical mission areas are communications, electromagnetic guidance and control, surveillance of ground and aerospace objects, intelligence data collection and handling, information system technology, ionospheric propagation, solid state sciences, microwave physics and electronic reliability, maintainability and compatibility.